Expanding the Scope of the Asymmetric Allenic Pauson–Khand Reaction Towards the Synthesis of Thapsigargin and Analogues

by

Eric David Deihl

B. S. Chemistry, University of Pittsburgh at Greensburg, 2015

Submitted to the Graduate Faculty of the

Dietrich School of Arts and Sciences in partial fulfillment

of the requirements for the degree of

Doctor of Philosophy

University of Pittsburgh

2022

UNIVERSITY OF PITTSBURGH

DIETRICH SCHOOL OF ARTS AND SCIENCES

This dissertation was presented

by

Eric David Deihl

It was defended on

June 13, 2022

and approved by

Paul E. Floreancig, Professor, Department of Chemistry

Yiming Wang, Assistant Professor, Department of Chemistry

Jeffrey L. Brodsky, Professor, Department of Biological Sciences

Dissertation Director: Kay M. Brummond, Professor and Associate Dean for Faculty, Department of Chemistry

Expanding the Scope of the Asymmetric Allenic Pauson–Khand Reaction Towards the Synthesis of Thapsigargin and Analogues

Eric David Deihl, PhD

University of Pittsburgh, 2022

Thapsigargin is a potent inhibitor of sarco/endoplasmic reticulum calcium ATPase. A prodrug of thapsigargin called mipsagargin has been investigated in clinical trials for treating several types of cancer. The ability to synthesize thapsigargin analogues would further the structure activity relationship studies of this biologically important compound. The asymmetric allenic Pauson–Khand reaction affords enantioenriched cyclopentenones in a dynamic kinetic asymmetric transformation process. Herein we report the use of the asymmetric allenic Pauson–Khand reaction of furanyl tethered allene-ynes to rapidly form the carbocyclic core ring system of thapsigargin with good yields and enantioselectivities. The highest enantioselectivities observed in the asymmetric allenic Pauson–Khand reaction were with an allene-yne having a chloroacetate group. Computational results show the good enantioselectivity is due to a high activation barrier for the competing racemic background reaction. Expanding the substrate scope to include a benzene tethered allene-yne resulted in low enantioselectivities. The products of the allenic Pauson–Khand reaction were further functionalized via hydrolysis and hydrogenation reactions. The asymmetric allenic Pauson–Khand reaction of an allene-yne having a butanoyl group on the tether afforded products containing this important C8 group present in thapsigargin. The asymmetric allenic Pauson–Khand reaction is poised to be used in the synthesis of thapsigargin and thapsigargin analogues.

Table of Contents

List of Tables

List of Figures

List of Schemes

Preface

The journey to completing my doctorate has been a long and fulfilling process. I could not have done it alone. I would first like to thank my PhD advisor Professor Kay Brummond for her support over the years. Her hard work was an inspiration and helped me become a better chemist. I would like to thank my committee members Professor Paul Floreancig, Professor Yiming Wang, and Professor Jeffrey Brodsky for their helpful advice. I would also like to thank Professor Peng Liu, Luke Jesikiewicz and Logan Newman for their helpful collaboration. I would like to thank two of my professors from my undergraduate studies, Professor Matt Luderer and Professor Mark Stauffer, who encouraged and helped me to apply to graduate school.

I am lucky to have met so many great people in my time at the University of Pittsburgh. I would like to thank all of the past and present Brummond lab group members. I am fortunate to have had so many lab mates that made every day at work fun and enjoyable.

I would also like to thank my family and friends for their unwavering support. I could not have accomplished my goal of completing a doctorate without them.

1.0 Thapsigargin: a biologically active guaianolide natural product

Thapsigargin (Tg, **1.1**) is a sesquiterpene lactone of the guaianolide family of natural products (Figure 1). Tg was first isolated in 1978 by Christensen and coworkers from the plant *Thapsia garganica*, and the absolute configuration was assigned in 1985.[1] The discovery that Tg is a sub-nanomolar inhibitor of sarco/endoplasmic reticulum calcium ATPase (SERCA) in 1990 spurred extensive research into this molecule.[2, 3] SERCA is a calcium ion pump that is responsible for calcium homeostasis in cells. Inhibition of SERCA by Tg results in increased Ca^{2+} concentrations in the cytosol and leads to apoptosis.[4] The ability of Tg to induce apoptosis motivated research into its use as a cancer treatment.[5, 6]

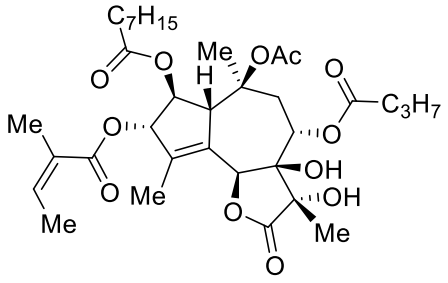

(–)-Tg, 1.1

Figure 1. Structure of thapsigargin

1.1 Mipsagargin a prodrug of thapsigargin

Because SERCA is found in healthy cells as well as cancer cells, Tg will indiscriminately kill cells. To avoid killing healthy cells, inactive prodrugs of Tg have been developed that are activated at the site of the tumor.[5] Structure activity relationship (SAR) studies were performed to

determine the appropriate site for an inactivating peptide on the molecule.[7] These SAR studies showed the C8 position was tolerant of a long carbon linker connecting the peptide to Tg. The prodrug mipsagargin (**1.2**) contains a long carbon linker connected to a small peptide residue. Mipsagargin does not inhibit SERCA, but in the presence of prostate specific membrane antigen (PSMA), the peptide is cleaved to release 12ADT-asp (**1.3**), a compound nearly equipotent to Tg (Scheme 1). Despite its name, prostate specific membrane antigen is expressed in the neovasculature of certain cancers allowing mipsagargin to potentially treat several types of cancer.[8]

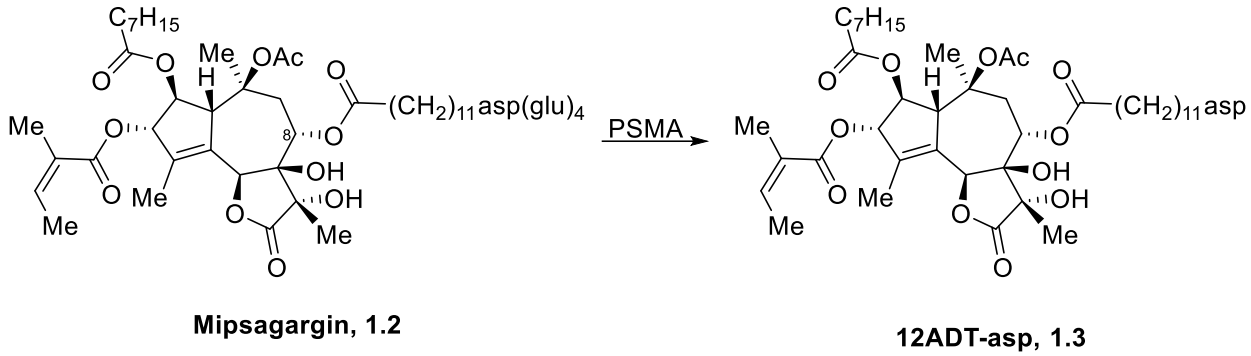

Mipsagargin, 1.2 **12ADT-asp, 1.3**

Scheme 1. PSMA activation of mipsagargin

1.1.1 Clinical trial results of mipsagargin

Patients treated with mipsagargin in a phase I clinical trial tolerated the treatment well.[9] Patients in the phase I trial with hepatocellular carcinoma had disease stabilization which led to a Phase II clinical trial. In a phase II clinical trial of patients with sorafenib resistant hepatocellular carcinoma, mipsagargin doubled the median time to progression of disease from approximately 63 days in the historic control population to 134 days in the mipsagargin treated patients.[10] In a phase II clinical trial of patients with glioblastoma, 22% of patients experienced disease stabilization.[11]

Despite the positive results from the phase II clinical trial, mipsagargin is not currently being investigated in clinical trials.[6]

1.1.2 Other prodrug approaches to thapsigargin based cancer therapeutics

A Tg prodrug **1.4** has been investigated to treat acute lymphoblastic leukemia.[12] Acute lymphoblastic leukemia cells overexpress folate receptors making this an attractive target for a folic acid conjugated prodrug. Tg conjugated to folic acid was inactive at inhibiting SERCA but entered cells in the presence of folate receptors. Once inside cells, the folic acid was cleaved to afford a C8 hydroxy Tg derivative **1.5** (Scheme 2). Tg derivative **1.5** inhibits SERCA but is less potent than Tg, with a relative IC_{50} value ranging from 5.4 to 50 in two separate studies.[13, 14] The authors proposed future studies using a linker to conjugate folic acid to Tg to afford a more bioactive product following hydrolysis for which findings have not been reported.

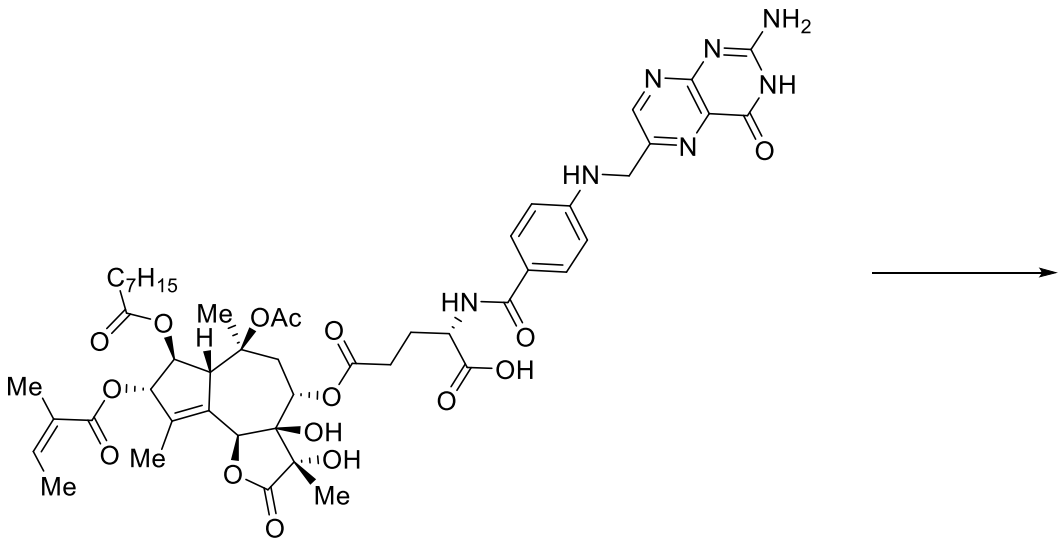

1.4

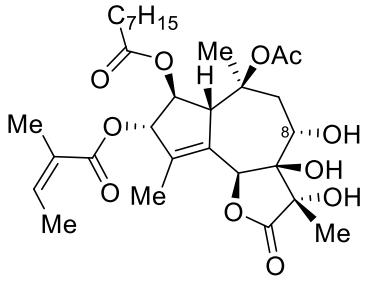

1.5

Scheme 2. Hydrolysis of folate conjugated thapsigargin analogue

Another approach to Tg-based prodrugs is linking albumin to Tg via a maleimide linker (Figure 2).[15] Albumin is a protein that is highly concentrated in prostate cancer cells. Albumin in prodrug **1.6** is readily cleaved in prostate cancer cells releasing a potent Tg analogue. This prodrug showed good results in killing prostate cancer cell lines *in vitro*.

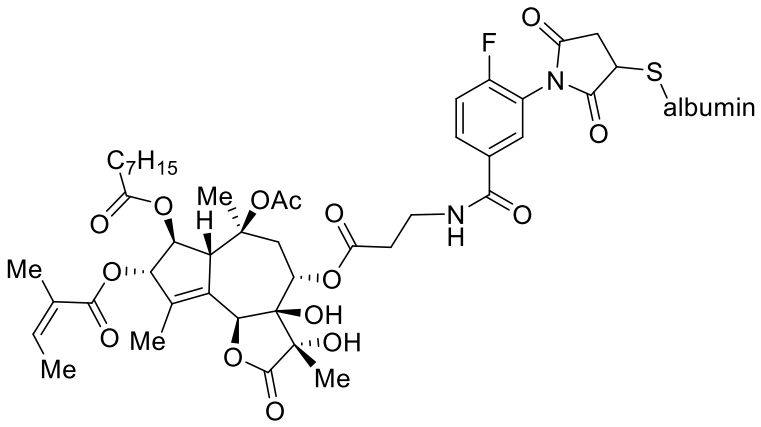

Figure 2. Albumin linked thapsigargin prodrug

1.2 Thapsigargin as a treatment for diseases other than cancer

Tg and Tg analogues have been investigated for treating several other diseases including malaria, sepsis, MRSA, and viruses such as influenza and SARS-CoV-2.[16-24] For example, priming Calu-3 cells with 0.5 µM Tg prior to infection decreased the relative virus copy number by 96.6%.[20] Treating cells infected with SARS-CoV-2 with 0.5 µM Tg 24 hours after infection resulted in an 81.4% relative decrease in virus copy number. Tg was highly effective against variants of SARS-CoV-2 including the highly transmissible Delta variant.[22]

1.3 Previous total syntheses of thapsigargin

Tg is isolated from *Thapsia garganica* in low quantities ranging from 0.2-4.91% by dry weight.[25, 26] Synthesis of Tg could reduce reliance on *Thapsia garganica* as the only commercial

source.[27] To date, there have been 3 total syntheses of Tg, each starting with carvone or dihydrocarvone (Scheme 3).[28-32] The first synthesis of Tg was completed in the lab of Steve Ley and used a Favorskii rearrangement to form the five-membered ring and a metathesis reaction of diene **1.8** to form the seven-membered ring.[28-30] The Baran lab's synthesis of Tg began with dihydrocarvone and formed the 5,7-ring system of Tg with a photochemical rearrangement of **1.10**.[31] P. A. Evan's synthesis of Tg began with (*R*)-carvone and formed the seven-membered ring via a pinacol coupling of **1.12**.[32]

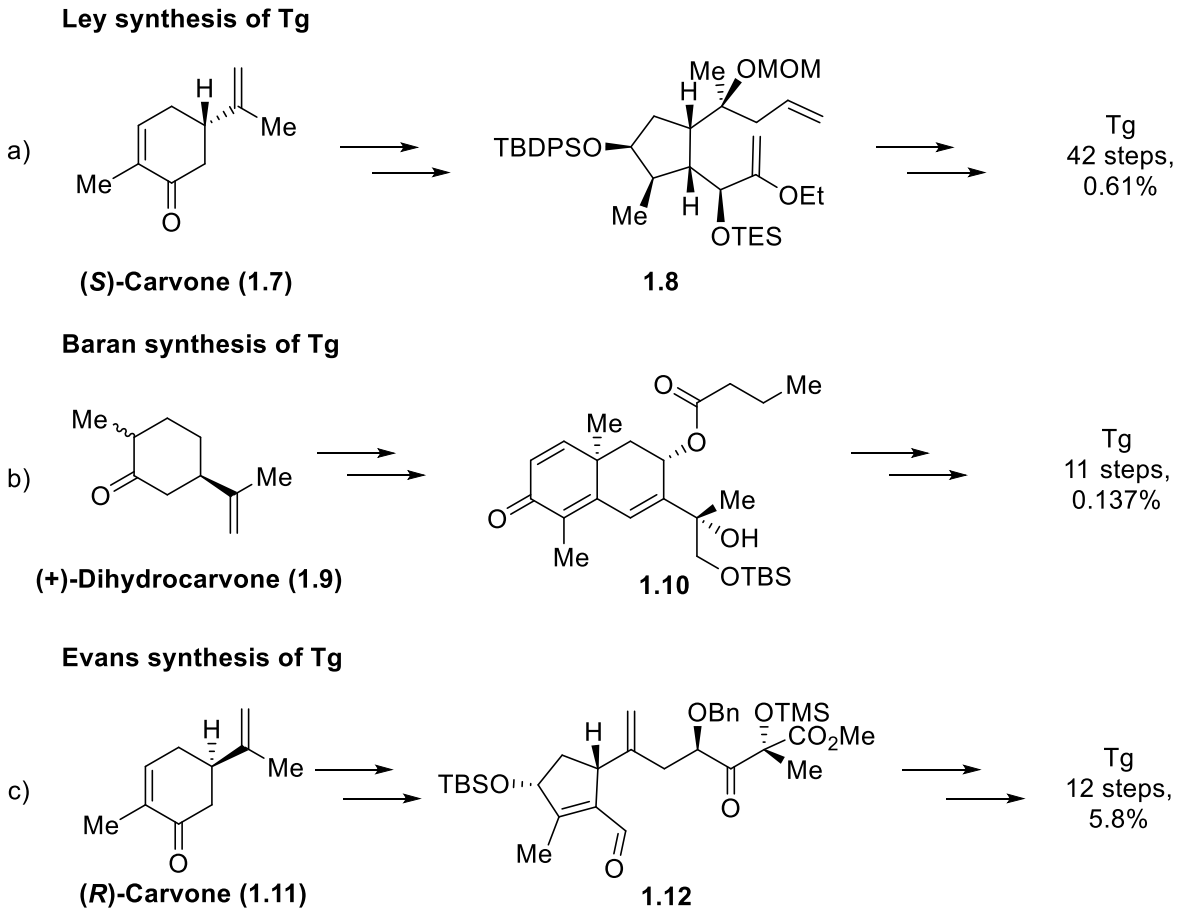

Scheme 3. Previous total syntheses of thapsigargin

1.3.1 Other synthetic strategies to access thapsigargin

Other groups' strategies directed towards the synthesis of Tg include metathesis, photochemical rearrangement, and allenic Pauson–Khand reactions.[33-39] Tg can be accessed via semi-synthesis in 4 steps from the natural product nortrilobolide (**1.13**), which is also isolated from *Thapsia garganica*.[40] Tg can also be accessed from the closely related natural product trilobolide (**1.14**) (Figure 3).[41] Trilobolide is isolated from the plant *Laser trilobum*, which grows abundantly in the Czech Republic.

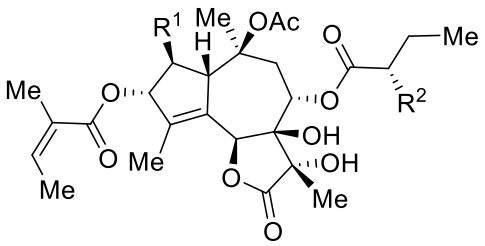

1.13 R^1= H, R^2= H
1.14 R^1= H, R^2= Me

Figure 3. Structures of nortrilobolide and trilobolide

1.3.2 Structure activity relationship studies of thapsigargin

SAR studies of Tg have been conducted mostly by extracting the natural product from *Thapsia garganica* and performing reactions to form new analogues.[7] Most Tg analogues have been generated by selective hydrolysis of the ester groups followed by re-esterification to form new ester groups. The structural diversity of the carbocyclic skeleton for analogues generated using this strategy is limited. A few highly potent analogues have been synthesized in the course of completing total syntheses of Tg.[42, 43]

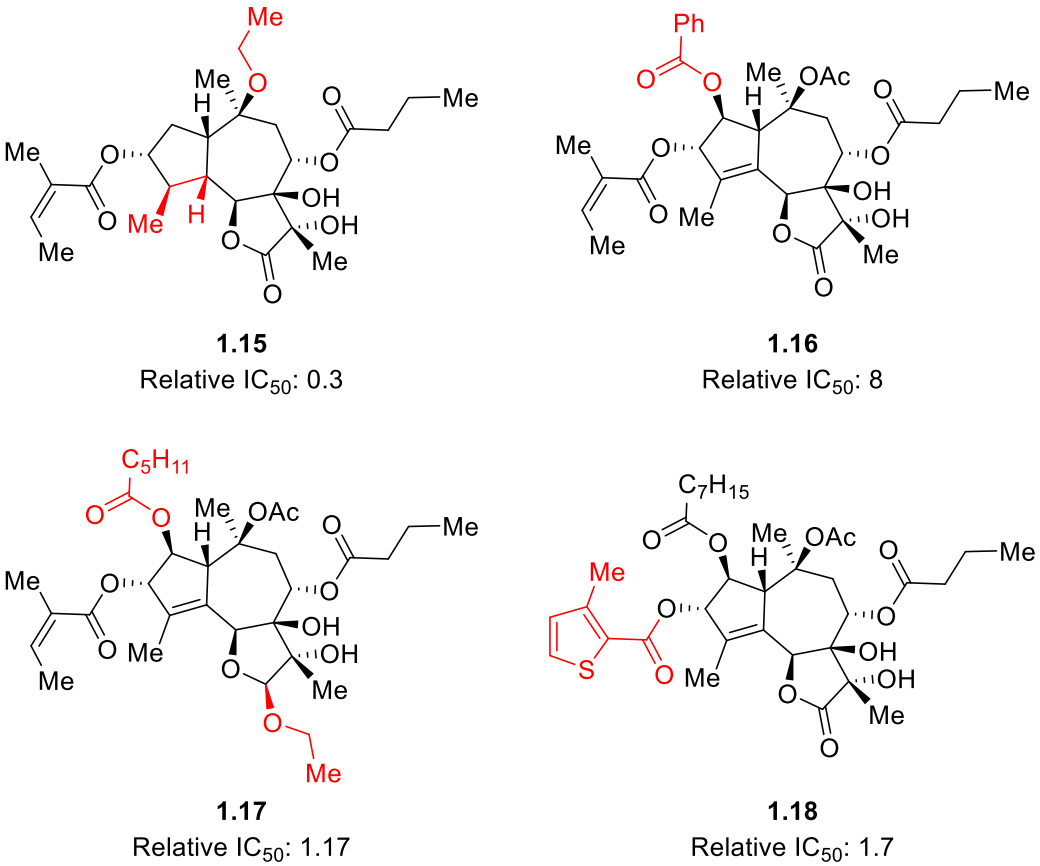

Figure 4. Some highly potent Tg analogues

Based on the SAR studies of Tg analogues, the most important groups to SERCA inhibition activity are the C3 angeloyl group, C7 hydroxyl group, C8 butanoyl group, C10 acetate group, and the C15 methyl group.[7, 44] Based on this information, we propose a pharmacophore model of Tg for the synthetic design of analogues where the portion of the molecule responsible for activity is highlighted in yellow (Figure 5).[45-48] This model is supported by SAR studies showing the lactone ring of Tg tolerates substantial changes with little to no decrease in SERCA inhibition activity.

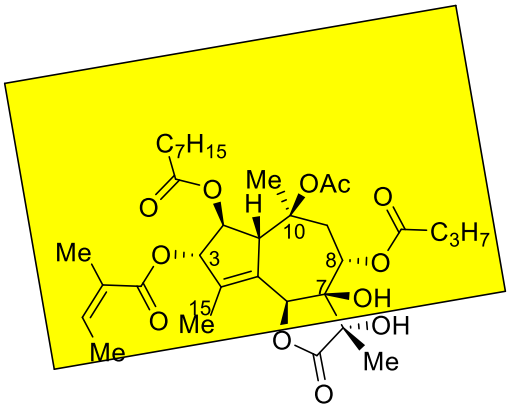

Tg, 1.1

Figure 5. Pharmacophore model of Tg

1.4 The allenic Pauson–Khand reaction

The Pauson–Khand reaction is a metal catalyzed [2+2+1] cyclocarbonylation reaction between an alkene, alkyne and carbon monoxide.[49-51] The allenic Pauson–Khand reaction (APKR) is a variant of the Pauson-Khand reaction involving an allene, alkyne, and carbon monoxide.[52, 53] Both intermolecular and intramolecular variants of the APKR have been developed.[54-56] The mechanism of the APKR involves an oxidative cyclization, CO insertion, and reductive elimination to afford the cyclopentenone product (Scheme 4).

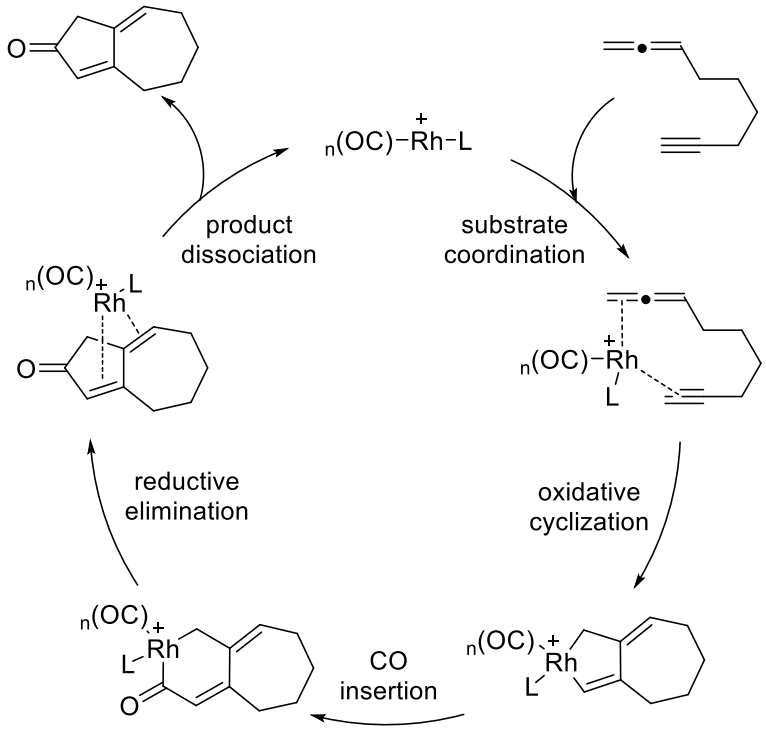

Scheme 4. Mechanism of the APKR

The metal catalyst plays an important role in the allene double bond selectivity of the APKR. For instance, molybdenum favors reaction with the proximal double bond of the allene in the intramolecular APKR while rhodium usually reacts preferentially with the distal double bond (Scheme 5).[57-61] A few examples of rhodium catalyzed APKRs reacting with the proximal double bond have been reported.[62-64] Reaction with the proximal double bond in these examples is the result of steric congestion, electronic factors or directing groups. DFT calculations show this double bond selectivity is influenced by the geometry of the metal center with rhodium adopting a square planar geometry in an early oxidative cyclization transition state, which favors reaction of the distal double bond of the allene.[65] Whereas in the case of molybdenum, the trigonal bipyramidal geometry of the oxidative cyclization step favors reaction with the proximal double bond. Other metals, including Co, Fe, Ir, Zr, and Ti, have been used in the APKR.[54, 56, 57, 66-68]

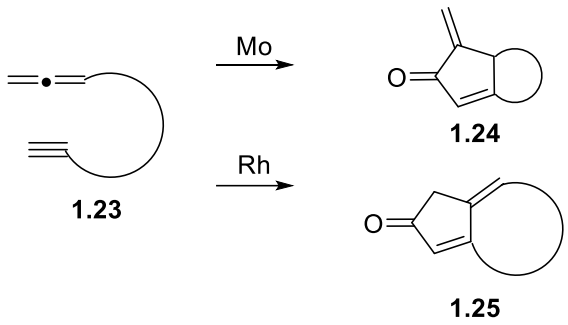

Scheme 5. Allene double bond selectivity of the APKR

1.4.1 Transfer of allene axial chirality to the asymmetric APKR product

Chiral, non-racemic allenes undergo the APKR with a transfer of the axial chirality to an sp^3 hybridized carbon to afford enantioenriched ring-fused cyclopentenones.[69, 70] For instance, enantioenriched allene **1.26** with an NTs containing tether underwent the APKR with complete transfer of chirality to afford enantioenriched α-methylcyclopentenone **1.27** (Scheme 6). Allenes with an oxygen or diester group in the tether experienced an erosion of the enantioselectivity due to scrambling of the axial chirality of the allene under the reaction conditions.

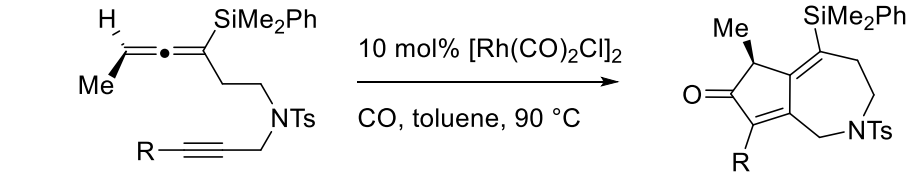

1.26
>93%ee
R= Me, Ph, H, TMS, cyclopropyl, 2-thiophene, 3-thiophene

1.27
>96% ee
66-95% yield

Scheme 6. Transfer of chirality in the APKR

1.4.2 The Asymmetric APKR

Chiral, racemic allenyl carboxyesters undergo a rhodium catalyzed asymmetric APKR in the presence of a chiral monodentate ligand.[71-73] Reacting racemic allene-yne **1.28** with $Rh(cod)_2BF_4$ and (*S*)-MonoPhos-alkene (**L1**) at 70 °C under a carbon monoxide atmosphere afforded enantioenriched cyclopentenone **1.29** in 79% yield and 18:82 er (Scheme 7).[73] Lauren Burrows, a former group member, demonstrated that this asymmetric APKR is an example of a Type I Dynamic Kinetic Asymmetric Transformation (DyKAT) (Scheme 8).[74-78] In this DyKAT process, the axial chirality of the allene is rapidly scrambled in the presence of the rhodium catalyst followed by a single enantiomer of the allene reacting preferentially with the chiral catalyst complex to form enantioenriched APKR product.

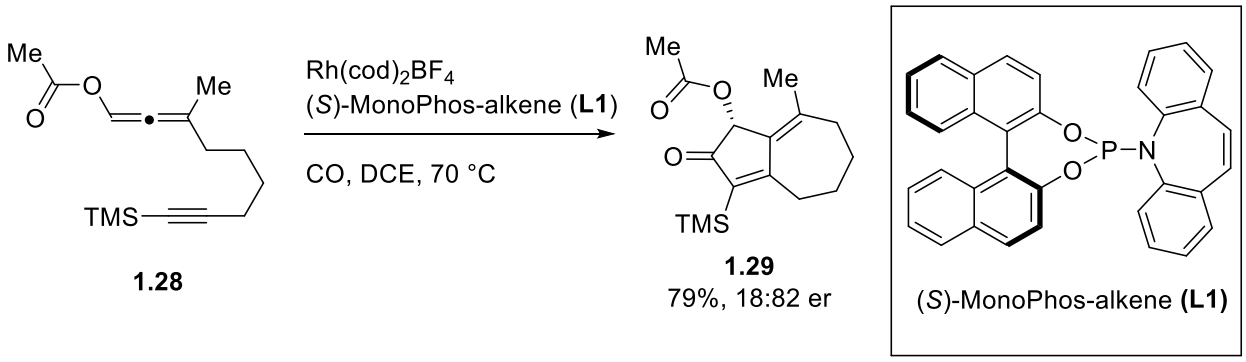

Scheme 7. Asymmetric APKR of carbon tethered allene-yne

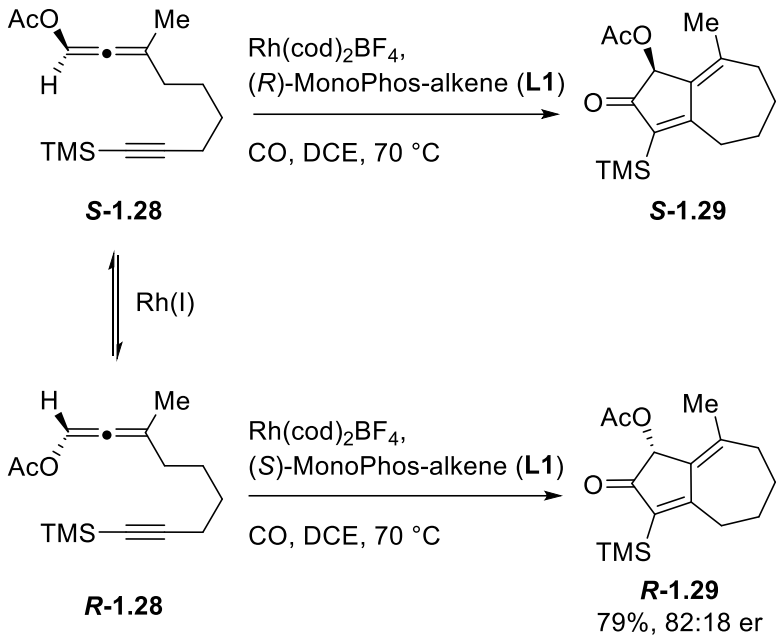

Scheme 8. Type I DyKAT process in the asymmetric APKR

1.5 Conclusions

Tg is an important biological tool and research into its clinical significance is continuing. Despite the failure of mipsagargin to advance to phase III clinical trials, Tg prodrugs conjugated to folic acid and albumin are being investigated to treat cancer. Tg as an antiviral drug is showing promise as a broad-spectrum inhibitor of viral replication. Large scale production of Tg has not been accomplished, but synthetic and semisynthetic production are potential options. The allenic Pauson–Khand reaction remains a viable strategy for the synthesis of Tg and Tg analogues.

2.0 The asymmetric APKR of furanyl tethered allene-ynes

This Chapter was adapted from a manuscript coauthored by Eric D. Deihl, Luke T. Jesikiewicz, Logan J. Newman, Peng Liu, and Kay M. Brummond.[79]

We have designed a retrosynthetic strategy for accessing Tg using an asymmetric allenic Pauson-Khand approach. We envision synthesizing Tg **1.1** from **2.1** by converting the furan into a butenolide using *m*-CPBA, epoxidation of the butenolide double bond and ring opening followed by reduction of the ketone and esterification (Scheme 9).[80] **2.1** can be accessed from carbamate **2.2** via a modified Hoffman–Löffler–Freytag C–H functionalization reaction and esterification of the resulting tertiary alcohol.[81, 82] **2.2** can be accessed from **2.3** by converting the C2 hydroxyl group to a carbamate. **2.3** could be accessed from APKR adduct **2.4** via hydrolysis of the acetyl group followed by a hydroxyl directed hydrogenation of the C1-C10 double bond.[83]

Formation of the carbocyclic 5,7,5-ring system of **2.4** can be accessed via the asymmetric APKR of allene-yne **2.5** to selectively form the C2 stereocenter with the absolute configuration of Tg.[73] Allene-yne **2.5** can be accessed from propargyl acetate **2.6** via a rhodium catalyzed rearrangement.[63] Propargyl acetate **2.6** can be accessed from methyl ketone **2.7** via addition of ethynylmagnesium bromide and trapping with acetyl chloride.[84, 85] Methyl ketone **2.7** can be accessed via conversion of the silyl group to a halogen and Sonogashira coupling and an amino acid catalyzed asymmetric aldol reaction of **2.8** and esterification of the resulting β-hydroxy group.[84-87] Furan **2.8** can be accessed via a silyl shift of TMS protected alcohol **2.9** followed by deprotonation and methylation.[88, 89]

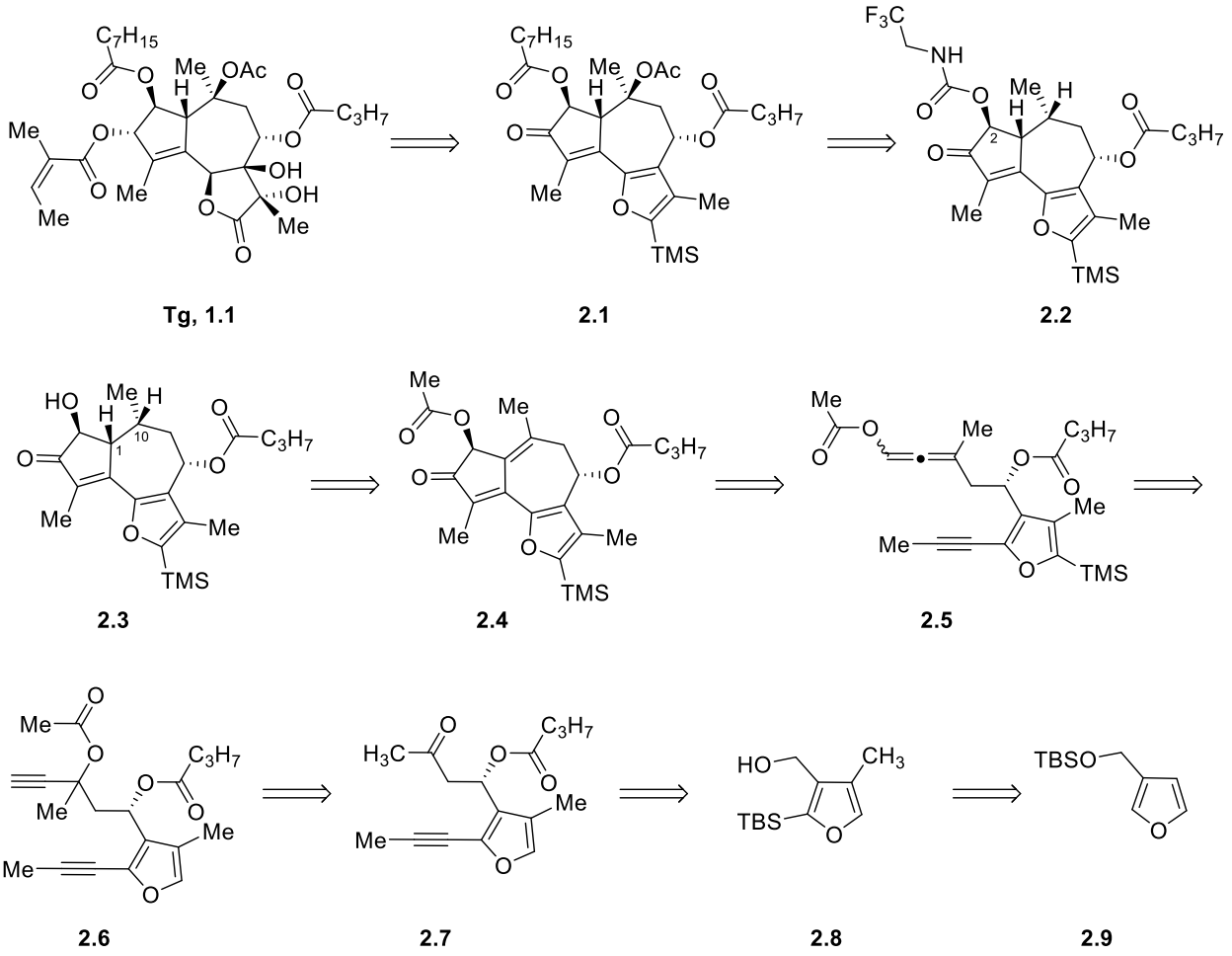

Scheme 9. Retrosynthetic strategy for thapsigargin

2.1 Synthesis of allene-ynes for the APKR

We began our synthesis of Tg and Tg analogues using model system **2.11** to study the asymmetric APKR of furanyl tethered allene-ynes (Scheme 10). We chose this model system because we were unsure of how the butanoyl group would impact this reaction and whether the furanyl ring would be tolerated in the asymmetric APKR.[90-92] We chose to include a furan in the tether of the allene-yne because it is a synthon for a lactone, and we were interested in testing

compounds containing furan rings, such as **2.12**, for their biological activity. Furans are present in some pharmaceuticals, but their metabolism to reactive compounds *in vivo* limits the testing of furan containing compounds in medicinal chemistry studies.[93] Based on previous work of a Tg analogue with a tetrahydrofuran giving nearly equipotent relative IC_{50} values, we believe that an analogue containing a furan ring may also be highly active (Figure 6).[7]

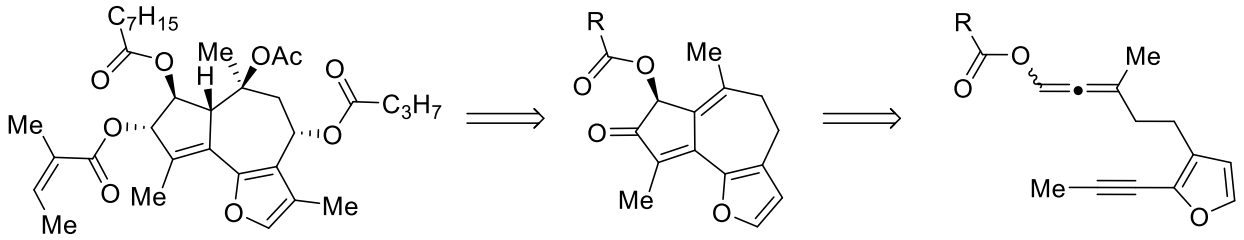

2.12 **2.11** **2.10**

Scheme 10. Model system to test the feasibility of the asymmetric APKR of furanyl tethered allen-ynes

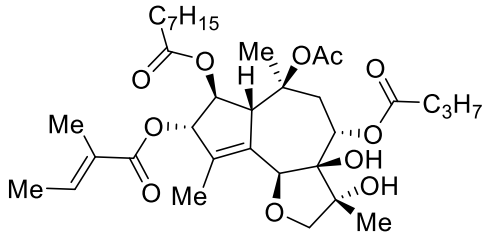

2.13
Relative IC_{50}: 1.06

Figure 6. Potent tetrahydrofuran containing thapsigargin analogue

We began our synthesis of allene-yne **2.10** by reacting 3-furfural (**2.14**) with propynylmagnesium bromide to afford propargyl alcohol **2.15** in 92% yield (Scheme 11). Propargyl alcohol **2.15** was reacted with *N*-bromosuccinimide (NBS) followed by 1 M HCl to afford furaldehyde **2.16** in 69% yield.[94] We initially performed this sequence of reactions in a one-pot two-step procedure, but the one-pot procedure was not always reproducible. For example, the first several times we performed the one-pot procedure we were able to obtain the desired product; however, the oxidative rearrangement reaction stopped working in the one-pot procedure for

unknown reasons, and we isolated the propargyl alcohol in low yields. Therefore, we opted for the two-pot procedure shown.

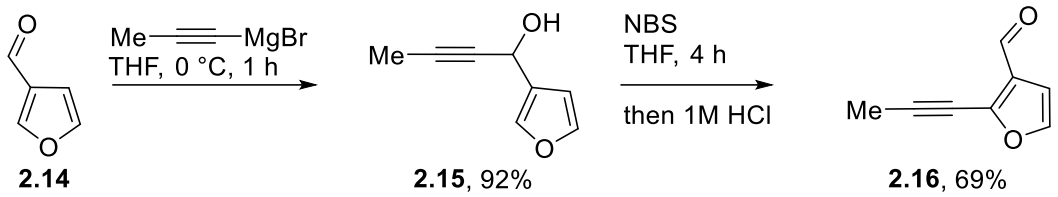

2.14 **2.15**, 92% **2.16**, 69%

Scheme 11. Installation of alkyne moiety via oxidative rearrangement

2.1.1 Horner-Wadsworth-Emmons reaction approach to the methyl ketone

We next sought to convert furaldehyde **2.16** to methyl ketone **2.20**. Our original strategy to synthesize methyl ketone **2.20** was to transform the aldehyde into an unsaturated nitrile using a Horner–Wadsworth–Emmons reaction followed by a reduction of the double bond and conversion of the nitrile to methyl ketone **2.20**.[95] Aldehyde **2.16** was converted to the unsaturated nitrile **2.17** in 84% yield as a 76:24 ratio of *E*:*Z* isomers that were not separated but taken on as a mixture to the next step (Scheme 12). Reduction of the double bond of **2.17** using 40 equiv of magnesium gave a 51% yield of nitrile **2.18**. The low yield was partially attributed to the formation of the over-reduced product **2.19**. Dibromoethane was required for magnesium activation.[96] Using less magnesium did not improve the isolated yield or gave recovered starting material. For example, using 20 equiv of magnesium afforded 60% crude yield of **2.18** and 12% crude yield of **2.19**. Using 10 equiv of magnesium resulted in 10% of recovered starting material and only 12% isolated yield **2.19**.

Reacting nitrile **2.18** with methylmagnesium bromide and heating in a microwave reactor at 100 °C followed by hydrolysis with 15% H_2SO_4 afforded methyl ketone **2.20** in low yield (35-49%).[97] Conventional heating (oil bath) did not furnish **2.20**. Performing the reaction in refluxing

THF with a catalytic amount of Cu(I)Br gave no product.[98] Using methyllithium and refluxing the reaction mixture in diethyl ether gave trace amounts of **2.20**.[99] Due to inconsistent and low yields, poor scalability, requirement for specialized heating equipment and a large excess of methylmagnesium bromide, we abandoned this route. Furthermore, conversion of an alkyl nitrile to a dialkyl ketone is problematic due to the acidity of the hydrogens alpha to the nitrile.[100, 101]

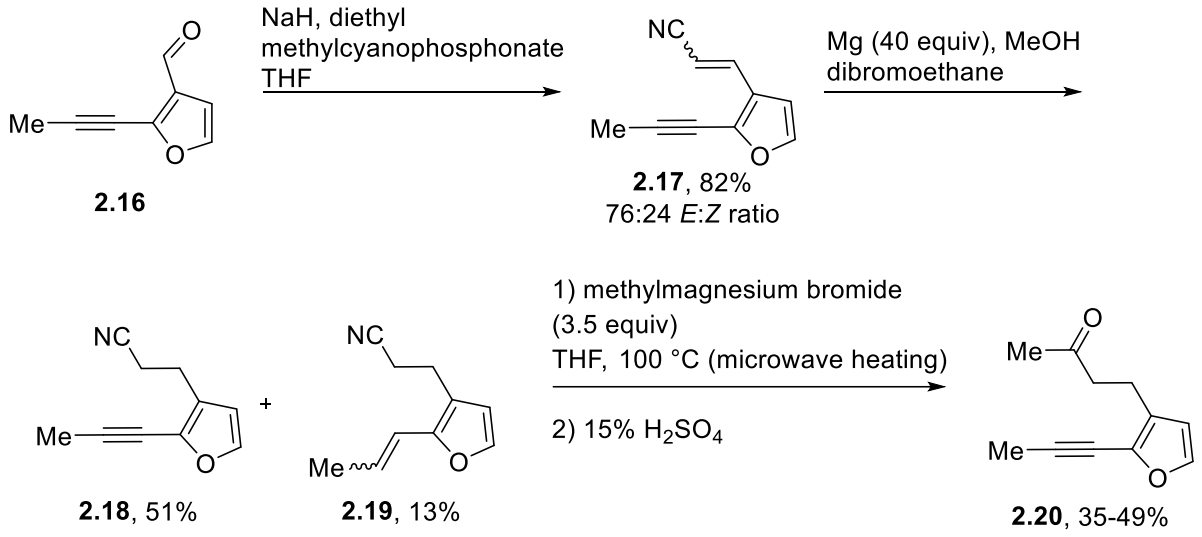

Scheme 12. Synthesis of methyl ketone 2.20 via nitrile intermediate

2.1.2 An unexpected electrocyclization reaction to form benzofurans

While investigating methods for reducing the double bond of unsaturated nitrile **2.17**, we attempted to form **2.18** using $NaBH_4$.[102] Subjecting **2.17** to $NaBH_4$ in isopropanol at 75 °C for 27 h resulted in quantitative yield of benzofuran byproduct **2.21** and none of the desired nitrile **2.18** (Scheme 13). The ^1H NMR of **2.21** showed two doublets at 7.66 and 6.78 ppm corresponding to H_a and H_b and two singlets at 7.88 and 7.43 ppm corresponding to H_c and H_d as well as a methyl singlet at 2.65 ppm. The ^{13}C NMR showed 9 signals from 106-157 ppm corresponding to the aromatic carbons and the nitrile carbon and the methyl carbon at 20.9 ppm. Mass spectrometry

data showed the exact mass of 158.0598 aligning with the benzofuran product. To determine whether this transformation was a thermal cyclization or promoted by $NaBH_4$, we heated **2.17** in isopropanol at 75 °C. After 22 h, only starting material was observed by ^1H NMR. At this point $NaBH_4$ was added and the reaction heated overnight at 75 °C. After purification, benzofuran **2.21** was isolated in 50% yield. These data demonstrate that $NaBH_4$ is required to form benzofuran **2.21**.

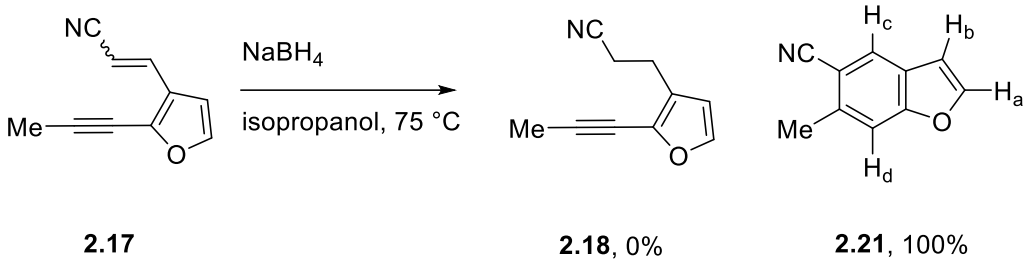

2.17 **2.18**, 0% **2.21**, 100%

Scheme 13. Formation of benzofuran byproduct from acrylonitrile 2.17

We hypothesized that $NaBH_4$ may be acting as a base to promote the cyclization reaction due to the use of bases in similar cyclization reactions.[103] To test this hypothesis, triethylamine was used in place of $NaBH_4$ and afforded only recovered starting material. Changing the solvent from isopropanol to chloroform and increasing the equivalents of triethylamine from 0.1 to 1.5 equiv gave only 90% recovered starting material.

To determine whether the methyl group on the alkyne was important to the reaction, we reacted **2.22** containing a phenyl substituted alkyne with $NaBH_4$ in isopropanol at 75 °C which afforded recovered starting material (Scheme 14). This result shows that the substituent on the terminus of the alkyne may play a role in the reaction either by sterics or another factor. Due to the limited substrate scope of this reaction, we did not pursue this methodology further.

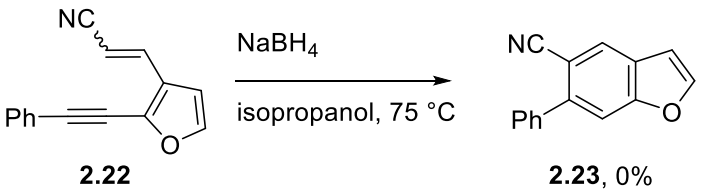

2.22 **2.23**, 0%

Scheme 14. Cyclization reaction of phenyl substituted alkyne

Based upon these results we propose that the $NaBH_4$ or sodium isopropoxide is promoting the isomerization of the propynyl group of **2.17** to an allene via a deprotonation/protonation sequence (Scheme 15). Allene **2.24** undergoes an electrocyclization reaction to afford **2.25** which undergoes a second protonation/deprotonation to afford benzofuran **2.21**.[104, 105] This mechanistic hypothesis takes into consideration the need for $NaBH_4$ and is consistent with the nonreactivity of the phenyl substituted alkyne, which cannot form an allene and undergo this cyclization.

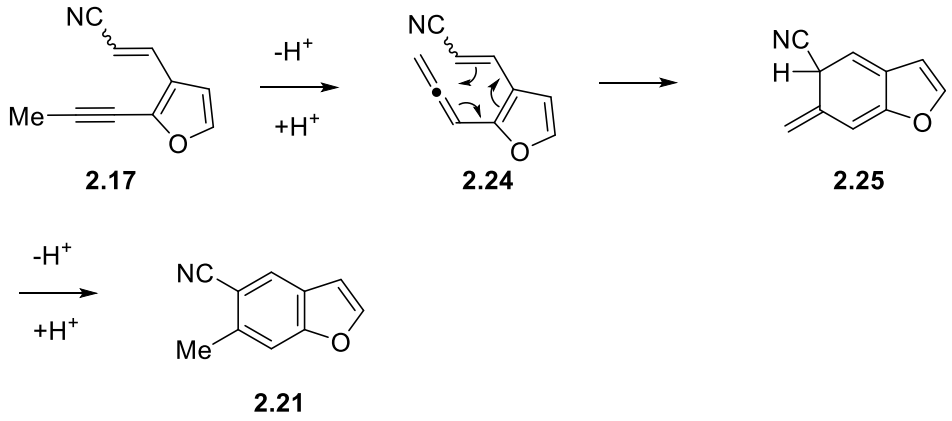

2.17 **2.24** **2.25**

2.21

Scheme 15. Proposed mechanism for the electrocyclization reaction of 2.17

2.1.3 Aldol condensation approach to methyl ketone 2.20

We attempted to improve the synthesis of methyl ketone **2.20** via an aldol condensation reaction between acetone and **2.16** followed by a conjugate reduction of the enone. Reacting furaldehyde **2.16** with acetone and sodium hydroxide at 0 °C afforded the α, β-unsaturated ketone **2.26** in 67% yield (Scheme 16).[106] Next a 1,4-reduction of **2.26** using diethyl 2,6-dimethyl-1,4-

dihydropyridine-3,5-dicarboxylate (Hantzsch ester, **2.27**) in refluxing benzene afforded some product but mostly starting material.[107] Performing the Hantzsch ester reduction in refluxing toluene afforded the desired product **2.20** in 74% yield with no recovered starting material.[108] Performing the reaction with Hantzsch ester **2.27** (3 equiv) and $TiCl_4$ (1.2 equiv) in THF resulted in an 83% yield of **2.20**.[109] Due to the operational simplicity, we chose to use conditions employing refluxing toluene with no $TiCl_4$. The aldol condensation strategy to form methyl ketone **2.20** was a great improvement over the Horner–Wadsworth–Emmons approach based upon a significantly higher yield of **2.20**, the reaction sequence could be performed on larger scale with oil bath heating, and a reduced number of steps. For example, the aldol strategy afforded 1.4 g of **2.20** in 50% yield in 2 steps from furan **2.16** compared to 80 mg of **2.20** in 15-20% yield in 3 steps for the Horner-Wadsworth-Emmons reaction sequence.

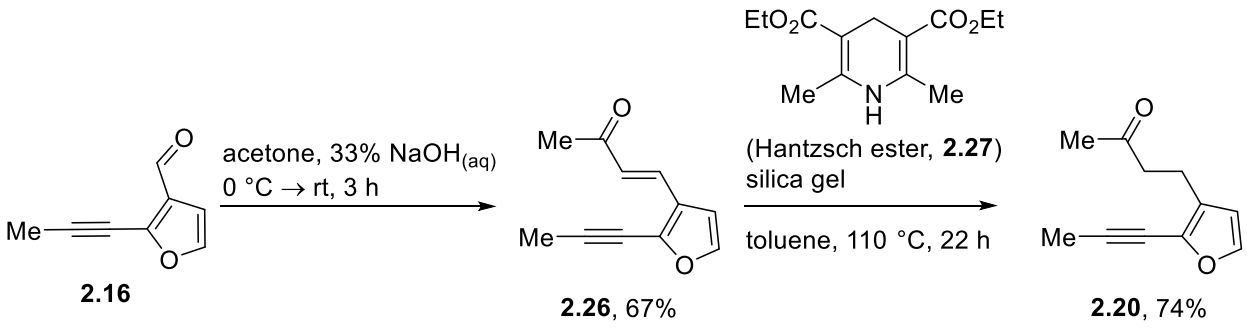

Scheme 16. Access to methyl ketone 2.20 via aldol condensation reaction

2.2 Synthesis of allenyl carboxyesters

With methyl ketone **2.20** in hand, we turned to conditions developed by previous Brummond group members to transform the methyl ketone into allenyl carboxyesters.[63, 73] Addition of ethynylmagnesium bromide followed by trapping of the resulting propargyl alkoxide

in situ with acetyl chloride afforded propargyl acetate **2.28a** in 59% yield (Scheme 17). Propargyl acetate **2.28a** was subjected to a Rh(II) catalyzed formal [3,3] sigmatropic rearrangement to afford allenyl acetate **2.10a** in 64% yield. Allenyl carboxyesters **2.10b**-**2.10g** were synthesized in a similar manner. For detailed information on the synthesis of **2.10a**-**2.10g**, see *Org. Lett*. **2022**, 995-999.[79]

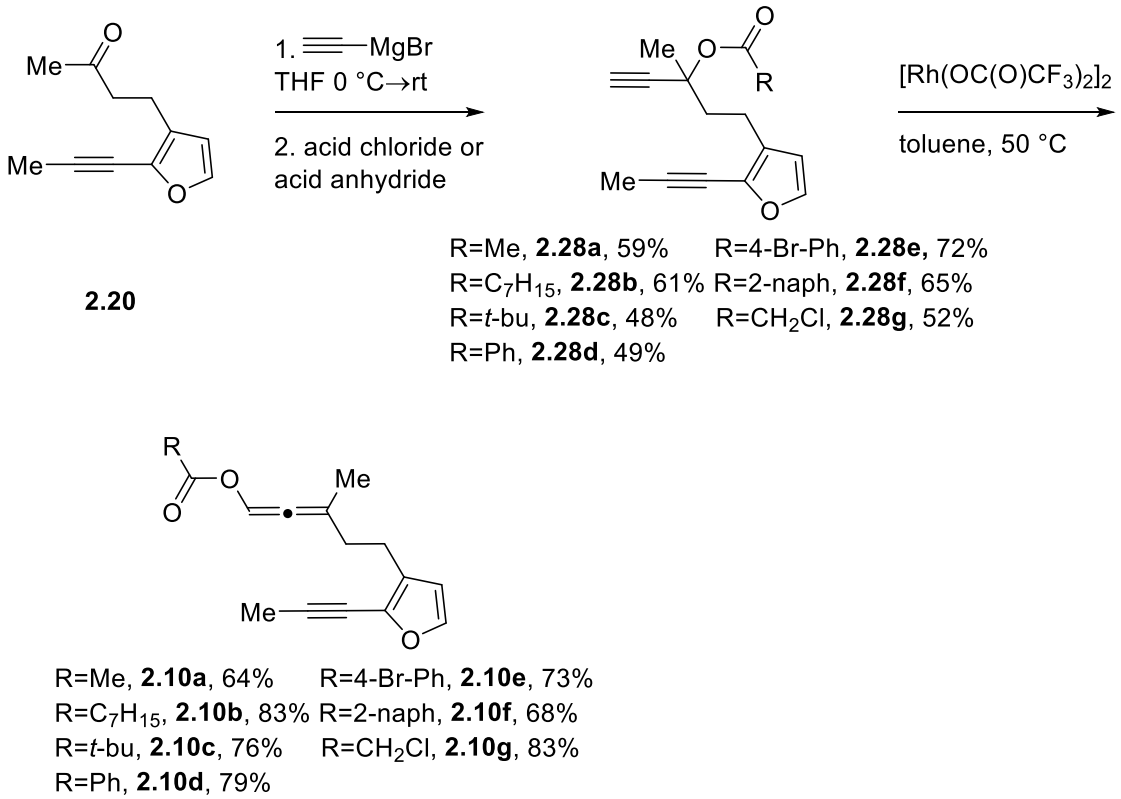

Scheme 17. Synthesis of allenyl carboxyesters

We synthesized allene-ynes **2.10a**-**2.10g** for the following reasons. The acetate group in **2.10a** would be used to benchmark the yield and enantiomeric ratios for the 5,7,5-ring systems against the 5,7-ring systems previously reported.[73] An octanoate group in **2.10b** is present in Tg. The pivalate group in **2.10c** is a bulky alkyl group that may afford a highly enantioenriched product. Benzoate containing allene-yne **2.10d** was selected due to high enantioselectivities previously seen in the asymmetric APKR of an allenyl benzoate substrate.[73] The chloroacetate in

2.10g was selected for its ease of hydrolysis of this group which would aid in the synthesis of Tg.[110]

2.3 Testing the feasibility of the APKR and optimizing the asymmetric APKR

We subjected allene-yne **2.10a** to the APKR conditions using triphenylphosphine (PPh_3) as a ligand, under carbon monoxide (1 atm, balloon) in DCE at 70 °C.[73] This reaction afforded the APKR adduct **2.11a** in 70% yield (Table 1, entry 1). When allene-yne **2.10a** was subjected to the asymmetric APKR with (*S*)-MonoPhos-alkene (**L1**) as ligand, the product was formed in 28% yield along with a side product, aldehyde **2.29** in 62% yield (Table 1, entry 2). We briefly examined different reaction conditions in an effort to increase the yield of the APKR product **2.11a** and decrease the formation of aldehyde **2.29**. Modifications to the CO concentration, solvent, temperature, and reaction concentration revealed that solvent concentration had the biggest impact on the yield of **2.11a**. For example, performing the APKR at higher dilution (0.01 M in DCE) afforded **2.11a** in 61% yield and aldehyde **2.29** in 21% yield (Table 1, compare entries 3 and 5). The enantioselectivity of the APKR was relatively unaffected by changes in reaction conditions when the reaction was performed in DCE. Performing the APKR in *o*-DCB afforded **2.11a** with an er of 74:26 (Table 1, entry 6).

Table 1. Optimization of the APKR of furanyl tethered allene-ynes

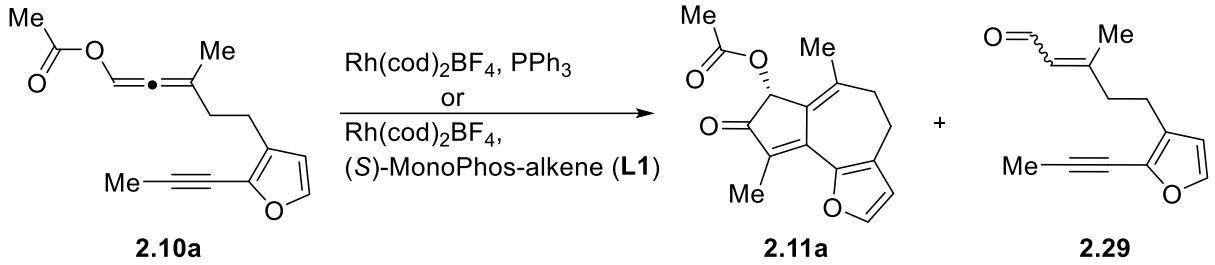

entry	ligand	CO atm (%)	temp (°C)	solvent	time (h)	conc (M)	product 2.11a yield (%)	er	aldehyde 2.29 yield (%)
1	PPh_3	100	70	DCE	4	0.02	70	-	0
2	L1	10	70	DCE	24	0.03	28	85:15	62
3	L1	100	70	DCE	4	0.03	36	83:17	26
4	L1	100	50	DCE	20	0.03	27	81:19	50
5	L1	100	70	DCE	20.5	0.01	61	82:18	21
6	L1	100	70	*o*-DCB	44	0.01	27 (34 brsm)	74:26	25 (31 brsm)

Adapted with permission from *Org. Lett.* 2022, 24, 4, 995–999. Copyright 2022 American Chemical Society.

With optimized conditions for the asymmetric APKR of furanyl tethered allene-ynes in hand, we examined allenyl carboxyesters **2.10b-g**. Allene-yne **2.10b** with an octanoate group afforded **2.11b** in 63% yield and 84:16 er (Scheme 18). Subjecting **2.10b** to the asymmetric APKR conditions with (*R*)-MonoPhos-alkene rather than (*S*)-MonoPhos-alkene afforded **2.10b** in 65% yield and 16:84 er with the C2 stereochemistry and carboxyester group present in Tg. Allene-yne **2.10c** with a bulky *t*-bu group afforded **2.11c** in 43% yield and 78:22 er, lower than those with less bulky alkyl groups. Allene-ynes having aryl groups (benzoate, **2.10d**; naphthoate **2.10e**; and 4-Br-benzoate, **2.10f**) afforded **2.11d**, **2.11e**, and **2.11f** in moderate yield with good enantioselectivities. Allene-yne **2.10g** containing a chloroacetate group afforded **2.11g** in 57% yield with a 97:3 er.

Due to the excellent enantioselectivity observed for this latter system, we scaled up this reaction to 95 mg, affording **2.11g** in 56% yield and a 90:10 er. We cannot explain the slightly lower enantioselectivity on this scale.

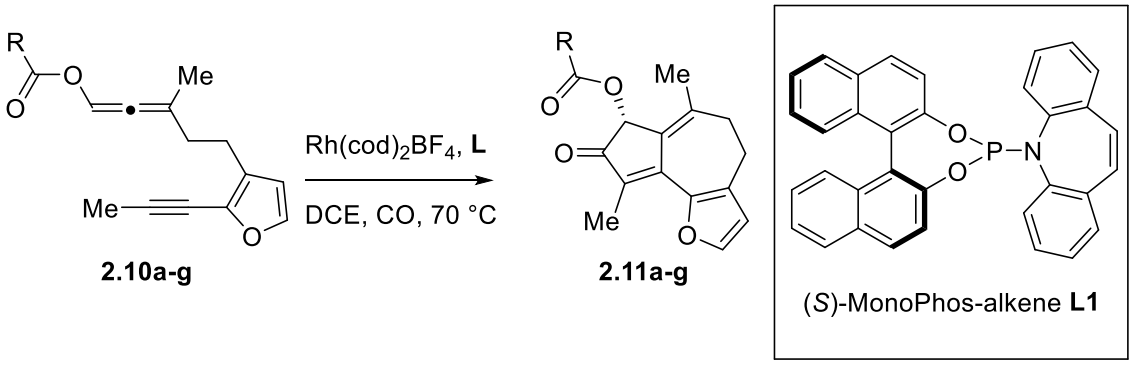

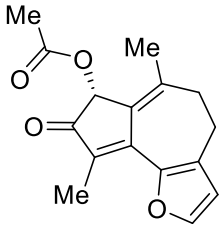

2.11a

L= PPh_3: 70%
L= **L1**: 61%, 82:18 er

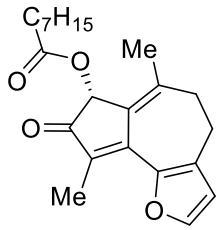

2.11b

L= PPh_3: 69%
L= **L1**: 63%, 84:16 er

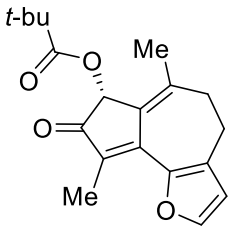

2.11c

L= PPh_3: 69%
L= **L1**: 43%, 78:22

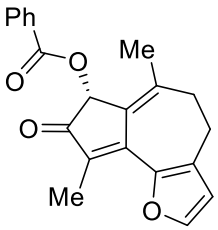

2.11d

L= PPh_3: 82%
L= **L1**: 55%, 93:7 er

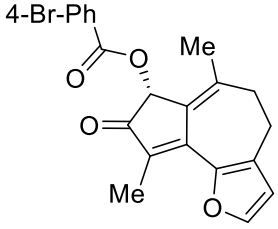

2.11e

L= PPh_3: 63%
L= **L1**: 46%, 84:16 er

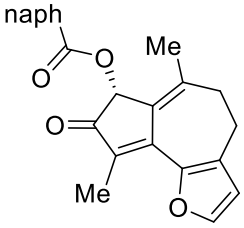

2.11f

L= PPh_3: 64%
L= **L1**: 42%, 90:10 er

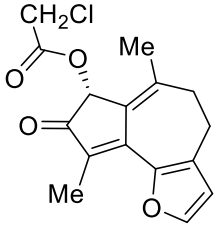

2.11g

L= PPh_3: 71%
L= **L1**: 57%, 97:3 er

Scheme 18. APKR of different carboxy ester groups

2.3.1 Computational results of the asymmetric APKR of furanyl tethered allene-ynes

We collaborated with the group of Professor Peng Liu to computationally understand the origin of the high enantioselectivity in the asymmetric APKR of allenyl chloroacetate **2.10g**. All DFT calculations were performed by Luke Jesikiewicz and Logan Newman at the M06/6-311+G(d,p)/SDD/SMD (DCE)//B3LYP/6-31G(d)/LANL2DZ level of theory. Calculations of **2.10g** show that TS1, the transition state leading to the major enantiomer of **2.11g**, is 3.5 kcal/mol lower in energy than TS2 (Figure 7). TS3, the transition state of the background reaction leading to racemic product with a rhodium metal containing three CO ligands and no phosphoramidite ligand, is 8.7 kcal/mol higher in energy than TS1. The difference in energies between TS1 and TS2 can be rationalized by a favorable π-π stacking between the furan ring and ligand in TS1 that does not occur in TS2 (Figure 8).

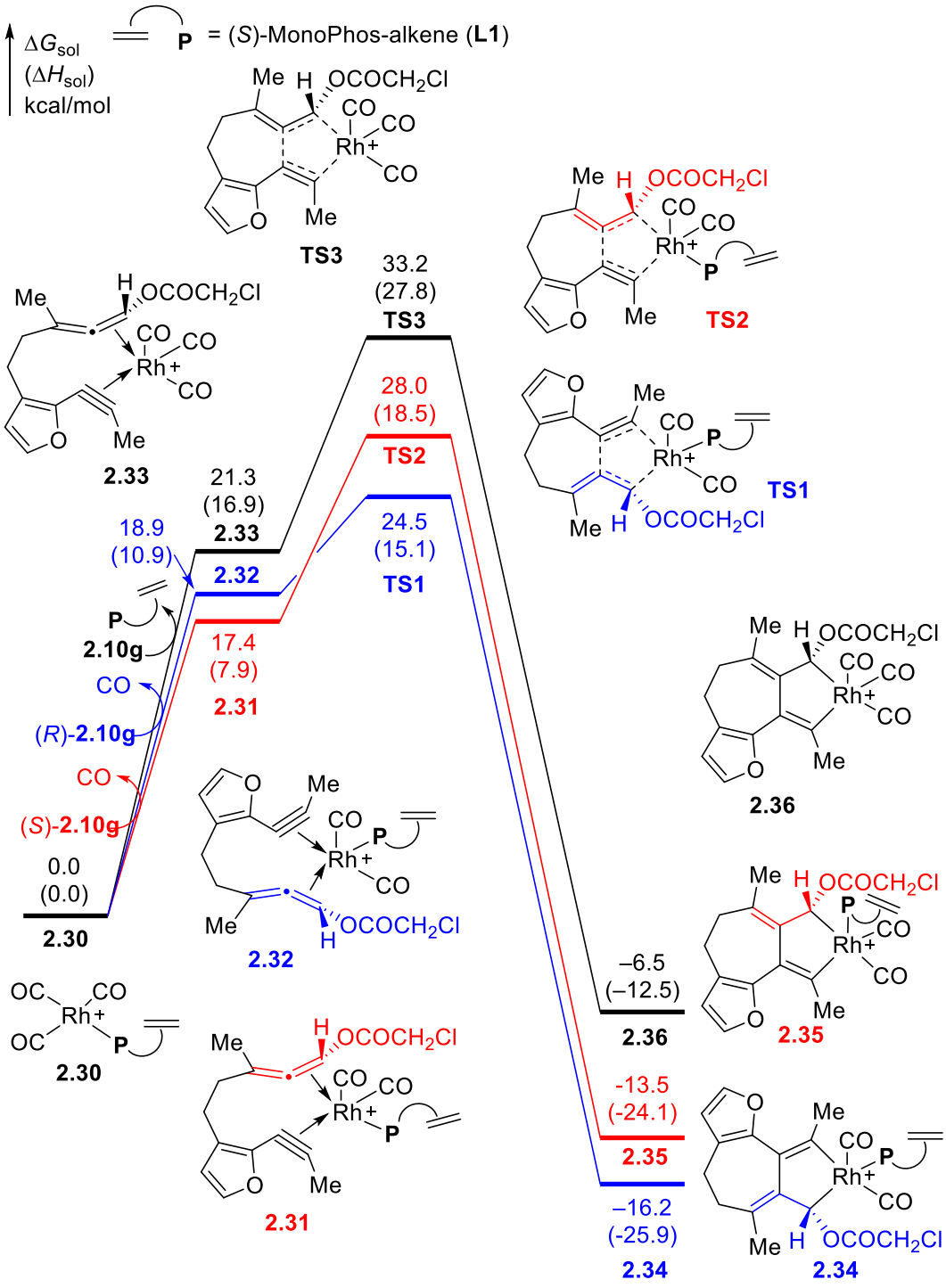

Figure 7. Enantioselectivity determining oxidative cyclization transition states for 2.10g

Adapted with permission from *Org. Lett.* 2022, 24, 4, 995–999. Copyright 2022 American Chemical Society.

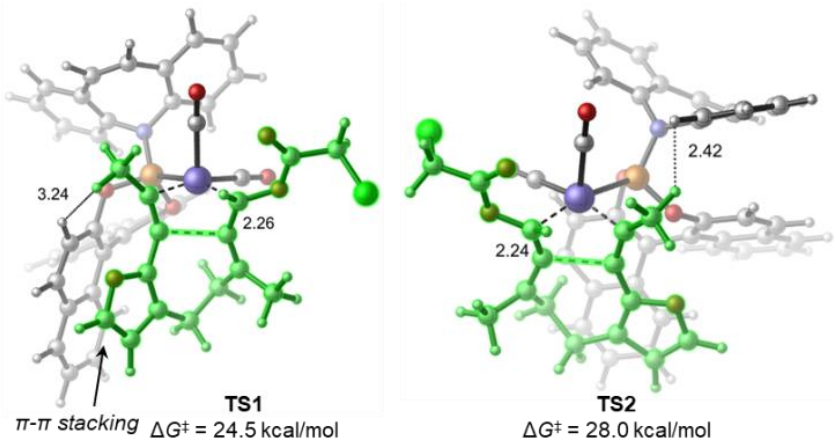

Figure 8. Transition state structures of chloroacetate 2.10g

Adapted with permission from *Org. Lett.* 2022, 24, 4, 995–999. Copyright 2022 American Chemical Society.

Calculations of **2.10a** show that TS4, the transition state leading to the major enantiomer of **2.11a**, is 3.9 kcal/mol lower in energy than TS5 (Figure 9). TS6, the transition state of the background reaction leading to racemic product with a rhodium metal containing three CO ligands and no phosphoramidite ligand, is 8.8 kcal/mol higher in energy than TS4. The greater energy differences between transition states for **2.10a** predict that the enantioselectivity of **2.11a** should be close to or greater than **2.11g**. The experimentally determined enantiomeric ratios are greater for **2.11g** than **2.11a** (97:3 versus 82:18) meaning there may be another transition state that has not been calculated that is important to this reaction. One possibility is that there is another background reaction catalyzed by a different active catalyst that is lower in energy than TS6 for **2.10a**. This lower energy transition state would cause erosion of enantioselectivity and lead to the experimentally observed enantioselectivities.

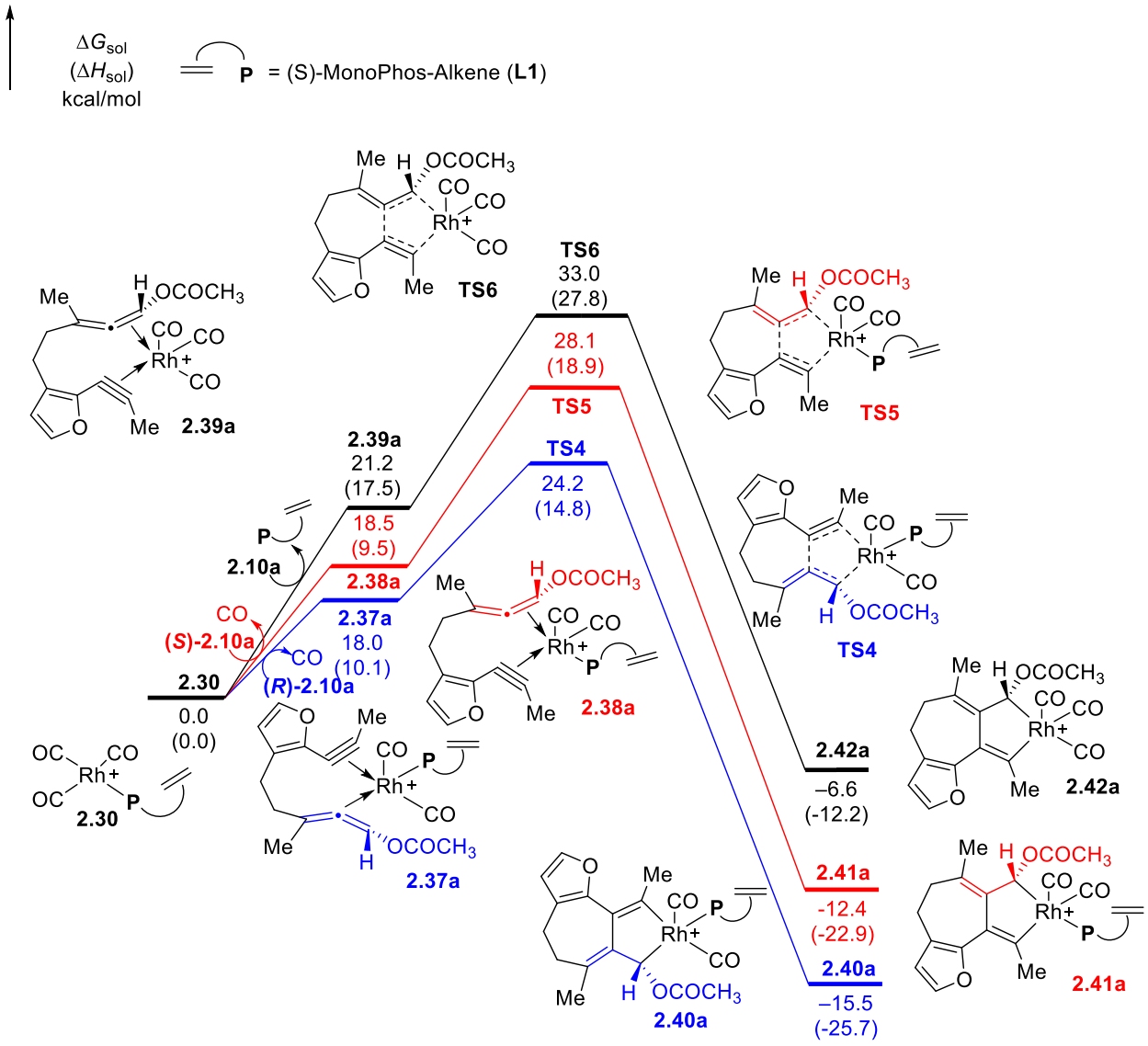

Figure 9. Enantioselectivity determining oxidative cyclization transition states for 2.10a

Adapted with permission from *Org. Lett.* 2022, 24, 4, 995–999. Copyright 2022 American Chemical Society.

2.3.2 NMR chemical shifts correlated to enantioselectivity

We compared the ^{13}C NMR chemical shift values of the proximal allene carbon of the allene-yne starting materials to the ΔG of the APKR. ΔG was calculated from the equation ΔG =

–RTln(*K*) where R is the gas constant, T is 70 °C, and *K* is the ratio of enantiomers. There was a low correlation when all 7 carboxyester groups, **2.10a-g**, were compared with an R^2 value of 0.7036 (Figure 10). When the alkyl and aromatic carboxyesters groups were compared separately, we saw good correlation with R^2 values of 0.9501 for alkyl carboxyester groups (Figure 11) and 0.9905 for aromatic groups (Figure 12). Substrates bearing alkyl carboxyester groups with proximal carbons with more downfield chemical shifts generally had higher er's. In contrast, substrates bearing aromatic carboxyester groups with proximal carbons with more upfield chemical shifts had higher er's. Despite the small sample size, the good correlation warrants additional investigation into whether ^{13}C NMR chemical shifts can be predictive of enantioselectivity in the APKR.

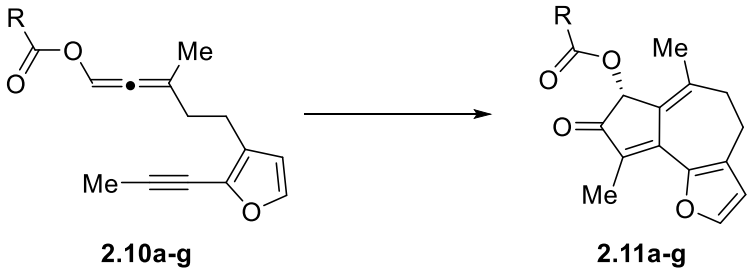

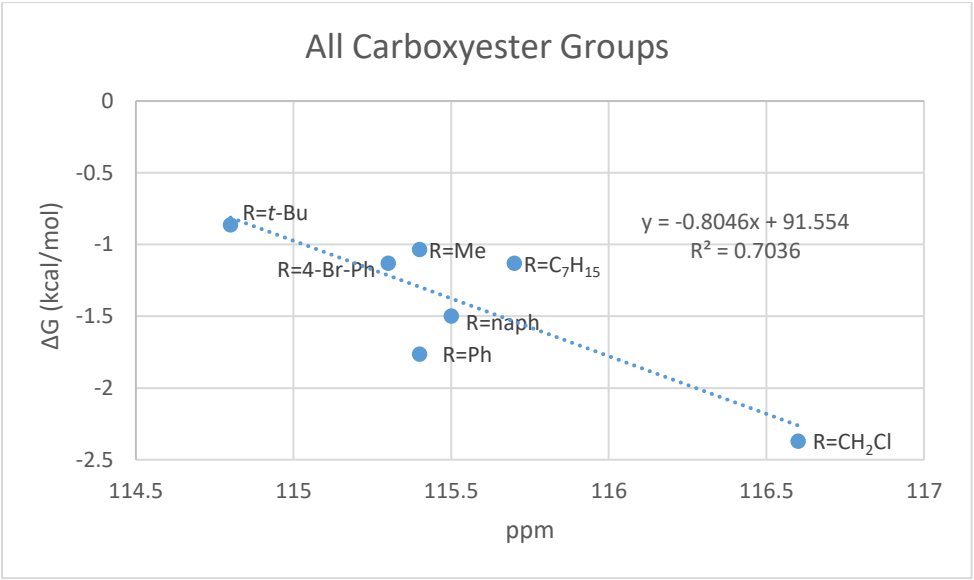

Figure 10. ^{13}C NMR chemical shift values vs $\Delta\Delta G^{\ddagger}$ for all carboxyester groups 2.10a-g

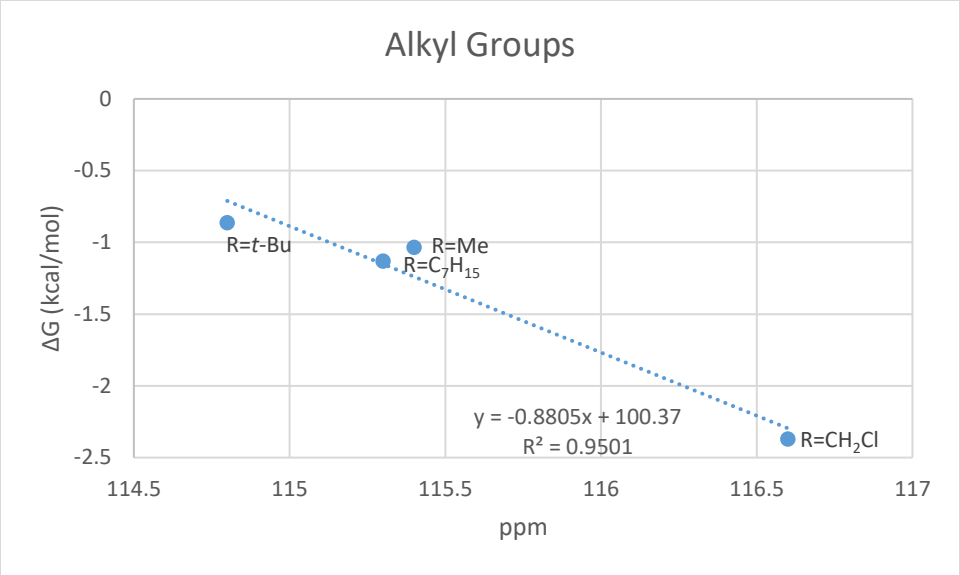

Figure 11. ^{13}C NMR chemical shift values vs $\Delta\Delta G^{\ddagger}$ for alkyl groups 2.10a-c and 2.10g

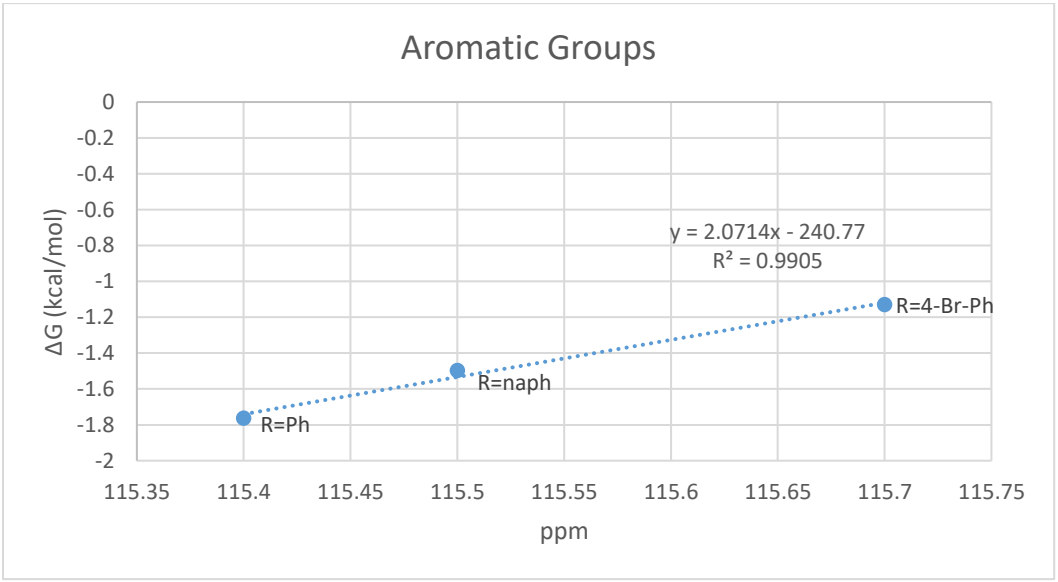

Figure 12. ^{13}C NMR chemical shift values vs $\Delta\Delta G^{\ddagger}$ for aromatic groups 2.10d-f

2.3.3 Hydrolysis of acyloxy cyclopentenones and determination of absolute stereochemistry

Computational results, as well as previous work on the asymmetric APKR, show that the *R* enantiomer is the predicted major enantiomer in the asymmetric APKR.[73] To confirm

stereochemistry, we grew an x-ray quality crystal of chloroacetate **2.11g** by slow diffusion in hexanes and DCM at 0 °C. X-ray analysis shows that the *R* enantiomer is the major enantiomer in the asymmetric APKR when (*S*)-MonoPhos-alkene is used (Figure 13).

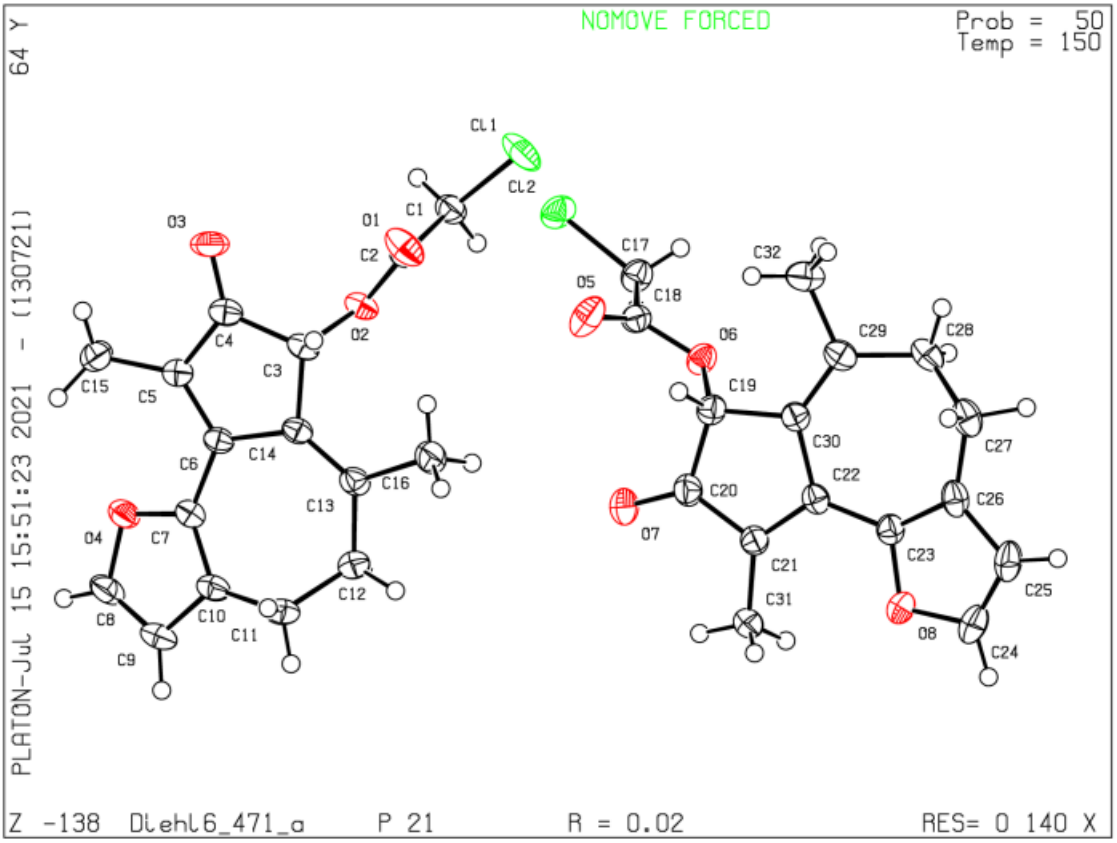

Figure 13. Thermal ellipsoid of 2.11g at 50% probability level

Adapted with permission from *Org. Lett.* 2022, 24, 4, 995–999. Copyright 2022 American Chemical Society.

We hypothesized that all of the substrates **2.10a-g** form the same major *R* enantiomer of products **2.11a-g**. To test this hypothesis, we hydrolyzed **2.11a**, **2.11d**, and **2.11g** using scandium triflate (Scheme 19).[111] Conditions developed by Hiyama and coworkers were used to hydrolyze acyloxy groups alpha to ketones while retaining stereochemistry. Hydrolysis of **2.11a**, **2.11d**, and **2.11g** afforded the same major enantiomeric product, alcohol **(*R*)-2.43** as determined by chiral

HPLC (Figure 14). We have assigned the absolute stereochemistry as the *R* enantiomer for **2.11b**, **2.11c**, **2.11e**, and **2.11f** by analogy.

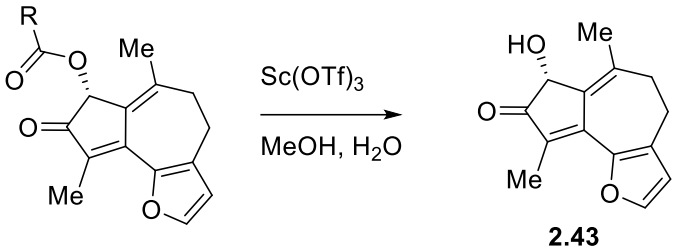

2.11a R=Me
2.11d R=Ph
2.11g R=CH_2Cl

2.43
R=Me, 50%
R=Ph, 33%
R=CH_2Cl, 67%

Scheme 19. Hydrolysis of APKR adduct

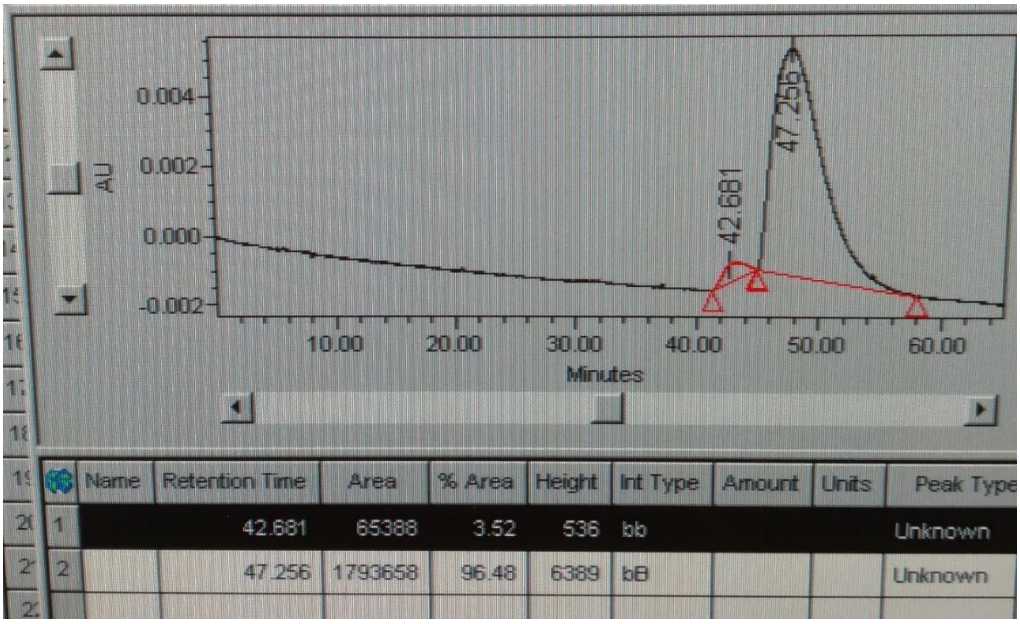

Figure 14. Chiral HPLC trace of 2.43 following hydrolysis of 2.11g

2.4 Synthesis of allene-ynes with different alkyne substituents

To determine the impact of the alkynyl group on yield and enantioselectivity in the asymmetric APKR of allene-ynes having a chloroacetate group, we synthesized three allene-ynes

having a phenyl, TMS, or a hydrogen group on the terminus of the alkyne in a manner similar to that used for allene-yne **2.10** in Scheme 17. Addition of phenylethynylmagnesium bromide to 3-furfural afforded propargyl alcohol **2.44**, which was subjected to an oxidative rearrangement to afford furaldehyde **2.45** in 75% yield (Scheme 20). **2.45** was reacted with acetone (10 equiv) and NaOH (0.4 equiv) to afford unsaturated ketone **2.46** in 77% yield. Using less acetone (2.5 equiv) resulted in **2.46** and the bis-aldol adduct **2.47**. Bis-aldol adduct **2.47** and unsaturated ketone **2.46** were not separable by column chromatography, so **2.47** was assigned via ^{1}H and ^{13}C NMR as the mixture. Evidence for **2.47** was supported by resonances at 7.77, 7.60-7.56, 6.91, and 6.68 ppm and lack of a methyl ketone singlet resonance at 2.38 ppm in the ^{1}H NMR. The ^{13}C NMR contains a carbonyl carbon at 188.5 ppm and no methyl ketone signal at 27.6 ppm.

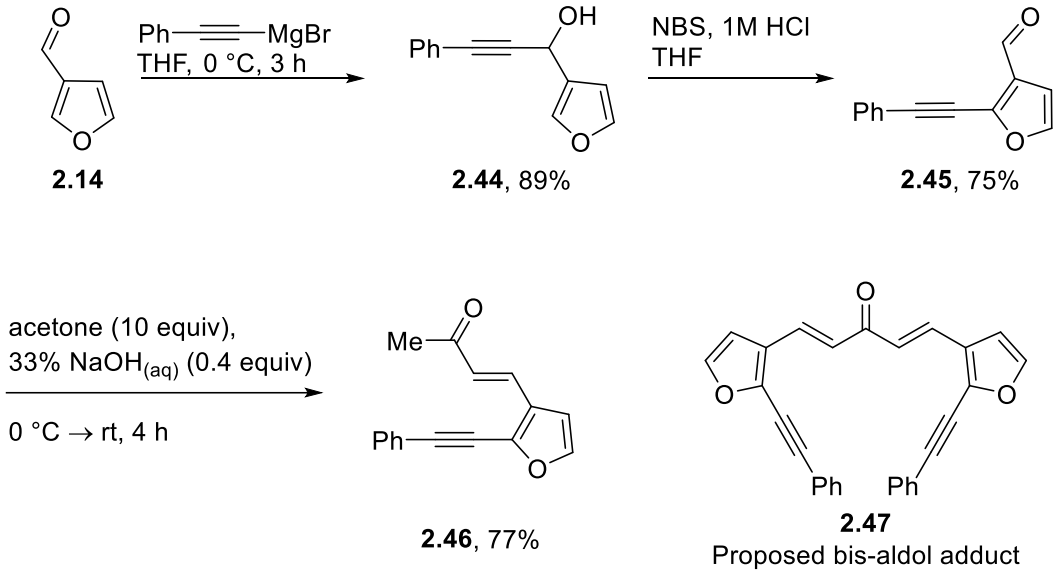

Scheme 20. Synthesis of Phenyl substituted alkyne substrate

Addition of the lithium trimethylsilyl acetylide to 3-furfural afforded propargyl alcohol **2.48** in 81% yield (Scheme 21). **2.48** was subjected to an oxidative rearrangement (NBS, H_2O) to afford furaldehyde **2.49** in 77% yield. Subjecting furaldehyde **2.49** to NaOH and acetone gave the desilylated alkyne **2.51** in 67% yield (Scheme 22). To access the desired TMS substituted alkyne,

furaldehyde **2.49** was subjected to a Horner-Wadsworth-Emmons reaction using dimethyl-2-oxopropyl phosphonate and cesium carbonate to afford unsaturated ketone **2.50** in 77% yield.

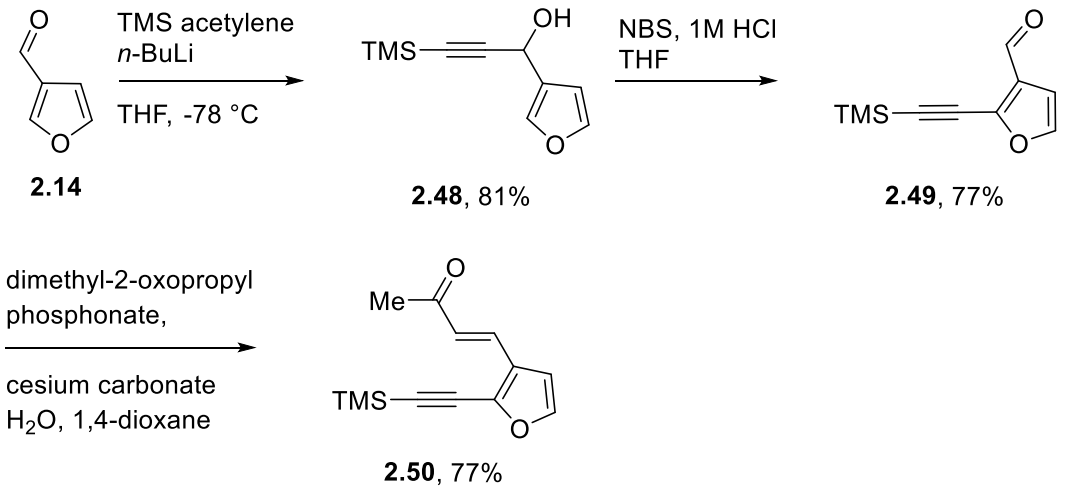

Scheme 21. Synthesis of TMS substituted alkyne substrate

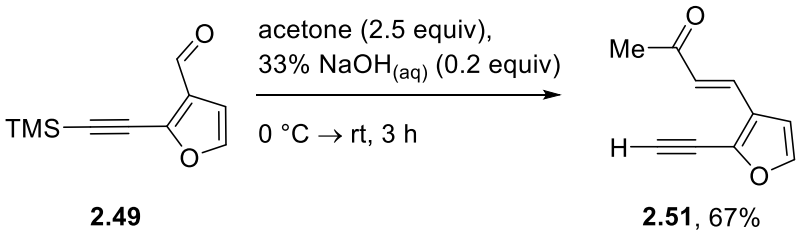

Scheme 22. Synthesis of terminal alkyne substrate

With unsaturated ketones **2.46**, **2.50**, and **2.51** in hand, we performed a 1,4-reduction using Hantzsch ester **2.27** and silica gel in refluxing toluene to afford saturated ketones **2.52a-c** (Scheme 23). Addition of ethynylmagensium bromide and trapping with chloroacetyl chloride in a one-pot procedure afforded propargyl chloroacetates **2.53a-c**. The chloroacetyl group was selected due to the high enantioselectivities seen in the APKR previously in the case of methyl substituted alkyne **2.10g**. Propargyl chloroacetates **2.53a-c** were then subjected to a rhodium catalyzed rearrangement to afford allenyl chloroacetates **2.54a-c**.

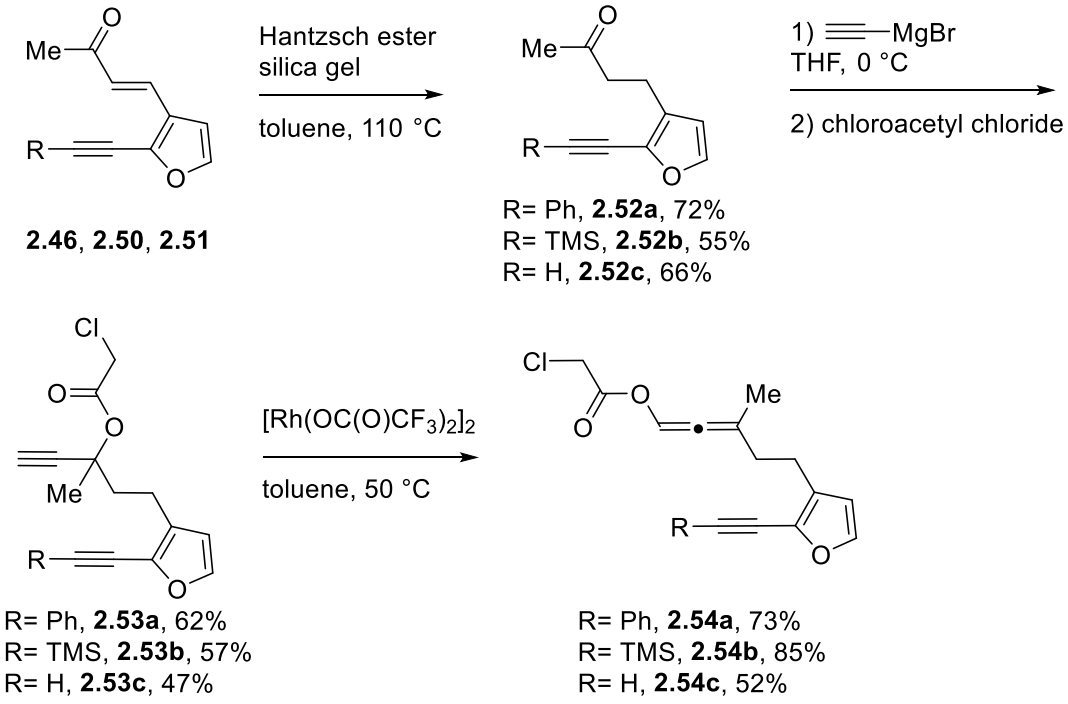

Scheme 23. Synthesis of allenyl chloroacetates with different alkynes

Subjecting allene-yne **2.54a** having a phenyl group on the terminus of the alkyne to the asymmetric APKR afforded **2.55a** in 59% yield with an excellent er of 99:1, the highest enantioselectivity of an asymmetric APKR to date (Scheme 24). Allene-yne **2.54b** containing a TMS group on the terminus of the alkyne afforded **2.55b** in moderate yields under both racemic and asymmetric conditions. The APKR of terminal alkyne **2.54c** afforded product **2.55c** in low yields under racemic and asymmetric conditions. The er's for both the TMS containing and terminal alkyne substrates **2.55b** and **2.55c** were both low relative to the chloroacetate containing substrates with methyl or phenyl substituted alkynes. We believe in the case of **2.55c** that this is due to the terminal alkyne reacting with the rhodium catalyst as evidenced by lower than expected ^{1}H NMR integrations for this hydrogen in the crude NMR. These low er's show that the chloroacetate group is not a group that will result in high enantioselectivities for all substrates, and other factors than the carboxyester group can influence the er of the asymmetric APKR.

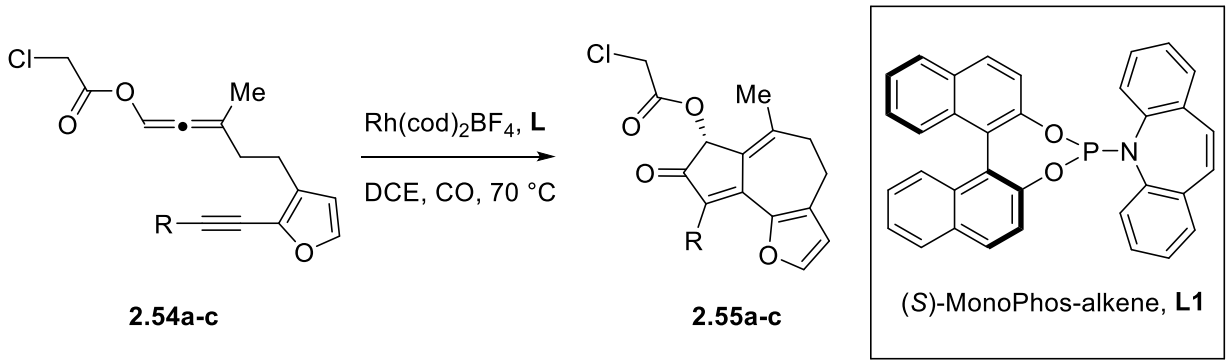

2.54a-c **2.55a-c**

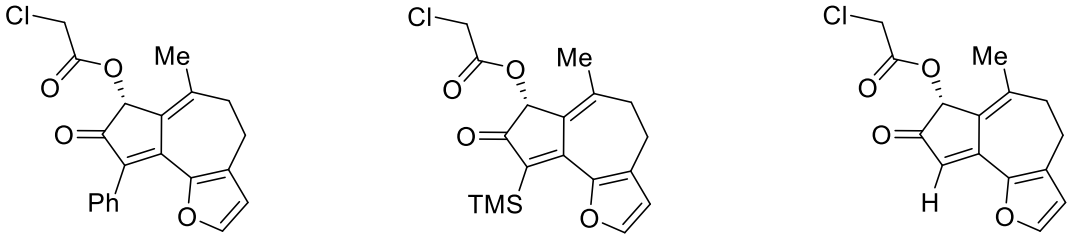

2.55a **2.55b** **2.55c**

L= PPh_3: 59%
L= **L1**: 46%, 99:1 er

L= PPh_3: 45%
L= **L1**: 48%, 78:22 er

L= PPh_3: 32%
L= **L1**: 32%, 77:23 er

Scheme 24. APKR results for different alkynes

2.5 Benzene tethered allene-yne in the APKR

To investigate the impact of the tether on the asymmetric APKR, a benzene ring tethered allen-yne was investigated (Scheme 25). Starting with 2-bromobenzaldehyde **2.56**, we performed a Sonogashira coupling with 1-propyne to afford alkyne **2.57** in 74% yield.[112] Reacting **2.57** with acetone and NaOH afforded unsaturated ketone **2.58** in 76% yield. Unsaturated ketone **2.58** was reacted with Hantzsch ester **2.27** in refluxing toluene to afford the saturated ketone product **2.59** in 77% yield. Addition of ethynylmagnesium bromide to ketone **2.59** afforded the corresponding propargyl alkoxide that was trapped with chloroacetyl chloride in a one-pot procedure to afford

propargyl chloroacetate **2.60** in 76% yield. Propargyl chloroacetate **2.60** was reacted with $[Rh(OC(O)CF_3)_2]_2$ to afford allene-yne **2.61** in 85% yield.

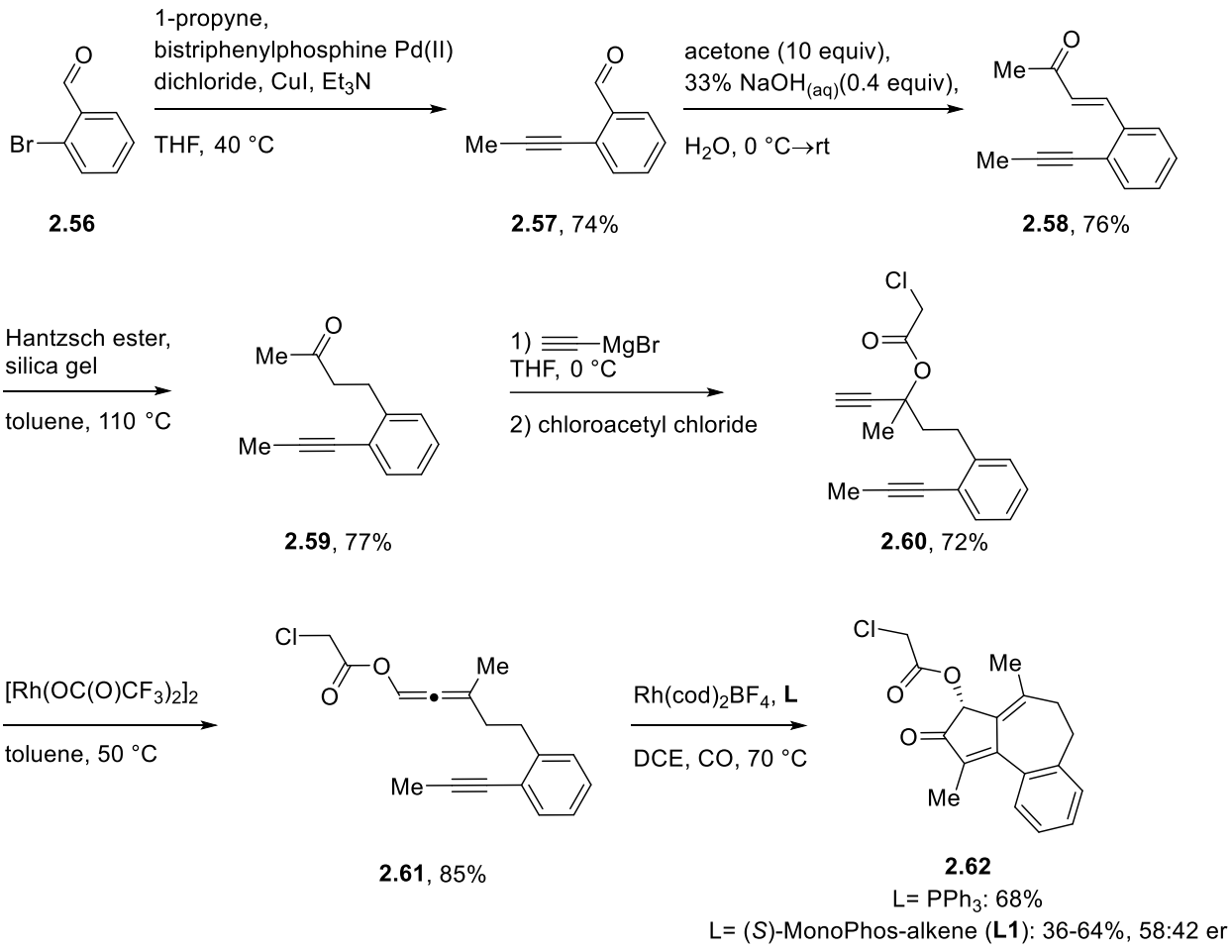

Scheme 25. Synthesis of benzene tethered allene-yne

With allene-yne **2.61** in hand, we next sought to investigate the effect of the benzene tether on the APKR. Performing the APKR with $Rh(cod)_2BF_4$ and PPh_3 afforded racemic **2.62** in 68% yield. Performing the asymmetric APKR with the optimized conditions for the furanyl-based systems ($Rh(cod)_2BF_4$, (*S*)-MonoPhos-alkene, 0.01M in DCE) gave inconsistent yields of the APKR adduct ranging from 36-64% over three runs. The er of the reaction was consistent with an average of 58:42. These results show that the furanyl ring is playing a role in the high

enantioselectivity of the asymmetric APKR. We postulate that the low er in the APKR of **2.61** is due to a developing $A^{1,3}$ interaction between a hydrogen of the phenyl ring and the methyl group of the alkyne in the transition state of the enantiodetermining oxidative cyclization (Figure 15).

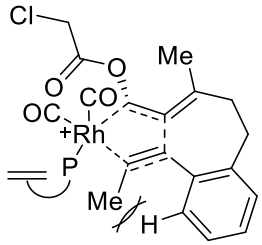

Figure 15. Destabilizing $A^{1,3}$ interaction in the oxidative cyclization transition state of 2.61 in the APKR

2.6 Isolation of an indene byproduct in the synthesis of a furanyl tethered allene-yne

Next, we investigated the impact of the substitution pattern of the furanyl tethered allene-yne by exploring a substrate with the alkyne at the 3-position of the furan and the allenyl group at the 2-position. 3-Bromofuran-2-carbaldehyde **2.63** was reacted with 1-propyne in THF to afford **2.64** in 95% yield (Scheme 26). **2.64** was reacted with acetone to give the unsaturated ketone **2.65** in 80% yield. **2.65** was subjected to conjugate reduction conditions using Hantzsch ester **2.27** in refluxing toluene to afford ketone **2.66** in 66% yield. Addition of ethynylmagnesium bromide to ketone **2.66** afforded the corresponding propargyl alkoxide that was trapped in situ with chloroacetyl chloride providing propargyl chloroacetate **2.67** in 63% yield.

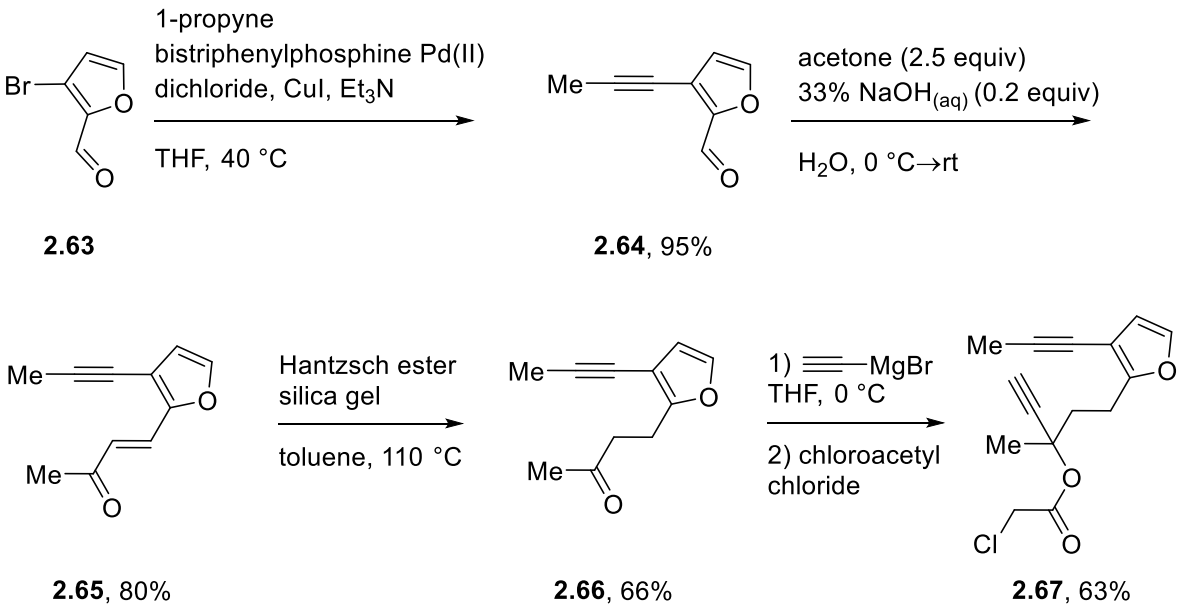

Scheme 26. Synthesis of a furan substrate with an allene at the 2-position

Attempts to convert propargyl chloroacetate **2.67** into allenyl chloroacetate **2.68** using our standard conditions ($[Rh(OC(O)CF_3)_2]_2$ in toluene at 50 °C for 23.5 h) did not give the desired allenyl chloroacetate (Scheme 27). Instead, a byproduct was obtained whose structure was confirmed as indene product **2.70** via x-ray crystallography (Figure 16). We propose that **2.70** is formed via a multi-step process involving an intramolecular Diels-Alder reaction of intermediate **2.68** to afford oxanorbornene **2.69** followed by rhodium catalyzed ring opening and aromatization.[113, 114] The transition-metal catalyzed ring opening of oxanorbornenes is a well-known process.[115] Stopping the reaction at 2 h, before all starting material was consumed, resulted in a 23% recovery of starting material **2.67** and 34% yield of a mixture of allene **2.68** and a byproduct that is possibly oxanorbornene **2.69** in a 1:0.15 ratio.

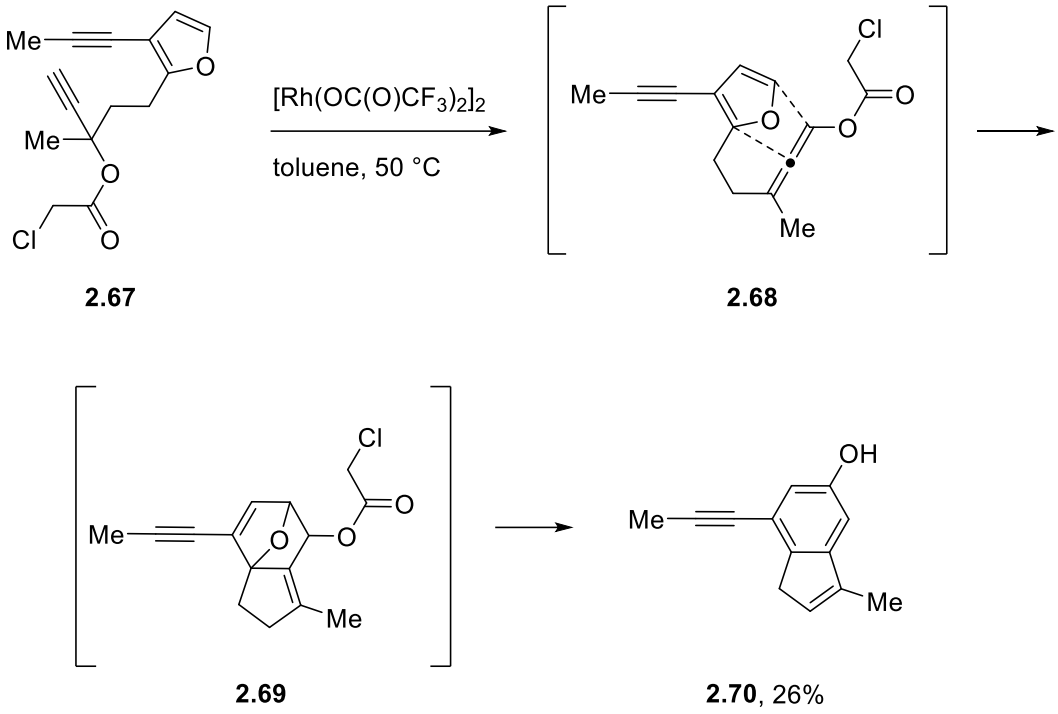

Scheme 27. Possible mechanism of indene byproduct 2.70 formation

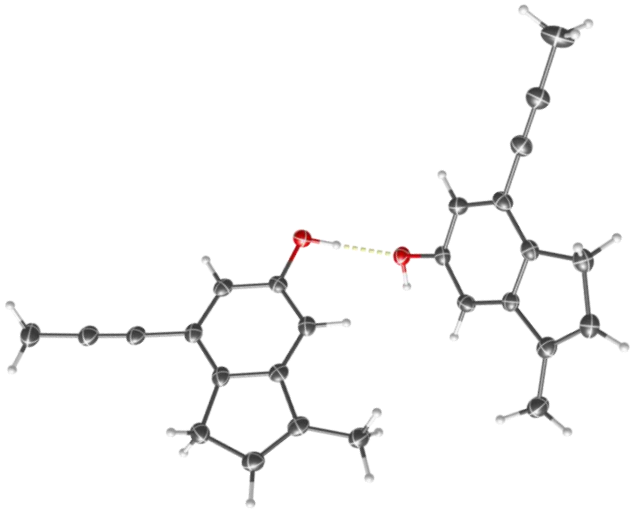

Figure 16. X-ray crystal structure of indene byproduct 2.70

We attempted to catalyze the rearrangement of the propargyl chloroacetate with transition metal catalysts other than rhodium to obtain the desired allenyl chloroacetate. To this end, we tested several different metals in this rearrangement reaction including $AuCl_3$, $PtCl_2$, and

$AgSbF_6$.[63, 116-118] Reacting **2.67** with $PtCl_2$ in toluene at room temperature for 94 h or $AgSbF_6$ in DCM at room temperature for 23 h afforded recovered starting material and decomposition byproducts. The reaction with $AuCl_3$ in toluene at room temperature afforded some product after 23 h, but the reaction appeared to stop progressing after just a few hours according to NMR aliquots. Due to the inability to selectively synthesize the desired product we did not pursue this allene-yne substrate further.

2.7 Probing the mechanism for the formation of aldehyde byproduct 2.29

To control the diverging reactivity of the allene-yne to favor the formation of the APKR product, we sought to understand the mechanism for the formation of aldehyde byproduct. We hypothesized that the rhodium catalyst was responsible for aldehyde formation. To test this hypothesis, we subjected **2.10a** to the APKR conditions excluding the rhodium catalyst. After 19.5 h, starting material was recovered with no evidence of aldehyde **2.29** by ^{1}H NMR (Scheme 28, entry a). Performing the reaction in the presence of the rhodium catalyst under a nitrogen atmosphere and furfuryl alcohol (1.0 equiv) afforded aldehyde **2.29** in 50% yield (Scheme 28, entry b). Furfuryl alcohol was added to trap the acetyl group but the corresponding acetylated product was not observed by ^{1}H NMR of the crude reaction mixture. These results provide evidence that the rhodium catalyst is essential for the formation of aldehyde **2.29**.

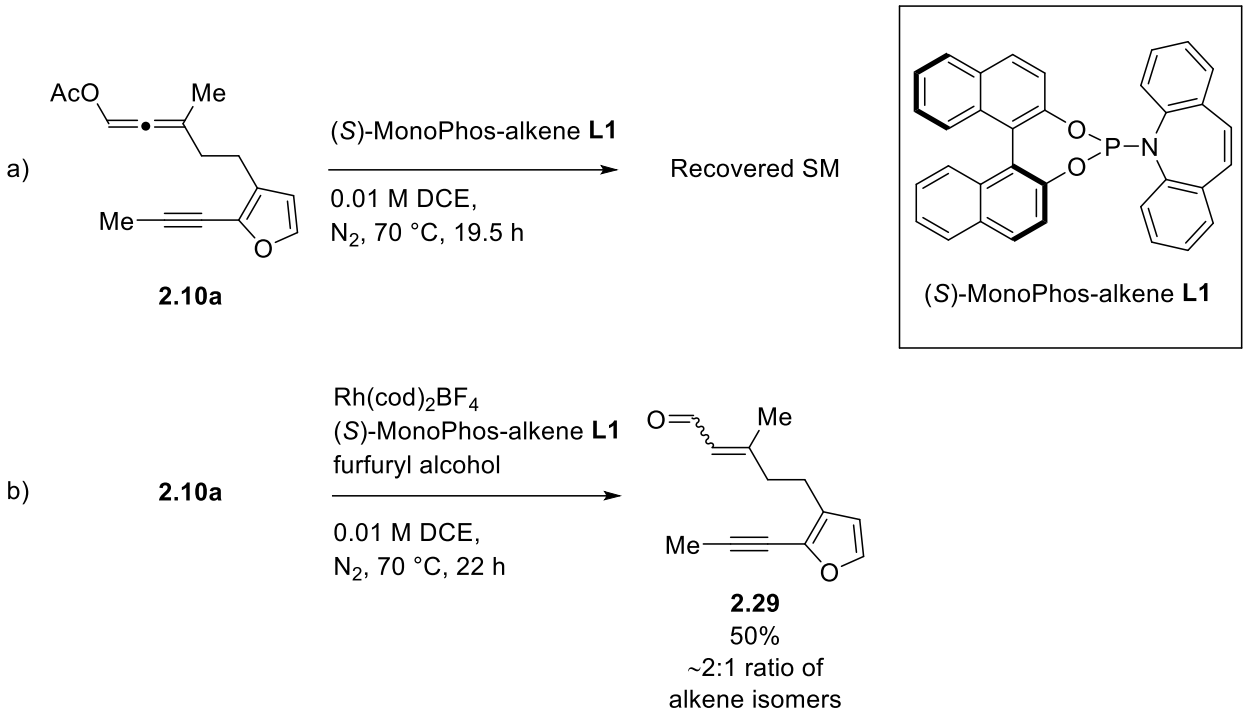

Scheme 28. Probing the mechanism of aldehyde 2.29 formation

To investigate the formation of aldehyde byproduct on a substrate that would not participate in the APKR, allene **2.73** was prepared which lacked the alkynyl group. Addition of ethynylmagnesium bromide to 2-octanone (**2.71**) followed by trapping with acetyl chloride afforded propargyl acetate **2.72** in 67% yield (Scheme 29). Reaction of propargyl acetate **2.72** to a rhodium catalyzed rearrangement afforded allenyl acetate **2.73**.

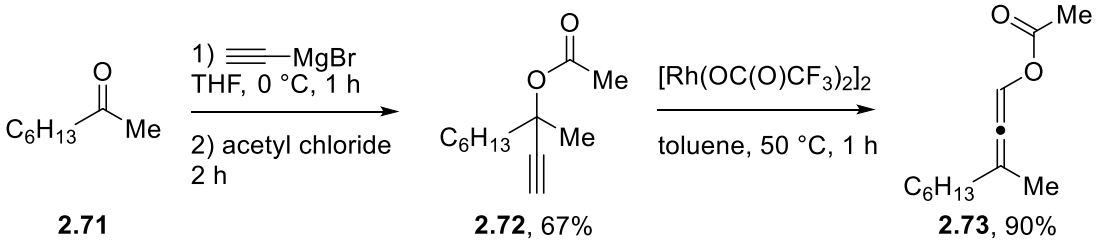

Scheme 29. Synthesis of a model allene substrate

With model allenyl acetate **2.73** in hand, we subjected it to the asymmetric APKR conditions in the presence of 5 equiv of D_2O (Scheme 30). Aldehyde **2.74** was obtained in 44% isolated yield along with **2.74-D**. The ratio of **2.74**:**2.74-D** was determined to be 75:25

corresponding to a 25% deuterium incorporation. The percent deuterium incorporation was based on the integration of the signal for the alkenyl resonance alpha to the aldehyde at 5.87 ppm relative to signals at 2.16 and 1.97 ppm in the ^{1}H NMR spectrum. The aldehyde signals for **2.74-D** show evidence of deuterium incorporation as the resonances at 9.99 and 9.95 ppm appear as singlets whereas the resonances for **2.74** appear as doublets at 9.99 (d, J = 8.4 Hz) and 9.95 (d, J = 8.0 Hz) ppm (Figure 17). This result shows that adventitious water may play some role in the hydrolysis of the allenyl acetate. However, an alternative mechanism must be operating as an excess of deuterium oxide gave only 25% deuterium incorporation. A possible mechanism for formation of **2.74-D** is shown in Scheme 31.

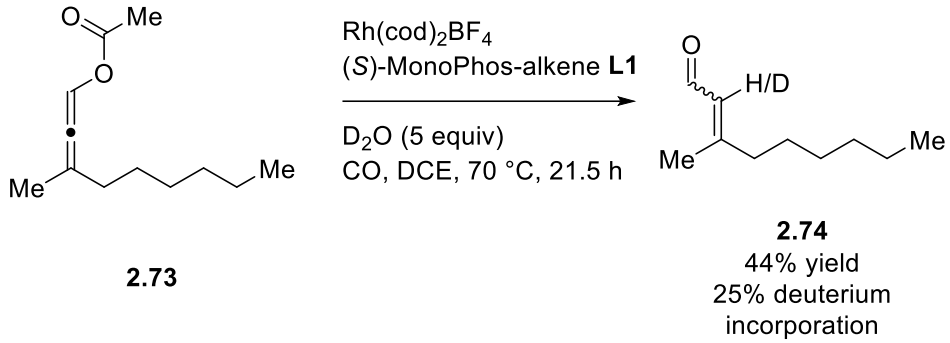

Scheme 30. APKR conditions for aldehyde synthesis from a model allene

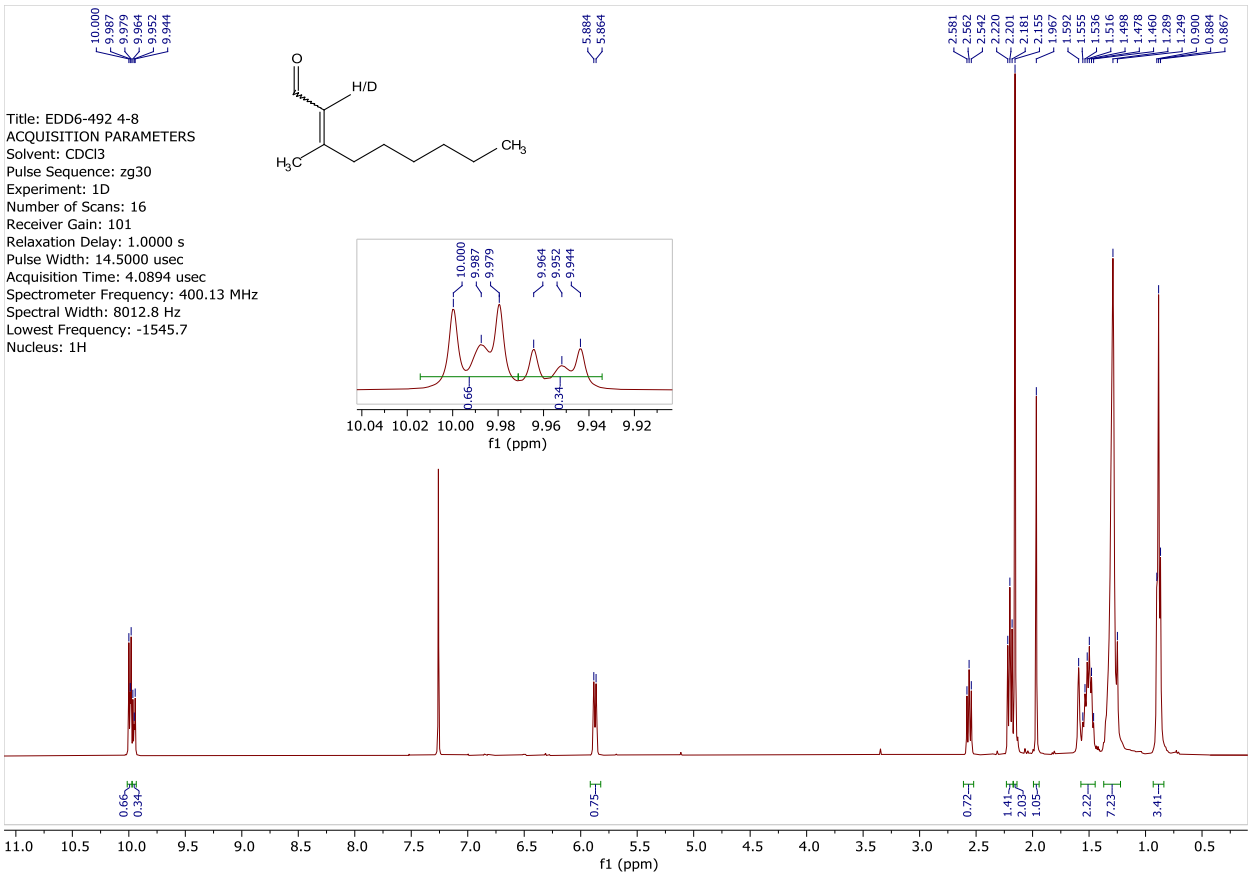

Figure 17. NMR spectrum of 2.74-D

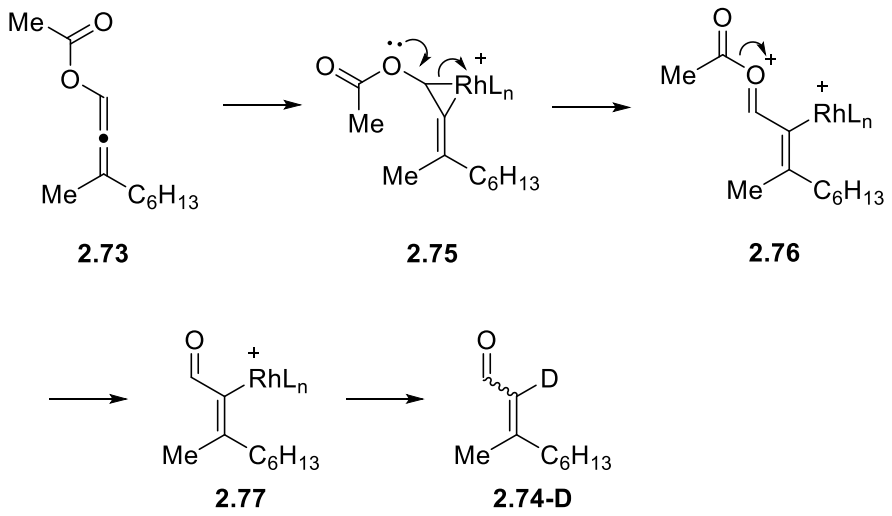

Scheme 31. Proposed mechanism of aldehyde formation and incorporation of deuterium

2.8 Hydroxyl-directed hydrogenation of the C1-C10 double bond

With an eye towards the synthesis of Tg and biologically active Tg analogues, we set out to selectively reduce the C1-C10 double bond of APKR adduct **2.11** and gain access to a 3-dimensional core resembling Tg. Because the facial selectivity of transition metal catalyzed hydrogenations can in principle be directed by a Lewis basic group, we focused our efforts on this reduction strategy having the C2 group serve as a directing group.[119] This strategy takes advantage of the C2 stereochemistry afforded by the asymmetric APKR. Moreover, this C2 group can be transformed into a variety of Lewis basic groups that have been used successfully in directed hydrogenation reactions, such as hydroxyl, amide, carbamate, and ester groups.[120, 121] One of the most common catalysts for directed hydrogenations is $[C_8H_{12}IrP(C_6H_{11})_3C_5H_5N]PF_6$ (Crabtree's catalyst).[83] This cationic 16-electron complex allows the directing group to coordinate to the metal center and direct the hydrogen to the same face of the alkene as the directing group.

Substrate **2.43** was selected over **2.11a-g** because a hydroxyl group, in some cases, serves as a better directing group than a carboxyester group.[120] We face a few challenges in this directed hydrogenation strategy of substrate **2.43**: 1) chemoselectivity may be an issue as there are three other carbon-carbon double bonds in **2.43**; 2) C1-C10 is tetrasubstituted and conjugated to an enone system, making it less reactive.

Reacting **2.43** with Crabtree's catalyst in DCM under a balloon of hydrogen at room temperature gave no reaction after 2 h (Scheme 32). Performing the same experiment using degassed (freeze-pump-thaw) DCM gave only recovered starting material after 24 h. A control experiment was performed to test the quality of Crabtree's catalyst by reacting 3-methyl-2-buten-1-ol **2.79** to the same reaction conditions. After 18 h, the reaction mixture was filtered through a plug of silica to afford the hydrogenated product **2.80** as evidenced by the disappearance of the

vinyl proton resonance. While a yield was not obtained, this result supports that our reaction protocol using Crabtree's catalyst was effective at hydrogenating allylic alcohol containing substrates. Investigations using the Crabtree catalyst under more forcing conditions to reduce the relatively inert alkene of **2.43** will be performed by Fatemeh Haghighi in the group.[122]

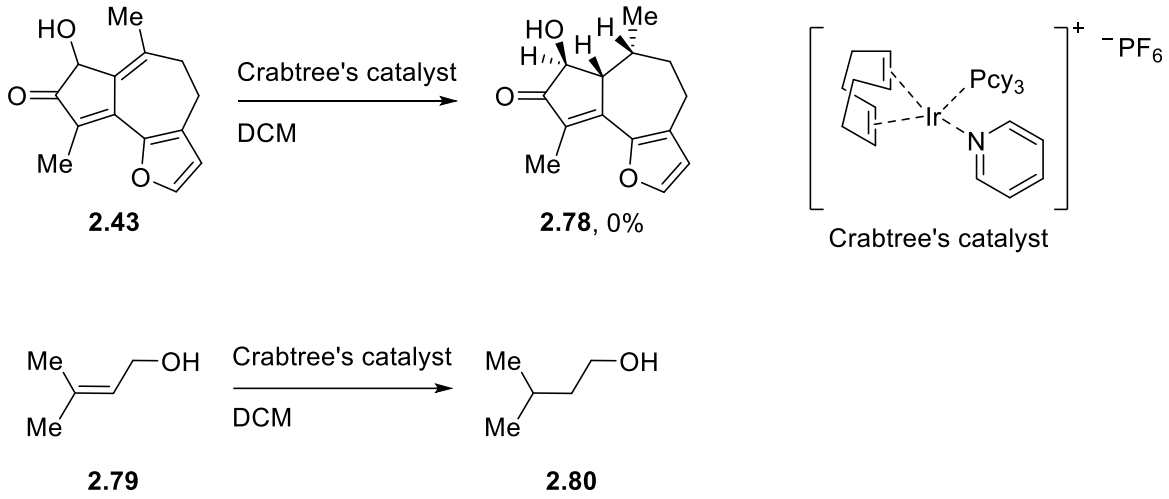

Scheme 32. Hydrogenation using Crabtree's catalyst

Due to the inability of Crabtree's catalyst to reduce the C1-C10 double bond of **2.43**, we investigated other catalysts to affect this transformation. Pd/C has been used previously to hydrogenate similar tetrasubstituted alkenes formed via the APKR and, in some cases, has been directed by hydroxyl groups.[123-125] Reacting **2.43** with 10% Pd/C (0.1 equiv) in a 4:1 methanol:ethyl acetate solvent system under a hydrogen atmosphere for 30 minutes resulted in a complex mixture of products, none of which appeared to be the desired product based upon disappearance of the furanyl resonances in the crude ^{1}H NMR. Pd/$BaSO_4$ has been used previously on similar tetrasubstituted alkenes.[126] Reacting **2.43** with Pd/$BaSO_4$ in ethyl acetate under a hydrogen atmosphere resulted in complete recovery of starting material after 20 h.

Next, we investigated the effect of solvent on the palladium catalyzed hydrogenation. Reacting **2.43** with 10% Pd/C in ethyl acetate under a hydrogen atmosphere afforded the desired

product **2.78** in 44% yield and approximately 1.4:1 dr (Scheme 33). The major diastereomer was assigned as the directed product via ^{1}H NMR coupling constants of the hydrogen alpha to the ketone. The coupling constant for H_a is 4.0 Hz and H_b is 7.0 Hz. Reported coupling constants for cyclopentenones are 2.2 Hz for *trans* hydrogens and 7.2 Hz for *cis* hydrogens.[127]

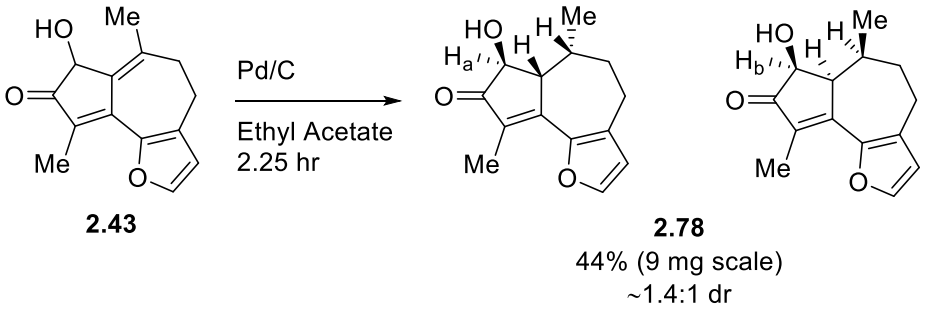

2.43

2.78
44% (9 mg scale)
~1.4:1 dr

Scheme 33. Hydrogenation of 2.43 using Pd/C

2.9 Conclusions

We have shown that furanyl tethered allene-ynes are tolerated in the asymmetric APKR, affording good yields and high enantioselectivities. The origin of the high enantioselectivities arises from a favorable π-π stacking between the furan ring and binap group of the phosphoramidite ligand according to computation. Allenyl chloroacetates afford high enantioselectivities in substrates bearing methyl and phenyl substituted alkynes. The moderate yielding asymmetric APKR is attributed to the propensity of the allenyl carboxy groups to form an aldehyde byproduct under the APKR reaction conditions. Performing the APKR under dilute conditions favors the formation of APKR product **2.11** over aldehyde **2.29**. We attribute this to the APKR being an intramolecular process while it is an intermolecular process that leads to aldehyde formation. A

hydroxyl directed hydrogenation of the APKR adduct using Crabtree's catalyst afforded no reaction. Using Pd/C for this hydrogenation worked with some diastereoselectivity.

Supporting Information

General Methods

All commercially available compounds were purchased and used as received unless otherwise noted. Tetrahydrofuran (THF), diethyl ether (Et_2O), and dichloromethane (DCM, CH_2Cl_2) were purified by passing through alumina using a Sol-Tek ST-002 solvent purification system. Toluene was purified by distilling from calcium hydride. Acetone was purified by refluxing over, and distillation from, $KMnO_4$ and stored over 4 Å molecular sieves. *o*-DCB was degassed using freeze-pump-thaw method (3x). Triphenylphosphine was purified by recrystallization with ethanol. Carbon monoxide (>99.99%) and 10% carbon monoxide in argon were purchased from Matheson. $33\%_{(w/w)}$ NaOH was prepared by dissolving NaOH in water. Purification of the compounds by flash column chromatography was performed using silica gel (40-63 μm particle size, 60 Å pore size). TLC analyses were performed on silica gel F254 glass plates (250 μm thickness). ^1H and ^{13}C NMR spectra were recorded on Bruker Avance 300, 400, or 500 MHz spectrometers. Spectra were referenced to residual chloroform (7.26 ppm, ^1H NMR; 77.16 ppm, ^{13}C NMR). Chemical shifts are reported in ppm, multiplicities are indicated by s (singlet), d (doublet), t (triplet), q (quartet), p (pentet), and m (multiplet). Coupling constants, *J*, are reported in hertz (Hz). All NMR spectra were obtained at rt. IR spectra were obtained using a Nicolet Avatar E.S.P. 360 FT-IR or Perkin Elmer Spectrum Two FT-IR. ESI mass spectrometry was performed on a Waters Micromass GCT high resolution mass spectrometer, while ES mass spectrometry was performed on a Waters Q-TOF Ultima API, Micromass UK Limited high resolution mass spectrometer. Chiral HPLC was performed on a Waters 600 HPLC using a Waters

996 photodiode array detector using a Chiralcel OD chiral column or ChiralPak IA-3 chiral column. All microwave reactions were carried out using a Biotage Initiator Exp. The microwave parameters were set to variable power, constant temperature, and the fixed hold time set to on. Optical rotations were measured using a Jasco P2000 polarimeter.

Synthesis of 3-acrylonitrile furan via Horner-Wadsworth-Emmons olefination

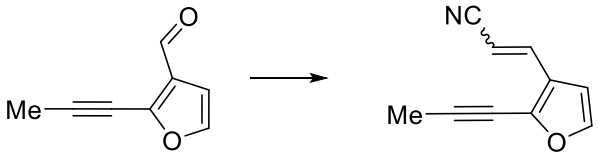

2.16 **2.17**

3-(2-(prop-1-yn-1-yl)furan-3-yl)acrylonitrile (2.17). This compound was prepared as previously reported with some modifications.[95] A flame-dried, 2-necked, 250-mL round-bottomed flask equipped with a magnetic stir bar, nitrogen inlet adapter, and septum was charged with NaH (550 mg of a 60% dispersion in mineral oil, 13.76 mmol) by temporary removal of the septum. The flask was evacuated and refilled with nitrogen (3 x) using a Schlenk manifold and nitrogen inlet adapter. THF (28.6 mL) was added and the solution was cooled by placing the flask in an ice-bath. A solution of diethyl cyanomethylphosphonate (2.1 mL, 13.1 mmol) in THF (9.8 mL) was added dropwise via syringe over 5 min. After stirring for 10 min, the ice-bath was removed, and the solution maintained for an additional 40 min. The reaction was cooled by placing in an ice-bath and a solution of 2-(prop-1-yn-1-yl)furan-3-carbaldehyde (**2.16**) (1.407 g, 10.55 mmol) in THF (9.3 mL) was added dropwise over 10 min via syringe. After 1 h at 0 °C, ^{1}H NMR showed complete consumption of starting material. Water (15 mL) was added to the flask, and the contents of the flask were transferred to a separatory funnel and extracted with diethyl ether (5 x 25 mL). The organic layers were combined, washed with brine (1 x 25 mL), dried over magnesium sulfate,

filtered, and concentrated *in vacuo*. The crude residue was purified by silica gel flash chromatography (10% ethyl acetate/hexanes) to afford 1.36 g (82%) of the title compound as a yellow solid in a 76:24 ratio of *E*:*Z* isomers. The isomers were not separated but taken on to the next step as a mixture.

EDD2-084

MP 151-163 °C

^{1}H NMR (400 MHz, $CDCl_3$)

7.35 (d, *J* = 2.0 Hz, 1 H)*, 7.33 (d, *J* = 16.4 Hz, 1 H)**, 7.30 (d, *J* = 2.0 Hz, 1 H)**, 7.27 (d, *J* = 2.0, 1 H)**, 7.13 (d, *J* = 11.6 Hz, 1 H)*, 6.48 (d, *J* = 2.0 Hz, 1 H)**, 5.65 (d, *J* = 16.8 Hz, 1 H)**, 5.30 (d, *J* = 11.6 Hz, 1 H)*, 2.18 (s, 3 H)**, 2.16 (s, 3 H)* ppm

* Indicates resonances corresponding to *Z* isomer where discernable

** Indicates resonances corresponding to *E* isomer where discernable

^{13}C NMR (100 MHz, $CDCl_3$)

143.9, 143.8, 140.7, 139.2, 138.7, 124.4, 118.4, 108.5, 107.5, 97.4, 96.0, 94.1, 68.6, 4.9 ppm

IR (Thin Film)

2214, 1631, 1147, 952 cm^{-1}

HRMS HRMS-ESI+ (m/z): $[M + H]^+$ calcd for $C_{10}H_8ON$, 158.0606; found: 158.0599

TLC R_f = 0.65 (35% ethyl acetate/hexanes); silica gel, UV, *p*-anisaldehyde

Synthesis of saturated nitrile via dissolving metal reduction

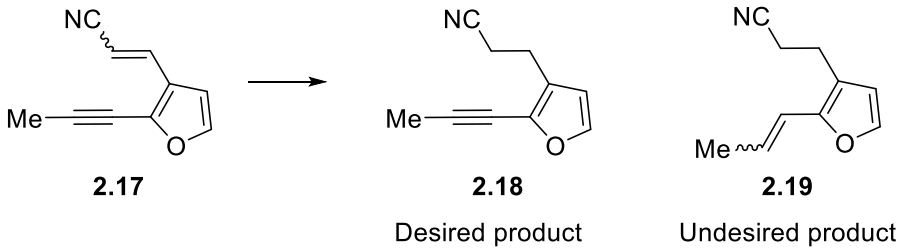

3-(2-(prop-yl-yl-1-yl)furan-3-yl)propanenitrile (2.18). This compound was prepared as previously reported with some modifications.[95] A flame-dried, 2-necked, 100-mL round-bottomed flask equipped with a magnetic stir bar, nitrogen inlet adapter, and septum was charged with magnesium turnings (2.48g, 101.8 mmol). The flask was evacuated and refilled 3 times with nitrogen. 3-(2-(prop-1-yn-1-yl)furan-3-yl)Acrylonitrile (**2.17**) (400 mg, 2.54 mmol) and methanol (22.2 mL) were added to the flask and the solution was cooled by placing the flask in an ice-bath. Dibromoethane (0.8 mL, 9.28 mmol) was added dropwise over 2 min. After 4 h, ^{1}H NMR showed complete consumption of starting material and a 4:1 ratio of product **2.18** to byproduct **2.19**. The reaction was diluted with dichloromethane (10 mL) and transferred to a beaker filled with cold HCl (0.5 M, 400 mL) and placed in an ice-bath. Concentrated HCl was added dropwise until magnesium was no longer visible. The contents of the beaker were transferred to a separatory funnel and extracted with dichloromethane (4 x 75 mL). The combined organic layers were washed with $NaHCO_3$ (1 x 50 mL), dried over magnesium sulfate, filtered, and concentrated *in vacuo*. The crude residue (273 mg) was carried forward to the next step without further purification. A small amount of the crude residue was purified silica gel flash chromatography (5% ethyl acetate/ hexanes) for characterization purposes.

EDD2-092

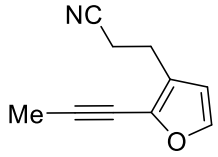

2.18

^{1}H NMR (400 MHz, $CDCl_3$)

7.27 (d, *J* = 1.6 Hz, 1 H), 6.35 (d, *J* = 2.0 Hz, 1 H), 2.84 (t, *J* = 7.6 Hz, 2 H), 2.58 (t, *J* = 7.2 Hz, 2 H), 2.11 (s, 3 H) ppm

^{13}C NMR (100 MHz, $CDCl_3$)

142.9, 135.5, 125.0, 119.3, 111.2, 93.8, 68.9, 21.8, 18.0, 4.8 ppm

IR (Thin Film)

2919, 2248, 1495, 1427, 1180, 1145, 1076, 889, 752 cm^{-1}

HRMS HRMS-ESI+ (m/z): $[M + H]^+$ calcd for $C_{10}H_{10}ON$, 160.0762; found: 160.0753

TLC R_f = 0.57 (35% ethyl acetate/hexanes); silica gel, UV, *p*-anisaldehyde

Byproduct of the dissolving metal reduction reaction of acrylonitrile 2.17

3-(2-(prop-1-en-1-yl)furan-3-yl)propanenitrile (2.19). Obtained as a byproduct in the dissolving metal reduction of acrylonitrile **2.17** in a 53:47 ratio of *E*:*Z* isomers that were inseparable by column chromatography.

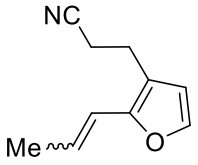

2.19

^{1}H NMR (400 MHz, $CDCl_3$)

7.38 (d, *J* = 2.0 Hz, 1 H), 7.27 (d, *J* = 1.6 Hz, 1 H)*, 6.35 (d, *J* = 2.0 Hz, 1 H), 6.31 (d, *J* = 2.0 Hz, 1 H)*, 6.21-6.18 (m, 2 H), 6.11-6.08 (m, 1 H), 5.73-5.64 (m, 1 H)*,

2.79 (t, *J* = 7.2 Hz, 4 H), 2.53 (t, *J* = 7.2 Hz, 4 H), 2.05 (dd, *J* = 1.6, 7.2 Hz, 3 H), 1.88 (dd, *J* = 1.2, 3.6 Hz, 3 H)* ppm

* Indicates *E* isomer

^{13}C NMR (100 MHz, $CDCl_3$)

150.1, 149.4, 141.6, 141.4, 126.3, 125.6, 119.3, 118.9, 117.3, 116.4, 115.1, 111.7, 111.3, 21.5, 21.2, 18.7, 18.7, 15.3 ppm

HRMS HRMS-ESI+ (m/z): $[M + H]^+$ calcd for $C_{10}H_{12}ON$, 162.0913; found: 162.0910

TLC R_f = 0.61 (35% ethyl acetate/hexanes); silica gel, UV, *p*-anisaldehyde

Synthesis of methyl ketone via addition of Grignard reagent to nitrile

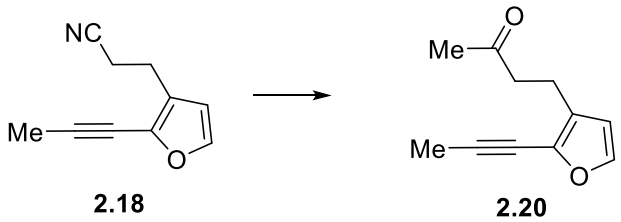

4-(2-(prop-1-yn-1-yl)furan-3-yl)butan-2-one (2.20). This compound was prepared as previously reported with some modifications.[97] An oven-dried 2-5 mL microwave vial (part no. 351521) containing a magnetic stir bar and crimp cap (part no. 50-231-1209) was charged with 3-(2-(prop-yl-yl-1-yl)furan-3-yl)propanenitrile (**2.18**) (50 mg, 0.314 mmol) and THF (0.95 mL) under a nitrogen atmosphere. Methylmagnesium bromide (1.1 mL 1 M solution in THF, 1.10 mmol, 3.5 equiv) was added dropwise via syringe over 3 min at rt. The solution was heated to 100 °C for 10 min in a Biotage Initiator microwave. The reaction was allowed to cool to rt and deionized water (0.08 mL) followed by sulfuric acid (15% v/v, 0.5 mL) were added dropwise via syringe and stirred at rt for 2 h. The resulting solution was transferred to a separatory funnel and extracted with diethyl ether (3 x 10 mL). The combined organic layers were washed with brine (1 x 10 mL), dried over magnesium sulfate, filtered, and concentrated *in vacuo*. The crude residue

was purified by silica gel flash chromatography (5% ethyl acetate/hexanes) to afford 27 mg (49%) of the title compound as a pale-yellow liquid.

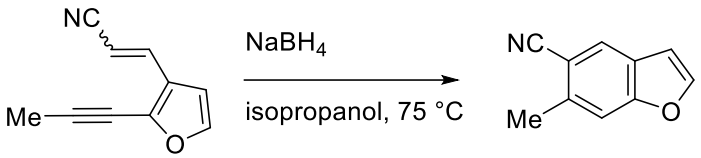

2.17 **2.21**

6-methylbenzofuran-5-carbonitrile (**2.21**). A flame-dried, 2-necked, 25-mL round-bottomed flask equipped with a magnetic stir bar, nitrogen inlet adapter, condenser, and septum was charged with $NaBH_4$ (9 mg, 0.24 mmol). The flask was evacuated and refilled 3 times with nitrogen. 3-(2-(prop-1-yn-1-yl)furan-3-yl)Acrylonitrile (**2.17**) (25 mg, 0.159 mmol) in 2-propanol (2.5 mL) was added to the flask and the solution was placed in an oil bath (75 °C) and refluxed for 27 h. The crude reaction mixture was filtered through a short plug of silica gel using ethyl acetate and the filtrate was concentrated *in vacuo* to yield 27 mg (100%) of the title compound.

EDD2-067

^{1}H NMR (400 MHz, $CDCl_3$)

7.88 (s, 1 H), 7.66 (d, J = 2.4 Hz, 1 H), 7.43 (s, 1 H), 6.78 (d, J = 2.0 Hz, 1 H), 2.65 (s, 3 H)

^{13}C NMR (100 MHz, $CDCl_3$)

157.1, 146.6, 138.1, 126.5, 125.9, 118.8, 113.3, 107.8, 106.4, 20.9 ppm

HRMS HRMS-ESI+ (m/z): $[M + H]^+$ calcd for $C_{10}H_{12}ON$, 158.0606; found: 158.0598

TLC R_f = 0.74 (35% ethyl acetate/hexanes); silica gel, UV, *p*-anisaldehyde

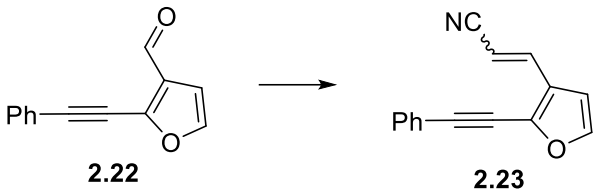

2.22 **2.23**

3-(2-(phenylethynyl)furan-3-yl)acrylonitrile (2.23). A flame-dried, 2-necked, 50-mL round-bottomed flask equipped with a magnetic stir bar, nitrogen inlet adapter, and septum was charged with NaH (148 mg of a 60% dispersion in mineral oil, 3.69 mmol). The flask was evacuated and refilled with nitrogen 3 times using a Schlenk manifold and nitrogen inlet adapter. THF (7.7 mL) was added and the solution was cooled by placing in an ice-bath. A solution of diethyl cyanomethylphosphonate (0.58 mL, 3.52 mmol) in THF (2.6 mL) was added dropwise via syringe over 5 min. After stirring for 10 min, the ice-bath was removed, and the solution stirred for an additional 40 min. The reaction was cooled again by placing in an ice-bath and a solution of 2-(phenylethynyl)furan-3-carbaldehyde (**2.22**) (550 mg, 2.01 mmol) in THF (2.5 mL) was added dropwise over 5 min via syringe. After 1 h at 0 °C, ^{1}H NMR showed complete consumption of starting material. The reaction was quenched with water and brine and extracted with diethyl ether (5 X 15 mL). The organic layers were combined, washed with brine (1 X 15 mL), dried over magnesium sulfate, gravity filtered, and concentrated *in vacuo*. The crude residue was purified by silica gel flash chromatography (10% ethyl acetate/hexanes) to afford 510 mg (83%) as a 78:22 ratio of *E*:*Z* isomers of the title compound as a beige solid.

EDD2-112

MP 39-42 °C

^{1}H NMR (400 MHz, $CDCl_3$)

7.58-7.56 (m, 2 H), 7.46-7.36 (m, 6 H), *7.23 (d, *J* = 11.8 Hz, 0.29 H), 6.57 (d, *J* = 2.4 Hz, 1H), 5.73 (d, *J* = 16.4 Hz, 1 H), *5.38 (d, *J* = 12.0 Hz, 0.29 H) ppm

* Indicates resonances corresponding to *Z* isomer where discernable

Impurity at 2.17 (s, 0.15 H)

^{13}C NMR (100 MHz, $CDCl_3$)

144.8, 144.7, 140.4, 138.6, 138.4, 131.8, 131.8, 129.8, 129.7, 128.8, 128.7, 125.5, 125.4, 121.3, 118.3, 108.9, 107.9, 99.6, 96.7, 94.8 ppm

IR (Thin Film)

2216, 1621, 1506, 1483, 1168 cm^{-1}

HRMS HRMS-ESI+ (m/z): $[M + H]^+$ calcd for $C_{15}H_{10}ON$, 220.0762; found: 220.0757

TLC R_f = 0.60 (35% ethyl acetate/hexanes); silica gel, UV, *p*-anisaldehyde

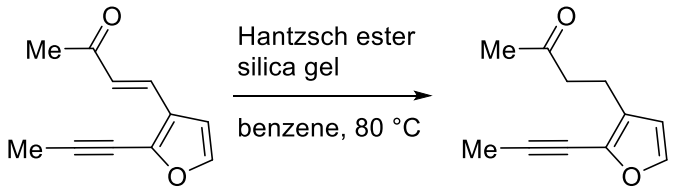

2.26 **2.20**

4-(2-(prop-1-yn-1-yl)furan-3-yl)butan-2-one (2.20). This compound was prepared as previously reported with some modifications.[107] A flame-dried, 2-necked, 10-mL, round-bottomed flask equipped with a magnetic stir bar, septa and nitrogen inlet adapter was charged with (*E*)-4-(2-(prop-1-yn-1-yl)furan-3-yl)but-3-en-2-one (**2.26**) (35 mg, 0.20 mmol) in benzene (2.87 mL, 0.07 M). Diethyl 2,6-dimethyl-1,4-dihydropyridine-3,5-dicarboxylate (Hantzsch ester, **2.27**) (64 mg, 0.25 mmol, 1.25 equiv) was added by temporary removal of the septa. The flask was lowered into a preheated oil bath (80 °C) and maintained for 21 h. TLC and NMR aliquots at this time showed incomplete consumption of starting material. The crude residue was concentrated *in vacuo* and purified by silica gel flash chromatography (2.5-5% ethyl acetate/hexanes) to afford a mixture of starting material, product, and Hantzsch pyridine.

EDD4-292

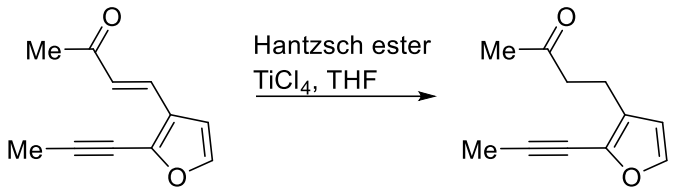

2.26 **2.20**

4-(2-(prop-1-yn-1-yl)furan-3-yl)butan-2-one (2.20). This compound was prepared as previously reported with some modifications.[109] A flame-dried, 2-necked, 10-mL, round-bottomed flask equipped with a magnetic stir bar, septa and nitrogen inlet adapter was charged with (*E*)-4-(2-(prop-1-yn-1-yl)furan-3-yl)but-3-en-2-one (**2.26**) (35 mg, 0.201 mmol) in THF (1.0 mL, 0.2M) via syringe. Diethyl 2,6-dimethyl-1,4-dihydropyridine-3,5-dicarboxylate (Hantzsch ester, **2.27**) (129 mg, 0.603 mmol, 3.0 equiv) was added by temporary removal of the septa. $TiCl_4$ (0.24 mL of a 1 M solution in DCM, 0.24 mmol, 1.2 equiv) was added via syringe over 2 min. After 1 h, TLC showed complete consumption of starting material. The solution was concentrated via rotary evaporation, the crude residue loaded onto a column, and purified via silica gel flash chromatography (5-10% EtOAc/ Hexanes) to afford 29 mg (83%) of the title compound as a yellow oil.

EDD4-302

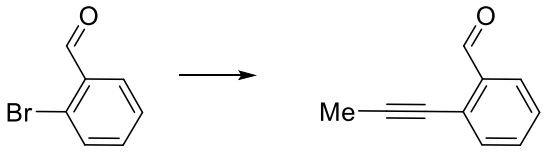

2.56 **2.57**

2-(prop-1-yn-1-yl)benzaldehyde (2.57). This compound was prepared as previously reported with some modifications.[112] A flame-dried, 2-necked, 100-mL, round bottomed flask equipped with a magnetic stir bar, nitrogen inlet needle, condenser, and septum was charged with 2-bromobenzaldehyde (**2.56**) (1.2 mL, 10.28 mmol), bistriphenylphosphine palladium(II)

dichloride (358 mg, 0.51 mmol), triethylamine (2.87 mL, 20.56 mmol), and THF (16.3 mL, 0.63 M). Nitrogen was bubbled through the solution for 5 min. 1-Propyne (11.3 mL of a 1 M in THF solution, 11.31 mmol), and CuI (50 mg, 0.26 mmol) was added and the flask lowered into a preheated oil bath (40 °C). After 2 h, an NMR aliquot showed complete consumption of starting material. The solution was concentrated *in vacuo* and purified via silica gel flash chromatography (5-10% ethyl acetate/hexanes) to afford 1.099g (74%) of the title compound as a brown oil.

EDD6-425

^{1}H NMR (300 MHz, $CDCl_3$)

10.53 (d, *J* = 0.6 Hz, 1 H), 7.88 (d, *J* = 7.5 Hz, 1 H), 7.55-7.48 (m, 2 H), 7.41-7.36 (m, 1 H), 2.14 (s, 3 H) ppm

^{13}C NMR (100 MHz, $CDCl_3$)

192.4, 136.2, 133.8, 133.4, 128.0, 128.0, 127.1, 93.7, 75.7, 4.7 ppm

IR (Thin Film)

2242, 1693, 760 cm^{-1}

HRMS HRMS-ESI+ (m/z): $[M + H]^+$ calcd for $C_{10}H_9O$, 145.0648; found: 145.0647

TLC R_f = 0.64 (35% ethyl acetate/hexanes); silica gel, UV, PAA

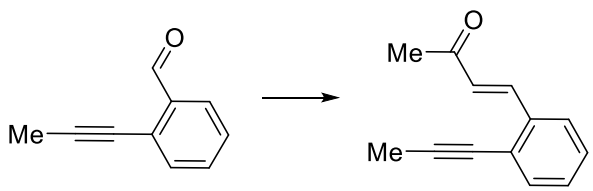

2.57 **2.58**

(*E*)-4-(2-(prop-1-yn-1-yl)phenyl)but-3-en-2-one (2.58). This compound was prepared as previously reported with some modifications.[106] A flame-dried, 2-necked, 50-mL, round-bottomed flask equipped with a magnetic stir bar, nitrogen inlet adapter, and septum was charged with 2-

(prop-1-yn-1-yl)benzaldehyde (**2.57**) (984 mg, 6.83 mmol), deionized water (5.7 mL, 1.2 M) and acetone (5.0 mL, 68.3 mmol) via syringe. The solution was cooled in an ice-bath, and 33% w/w aqueous NaOH (0.33 mL, 2.73 mmol) was added dropwise over 1 min. The solution was allowed to warm to rt and after 4 h, TLC showed complete consumption of starting material. 10% Sulfuric acid was added dropwise until the solution reached a pH 4 as determined using pH paper. The resulting solution was transferred to a separatory funnel and the organic layer separated. The aqueous layer was extracted with $CHCl_3$ (5 x 5 mL), the combined organic layers were dried over magnesium sulfate, filtered, and concentrated *in vacuo*. The crude residue was purified by silica gel flash chromatography (10-20% ethyl acetate/hexanes) to afford 953 mg (76% yield) of the title compound as a yellow oil.

EDD6-428

^{1}H NMR (400 MHz, $CDCl_3$)

8.04 (d, *J* = 16.4 Hz, 1 H), 7.63-7.61 (m, 1 H), 7.46-7.44 (m, 2 H), 7.33-7.29 (m, 2 H), 6.73 (d, *J* = 16.4 Hz, 1 H), 2.41 (s, 3 H), 2.15 (s, 3 H) ppm

^{13}C NMR (100 MHz, $CDCl_3$)

198.8, 141.9, 135.8, 133.1, 130.0, 128.5, 128.1, 126.0, 125.4, 92.6, 77.5, 27.4, 4.7 ppm

IR (Thin Film)

2246, 1668, 758 cm^{-1}

HRMS HRMS-ESI+ (m/z): $[M + H]^+$ calcd for $C_{13}H_{13}O$, 185.0961; found: 185.0962

TLC R_f = 0.56 (35% ethyl acetate/hexanes); silica gel, UV, PAA

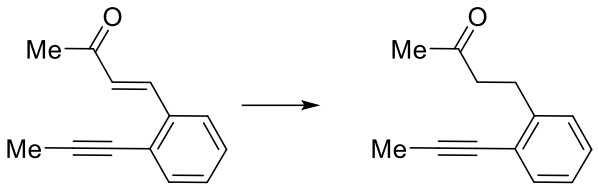

2.58 **2.59**

4-(2-(prop-1-yn-1-yl)phenyl)butan-2-one (2.59). A flame-dried, 2-necked, 100-mL round-bottomed flask equipped with a magnetic stir bar, nitrogen inlet adapter, and septum was charged with (*E*)-4-(2-(prop-1-yn-1-yl)phenyl)but-3-en-2-one (**2.58**) (740 mg, 4.02 mmol), toluene (40.2 mL, 0.01 M), Hantzsch ester (**2.27**) (3.564g, 14.07 mmol), and silica gel (6.03 g) and lowered into a preheated oil bath (110 °C). After 20.5 h, an NMR aliquot showed complete consumption of starting material. The solution was gravity filtered using a glass funnel fitted with filter paper. The filter paper was washed with ethyl acetate (25 mL), and the combined organics were concentrated *in vacuo*. The crude residue was diluted in ethyl acetate, transferred to a separatory funnel and washed with 2 N HCl (5 x 5 mL) and brine (1 x 5 mL), dried over magnesium sulfate, filtered, and concentrated *in vacuo.* The crude residue was purified by silica gel flash chromatography (5-15% ethyl acetate/ hexanes) to afford 577 mg (77%) of the title compound as a yellow oil.

EDD6-431

^{1}H NMR (400 MHz, $CDCl_3$)

7.36 (d, *J* = 7.6 Hz, 1 H), 7.21-7.11 (m, 3 H), 3.02 (t, *J* = 7.6 Hz, 2 H), 2.78 (t, *J* = 8.0 Hz, 2 H), 2.15 (s, 3 H), 2.08 (s, 3 H) ppm

^{13}C NMR (100 MHz, $CDCl_3$)

208.4, 142.9, 132.5, 128.9, 127.9, 126.2, 123.5, 89.9, 78.2, 44.4, 30.1, 29.0, 4.6 ppm

IR (Thin Film)

2249, 1712, 757 cm^{-1}

HRMS HRMS-ESI+ (m/z): $[M + H]^+$ calcd for $C_{13}H_{15}O$, 187.1117; found: 187.1119

TLC R_f = 0.59 (35% ethyl acetate/hexanes); silica gel, UV, PAA

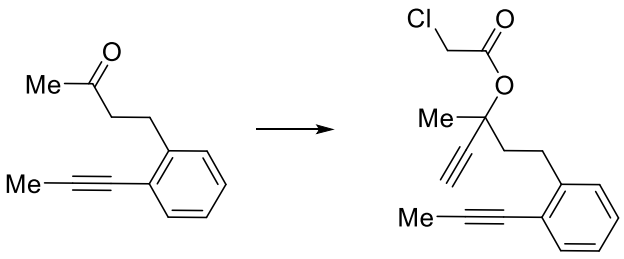

2.59 **2.60**

3-methyl-5-(2-(prop-1-yn-1-yl)phenyl)pent-1-yn-3-yl 2-chloroacetate (2.60). This compound was prepared as previously reported with some modifications.[73] A flame-dried, 2-necked, 100-mL, round bottomed flask equipped with a magnetic stir bar, nitrogen inlet adapter, and septum was charged with 4-(2-(prop-1-yn-1-yl)phenyl)butan-2-one (**2.59**) (570 mg, 3.06 mmol) and THF (10.2 mL). The solution was cooled by placing the flask in an ice-bath and ethynylmagnesium bromide (18.4 mL of a 0.5 M solution in THF, 9.18 mmol, 3.0 equiv) was added dropwise via syringe over 10 min. After allowing to warm to rt over 60 min, TLC showed complete consumption of starting material. The flask was placed in an ice-bath and chloroacetyl chloride (0.85 mL, 10.71 mmol, 3.5 equiv) was added dropwise via syringe over 2 min. After 2 h, TLC showed complete consumption of the propargyl alcohol intermediate. Diethyl ether (10 mL) and deionized water (5 mL) were added to the flask, the mixture was transferred to a separatory funnel, and the organic layer was separated. The aqueous layer was extracted with diethyl ether (3 x 10 mL). The combined organics were washed with brine, dried over magnesium sulfate, filtered, and concentrated *in vacuo*. The crude residue was purified by silica gel flash chromatography (5 to 15% ethyl acetate/hexanes) to give 636 mg (72%) of the title compound as a light-yellow oil.

EDD6-435

^{1}H NMR (400 MHz, $CDCl_3$)

7.37 (d, *J* = 7.6 Hz, 1 H), 7.21-7.18 (m, 2 H), 7.15-7.11 (m, 1 H), 4.00 (s, 2 H), 2.99-2.95 (m, 2 H), 2.67 (s, 1 H), 2.33-2.26 (m, 1 H), 2.20-2.13 (m, 1 H), 2.09 (s, 3 H), 1.81 (s, 3 H) ppm

^{13}C NMR (100 MHz, $CDCl_3$)

165.4, 142.9, 132.4, 129.0, 127.9, 126.2, 123.6, 89.7, 82.8, 78.2, 77.4, 74.6, 42.1, 41.5, 29.7, 26.5, 4.6 ppm

IR (Thin Film)

2119, 1761, 759 cm^{-1}

HRMS HRMS-ESI+ (m/z): $[M + H]^+$ calcd for $C_{17}H_{18}O_2Cl$, 289.0989; found: 289.0991

TLC R_f = 0.65 (35% ethyl acetate/hexanes); silica gel, UV, PAA

General Procedure A: Synthesis of allenyl esters via a formal [3,3]-sigmatropic rearrangement[73]

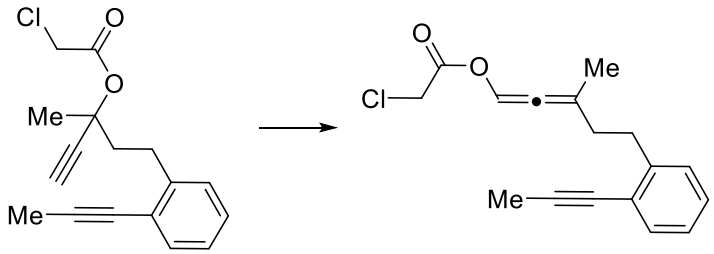

2.60 **2.61**

3-methyl-5-(2-(prop-1-yn-1-yl)phenyl)penta-1,2-dien-1-yl 2-chloroacetate (2.61). A flame-dried, single-necked, 25-mL, round bottomed flask equipped with a magnetic stir bar was charged with rhodium(II) trifluoroacetate dimer (0.05 equiv, 16.0 mg, 0.024 mmol) in a nitrogen filled glovebox and sealed with a septum before removal. The flask was placed under a nitrogen atmosphere using a nitrogen manifold and an inlet needle. A solution of 3-methyl-5-(2-(prop-1-

yn-1-yl)phenyl)pent-1-yn-3-yl 2-chloroacetate (**2.60**) (1 equiv, 139 mg, 0.48 mmol) in toluene (2.4 mL, 0.2 M) was added dropwise via syringe to the flask. The flask was lowered into a preheated 50 °C oil bath. After 2 h, consumption of starting material was observed by TLC. The flask was allowed to cool to rt, the volatiles were removed *in vacuo*, and the crude residue immediately purified by silica gel flash chromatography (2% ethyl acetate/hexanes) to give 118 mg (85%) of the title compound as a clear liquid.

EDD6-438

^{1}H NMR (400 MHz, $CDCl_3$)

7.36 (d, *J* = 7.6 Hz, 1 H), 7.31-7.30 (m, 1 H), 7.22-7.10 (m, 3 H), 4.12 (s, 2 H), 2.95-2.87 (m, 2 H), 2.46-2.37 (m, 2 H), 2.08 (s, 3 H), 1.89 (d, *J* = 1.6 Hz, 3 H) ppm

^{13}C NMR (100 MHz, $CDCl_3$)

189.8, 165.4, 143.2, 132.4, 128.7, 127.8, 126.1, 123.6, 117.1, 110.4, 89.7, 78.3, 40.9, 36.0, 32.6, 20.6, 4.6 ppm

IR (Thin Film)

2249, 1978, 1765, 756 cm^{-1}

HRMS HRMS-ESI+ (m/z): $[M + H]^+$ calcd for $C_{17}H_{18}O_2Cl$, 289.0989; found: 289.0992

TLC R_f = 0.71 (35% ethyl acetate/hexanes); silica gel, UV, PAA

General Procedure B: Racemic APKR

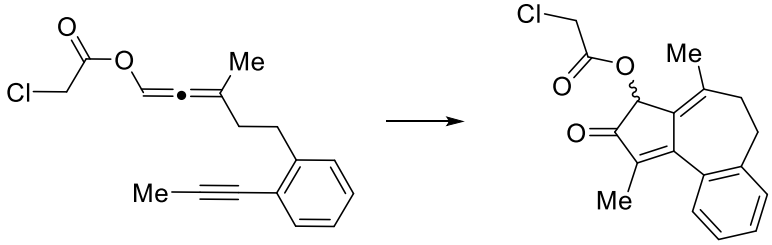

2.61 **2.62**

1,4-dimethyl-2-oxo-2,3,5,6-tetrahydrobenzo[e]azulen-3-yl 2-chloroacetate (2.62). Bis(1,5-cyclooctadiene)rhodium(I) tetrafluoroborate (0.1 equiv, 3.0 mg, 0.0073 mmol) was weighed into a flame-dried 5-mL pear-shaped flask in a nitrogen glovebox and sealed with a septum. DCE (0.7 mL) was added under nitrogen to the flask and the solution was transferred via syringe to a flame-dried 25-mL Schlenk tube equipped with magnetic stir bar and septum. In a separate flask, triphenylphosphine (0.15 equiv, 2.9 mg, 0.011 mmol) was dissolved in DCE (0.7 mL) and added to the Schlenk tube via syringe. The resulting solution was stirred at rt under nitrogen for 30 min. The Schlenk tube was evacuated via the inlet needle and refilled with 100% carbon monoxide (3 x) using a separate inlet needle and stirred for 1 h. 3-methyl-5-(2-(prop-1-yn-1-yl)phenyl)penta-1,2-dien-1-yl 2-chloroacetate (**2.61**) (1.0 equiv, 20 mg, 0.0693 mmol) in DCE (2.3 mL) was added dropwise via syringe over 2 min. The tube was lowered into a preheated 70 °C oil bath and the reaction stirred for 71 h until complete by TLC. The volatiles were removed *in vacuo*, and the product was purified by silica gel flash chromatography (5% to 10% ethyl acetate/hexanes) to give 15 mg (68%) of the title compound as a yellow solid.

EDD6-433

^{1}H NMR (400 MHz, $CDCl_3$)

7.38-7.34 (m, 2 H), 7.31-7.29 (d, *J* = 7.2 Hz, 1 H), 7.23-7.21 (m, 1 H), 5.88, (s, 1 H), 4.18 (s, 2 H), 3.18-3.11 (m, 1 H), 2.79-2.76 (m, 1 H), 2.53-2.50 (m, 2 H), 2.04 (s, 3 H), 1.83 (s, 3 H) ppm

^{13}C NMR (100 MHz, $CDCl_3$)

199.5, 166.4, 142.5, 140.2, 135.7, 133.5, 130.6, 130.6, 130.1, 128.9, 126.2, 74.6, 40.7, 37.3, 34.0, 23.3, 11.2 ppm

IR (Thin Film)

1746, 1698, 756 cm^{-1}

HRMS HRMS-ESI+ (m/z): $[M + H]^+$ calcd for $C_{18}H_{18}O_3Cl$, 317.0939; found: 317.0925

TLC R_f = 0.48 (35% ethyl acetate/hexanes); silica gel, UV, PAA

Waters 600 HPLC, UV/PDA detector, 318 nm, Daicel CHIRALCEL-OD, 250 X 4.6 mm column, 1% *i*PrOH/hexanes, Flow rate: 1 mL/min

Table 2. HPLC results for racemic 2.62

Peak	Retention Time (min)	Peak area (%)
Peak 1	22.75	50.44
Peak 2	34.25	49.56

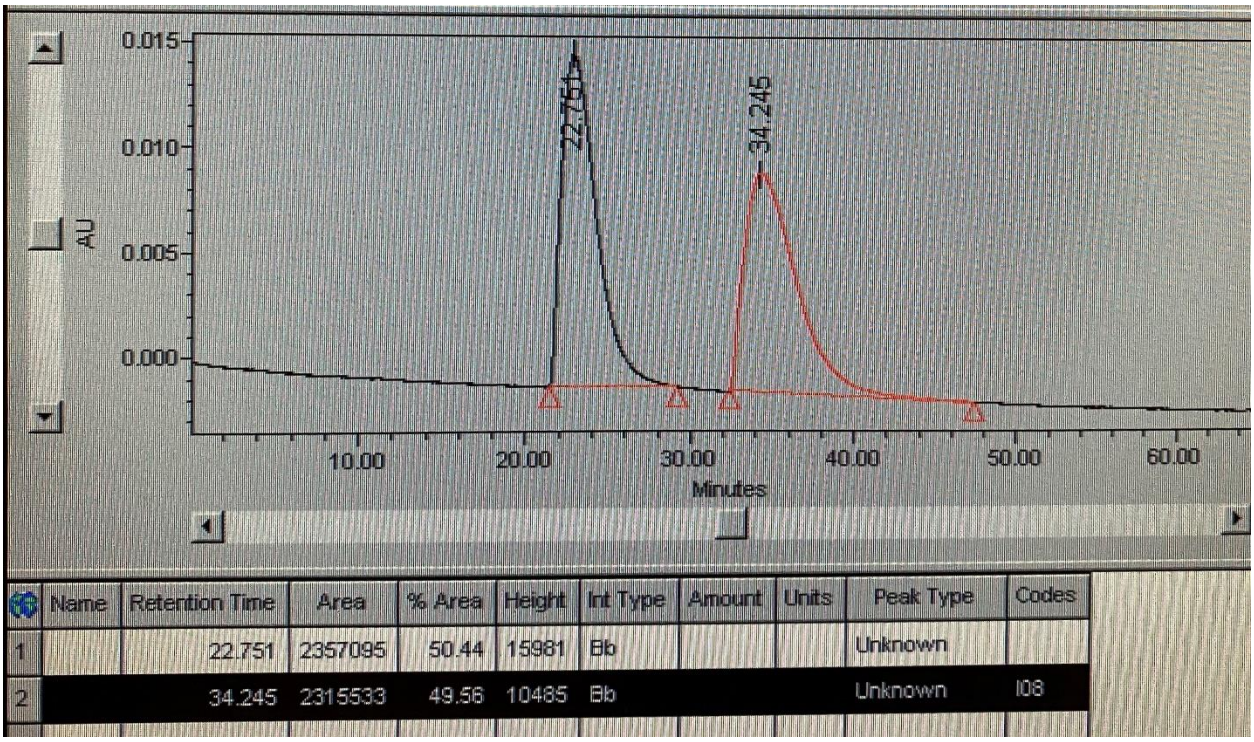

Figure 18. Chiral HPLC trace for racemic 2.62

General Procedure C: Asymmetric APKR

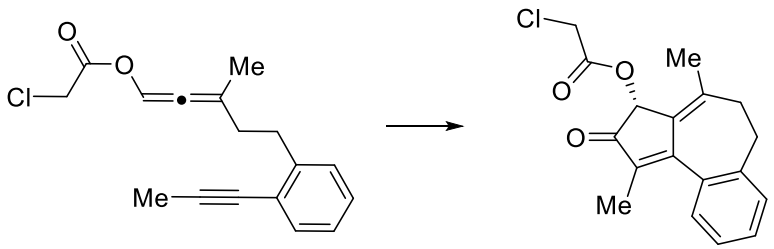

2.61 **2.62**

(*R*)-1,4-dimethyl-2-oxo-2,3,5,6-tetrahydrobenzo[e]azulen-3-yl 2-chloroacetate (2.62). Bis(1,5-cyclooctadiene)rhodium(I) tetrafluoroborate (0.1 equiv, 2.8 mg, 0.0069 mmol) and (*S*)-MonoPhos-alkene (**L1**) (0.15 equiv, 4.1 mg, 0.010 mmol) were weighed into separate flame-dried 5-mL pear-shaped flasks in a nitrogen glovebox and each sealed with a septum. The flasks were placed under a nitrogen atmosphere via a Schlenk manifold and an inlet needle. Bis(1,5-cyclooctadiene)rhodium(I) tetrafluoroborate and (*S*)-MonoPhos-alkene (**L1**) were each dissolved in DCE (1.0 mL each) and the resulting solutions transferred via syringe to a flame dried Schlenk tube and stirred under nitrogen for 30 min. The tube was evacuated via the inlet needle for a few seconds and refilled with carbon monoxide (100%) using a separate inlet needle attached to a balloon of CO and stirred for 1 h. 3-methyl-5-(2-(prop-1-yn-1-yl)phenyl)penta-1,2-dien-1-yl 2-chloroacetate (**2.61**) (1.0 equiv, 20 mg, 0.069 mmol) in DCE (0.01 M, 6.9 mL) was added dropwise via syringe. The tube was lowered into a preheated 70 °C oil bath and stirred until TLC showed complete consumption of starting material (69 h). The solution was concentrated *in vacuo*, and the product purified using silica gel flash chromatography (5% ethyl acetate/hexanes) to give the title compound (8 mg, 36%) as a yellow oil in a 59:41 ratio of enantiomers.

EDD6-434

Waters 600 HPLC, UV/PDA detector, 318 nm, Daicel CHIRALCEL-OD, 250 X 4.6 mm column, 1% *i*PrOH/hexanes, Flow rate: 1 mL/min

Table 3. Chiral HPLC data for enantioenriched 2.62 run 1

Peak	Retention Time (min)	Peak area (%)
Peak 1	24.19	58.61
Peak 2	36.84	41.39

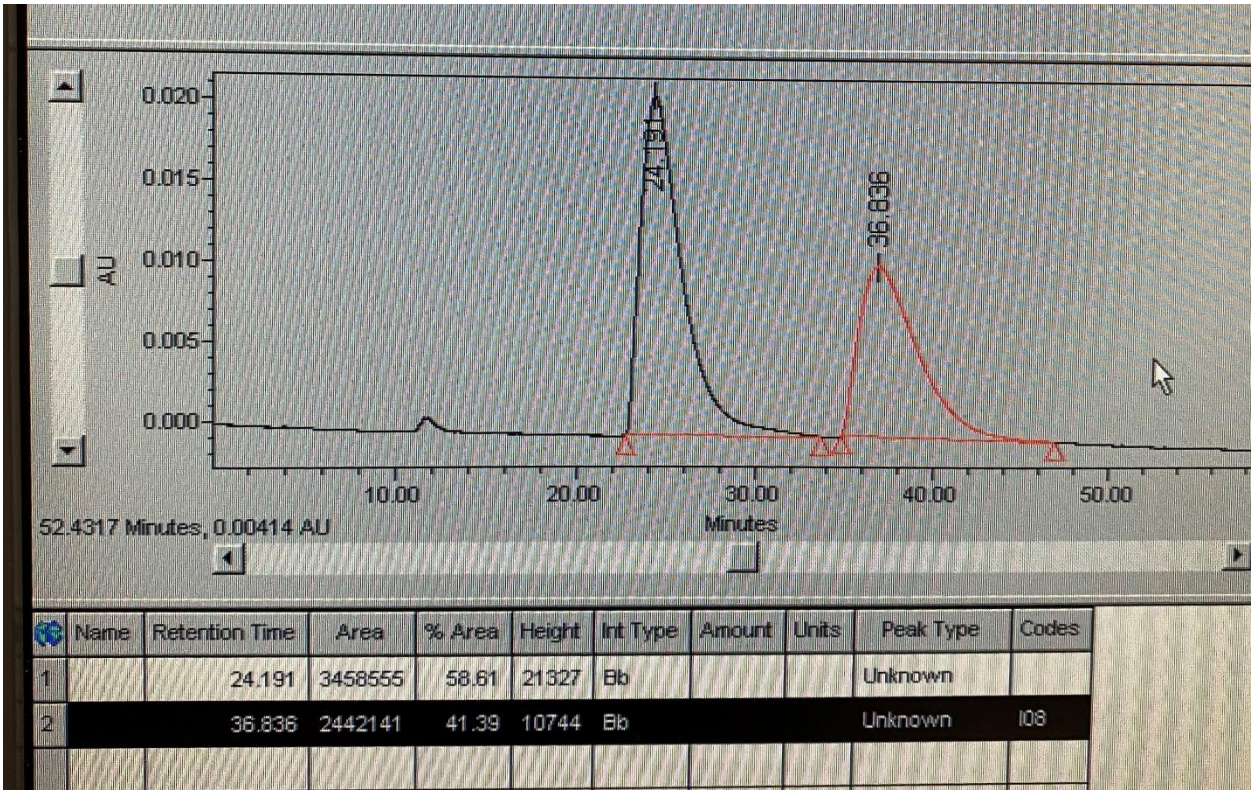

Figure 19. Chiral HPLC trace for enantioenriched 2.62 run 1

Run 2: Follows general procedure C: Bis(1,5-cyclooctadiene)rhodium(I) tetrafluoroborate (2.8 mg, 0.0069 mmol), (*S*)-MonoPhos-alkene (**L1**) (4.1 mg, 0.010 mmol), carbon monoxide (100%), 3-methyl-5-(2-(prop-1-yn-1-yl)phenyl)penta-1,2-dien-1-yl 2-chloroacetate (**2.61**) (20 mg, 0.069 mmol), DCE (6.9 mL, 0.01 M). The reaction was stirred for 69 h in an oil bath (70 °C). The crude residue was purified via silica gel flash chromatography (5% ethyl acetate/hexanes) to give 14 mg (64%) of the title compound as a yellow solid. The ^{1}H NMR matched that of racemic **2.62**.

EDD6-436

$[\alpha]^{23.7}_{D}$ = -0.72 (c. = 0.65, $CHCl_3$)

Waters 600 HPLC, UV/PDA detector, 318 nm, Daicel CHIRALCEL-OD, 250 X 4.6 mm column, 1% *i*PrOH/hexanes, Flow rate: 1 mL/min

Table 4. Chiral HPLC data for enantioenriched 2.26 run 2

Peak	Retention Time (min)	Peak area (%)
Peak 1	24.29	58.39
Peak 2	37.00	41.61

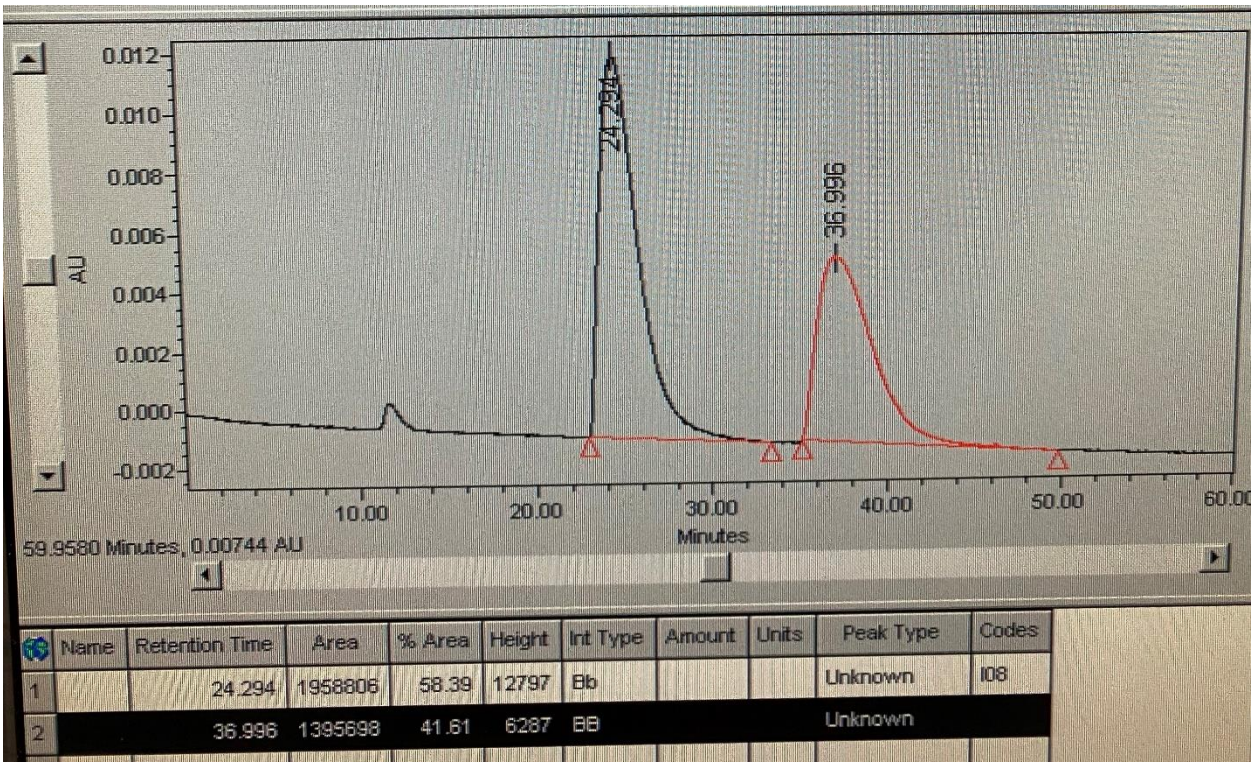

Figure 20. Chiral HPLC trace for enantioenriched 2.26 run 2

Run 3: Follows general procedure C: Bis(1,5-cyclooctadiene)rhodium(I) tetrafluoroborate (2.8 mg, 0.0069 mmol), (*S*)-MonoPhos-alkene (**L1**) (4.1 mg, 0.010 mmol), carbon monoxide (100%), 3-methyl-5-(2-(prop-1-yn-1-yl)phenyl)penta-1,2-dien-1-yl 2-chloroacetate (**2.61**) (20 mg, 0.069 mmol), DCE (6.9 mL, 0.01 M). The reaction was stirred for 63 h in an oil bath (70 °C). The

crude residue was purified via silica gel flash chromatography (5% ethyl acetate/hexanes) to give 11 mg (50%) of the title compound as a yellow solid. The ^{1}H NMR matched that of racemic **2.62**.

EDD6-439

Waters 600 HPLC, UV/PDA detector, 318 nm, Daicel CHIRALCEL-OD, 250 X 4.6 mm column, 1% *i*PrOH/hexanes, Flow rate: 1 mL/min

Table 5. Chiral HPLC data for enantioenriched 2.26 run 3

Peak	Retention Time (min)	Peak area (%)
Peak 1	24.18	57.31
Peak 2	36.78	42.69

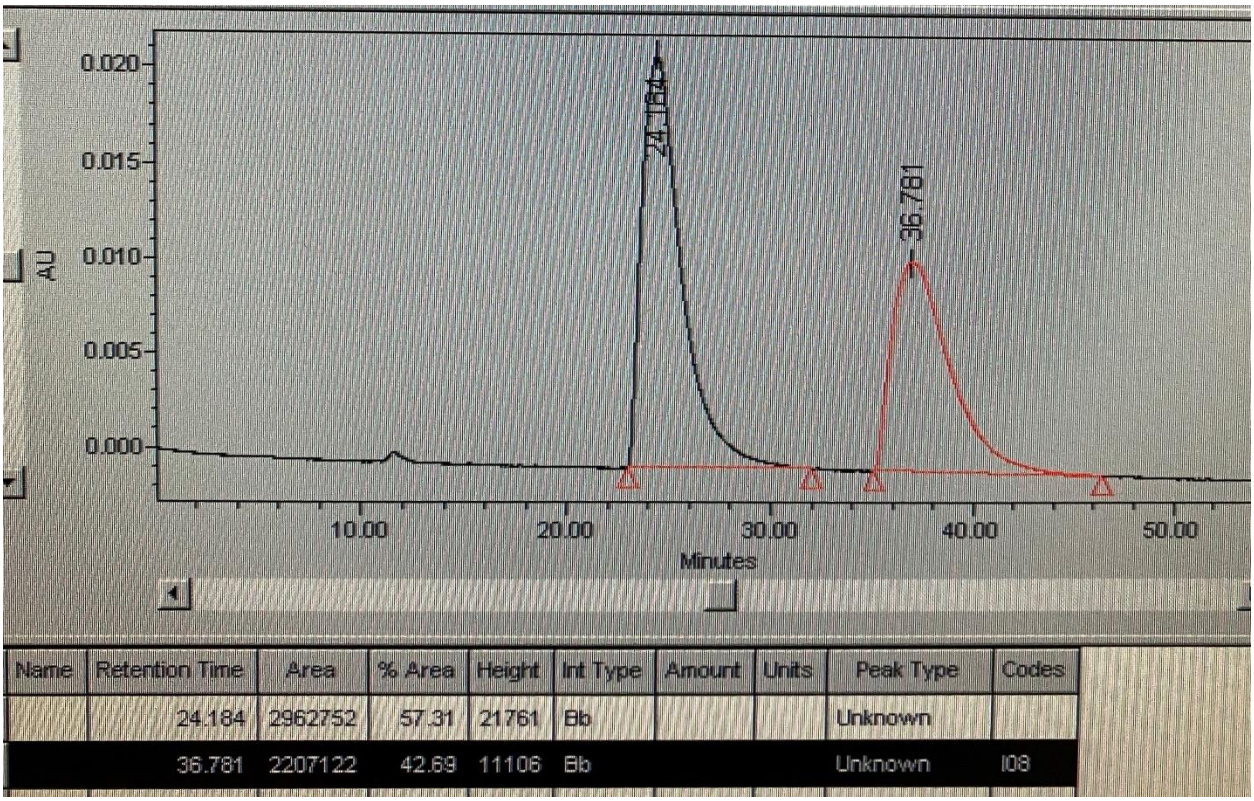

Figure 21.Chiral HPLC trace for enantioenriched 2.26 run 3

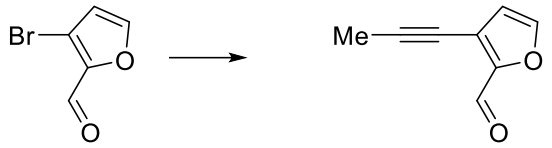

2.63 **2.64**

3-(prop-1-yn-1-yl)furan-2-carbaldehyde (2.64). This compound was prepared as previously reported with some modifications.[112] A flame-dried, 2-necked, 50-mL, round bottomed flask equipped with a magnetic stir bar, nitrogen inlet adapter, and septum was charged with 3-bromofuran-2-carbaldehyde (**2.63**) (1.00 g, 5.72 mmol), bistriphenylphosphine palladium(II) dichloride (201 mg, 0.286 mmol, 0.05 equiv), triethylamine (1.6 mL, 11.43 mmol, 2 equiv), and THF (9.1 mL, 0.63 M). Nitrogen gas was bubbled through into the solution for 5 min using a needle. 1-Propyne (6.3 mL of a 1 M solution in THF, 6.29 mmol, 1.1 equiv), and CuI (27 mg, 0.14 mmol, 0.025 equiv) were added and the flask was lowered into a preheated oil bath (40 °C). After 4 h, NMR showed complete consumption of starting material. The solution was concentrated *in vacuo* and purified by silica gel flash chromatography (5-20% ethyl acetate/hexanes) to give 725 mg (95%) of the title compound as a sticky brown solid.

EDD6-445

^{1}H NMR (400 MHz, $CDCl_3$)

9.75 (d, *J* = 0.4 Hz, 1 H), 7.58 (t, *J* = 0.8 Hz, 1 H), 6.54 (d, *J* = 1.6 Hz, 1 H), 2.11 (s, 3 H) ppm

^{13}C NMR (100 MHz, $CDCl_3$)

176.4, 153.0, 147.5, 120.6, 115.6, 95.3, 69.2, 4.8 ppm

IR (Thin Film)

2247, 1672 cm^{-1}

HRMS HRMS-ESI+ (m/z): $[M + H]^+$ calcd for $C_8H_7O_2$, 135.0446; found: 135.0443

TLC R_f = 0.6 (35% ethyl acetate/hexanes); silica gel, UV, PAA

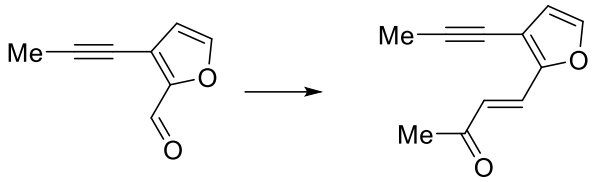

2.64 **2.65**

(*E*)-4-(3-(prop-1-yn-1-yl)furan-2-yl)but-3-en-2-one (2.65). A flame-dried, 2-necked, 50-mL, round bottomed flask equipped with a magnetic stir bar, nitrogen inlet adapter, and septum was charged with 3-(prop-1-yn-1-yl)furan-2-carbaldehyde (**2.64**) (724 mg, 5.40 mmol), water (4.5 mL, 252.1 mmol, 46.7 equiv), and acetone (0.99 mL, 13.50 mmol, 2.5 equiv) via syringe. The solution was cooled in an ice-bath, and 33%$_{(w/w)}$ NaOH (0.17 mL, 1.39 mmol) was added dropwise over 1 min. After allowing to warm to rt after 5 h, TLC showed complete consumption of starting material. 10% Sulfuric acid was added until the solution reached a pH 4 as determined using pH paper. The resulting solution was transferred to a separatory funnel and the organic layer separated. The aqueous layer was extracted with $CHCl_3$ (5 x 5 mL), the combined organic layers were dried over magnesium sulfate, filtered, and concentrated *in vacuo*. The crude residue was purified by silica gel flash chromatography (10-15% ethyl acetate/hexanes) to afford 748 mg (80% yield) of the title compound as a brown solid.

EDD6-446

MP 43.6-49.1 °C

^{1}H NMR (400 MHz, $CDCl_3$)

7.40 (d, *J* = 16.0 Hz, 1 H), 7.39 (d, *J* = 2.0 Hz, 1 H), 6.68 (d, *J* = 16.4, 1 H), 6.45 (d, *J* = 2.0 Hz, 1 H), 2.35 (s, 3 H), 2.10 (s, 3 H) ppm

^{13}C NMR (100 MHz, $CDCl_3$)

198.1, 152.8, 144.4, 127.5, 124.7, 115.3, 113.4, 93.9, 70.7, 28.1, 4.9 ppm

IR (Thin Film)

2249, 1666, 1606 cm^{-1}

HRMS HRMS-ESI+ (m/z): $[M + H]^+$ calcd for $C_{11}H_1O_2$, 175.0759 found: 175.0757

TLC R_f = 0.5 (35% ethyl acetate/hexanes); silica gel, UV, PAA

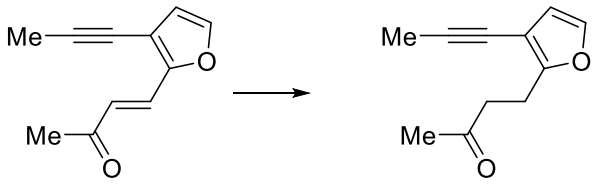

2.65 **2.66**

4-(3-(prop-1-yn-1-yl)furan-2-yl)butan-2-one (2.66). A flame-dried, 2-necked, 100-mL round-bottomed flask equipped with a magnetic stir bar, nitrogen inlet adapter, and septum was charged with (*E*)-4-(3-(prop-1-yn-1-yl)furan-2-yl)but-3-en-2-one (**2.65**) (548 mg, 3.15 mmol), toluene (31.5 mL, 0.1 M), Hantzsch ester (**2.27**) (2.794g, 11.03 mmol), and silica gel (4.725 g) and lowered into a preheated oil bath (110 °C). After 46 h, an NMR aliquot showed complete consumption of starting material. The solution was gravity filtered through filter paper using a glass funnel. The filter paper was washed with ethyl acetate (25 mL), and the organics concentrated *in vacuo*. The crude material was dissolved in ethyl acetate, transferred to a separatory funnel, extracted with 2 N HCl (5 x 5 mL), organic layer washed with brine (1 x 5 mL), dried over magnesium sulfate, filtered, and concentrated *in vacuo.* The crude residue was purified by silica gel flash chromatography (5-10% ethyl acetate/ hexanes) to afford 366 mg (66%) of the title compound as a yellow oil.

EDD6-454

^{1}H NMR (400 MHz, $CDCl_3$)

7.17 (d, *J* = 1.6 Hz, 1 H), 6.28 (d, *J* = 1.6 Hz, 1 H), 2.98 (t, *J* = 7.2 Hz, 2 H), 2.81 (t, *J* = 8.0 Hz, 2 H), 2.17 (s, 3 H), 2.01 (s, 3 H) ppm

^{13}C NMR (100 MHz, $CDCl_3$)

207.3, 157.2, 140.5, 113.1, 103.8, 88.6, 71.2, 41.4, 29.9, 21.4, 4.5 ppm

IR (Thin Film)

2918, 1715cm^{-1}

HRMS HRMS-ESI+ (m/z): $[M + H]^+$ calcd for $C_{11}H_{13}O_2$, 177.0910; found: 177.0911

TLC R_f = 0.52 (35% ethyl acetate/hexanes); silica gel, UV, PAA

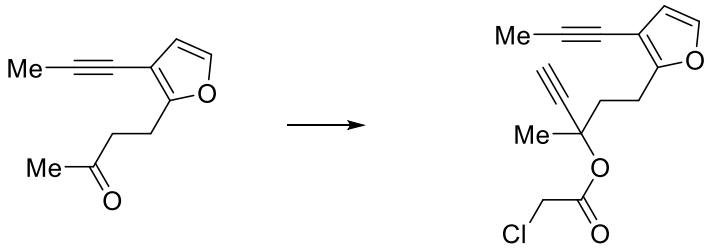

2.66 **2.67**

3-methyl-5-(3-(prop-1-yn-1-yl)furan-2-yl)pent-1-yn-3-yl 2-chloroacetate (2.67). This compound was prepared in a manner similar to that previously reported with some modifications.[73] A flame-dried, 2-necked, 25-mL, round bottomed flask equipped with a magnetic stir bar, nitrogen inlet adapter, and septum was charged with 4-(3-(prop-1-yn-1-yl)furan-2-yl)butan-2-one (**2.66**) (107 mg, 0.607 mmol) and THF (2.0 mL). The solution was cooled by placing the flask in an ice-bath and ethynylmagnesium bromide (3.6 mL of a 0.5 M solution in THF, 1.82 mmol, 3.0 equiv) was added dropwise via syringe over 5 min. After allowing to warm to room temp over 60 min, TLC showed complete consumption of starting material. The flask was placed in an ice-bath and chloroacetyl chloride (0.17 mL, 2.12 mmol, 3.5 equiv) was added dropwise via syringe over 1 min. After 2 h, TLC showed complete consumption of the propargyl alcohol intermediate. Diethyl ether

(5 mL) and deionized water (3 mL) were added to the flask, the mixture was transferred to a separatory funnel, and the organic layer was separated. The aqueous layer was extracted with diethyl ether (3 x 5 mL), washed with brine, dried over magnesium sulfate, filtered, and concentrated *in vacuo*. The crude residue was purified by silica gel flash chromatography (5% ethyl acetate/hexanes) to give 107 mg (63%) of the title compound as a light-yellow oil.

EDD6-448

^{1}H NMR (400 MHz, $CDCl_3$)

7.19 (d, J = 2.0 Hz, 1 H), 6.29 (d, J = 2.0 Hz, 1 H), 4.04-3.96 (ABq, J_{AB} = 14.8 Hz, 2 H), 2.97-2.93 (m, 2 H), 2.64 (s, 1 H), 2.37-2.18 (m, 2 H), 2.02 (s, 3 H), 1.77 (s, 3 H) ppm

^{13}C NMR (100 MHz, $CDCl_3$)

165.4, 157.4, 140.5, 113.1, 103.9, 88.6, 82.2, 76.6, 74.9, 71.3, 41.5, 39.3, 26.3, 22.2, 4.5 ppm

IR (Thin Film)

2120, 1763 cm^{-1}

HRMS HRMS-ESI+ (m/z): $[M + H]^+$ calcd for $C_{15}H_{16}O_3Cl$, 279.0783 found: 279.0790

TLC R_f = 0.68 (35% ethyl acetate/hexanes); silica gel, UV, PAA

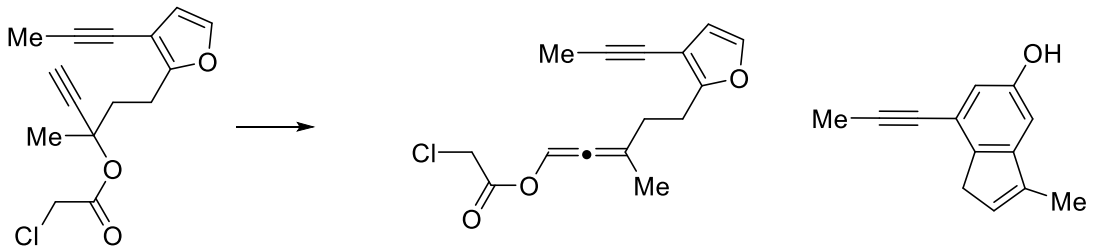

2.67 **2.68** desired product **2.70** isolated product

3-methyl-7-(prop-1-yn-1-yl)-1H-inden-5-ol (2.70). A flame-dried, single-necked, 10-mL, round bottomed flask equipped with a magnetic stir bar was charged with rhodium(II) trifluoroacetate dimer (0.05 equiv, 12.5 mg, 0.019 mmol) in a nitrogen filled glovebox and sealed with a septum before removal. The flask was placed under a nitrogen atmosphere using a nitrogen manifold and an inlet needle. A solution of 3-methyl-5-(3-(prop-1-yn-1-yl)furan-2-yl)pent-1-yn-3-yl 2-chloroacetate (**2.67**) (1 equiv, 103 mg, 0.37 mmol) in toluene (1.85 mL, 0.2 M) was added dropwise via syringe to the flask. The flask was lowered into a preheated oil bath (50 °C). After 23.5 h, consumption of starting material was observed by TLC. The flask was allowed to cool to rt, the volatiles were removed *in vacuo*, and the crude residue immediately purified by silica gel flash chromatography (2-5% ethyl acetate/hexanes) to give 18 mg (26%) of the title compound as a yellow solid.

EDD6-449

^{1}H NMR (400 MHz, $CDCl_3$)

6.76 (d, J = 2.4 Hz, 1 H), 6.71 (d, J = 1.6 Hz, 1 H), 6.25 (d, J = 2.0 Hz, 1 H), 4.81 (bs, 1 H), 3.28 (t, J = 2.0 Hz, 2 H), 2.09 (s, 6 H) ppm

^{13}C NMR (100 MHz, $CDCl_3$)

154.6, 147.7, 139.5, 139.2, 130.7, 119.8, 114.2, 106.5, 106.5 88.5, 37.1, 13.2, 4.6 ppm

IR (Thin Film)

3369, 2236 cm^{-1}

HRMS HRMS-ESI+ (m/z): $[M + H]^+$ calcd for $C_{13}H_{13}O$, 185.0961 found: 185.0976

TLC R_f = 0.50 (35% ethyl acetate/hexanes); silica gel, UV, PAA

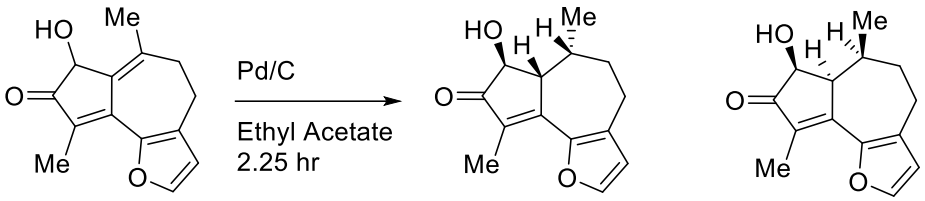

2.43 **2.78**

7-hydroxy-6,9-dimethyl-5,6,6a,7-tetrahydroazuleno[4,5-*b*]furan-8(*4H*)-one (**2.78**). A flame-dried, single-necked, 5-mL, round bottomed flask equipped with a magnetic stir bar was charged with Pd/C (10%) and the flask was evacuated and refilled 3 times with nitrogen. 7-Hydroxy-6,9-dimethyl-5,7-dihydroazuleno[4,5-*b*]furan-8(*4H*)-one (**2.43**) (9 mg, 0.39 mmol) was added in ethyl acetate (0.78 mL, 0.05M) was added to the flask via syringe. The flask was evacuated and refilled 3 times with hydrogen gas. After 2.25 h, TLC showed consumption of starting material. The reaction solution was filtered through a pad of Celite using ethyl acetate (5 mL), the volatiles were removed *in vacuo*, and the crude residue purified by silica gel flash chromatography (30% ethyl acetate/hexanes) to give 4 mg (44%) of the title compound as a yellow oil in a 1.4:1 dr.

EDD4-253

^{1}H NMR (500 MHz, $CDCl_3$)

7.54 (d, *J* = 2.0 Hz, 1.34 H), 7.50 (d, *J* = 1.5 Hz, 1 H), 6.35 (d, *J* = 1.5 Hz, 1 H), 6.34 (d, *J* = 2.0 Hz, 1.44 H), 4.31 (d, *J* = 7.0 Hz, 1 H), 4.11 (d, *J* = 4.0 Hz, 1.57 H), 3.32-3.30 (m, 1.24 H), 2.93-2.91 (m, 1.71 H), 2.81-2.56 (m, 10 H), 2.12 (d, *J* = 2.5 Hz, 4.6 H), 2.08 (d, *J* = 1.5 Hz, 3.5 H), 2.02-1.97 (m, 2.86 H), 1.84-1.78 (m, 2.28 H), 0.89 (d, *J* = 7.0 Hz, 4.86 H), 0.67 (d, *J* = 6.5 Hz, 3.48 H) ppm

^{13}C NMR (125 MHz, $CDCl_3$)

208.3, 207.2, 154.7, 153.1, 148.1, 147.6, 145.0, 144.5, 132.4, 132.3, 131.1, 130.8, 115.0, 114.6, 74.9, 73.2, 54.1, 48.9, 34.6, 32.8, 31.2, 29.5, 22.9, 22.6, 14.5, 11.7, 10.1, 9.3 ppm

IR (Thin Film)

3389, 1687, 1605 cm^{-1}

HRMS HRMS-ESI+ (m/z): $[M + H]^+$ calcd for $C_{14}H_{17}O_3$ 233.1172, found: 233.1195

TLC R_f = 0.20 (35% ethyl acetate/hexanes); silica gel, UV, PAA

3.0 Effect of a remote C8 carboxy group on the asymmetric APKR

3.1 Importance of the C8 group of thapsigargin

The C8 group of Tg is important for a few reasons. First, this position is used to tether a peptide-containing group to Tg to create the inactive prodrug mipsagargin.[10] Second, this group is important to the bioactivity of Tg by hydrogen bonding with water and interacting with hydrophobic residues of SERCA.[7] The stereochemistry at the C8 position of Tg is also important to its inhibitory activity. For example, an analogue with a group having the opposite stereochemistry at C8 of Tg is over 3000 times less potent than Tg at inhibiting SERCA.[128] With conditions in hand for the asymmetric APKR, we investigated the impact of a C8 butanoyl group on the enantioselectivity, reactivity, and yield of this reaction.

3.2 First generation synthesis of a C8 carboxy substituted allene-yne via an aldol reaction using a β-keto ester

To synthesize the C8 (Tg numbering) carboxy substituted allene-yne aldehyde **2.16** was reacted with allyl acetoacetate, triethylamine (Et_3N), and trimethylsilyl chloride (TMSCl) in DMF and DCM (Scheme 34).[129] This multicomponent reaction afforded **3.1** in 30% yield. Decarboxylation of **3.1** using palladium(0) tetrakistriphenylphosphine ($Pd(PPh_3)_4$) and morpholine in THF afforded **3.2** in 59% yield.[130] Addition of ethynylmagnesium bromide to **3.2** followed by trapping of the corresponding alkoxide in situ with acetyl chloride resulted in

diacetylated product **3.4** in 18% yield and none of the desired product **3.3**. Due to the poor yielding steps in this synthetic route and the lability of the trimethylsilyl protecting group, we investigated other ways to synthesize a C8 substituted allene-yne.

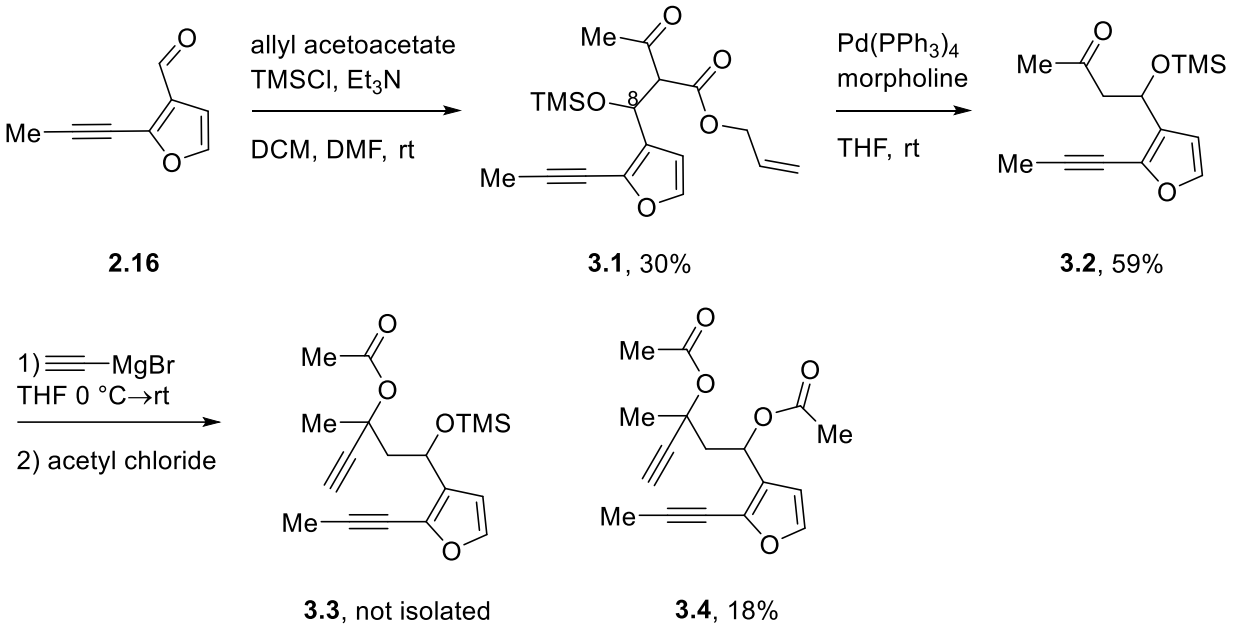

Scheme 34. β-Keto ester route to C8 carboxy containing allene-yne

3.3 Second generation synthesis of a C8 carboxy containing allene-yne via an aldol reaction using acetone

Next, we investigated a more direct route to prepare an allene-yne having a C8 carboxy group. Reacting **2.16** with acetone and 2%$_{(w/w)}$ aqueous NaOH at –10 °C afforded the racemic aldol addition product **3.5** in 72% yield (Scheme 35).[131] It is important to note here that this successful 1,2-addition of acetone to **2.16** lays the foundation for future studies using a chiral organocatalyst to afford the either enantiomer of **3.5** enantioselectively.[86, 87, 132] Esterification of

3.5 with butyric anhydride in the presence of Et_3N and DMAP afforded **3.6** in 72% yield. Addition of ethynylmagnesium bromide to **3.6** and trapping with acetyl chloride or chloroacetyl chloride afforded propargyl acetate **3.7a** in 50% yield and propargyl chloroacetate **3.7b** in 29% yield, respectively. Migration of the C8 butanoyl group to the newly formed tertiary alkoxide did not occur during addition of ethynylmagnesium bromide; this was confirmed at a later stage in the synthesis by the selective hydrolysis of the C2 carboxyester group in **3.9a** that showed the disappearance of the resonance at 1.94 ppm in the ^{1}H NMR spectrum (methyl singlet of C2 acetate group). Rhodium(II)-catalyzed rearrangement of **3.7a** and **3.7b** afforded **3.8a** in 76% yield and **3.8b** in 37% yield.

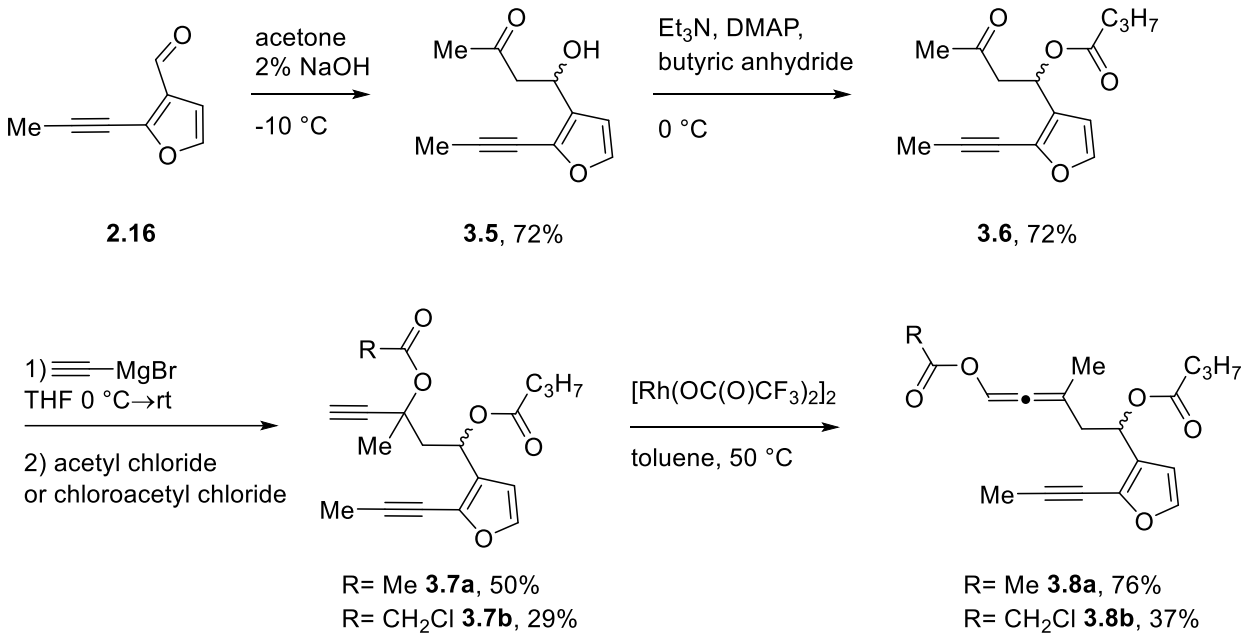

Scheme 35. Aldol addition strategy for the synthesis of C8 butanoyl allene-ynes

3.4 APKR of butanoyl containing allene-yne

Reacting **3.8a** with $Rh(cod)_2BF_4$ and PPh_3 under a CO atmosphere at 70 °C for 7 days afforded APKR adduct **3.9a** in 53% yield with a 2:1 dr according to resonances at 5.94 and 6.02 ppm in the NMR of the crude residue (Table 6, entry 1). Reacting **3.8a** under the optimized conditions established for the Rh(I)-catalyzed asymmetric APKR with 0.15 equiv of (*S*)-MonoPhos alkene (**L1**) as the chiral ligand resulted in a 53% yield of product **3.9a** with a 1:1 dr. Increasing the temperature of the reaction from 70 °C to 90 °C shortened the reaction time from 7 days to 3 days and afforded the product in 44% yield (entry 3). Performing the APKR with 0.3 equiv of **L1** at 90 °C resulted in a slower reaction (6 days vs 3 days) and 19% yield of the desired product (entry 4). Using (*R*)-MonoPhos-alkene afforded **3.9a** in 43% yield with a 1:1 dr (entry 5). The APKR of **3.8b** using PPh_3 as a ligand afforded **3.9b** in 52% yield and a 2:1 dr according to resonances at 5.83 and 5.88 ppm (entry 6). The asymmetric APKR of **3.8b** using (*S*)-MonoPhos alkene (**L1**) afforded **3.9b** in 47% yield and a 1.4:1 dr (entry 7). The yields obtained for compounds **3.9a** and **3.9b** having a C8 carboxy group are slightly lower than APKR products **2.11a**, and **2.11g** not having this group. Unfortunately, the cis and trans isomers of **3.9a** and **3.9b** were inseparable via column chromatography so the er's for each diastereomer cannot be determined with certainty.

Table 6. APKR of C8 substituted allene-ynes

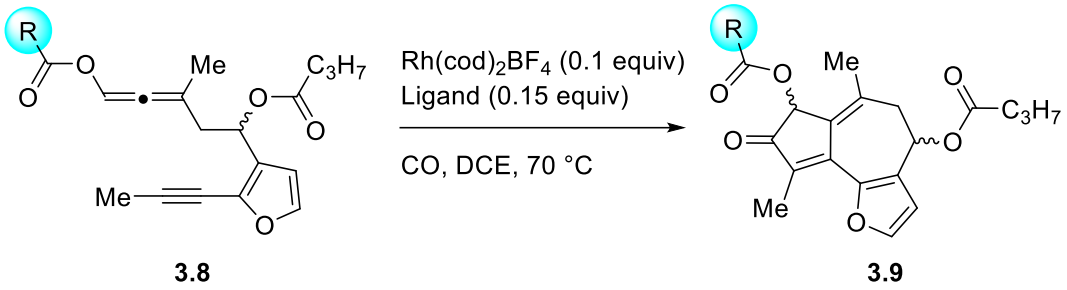

3.8 **3.9**

Entry	R	Ligand	Time	Yield (%)	dr	Approximate er [e]
1	Me	PPh_3	7 d	53%	2:1	-
2	Me	(*S*)-MonoPhos-alkene	7 d	53%	1:1	[c]
3[a]	Me	(*S*)-MonoPhos-alkene	3 d	44%	1:1	[c]
4[a]	Me	(*S*)-MonoPhos-alkene[b]	6 d	19%	1:1	[c]
5	Me	(*R*)-MonoPhos-alkene	5 d	43%	1:1	84:16 and 79:21[d]
6	CH_2Cl	PPh_3	5 d	52%	2:1	-
7	CH_2Cl	(*S*)-MonoPhos-alkene	6 d	47%	1.4:1	78:22 and 63:37[d]

[a] 90 °C, [b] 0.3 equiv, [c] er not determined, [d] er's determined by ^{1}H NMR via chiral shift reagent, [e] Baseline resolution of NMR resonances were not observed

3.4.1 Determination of enantiomeric ratios via chiral shift reagent

Subjecting **3.9a** to several chiral HPLC conditions (Chiralcel OD and ChiralPak IA-3 columns, different solvent systems, concentrations) resulted in incomplete separation of enantiomers. Because of the difficulty in separating all 4 stereoisomers of **3.9a** (2*R*8*R*; 2*S*8*S*; 2*R*8*S*;

2*S*8*R*) by chiral chromatography, we used a chiral shift reagent to determine the approximate er's for products **3.9a** and **3.9b** (entries 5 and 7, Table 6).[133]

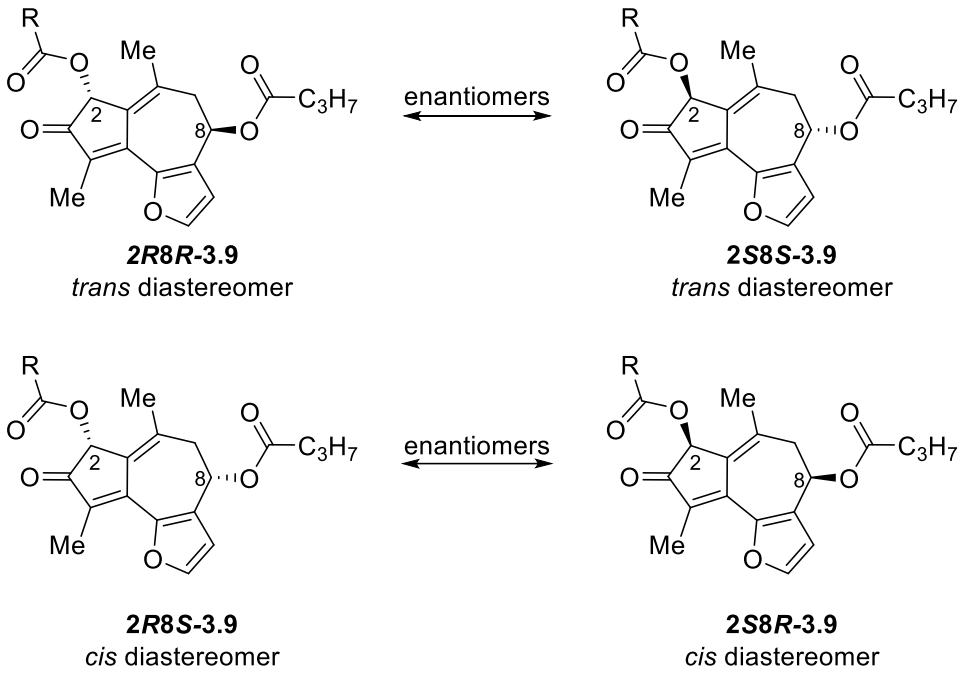

***2R*8*R*-3.9**
trans diastereomer

2*S*8*S*-3.9
trans diastereomer

2*R*8*S*-3.9
cis diastereomer

2*S*8*R*-3.9
cis diastereomer

Figure 22. Structures of all four stereoisomers of the APKR

Chiral shift reagent europium tris[3-(heptafluoropropylhydroxymethylene)-(+)-camphorate ($Eu(hfc)_3$, 10 mg) was dissolved in $CDCl_3$ (0.1 mL) and added to an NMR tube containing **3.9a** in $CDCl_3$ (Figure 23). Gradual addition of aliquots of the preprepared $Eu(hfc)_3/CDCl_3$ solution to **3.9a** in $CDCl_3$ showed the methyl singlet at 1.94 ppm splitting into four resonances at 2.07, 2.06, 2.04, and 2.02 ppm (Figure 24). Because baseline separation was not observed we estimate that the er for both the cis and trans diastereomers is approximately 82:18. This er value is based upon the products being formed with a 1:1 dr as determined by ^1H NMR and that the first set of peaks (2.07 and 2.06 ppm) correspond to the major enantiomer for both the cis and trans diastereomers and the second set of peaks (2.04 and 2.02 ppm) correspond to the minor enantiomer for both the cis and trans diastereomers. Based upon previous studies, the major

enantiomer for both diastereomers is assumed to have the *S* absolute configuration at C2 (Figure 25). Work is ongoing in our lab by Fatemeh Haghighi to confirm that this is the case.

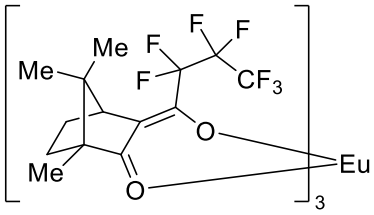

Figure 23. Structure of chiral shift reagent Eu(hfc)$_3$

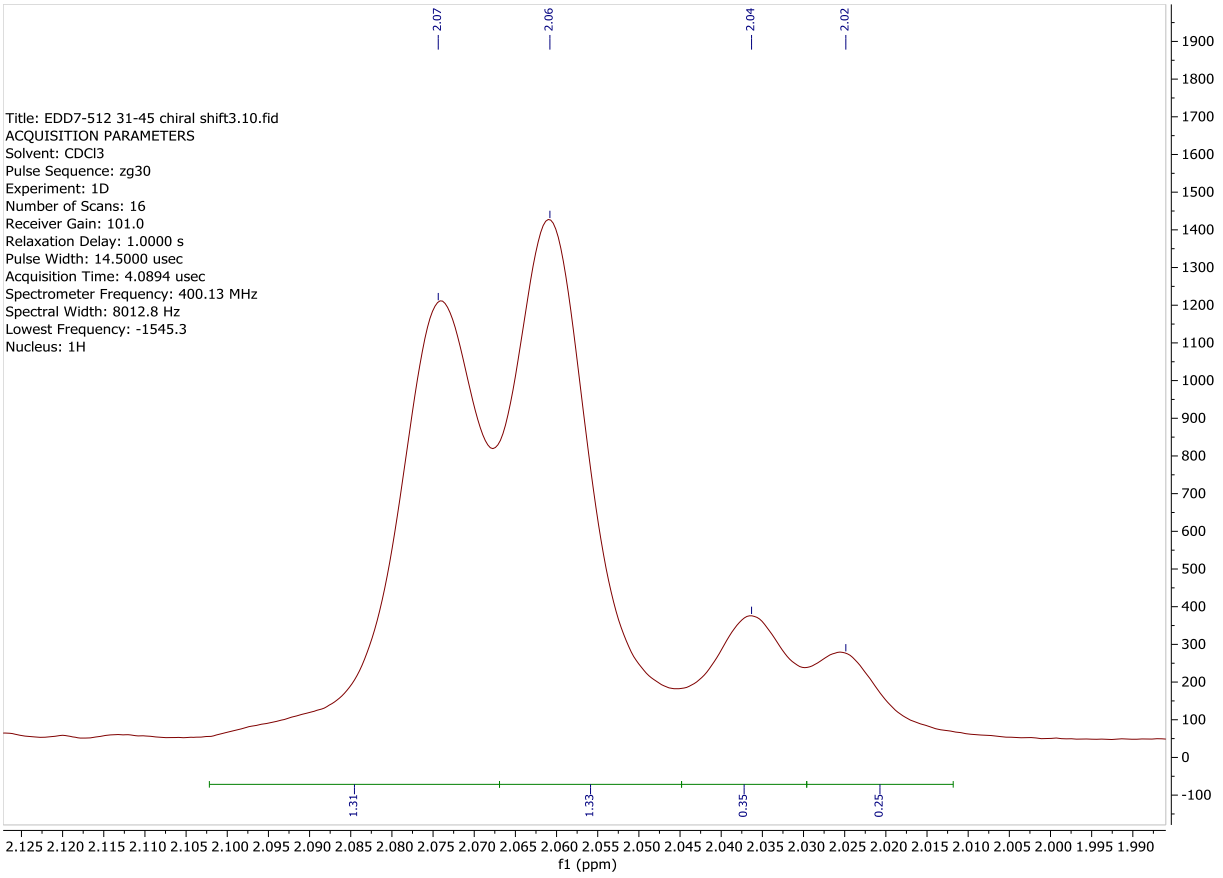

Figure 24. ^{1}H NMR of 3.9a with chiral shift reagent Eu(hfc)$_3$

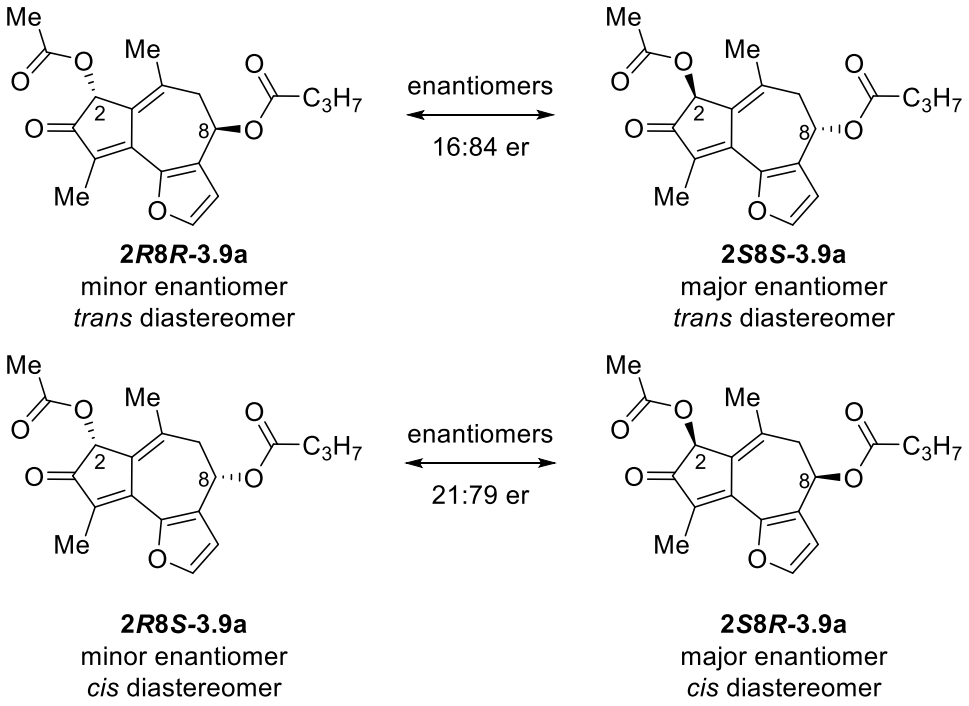

Figure 25. Hypothesized enantiomers and diastereomers of 3.9a

Repeating the protocol described above for determining the er's for **3.9a**, the ^{1}H NMR of **3.9b** showed the resonances for the two diastereomers at 5.88 and 5.83 ppm (hydrogen alpha to the ketone) splitting into four peaks at 6.03, 5.99, 5.97, and 5.94 ppm (Figure 26). The er's based on the integrations of these peaks resulted in a 78:22 er and 63:37 er (Figure 27). It is important to note that the peaks at 5.99 and 5.97 ppm were not fully resolved so these ratios are approximations. The enantiomeric pairs were able to be assigned due to the dr of the purified products being approximately 1.6:1. This corresponds to resonances at 6.03 and 5.99 ppm being enantiomeric pairs and resonances at 5.97 and 5.94 ppm being enantiomeric pairs. The major diastereomer is

predicted to be the *trans* product, and the major enantiomer at C2 is the *R*-enantiomer when (*S*)-MonoPhos-alkene is used.

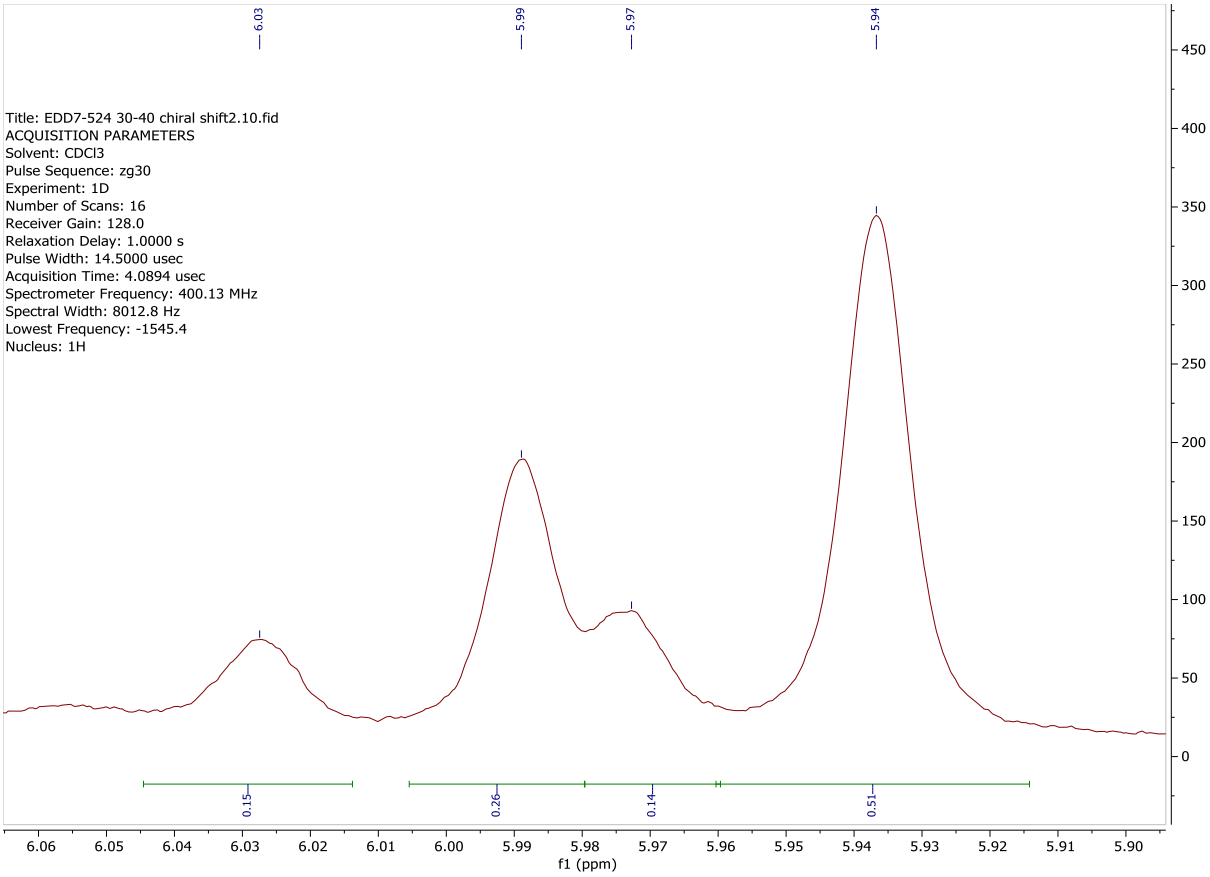

Figure 26. ^{1}H NMR of 3.9b with chiral shift reagent Eu(hfc)$_3$

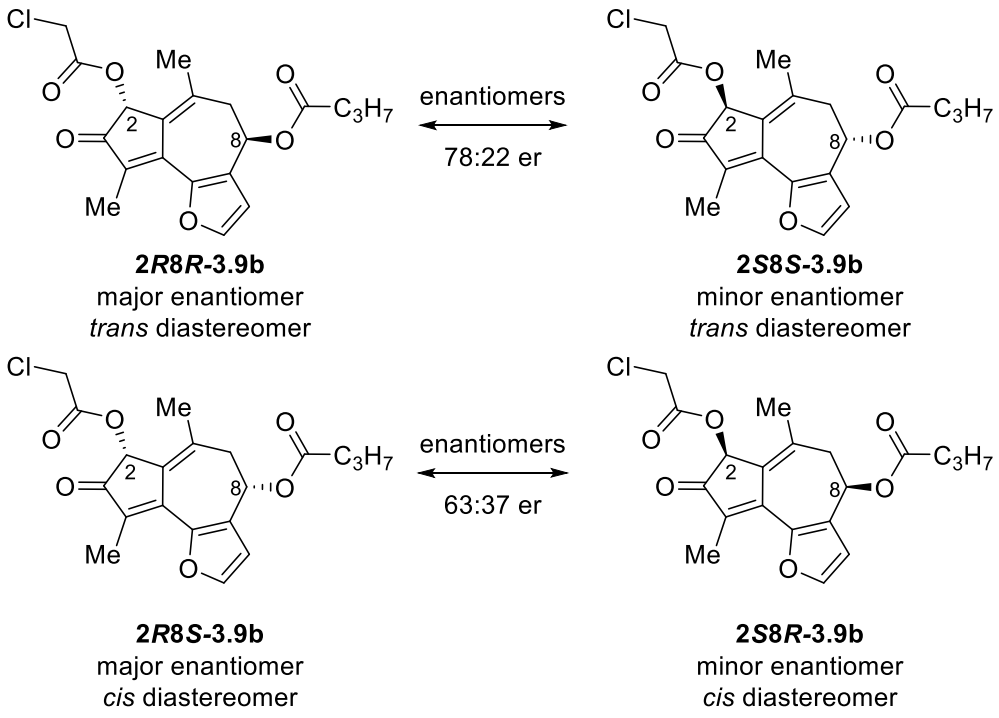

Figure 27. Hypothesized enantiomers and diastereomers of 3.9b

Because we did not get complete baseline resolution, we can only qualitatively interpret the er's of the products of each reaction. The er's for both diastereomers of acetate **3.9a** are similar to allenyl acetate **2.11a** with no remote stereocenter; however, both diastereomers of chloroacetate **3.9b** have much lower er's than the analogous **2.11g**. The remote stereocenter also plays a role in the er of *cis* and *trans* diastereomers. For example, **3.9b** has an er of approximately 78:22 for the major diastereomer and approximately 63:37 for the minor diastereomer. The low er for the minor diastereomer may be due to a destabilizing interaction between the butanoyl group and the phosphoramidite ligand in the transition state leading to the *cis* product (Figure 28). The transition state structures calculated for **2.11g** show the (*S*)-MonoPhos-alkene (**L1**) ligand in position to sterically clash with the butanoyl group at C8 for the *cis* product in **TS1**.

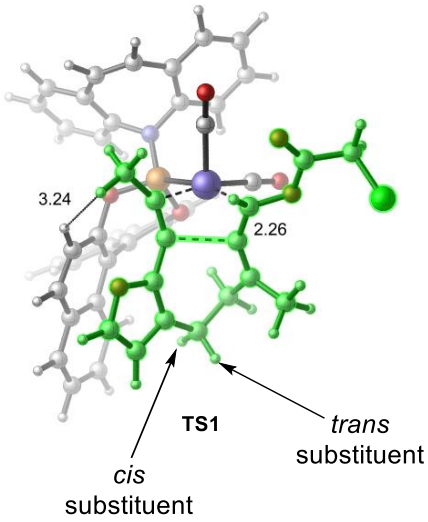

Figure 28. Transition state structure of 2.11g with no remote stereocenter

3.5 Conclusions

The direct addition of acetone to **2.16** using an aldol addition strategy afforded the C8 butanoyl containing allene-ynes in good yield. The APKR of C8 butanoyl allene-ynes **3.8a** and **3.8b** afforded products **3.9a** (allenyl acetate) and **3.9b** (allenyl chloroactate) in moderate yields. The long reaction times for both **3.8a** and **3.8b** could be decreased by using higher reaction temperatures but at the expense of product yield. The er's for the APKR of **3.9a** having a remote stereocenter, a C8 carboxy group, were comparable to that of **2.11a**, not having a group at C8; however, the er's of **3.9b** were much lower than **2.11g**. Work is ongoing in the lab to further develop the asymmetric APKR for C8 substituted allene-ynes and to demonstrate the utility of this asymmetric APKR approach in the synthesis of Tg and Tg analogues.

Supporting Information

Chapter 3

General Methods

All commercially available compounds were purchased and used as received unless otherwise noted. Tetrahydrofuran (THF), diethyl ether (Et_2O), and dichloromethane (DCM, CH_2Cl_2) were purified by passing through alumina using a Sol-Tek ST-002 solvent purification system. Toluene was purified by distilling from calcium hydride. Acetone was purified by refluxing over, and distillation from, $KMnO_4$ and stored over 4 Å molecular sieves. *o*-DCB was degassed using freeze-pump-thaw method (3x). Triphenylphosphine was purified by recrystallization with ethanol. Carbon monoxide (>99.99%) and 10% carbon monoxide in argon were purchased from Matheson. $2\%_{(w/w)}$ NaOH was prepared. Purification of the compounds by flash column chromatography was performed using silica gel (40-63 μm particle size, 60 Å pore size). TLC analyses were performed on silica gel F254 glass plates (250 μm thickness). ^{1}H and ^{13}C NMR spectra were recorded on Bruker Avance 300, 400, or 500 MHz spectrometers. Spectra were referenced to residual chloroform (7.26 ppm, ^{1}H NMR; 77.16 ppm, ^{13}C NMR). Chemical shifts are reported in ppm, multiplicities are indicated by s (singlet), d (doublet), t (triplet), q (quartet), p (pentet), and m (multiplet). Coupling constants, *J*, are reported in hertz (Hz). All NMR spectra were obtained at rt. IR spectra were obtained using a Nicolet Avatar E.S.P. 360 FT-IR or Perkin Elmer Spectrum Two FT-IR. ESI mass spectrometry was performed on a Waters Micromass GCT high resolution mass spectrometer, while ES mass spectrometry was performed on a Waters Q-TOF Ultima API, Micromass UK Limited high resolution mass spectrometer. Chiral HPLC was

performed on a Waters 600 HPLC using a Waters 996 photodiode array detector using a Chiralcel OD chiral column or ChiralPak IA-3 chiral column. Optical rotations were measured using a Jasco P2000 polarimeter.

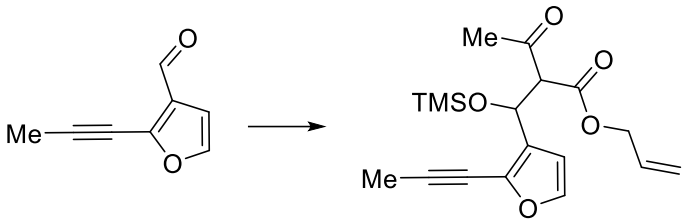

2.16 **3.1**

allyl 3-oxo-2-((2-(prop-1-yn-1-yl)furan-3-yl)((trimethylsilyl)oxy)methyl)butanoate (3.1). This compound was prepared in a manner similar to that previously reported with some modifications.[129] A flame-dried, 2-necked, 10-mL, round bottomed flask equipped with a magnetic stir bar, nitrogen inlet adapter, and septum was charged with triethylamine (0.24 mL, 1.73 mmol), allyl acetoacetate (0.15 mL, 1.13 mmol), TMSCl (0.19 mL, 1.5 mmol), and DMF (0.18 mL, 0.23 mmol). 2-(prop-1-yn-1-yl)furan-3-carbaldehyde (**2.16**) (100 mg, 0.75 mmol) in DCM (1.63 mL, 0.46 M) was added to the flask. After 23 h, aqueous $NaHCO_3$ was added and the contents of the reaction transferred to a separatory funnel. The aqueous layer was extracted with DCM (5 x 3 mL), and the combined organic layers dried over magnesium sulfate, filtered, and concentrated *in vacuo*. The crude residue was purified by silica gel flash chromatography (2.5-10% ethyl acetate/hexanes) to give 86 mg (30%) of the title compound as a yellow oil.

EDD3-189

^{1}H NMR (400 MHz, $CDCl_3$)

7.24-7.23 (m, 1 H), 6.41-6.40 (m, 1 H), 5.98-5.71 (m, 1 H), 5.39-5.35 (m, 1 H), 5.33-5.15 (m, 2 H), 4.72-4.60 (m, 1 H), 4.48-4.45 (m, 1 H), 3.97 (dd, *J* = 6.4, 10.0

Hz, 1 H), 2.35 (s, 1.5 H)*, 2.15 (s, 1.5 H)*, 2.13 (s, 1.5 H)*, 2.09 (s, 1.5 H)*, 0.01 (s, 4.5 H)*, 0.00 (s, 4.5 H)* ppm

*denotes single diastereomer where discernable

^{13}C NMR (100 MHz, $CDCl_3$)

201.5, 200.2, 167.3, 166.1, 143.2, 142.9, 135.4, 135.2, 131.8, 131.6, 128.5, 128.3, 119.0, 118.7, 109.5, 94.4, 94.0, 69.0, 68.8, 68.2, 66.6, 66.6, 66.2, 66.1, 65.5, 31.2, 29.9, 4.8, 4.8, -0.05, -0.1 ppm

IR (Thin Film)

1749, 1721, 843, 764 cm^{-1}

HRMS HRMS-ESI+ (m/z): $[M + Na]^+$ calcd for $C_{18}H_{24}O_5SiNa$, 371.1285, found: 371.1278

TLC R_f = 0.69 (35% ethyl acetate/hexanes); silica gel, UV, PAA

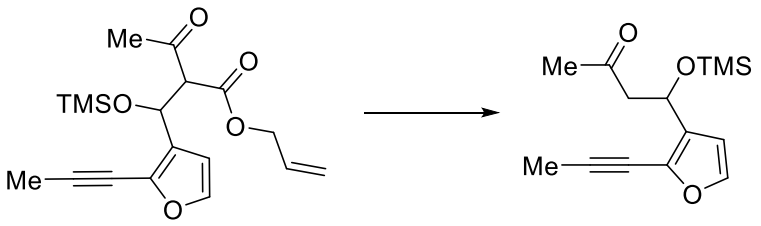

3.1 **3.2**

4-(2-(prop-1-yn-1-yl)furan-3-yl)-4-((trimethylsilyl)oxy)butan-2-one (3.2). This compound was prepared in a manner similar to that previously reported with some modifications.[130] A flame-dried, 2-necked, 50-mL, round bottomed flask equipped with a magnetic stir bar, nitrogen inlet adapter, and septum was charged with allyl 3-oxo-2-((2-(prop-1-yn-1-yl)furan-3-yl)((trimethylsilyl)oxy)methyl)butanoate (**3.1**) (86 mg, 0.25 mmol) in THF (12.4 mL, 0.02M), morpholine (64 µL, 0.74 mmol), and $Pd(PPh_3)_4$ (29 mg, 0.025 mmol). After 30 minutes, TLC showed complete consumption of starting material. The solution was concentrated *in vacuo*, and

the crude residue was purified by silica gel flash chromatography (2.5-15% ethyl acetate/hexanes) to give 86 mg (30%) of the title compound as a clear oil.

EDD3-191

^{1}H NMR (500 MHz, $CDCl_3$)

7.23 (d, *J* = 2.0 Hz, 1 H), 6.41 (d, *J* = 2.0 Hz, 1 H), 5.22 (dd, *J* = 4.0, 5.0 Hz, 1 H), 2.99-2.94 (m, 1 H), 2.57-2.53 (m, 1 H), 2.17 (s, 3 H), 2.12 (s, 3 H), 0.04 (s, 9 H) ppm

^{13}C NMR (125 MHz, $CDCl_3$)

206.8, 142.8, 133.8, 131.2, 109.5, 94.0, 69.1, 63.8, 52.2, 31.5, 4.8, 0.01 ppm

IR (Thin Film)

1717, 841, 764 cm^{-1}

HRMS HRMS-ESI+ (m/z): $[M + H]^+$ calcd for $C_{14}H_{21}O_3Si$, 265.1260 found: 263.1092. All other data supports the proposed structure, but the HRMS is 2 atomic units lower than predicted.

TLC R_f = 0.7 (35% ethyl acetate/hexanes); silica gel, UV, PAA

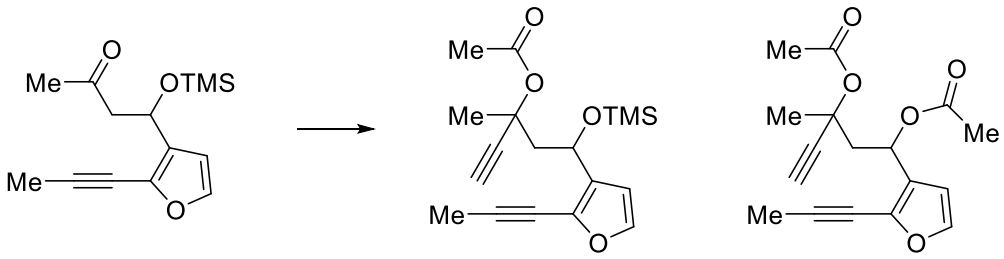

3.2 **3.3**, not isolated **3.4**, 18%

3-methyl-1-(2-(prop-1-yn-1-yl)furan-3-yl)pent-4-yne-1,3-diyl diacetate (3.4). A flame-dried, 2-necked, 50-mL, round bottomed flask equipped with a magnetic stir bar, nitrogen inlet adapter, and septum was charged with 4-(2-(prop-1-yn-1-yl)furan-3-yl)-4-((trimethylsilyl)oxy)butan-2-one (**3.2**) (30 mg, 0.113 mmol) in THF (0.38 mL, 0.3M). The solution

was cooled by placing the flask in an ice-bath and ethynylmagnesium bromide (0.68 mL of a 0.5 M solution in THF, 0.34 mmol, 3 equiv) was added dropwise via syringe over 3 min. After allowing to warm to rt over 90 min, TLC showed complete consumption of starting material. The flask was placed in an ice-bath and acetyl chloride (40 µL, 0.57 mmol) was added dropwise via syringe over 1 min. After 2.5 h, TLC showed complete consumption of the propargyl alcohol intermediate. Diethyl ether (3 mL) and deionized water (3 mL) were added to the flask, the mixture was transferred to a separatory funnel, and the organic layer was separated. The aqueous layer was extracted with diethyl ether (3 x 3 mL), washed with brine (1 x 2 mL), the combined aqueous layers back extracted with diethyl ether (1 x 3 mL), dried over magnesium sulfate, filtered, and concentrated *in vacuo*. The crude residue was purified by silica gel flash chromatography (2.5-25% ethyl acetate/hexanes) to give 6 mg (18%) of the title compound as a yellow oil.

EDD3-193

^{1}H NMR (500 MHz, $CDCl_3$)

7.25 (d, *J* = 2.0 Hz, 1 H), 6.38 (d, *J* = 2.0 Hz, 1 H), 6.16 (dd, *J* = 2.0, 5.5 Hz, 1 H), 2.65-2.61 (m, 1 H), 2.56 (s, 1 H), 2.45-2.41 (m, 1 H), 2.12 (s, 3 H), 2.04 (s, 3 H), 1.94 (s, 3 H), 1.74 (s, 3 H) ppm

^{13}C NMR (125 MHz, $CDCl_3$)

169.9, 169.2, 142.7, 135.2, 127.7, 109.9, 94.1, 83.4, 73.9, 73.0, 68.9, 65.3, 45.2, 26.9, 21.9, 21.3, 4.8 ppm; impurity at 29.8 ppm

IR (Thin Film)

3283, 1741 cm^{-1}

HRMS HRMS-ESI+ (m/z): $[M + H]^+$ calcd for $C_{17}H_{18}O_5Na$, 325.1046 found: 325.1047

TLC R_f = 0.52 (35% ethyl acetate/hexanes); silica gel, UV, PAA

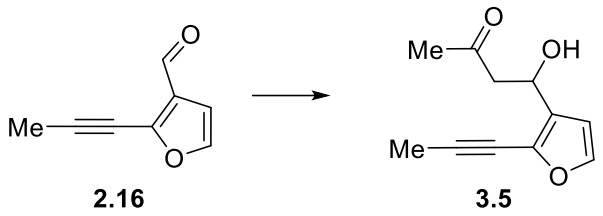

4-hydroxy-4-(2-(prop-1-yn-1-yl)furan-3-yl)butan-2-one (3.5). This compound was prepared in a manner similar to that previously reported with some modifications.[131] A flame-dried, 2-necked, 10-mL, round bottomed flask equipped with a magnetic stir bar, nitrogen inlet adapter, and septum was charged with 2-(prop-1-yn-1-yl)furan-3-carbaldehyde (**2.16**) (97 mg, 0.72 mmol) and acetone (1.25 mL, 0.58 M). The flask was lowered into a -10 °C bath and 2% aqueous $NaOH_{(w/w)}$ (0.17 mL, 4.2 M) was added dropwise. After 5.5 h, TLC showed complete consumption of starting material. The solution was neutralized with aqueous 0.5 M HCl, concentrated, diluted with H_2O, extracted with ethyl acetate (5 x 3 mL), dried over magnesium sulfate, filtered, and concentrated *in vacuo*. The crude residue was purified by silica gel flash chromatography (10-30% ethyl acetate/hexanes) to give 100 mg (72%) of the title compound as a yellow oil.

EDD4-277

^{1}H NMR (300 MHz, $CDCl_3$)

7.27 (s, 1 H), 6.45 (d, *J* = 3.0 Hz, 1 H), 5.23-5.18 (m, 1 H), 3.20 (d, *J* = 3.6 Hz, 1 H), 3.00-2.77 (m, 2 H), 2.22 (s, 3 H), 2.11 (s, 3 H) ppm

^{13}C NMR (500 MHz, $CDCl_3$)

209.1, 142.9, 134.1, 130.0, 109.5, 94.0, 69.1, 62.9, 50.2, 30.8, 4.8 ppm

IR (Thin Film)

3416, 2235, 1707 cm^{-1}

HRMS HRMS-ESI+ (m/z): $[M + H]^+$ calcd for $C_{11}H_{11}O_3$, 191.0708 found: 191.0708

TLC R_f = 0.19 (35% ethyl acetate/hexanes); silica gel, UV, PAA

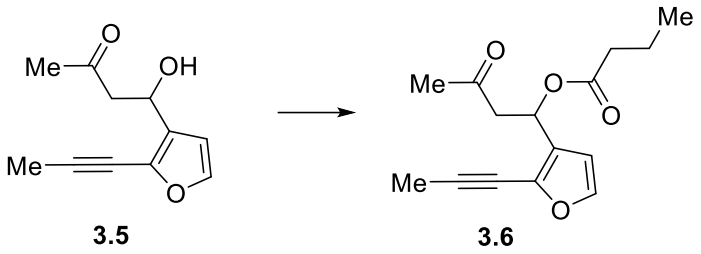

3-oxo-1-(2-(prop-1-yn-1-yl)furan-3-yl)butyl butyrate (3.6). A flame-dried, 2-necked, 10-mL, round bottomed flask equipped with a magnetic stir bar, nitrogen inlet adapter, and septum was charged with 4-hydroxy-4-(2-(prop-1-yn-1-yl)furan-3-yl)butan-2-one (**3.5**) (108 mg, 0.56 mmol) in DCM (0.94 mL, 0.6 M), triethylamine (0.09 mL, 0.62 mmol, 1.1 equiv), and 4-dimethylaminopyridine (21 mg, 0.17 mmol, 0.3 equiv). The flask was cooled by placing in an ice-bath and butyric anhydride (0.1 mL, 0.62 mmol, 1.1 equiv) was added dropwise. After 5 min, TLC showed complete consumption of starting material. Saturated aqueous ammonium chloride (3 mL) was added and the solution transferred to a separatory funnel, extracted with diethyl ether (5 x 3 mL), dried over magnesium sulfate, filtered and concentrated. The crude residue was purified by silica gel flash chromatography (15% ethyl acetate/hexanes) to give 112 mg (76%) of the title compound as a yellow oil and unsaturated ketone **2.26** (9%) as a byproduct.

EDD4-284

^{1}H NMR (400 MHz, $CDCl_3$)

7.24 (d, *J* = 2.0 Hz, 1 H), 6.36 (d, *J* = 2.0 Hz, 1 H), 6.25-6.21 (m, 1 H), 3.14-3.07 (m, 1 H), 2.89-2.84 (m, 1 H), 2.26 (t, *J* = 6.8 Hz, 2 H), 2.18 (s, 3 H), 2.13 (s, 3 H), 1.67-1.60 (m, 2 H), 0.91 (t, *J* = 8.0 Hz, 3 H) ppm

^{13}C NMR (100 MHz, $CDCl_3$)

204.6, 172.6, 143.8, 142.8, 135.2, 133.4, 127.6, 126.8, 125.1, 109.9, 108.1, 94.3, 68.9, 64.6, 48.5, 36.3, 30.4, 27.6, 18.5, 18.3, 13.7, 5.0, 4.9 ppm

IR (Thin Film)

2235, 1729 cm^{-1}

HRMS HRMS-ESI+ (m/z): $[M + H]^+$ calcd for $C_{15}H_{18}O_4Na$, 285.1103, found: 285.1085

TLC R_f = 0.48 (35% ethyl acetate/hexanes); silica gel, UV, PAA

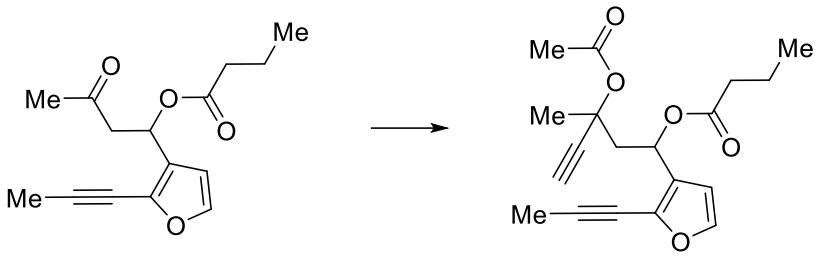

3.6 **3.7a**

3-acetoxy-3-methyl-1-(2-(prop-1-yn-1-yl)furan-3-yl)pent-4-yn-1-yl butyrate (3.7a). A flame-dried, 2-necked, 25-mL, round bottomed flask equipped with a magnetic stir bar, nitrogen inlet adapter, and septum was charged with 3-oxo-1-(2-(prop-1-yn-1-yl)furan-3-yl)butyl (**3.6**) (345 mg, 1.32 mmol) and THF (4.4 mL). The solution was cooled by placing the flask in an ice-bath and ethynylmagnesium bromide (7.9 mL of a 0.5 M solution in THF, 3.96 mmol, 3 equiv), was added dropwise via syringe over 5 min. After allowing to warm to rt over 90 min, TLC showed complete consumption of starting material. The flask was placed in an ice-bath and acetyl chloride (0.47 mL, 6.6 mmol) was added dropwise via syringe over 2 min. After 2 h, TLC showed complete consumption of the propargyl alcohol intermediate. Diethyl ether (5 mL) and deionized water (5 mL) were added to the flask, the mixture was transferred to a separatory funnel, and the organic layer was separated. The aqueous layer was extracted with diethyl ether (3 x 15 mL), washed with brine, and the combined aqueous layers back extracted with diethyl ether (1 x 15 mL). The combined organic layers were dried over magnesium sulfate, filtered, and concentrated *in vacuo*. The crude residue was purified by silica gel flash chromatography (5-20% ethyl acetate/hexanes) to give 217 mg (50%) of the title compound as a brown liquid.

EDD4-285

^{1}H NMR (300 MHz, $CDCl_3$)

7.23 (d, *J* = 2.1 Hz, 1 H), 6.37 (d, *J* = 2.8 Hz, 1 H), 6.22-6.13 (m, 1 H), 2.62 (s, 1 H), 2.60-2.42 (m, 2 H), 2.65 (t, *J* = 7.5 Hz, 2 H), 2.12 (s, 3 H), 1.94 (s, 3 H), 1.74 (s, 3 H), 1.67-1.60 (m, 2 H), 0.92 (t, *J* = 7.2, 3 H) ppm

^{13}C NMR (75 MHz, $CDCl_3$)

172.5, 169.3, 142.7, 142.6, 135.2, 128.0, 127.9, 109.9, 109.8, 94.1, 82.9, 74.3, 73.9, 73.0, 73.0, 65.4, 65.1, 45.5, 45.2, 36.4, 27.4, 26.8, 21.9, 18.4, 13.8, 4.8 ppm

IR (Thin Film)

1740, 1236 cm^{-1}

HRMS HRMS-ESI+ (m/z): $[M + H]^+$ calcd for $C_{19}H_{22}O_5Na$, 353.1365, found: 353.1335

TLC R_f = 0.54 (35% ethyl acetate/hexanes); silica gel, UV, PAA

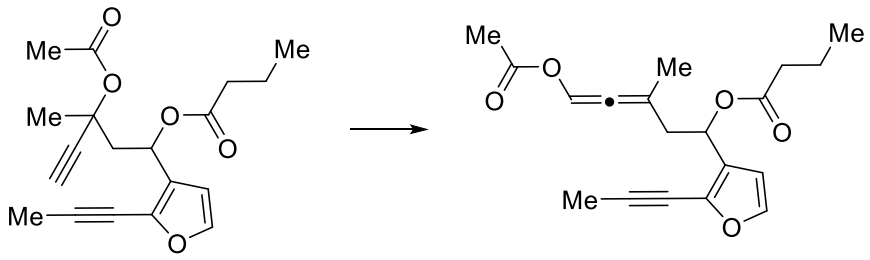

3.7a **3.8a**

5-acetoxy-3-methyl-1-(2-(prop-1-yn-1-yl)furan-3-yl)penta-3,4-dien-1-yl butyrate (3.8a). Follows General Procedure A: Rhodium(II) trifluoroacetate dimer (4.0 mg, 0.006 mmol), 3-acetoxy-3-methyl-1-(2-(prop-1-yn-1-yl)furan-3-yl)pent-4-yn-1-yl butyrate (**3.7a**) (42 mg, 0.127 mmol), toluene (0.64 mL, 0.2 M). Silicycle SiliaMetS silica gel (200 mg, 40 equiv, 1.19 mmol/g) was added to the flask and stirred overnight. The solution was filtered through celite and the crude residue was purified by silica gel flash chromatography (3-5% ethyl acetate/hexanes) to give 32 mg (76%) of the title compound as a clear liquid.

EDD4-272

^{1}H NMR (500 MHz, $CDCl_3$)

7.29-7.28 (m, 1 H), 7.24 (d, *J* = 2.0 Hz, 0.5 H)*, 7.23 (d, *J* = 2.0 Hz, 0.5 H)*, 6.37 (d, *J* = 2.0 Hz, 0.5 H)*, 6.36 (d, *J* = 2.0 Hz, 0.5 H)*, 6.01-5.97 (m, 1 H), 2.75-2.68 (m, 1 H), 2.57-2.48 (m, 1 H), 2.30-2.26 (m, 2 H), 2.11 (s, 3 H), 2.10 (s, 3 H), 1.86 (d, *J* = 2.0 Hz, 1.5 H)*, 1.85 (d, *J* = 2.0 Hz, 1.5 H)*, 1.67-1.60 (m, 2 H), 0.94-0.91 (m, 3 H) ppm

*denotes single diastereomer where discernable

^{13}C NMR (125 MHz, $CDCl_3$)

191.5, 191.4, 172.8, 172.7, 168.7, 168.7, 142.6, 142.6, 135.8, 135.5, 127.1, 127.0, 110.9, 110.0, 109.8, 109.7, 109.7, 94.0, 69.0, 69.0, 66.5, 66.4, 40.6, 40.6, 36.4, 36.3, 21.0, 21.0, 20.8, 20.7, 18.5, 13.8, 4.8, 4.8 ppm

IR (Thin Film)

1744, 1215 cm^{-1}

HRMS HRMS-ESI+ (m/z): $[M + H]^+$ calcd for $C_{19}H_{22}O_5Na$, 353.1365 found: 353.1334

TLC R_f = 0.58 (35% ethyl acetate/hexanes); silica gel, UV, PAA

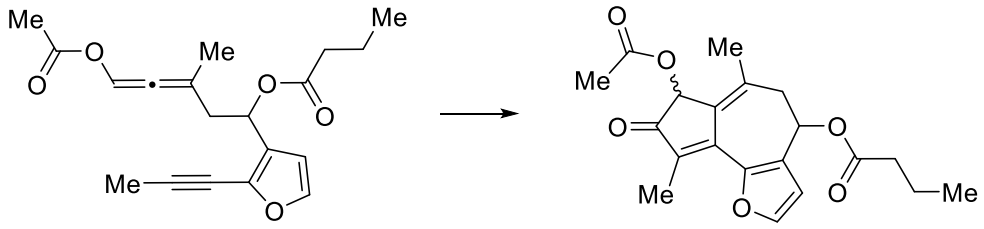

3.8a **3.9a**

7-acetoxy-6,9-dimethyl-8-oxo-4,5,7,8-tetrahydroazuleno[4,5-b]furan-4-yl butyrate (3.9a). Follows general procedure B: Bis(1,5-cyclooctadiene)rhodium(I) tetrafluoroborate (1.9

mg, 0.0048 mmol), triphenyl phosphine (1.9 mg, 0.0072 mmol), carbon monoxide (100%), 5-acetoxy-3-methyl-1-(2-(prop-1-yn-1-yl)furan-3-yl)penta-3,4-dien-1-yl butyrate (**3.8a**) (16 mg, 0.048 mmol), DCE (2.4 mL, 0.02 M). The reaction was stirred for 165 h in an oil bath (70 °C). The crude residue was purified via silica gel flash chromatography (10-20% ethyl acetate/hexanes) to give the title compound (9 mg, 53%) as a yellow oil in an approximately 2:1 dr.

EDD4-275

^{1}H NMR (500 MHz, $CDCl_3$)

7.58 (d, *J* = 2.0 Hz, 1 H), 6.55 (d, *J* = 1.5 Hz, 0.36 H), 6.54 (d, *J* = 2.0 Hz, 0.61 H), 6.02 (t, *J* = 5.5 Hz, 0.35 H), 5.94 (dd, *J* = 2.5 Hz, 8.5 Hz, 0.70 H), 5.82 (s, 0.34 H), 5.80 (s, 0.61 H), 2.92-2.68 (m, 2 H), 2.35-2.31 (m, 2 H), 2.22 (s, 3 H), 2.15 (s, 1 H), 2.15 (s, 2 H), 1.94 (d, *J* = 3.0 Hz, 3 H), 1.70-1.64 (m, 2 H), 0.95 (q, *J* = 7.5 Hz, 3 H) ppm

^{13}C NMR (125 MHz, $CDCl_3$)

199.6, 199.5, 173.1, 173.0, 169.9, 169.8, 148.2, 146.9, 145.0, 145.0, 134.0, 133.9, 133.0, 132.4, 130.7, 130.5, 128.4, 128.3, 112.6, 112.6, 71.8, 71.7, 66.0, 65.8, 40.1, 39.8, 36.4, 36.4, 25.2, 24.9, 20.8, 18.6, 18.6, 13.8, 13.8, 10.3 ppm

IR (Thin Film)

2931, 1739, 1699 cm^{-1}

HRMS HRMS-ESI+ (m/z): $[M + H]^+$ calcd for $C_{20}H_{22}O_6Na$, 381.1281 found: 381.1314

TLC R_f = 0.43 (35% ethyl acetate/hexanes); silica gel, UV, PAA

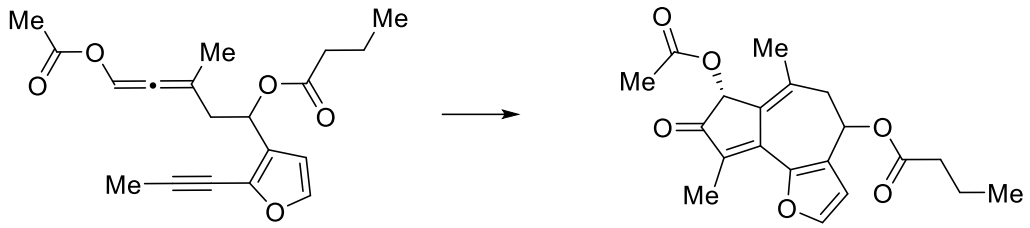

3.8a **3.9a**

(7*R*)-7-acetoxy-6,9-dimethyl-8-oxo-4,5,7,8-tetrahydroazuleno[4,5-b]furan-4-yl butyrate (3.9a). Follows general procedure C: Bis(1,5-cyclooctadiene)rhodium(I) tetrafluoroborate (1.9 mg, 0.0048 mmol), (*S*)-MonoPhos-alkene (3.0 mg, 0.0072 mmol), carbon monoxide (100%), 5-acetoxy-3-methyl-1-(2-(prop-1-yn-1-yl)furan-3-yl)penta-3,4-dien-1-yl butyrate (**3.8a**) (16 mg, 0.048 mmol), DCE (4.8 mL, 0.01 M). The reaction was stirred for 7 d in an oil bath (70 °C). The crude residue was purified via silica gel flash chromatography (10-20% ethyl acetate/hexanes) to give the title compound (9 mg, 53%) as a yellow oil. The ^{1}H NMR matched that of racemic **3.9a**.

EDD4-279

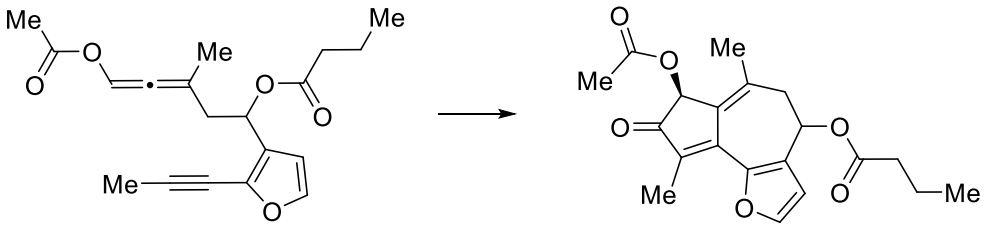

3.8a **3.9a**

(7*S*)-7-acetoxy-6,9-dimethyl-8-oxo-4,5,7,8-tetrahydroazuleno[4,5-b]furan-4-yl butyrate (3.9a). Follows general procedure C: Bis(1,5-cyclooctadiene)rhodium(I) tetrafluoroborate (2.4 mg, 0.0058 mmol), (*R*)-MonoPhos-alkene (3.6 mg, 0.0087 mmol), carbon monoxide (100%), 5-acetoxy-3-methyl-1-(2-(prop-1-yn-1-yl)furan-3-yl)penta-3,4-dien-1-yl butyrate (**3.8a**) (19 mg, 0.058 mmol), DCE (5.8 mL, 0.01 M). The reaction was stirred for 115 in an oil bath (70 °C). The crude residue was purified via silica gel flash chromatography (5-15%

ethyl acetate/hexanes) to give the title compound (9 mg, 43%) as a yellow oil. The ^{1}H NMR matched that of racemic **3.9a**.

EDD7-512

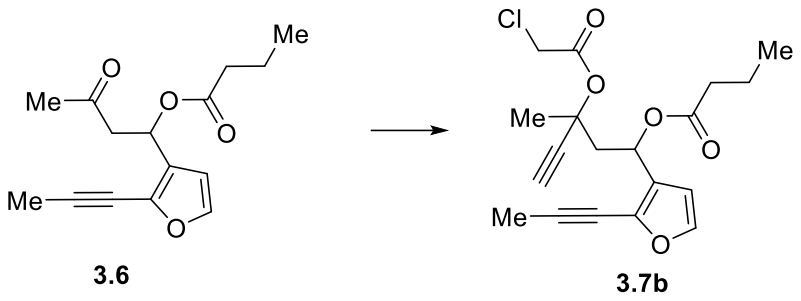

3-(2-chloroacetoxy)-3-methyl-1-(2-(prop-1-yn-1-yl)furan-3-yl)pent-4-yn-1-yl butyrate (3.7b). A flame-dried, 2-necked, 50-mL, round bottomed flask equipped with a magnetic stir bar, nitrogen inlet adapter, and septum was charged with 3-oxo-1-(2-(prop-1-yn-1-yl)furan-3-yl)butyl (**3.6**) (627 mg, 470 mg accounting for contaminant **2.26** in starting material, 2.4 mmol) and THF (8.0 mL). The solution was cooled by placing the flask in an ice-bath and ethynylmagnesium bromide (14.4 mL of a 0.5 M solution in THF, 7.2 mmol, 3 equiv), was added dropwise via syringe over 5 min. After allowing to warm to rt over 60 min, TLC showed complete consumption of starting material. The flask was placed in an ice-bath and chloroacetyl chloride (0.67 mL, 8.4 mmol) was added dropwise via syringe over 2 min. After 2 h, TLC showed complete consumption of the propargyl alcohol intermediate. Diethyl ether (5 mL) and deionized water (5 mL) were added to the flask, the mixture was transferred to a separatory funnel, and the organic layer was separated. The aqueous layer was extracted with diethyl ether (3 x 15 mL), and the combined organic layers were washed with brine, dried over magnesium sulfate, filtered, and concentrated *in vacuo*. The crude residue was purified by silica gel flash chromatography (5-30%

ethyl acetate/hexanes) to give 190 mg (29% accounting for contaminant in SM) of the title compound as a brown liquid.

EDD7-521

^{1}H NMR (400 MHz, $CDCl_3$)

7.25 (d, *J* = 2.0 Hz, 1 H), 6.38-6.37 (m, 1 H), 6.20 (t, *J* = 6.0 Hz, 0.5 H), 6.13 (t, *J* = 6.0 Hz, 0.5 H), 3.95-3.85 (m, 2 H), 2.67-2.46 (m, 2 H), 2.66 (s, 0.5 H), 2.61 (s, 0.5 H), 2.27 (t, *J* = 8.0, 2 H), 2.12 (d, *J* = 2.8 Hz, 3 H), 1.78 (s, 3 H), 1.63 (s, *J* = 7.2, 7.6, 7.6 Hz, 2 H), 0.92 (t, *J* = 7.6 Hz, 3 H) ppm

^{13}C NMR (100 MHz, $CDCl_3$)

172.5, 172.5, 165.3, 165.3, 142.8, 142.7, 135.3, 135.3, 127.8, 127.6, 109.8, 109.8, 94.3, 82.5, 81.9, 75.3, 75.3, 75.2, 74.9, 68.9, 68.9, 65.2, 64.9, 45.3, 44.9, 41.4, 41.3, 36.4, 27.3, 26.7, 18.4, 18.4, 13.8, 4.8 ppm

IR (Thin Film)

2121, 1765, 1733 cm^{-1}

HRMS HRMS-ESI+ (m/z): $[M + H]^+$ calcd for $C_{19}H_{21}O_5ClNH_4$, 382.1416 found: 382.1404

TLC R_f = 0.53 (35% ethyl acetate/hexanes); silica gel, UV, PAA

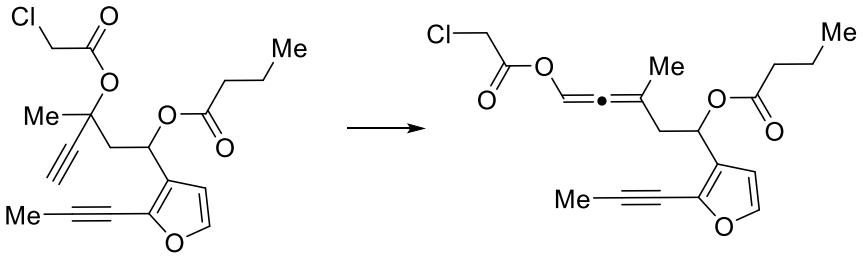

3.7b **3.8b**

5-(2-chloroacetoxy)-3-methyl-1-(2-(prop-1-yn-1-yl)furan-3-yl)penta-3,4-dien-1-yl butyrate (3.8b). Follows General Procedure A: Rhodium(II) trifluoroacetate dimer (4.0 mg, 0.006

mmol), 3-acetoxy-3-methyl-1-(2-(prop-1-yn-1-yl)furan-3-yl)pent-4-yn-1-yl butyrate (**3.7b**) (42 mg, 0.127 mmol), toluene (0.64 mL, 0.2 M). The crude residue was purified by silica gel flash chromatography (3-10% ethyl acetate/hexanes). The product was blue-green in color. The product was dissolved in toluene (2.5 mL, 0.2 M) and Silicycle SiliaMetS silica gel (580 mg, 40 equiv, 1.28 mmol/g) was added to the flask and stirred for 4 h. The solution was filtered through celite and the crude residue was purified by silica gel flash chromatography (2-10% ethyl acetate/hexanes) to give 67 mg (37%) of the title compound as a clear liquid.

EDD7-522

^{1}H NMR (400 MHz, $CDCl_3$)

7.30-7.29 (m, 0.5 H)*, 7.25-7.23 (m, 1.5 H), 6.37 (d, J = 1.6 Hz, 0.5 H)*, 6.36 (d, J = 2.0 Hz, 0.5 H)*, 5.98 (t, J = 6.8 Hz, 1 H), 4.14-4.06 (ABq, J_{AB} = 14.8 Hz, 1 H)*, 4.11 (s, 1H)*, 2.76-2.69 (m, 1 H), 2.60-2.50 (m, 1 H), 2.28 (t, J = 7.6 Hz, 1 H)*, 2.28 (t, J = 7.6 Hz, 1 H)*, 2.12 (s, 1.5 H)*, 2.11 (s, 1.5 H)*, 1.87 (t, J = 1.6, 3 H), 1.69-1.59 (m, 2 H), 0.93 (t, J = 7.6 Hz, 3 H) ppm

*denotes single diasteromer where discernable

^{13}C NMR (100 MHz, $CDCl_3$)

191.6, 191.3, 172.7, 172.7, 165.1, 142.7, 142.7, 136.0, 127.0. 126.8, 112.3, 112.2, 110.4, 110.3, 109.7, 109.6, 94.1, 69.0, 68.9, 66.4, 66.3, 40.8, 40.8, 40.5, 40.4, 36.4, 36.3, 20.8, 20.7, 18.5, 13.8, 4.8, 4.8 ppm

IR (Thin Film)

1982, 1771, 1739 cm^{-1}

HRMS HRMS-ESI+ (m/z): $[M + H]^+$ calcd for $C_{19}H_{21}O_5ClNH_4$, 384.1416 found: 384.1404

TLC R_f = 0.53 (35% ethyl acetate/hexanes); silica gel, UV, PAA

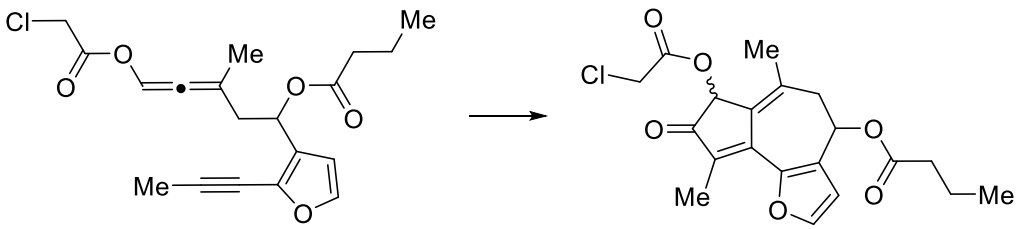

7-(2-chloroacetoxy)-6,9-dimethyl-8-oxo-4,5,7,8-tetrahydroazuleno[4,5-b]furan-4-yl butyrate (3.9b). Follows general procedure B: Bis(1,5-cyclooctadiene)rhodium(I) tetrafluoroborate (2.2 mg, 0.0055 mmol), triphenyl phosphine (2.2 mg, 0.0083 mmol), carbon monoxide (100%), 5-(2-chloroacetoxy)-3-methyl-1-(2-(prop-1-yn-1-yl)furan-3-yl)penta-3,4-dien-1-yl butyrate (**3.8b**) (20 mg, 0.055 mmol), DCE (2.8 mL, 0.02 M). The reaction was stirred for 114 h in an oil bath (70 °C). The crude residue was purified via silica gel flash chromatography (5-20% ethyl acetate/hexanes) to give the title compound (11.5 mg, 52%) as a yellow oil and a 2:1 dr by crude NMR and ~3.5:1 dr after purification.

EDD7-523

^{1}H NMR (300 MHz, $CDCl_3$)

7.59 (d, *J* = 1.5 Hz, 1 H), 6.55 (d, *J* = 1.5 Hz, 1 H), 6.02 (t, *J* = 6.0 Hz, 0.23 H), 5.95 (dd, *J* = 2.5 Hz, 8.0 Hz, 0.83 H), 5.88 (s, 0.21 H), 5.83 (s, 0.77 H), 4.17-4.10 (m, 2 H), 2.93-2.71 (m, 2 H), 2.36-2.31 (m, 2 H), 2.23 (s, 3 H), 1.97 (s, 2.42 H), 1.96 (s, 0.64 H), 1.68-1.63 (m, 2 H), 0.98-0.92 (m, 3 H) ppm

^{13}C NMR (75 MHz, $CDCl_3$)

198.6, 173.1, 166.3, 148.5, 146.9, 145.2, 134.0, 133.4, 130.9, 127.6, 112.8, 73.2, 65.7, 40.7, 40.1, 36.4, 29.9, 25.5, 25.2, 18.6, 18.6, 13.8, 10.3 ppm

IR (Thin Film)

1733, 1700, 1695 cm^{-1}

HRMS HRMS-ESI+ (m/z): $[M + H]^+$ calcd for $C_{20}H_{22}O_6Cl$, 393.1099 found: 393.1088

TLC R_f = 0.31 (35% ethyl acetate/hexanes); silica gel, UV, PAA

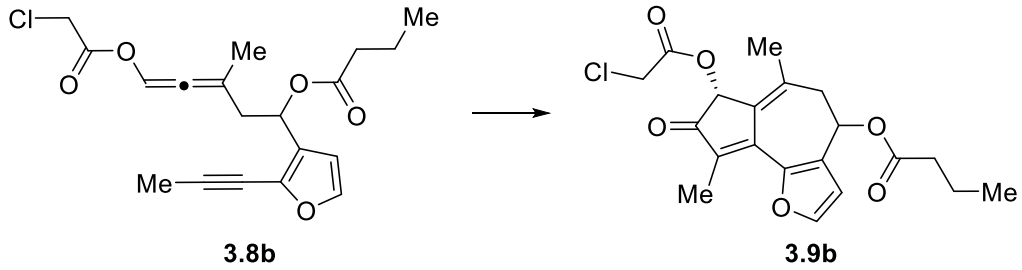

3.8b **3.9b**

(7*R*)-7-(2-chloroacetoxy)-6,9-dimethyl-8-oxo-4,5,7,8-tetrahydroazuleno[4,5-b]furan-4-yl butyrate (3.9b). Follows general procedure C: Bis(1,5-cyclooctadiene)rhodium(I) tetrafluoroborate (2.2 mg, 0.0055 mmol), (*S*)-MonoPhos-alkene (3.4 mg, 0.0083 mmol), carbon monoxide (100%), 5-(2-chloroacetoxy)-3-methyl-1-(2-(prop-1-yn-1-yl)furan-3-yl)penta-3,4-dien-1-yl butyrate (**3.8b**) (20 mg, 0.055 mmol), DCE (5.5 mL, 0.01 M). The reaction was stirred for 137 h in an oil bath (70 °C). The crude residue was purified via silica gel flash chromatography (10-20% ethyl acetate/hexanes) to give the title compound (10.3 mg, 47%) as a 1.4:1 dr by crude NMR and 1.8:1 dr after purification as a yellow oil. The ^{1}H NMR matched that of racemic **3.9b**.

EDD7-524

Appendix A NMR Spectra

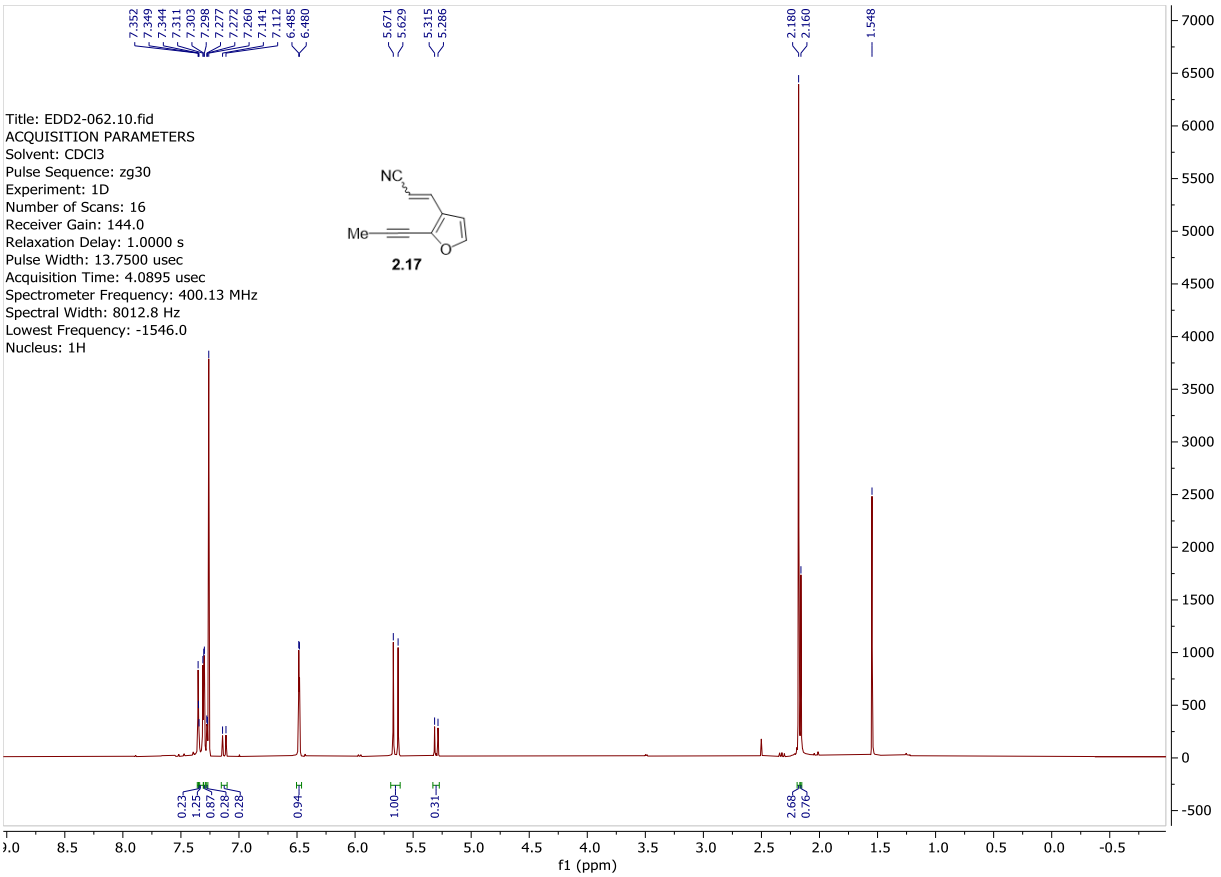
Title: EDD2-062.10.fid
ACQUISITION PARAMETERS
Solvent: CDCl3
Pulse Sequence: zg30
Experiment: 1D
Number of Scans: 16
Receiver Gain: 144.0
Relaxation Delay: 1.0000 s
Pulse Width: 13.7500 usec
Acquisition Time: 4.0895 usec
Spectrometer Frequency: 400.13 MHz
Spectral Width: 8012.8 Hz
Lowest Frequency: -1546.0
Nucleus: 1H
NC
Me
O
2.17
7.352
7.349
7.344
7.311
7.303
7.298
7.277
7.272
7.260
7.141
7.112
6.485
6.480
5.671
5.629
5.315
5.286
2.180
2.160
1.548
0.23
1.25
0.87
0.28
0.28
0.94
1.00
0.31
2.68
0.76
f1 (ppm)

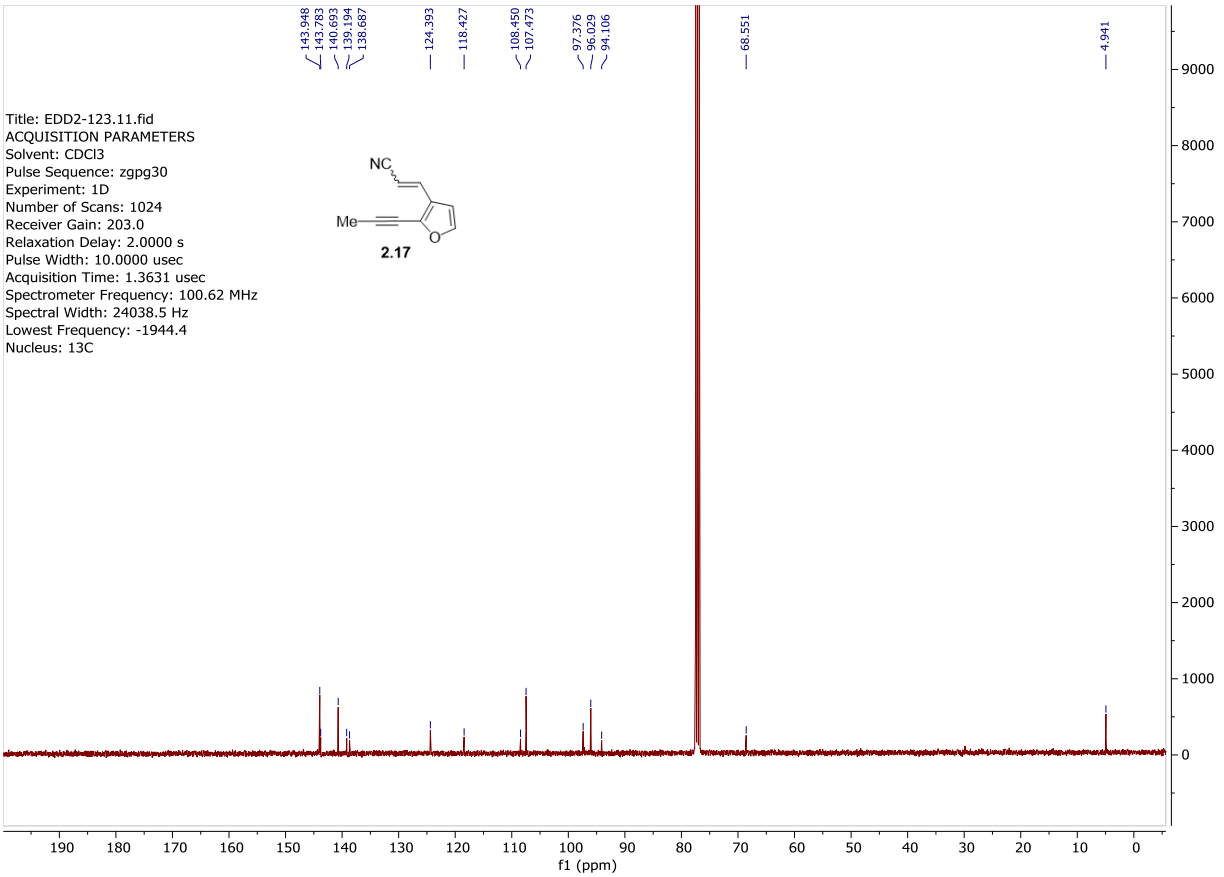
143.948
143.783
140.693
139.194
138.687
124.393
118.427
108.450
107.473
97.376
96.029
94.106
68.551
4.941
Title: EDD2-123.11.fid
ACQUISITION PARAMETERS
Solvent: CDCl3
Pulse Sequence: zgpg30
Experiment: 1D
Number of Scans: 1024
Receiver Gain: 203.0
Relaxation Delay: 2.0000 s
Pulse Width: 10.0000 usec
Acquisition Time: 1.3631 usec
Spectrometer Frequency: 100.62 MHz
Spectral Width: 24038.5 Hz
Lowest Frequency: -1944.4
Nucleus: 13C
NC
Me
O
2.17
9000
8000
7000
6000
5000
4000
3000
2000
1000
0
190
180
170
160
150
140
130
120
110
100
90
80
70
60
50
40
30
20
10
0
f1 (ppm)

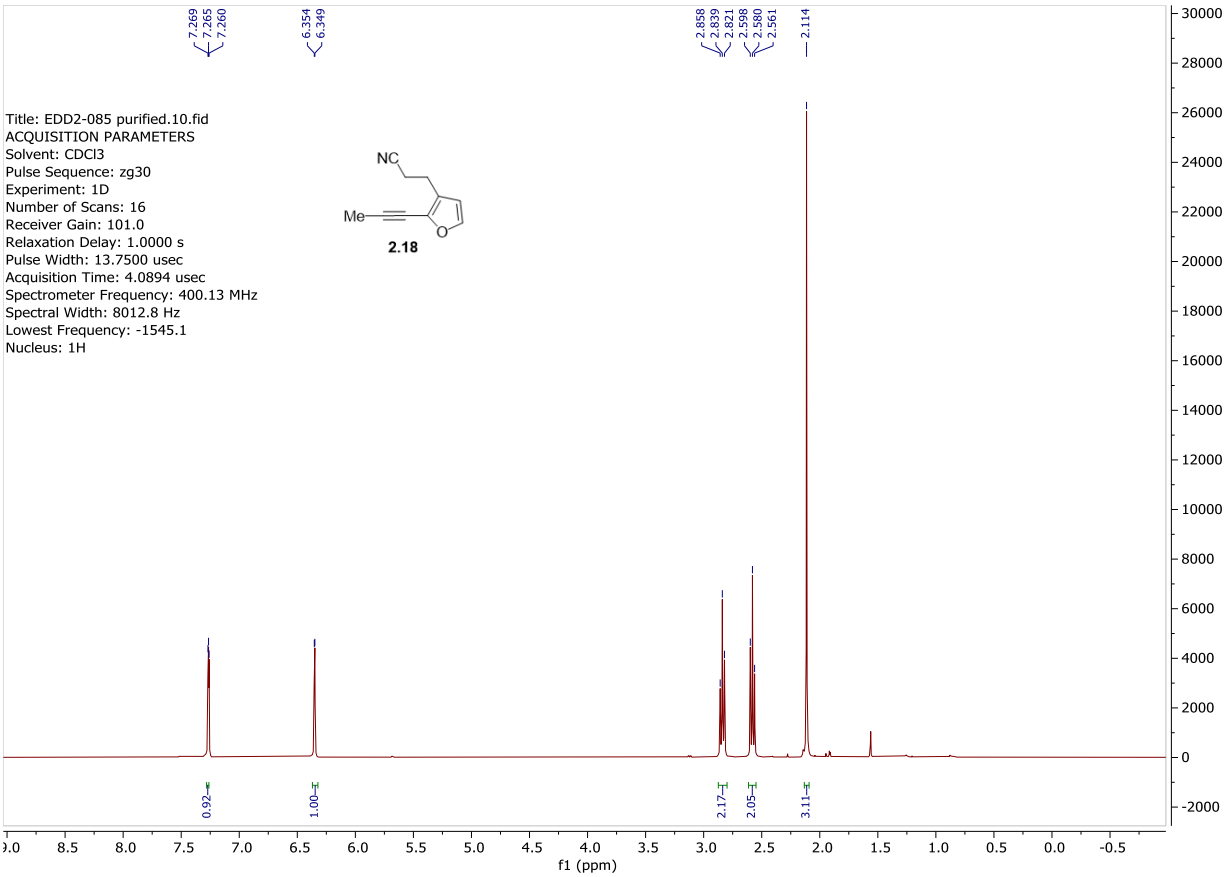
7.269
7.265
7.260
6.354
6.349
2.858
2.839
2.821
2.598
2.580
2.561
2.114
Title: EDD2-085 purified.10.fid
ACQUISITION PARAMETERS
Solvent: CDCl3
Pulse Sequence: zg30
Experiment: 1D
Number of Scans: 16
Receiver Gain: 101.0
Relaxation Delay: 1.0000 s
Pulse Width: 13.7500 usec
Acquisition Time: 4.0894 usec
Spectrometer Frequency: 400.13 MHz
Spectral Width: 8012.8 Hz
Lowest Frequency: -1545.1
Nucleus: 1H
NC
Me
O
2.18
0.92
1.00
2.17
2.05
3.11
f1 (ppm)

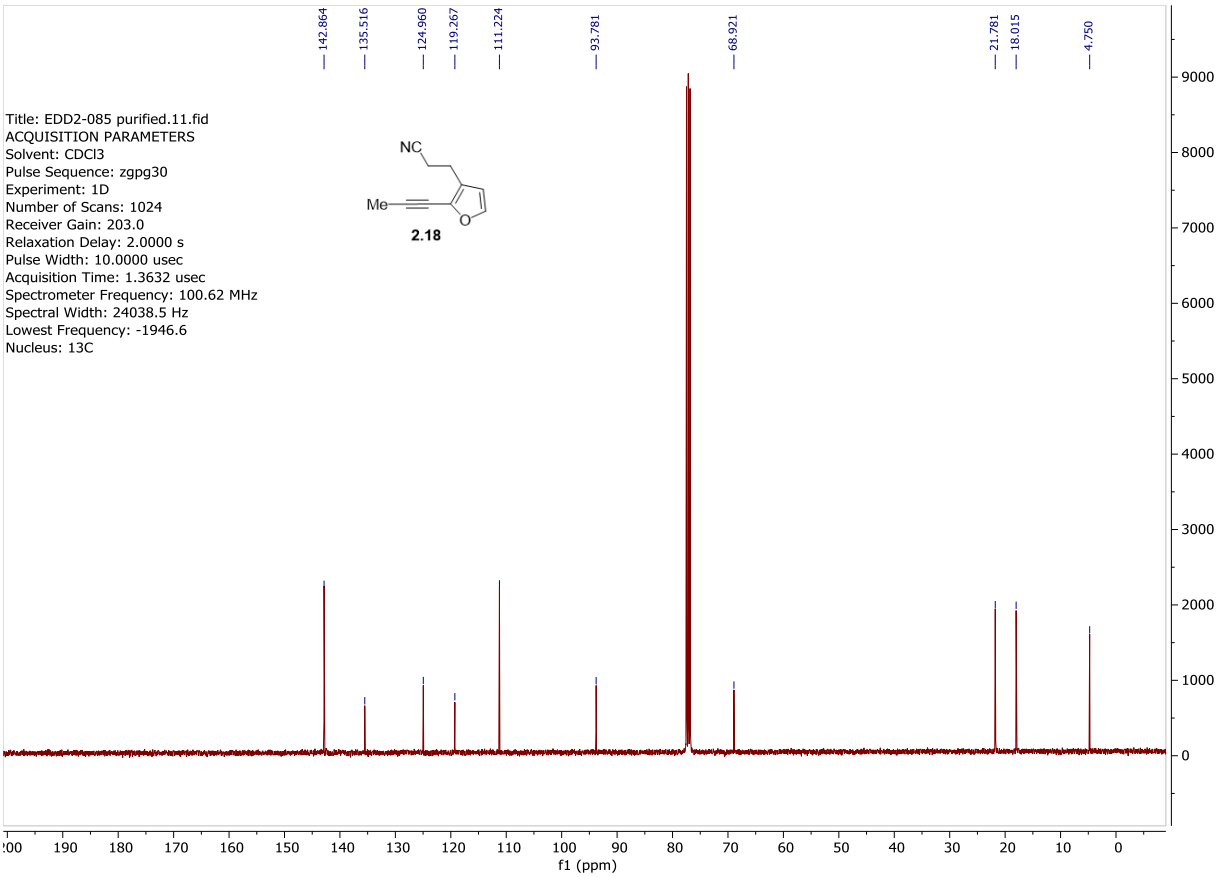
142.864
135.516
124.960
119.267
111.224
93.781
68.921
21.781
18.015
4.750
Title: EDD2-085 purified.11.fid
ACQUISITION PARAMETERS
Solvent: CDCl3
Pulse Sequence: zgpg30
Experiment: 1D
Number of Scans: 1024
Receiver Gain: 203.0
Relaxation Delay: 2.0000 s
Pulse Width: 10.0000 usec
Acquisition Time: 1.3632 usec
Spectrometer Frequency: 100.62 MHz
Spectral Width: 24038.5 Hz
Lowest Frequency: -1946.6
Nucleus: 13C
NC
Me
O
2.18
9000
8000
7000
6000
5000
4000
3000
2000
1000
0
200 190 180 170 160 150 140 130 120 110 100 90 80 70 60 50 40 30 20 10 0
f1 (ppm)

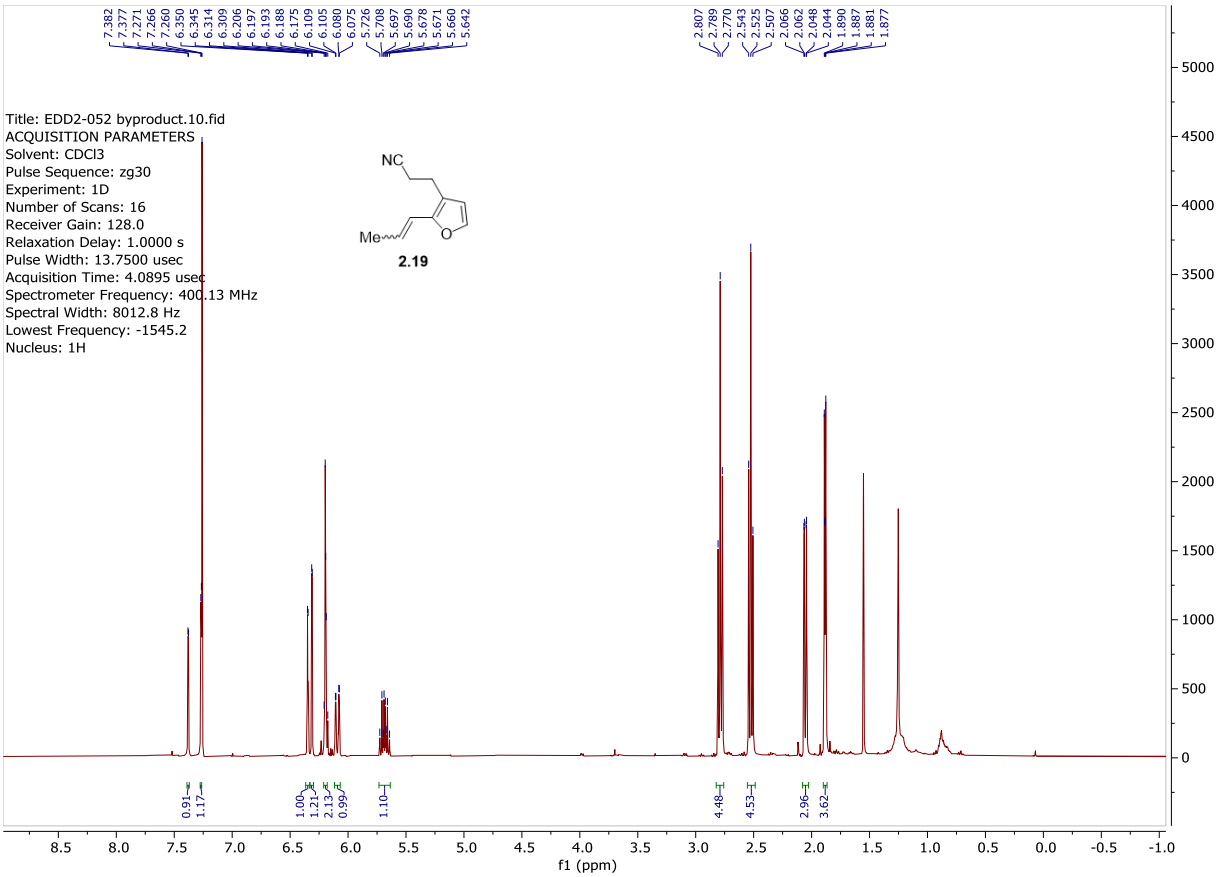
Title: EDD2-052 byproduct.10.fid
ACQUISITION PARAMETERS
Solvent: CDCl3
Pulse Sequence: zg30
Experiment: 1D
Number of Scans: 16
Receiver Gain: 128.0
Relaxation Delay: 1.0000 s
Pulse Width: 13.7500 usec
Acquisition Time: 4.0895 usec
Spectrometer Frequency: 400.13 MHz
Spectral Width: 8012.8 Hz
Lowest Frequency: -1545.2
Nucleus: 1H
NC
Me
O
2.19
f1 (ppm)

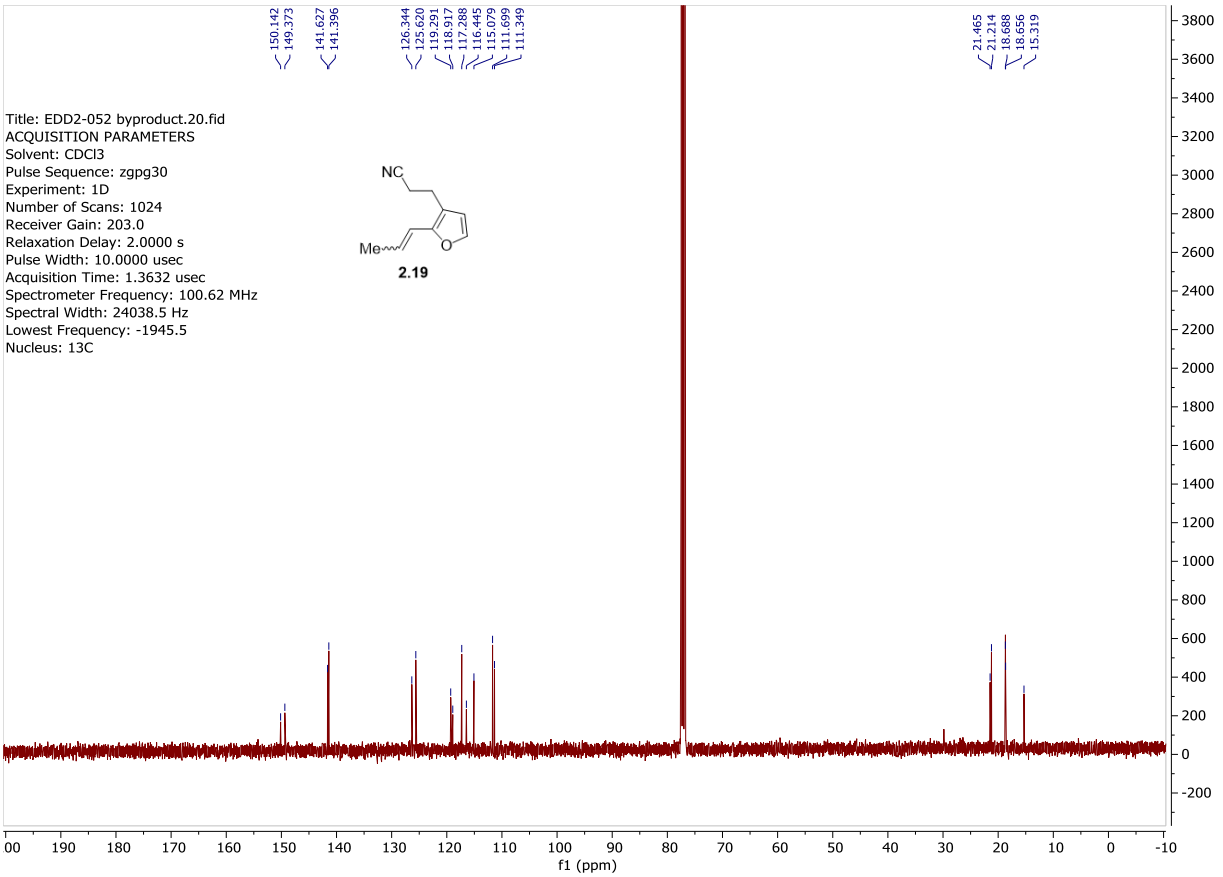
150.142
149.373
141.627
141.396
126.344
125.620
119.291
118.917
117.288
116.445
115.079
111.699
111.349
21.465
21.214
18.688
18.656
15.319
Title: EDD2-052 byproduct.20.fid
ACQUISITION PARAMETERS
Solvent: CDCl3
Pulse Sequence: zgpg30
Experiment: 1D
Number of Scans: 1024
Receiver Gain: 203.0
Relaxation Delay: 2.0000 s
Pulse Width: 10.0000 usec
Acquisition Time: 1.3632 usec
Spectrometer Frequency: 100.62 MHz
Spectral Width: 24038.5 Hz
Lowest Frequency: -1945.5
Nucleus: 13C
NC
Me
O
2.19
f1 (ppm)

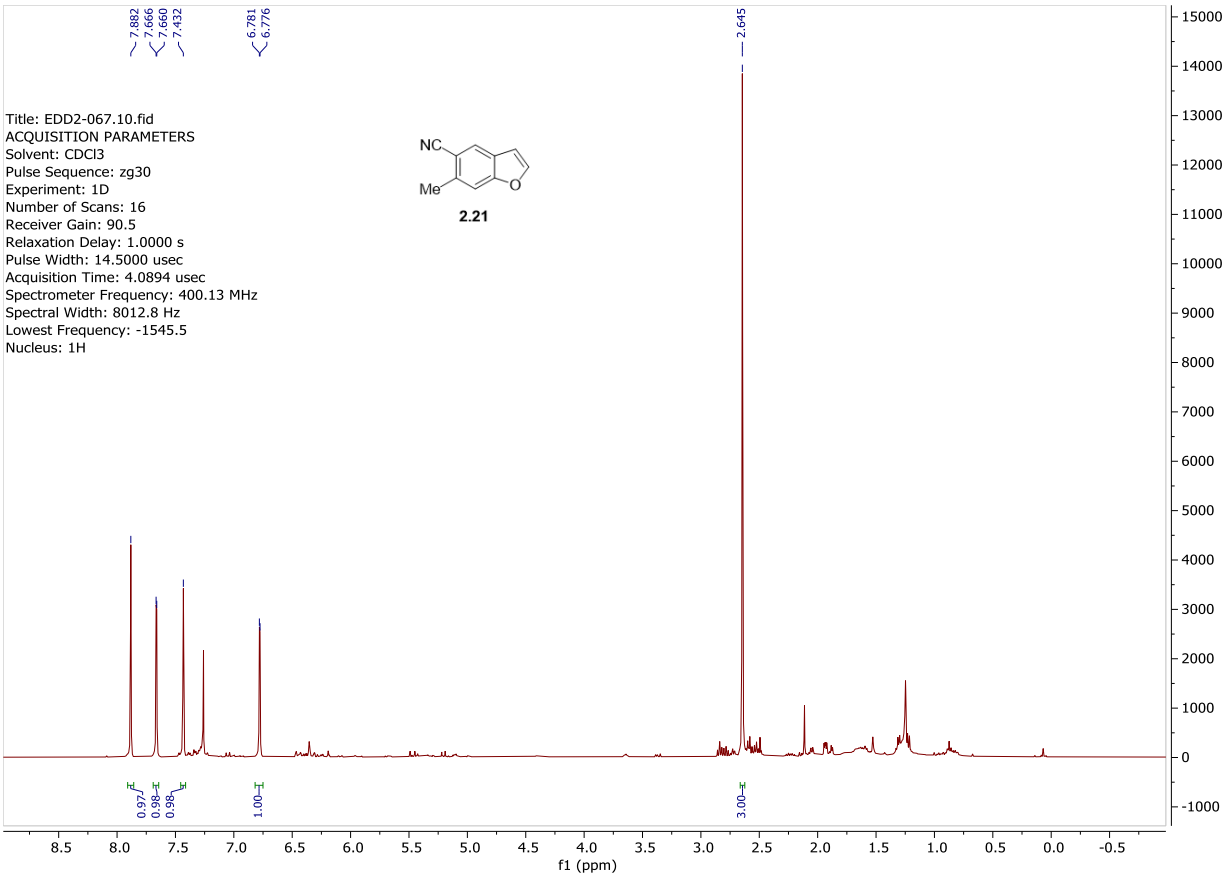
7.882
7.666
7.660
7.432
6.781
6.776
2.645
Title: EDD2-067.10.fid
ACQUISITION PARAMETERS
Solvent: CDCl3
Pulse Sequence: zg30
Experiment: 1D
Number of Scans: 16
Receiver Gain: 90.5
Relaxation Delay: 1.0000 s
Pulse Width: 14.5000 usec
Acquisition Time: 4.0894 usec
Spectrometer Frequency: 400.13 MHz
Spectral Width: 8012.8 Hz
Lowest Frequency: -1545.5
Nucleus: 1H
NC
Me
O
2.21
0.97
0.98
0.98
1.00
3.00
f1 (ppm)

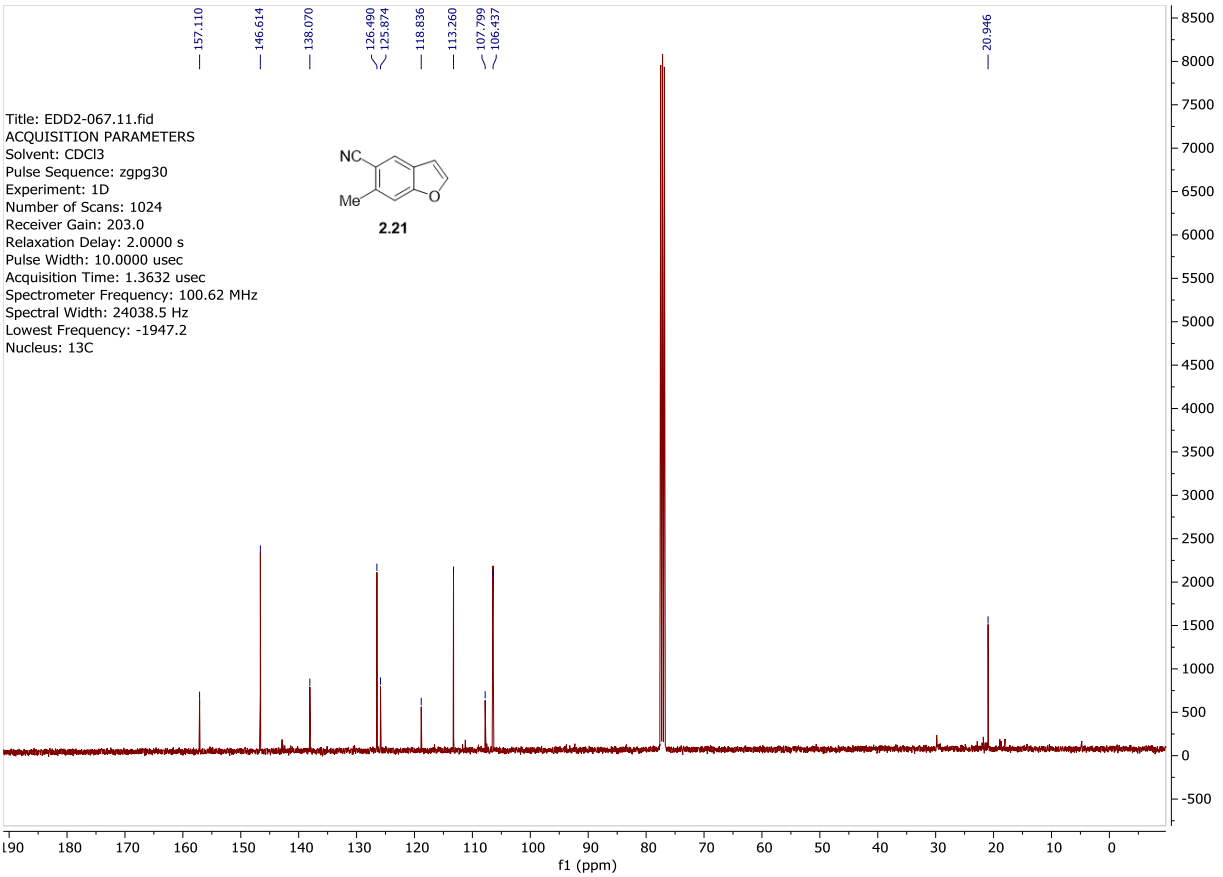
157.110
146.614
138.070
126.490
125.874
118.836
113.260
107.799
106.437
20.946
Title: EDD2-067.11.fid
ACQUISITION PARAMETERS
Solvent: CDCl3
Pulse Sequence: zgpg30
Experiment: 1D
Number of Scans: 1024
Receiver Gain: 203.0
Relaxation Delay: 2.0000 s
Pulse Width: 10.0000 usec
Acquisition Time: 1.3632 usec
Spectrometer Frequency: 100.62 MHz
Spectral Width: 24038.5 Hz
Lowest Frequency: -1947.2
Nucleus: 13C
NC
Me
O
2.21
f1 (ppm)

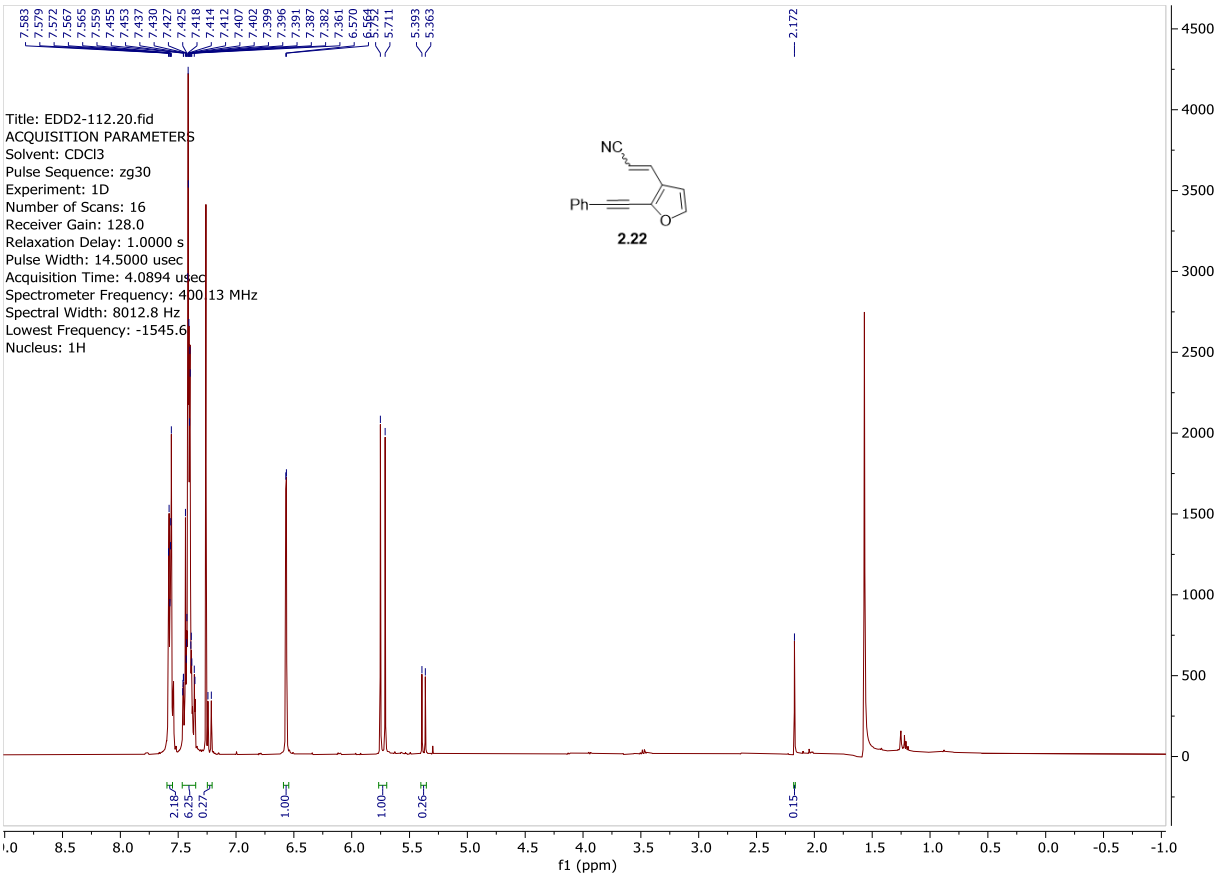
7.583
7.579
7.572
7.567
7.565
7.559
7.455
7.453
7.437
7.430
7.427
7.425
7.418
7.414
7.412
7.407
7.402
7.399
7.396
7.391
7.387
7.382
7.361
6.570
6.564
5.752
5.711
5.393
5.363
2.172
Title: EDD2-112.20.fid
ACQUISITION PARAMETERS
Solvent: CDCl3
Pulse Sequence: zg30
Experiment: 1D
Number of Scans: 16
Receiver Gain: 128.0
Relaxation Delay: 1.0000 s
Pulse Width: 14.5000 usec
Acquisition Time: 4.0894 usec
Spectrometer Frequency: 400.13 MHz
Spectral Width: 8012.8 Hz
Lowest Frequency: -1545.6
Nucleus: 1H
NC
Ph
O
2.22
2.18
6.25
0.27
1.00
1.00
0.26
0.15
f1 (ppm)

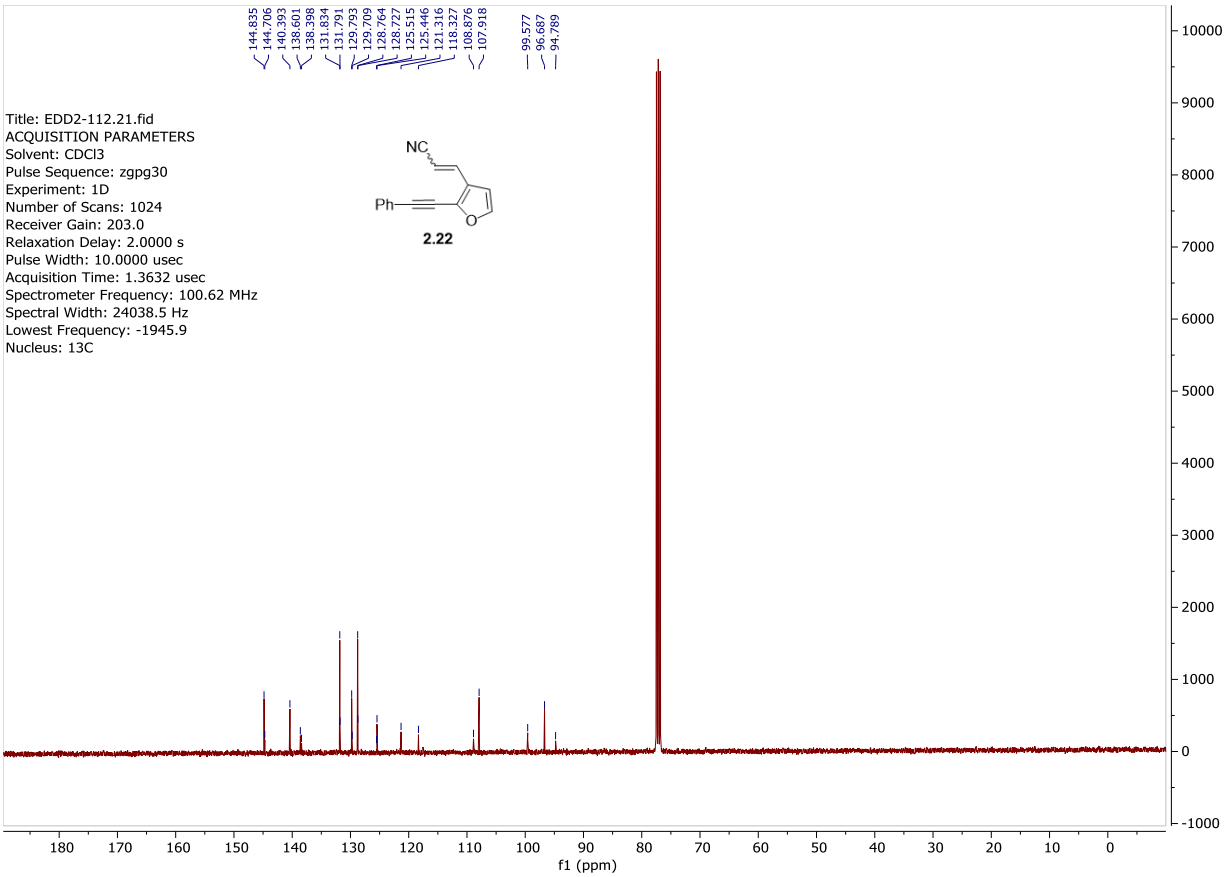
144.835
144.706
140.393
138.601
138.398
131.834
131.791
129.793
129.709
128.764
128.727
125.515
125.446
121.316
118.327
108.876
107.918
99.577
96.687
94.789
Title: EDD2-112.21.fid
ACQUISITION PARAMETERS
Solvent: CDCl3
Pulse Sequence: zgpg30
Experiment: 1D
Number of Scans: 1024
Receiver Gain: 203.0
Relaxation Delay: 2.0000 s
Pulse Width: 10.0000 usec
Acquisition Time: 1.3632 usec
Spectrometer Frequency: 100.62 MHz
Spectral Width: 24038.5 Hz
Lowest Frequency: -1945.9
Nucleus: 13C
NC
Ph
O
2.22
10000
9000
8000
7000
6000
5000
4000
3000
2000
1000
0
-1000
180
170
160
150
140
130
120
110
100
90
80
70
60
50
40
30
20
10
0
f1 (ppm)

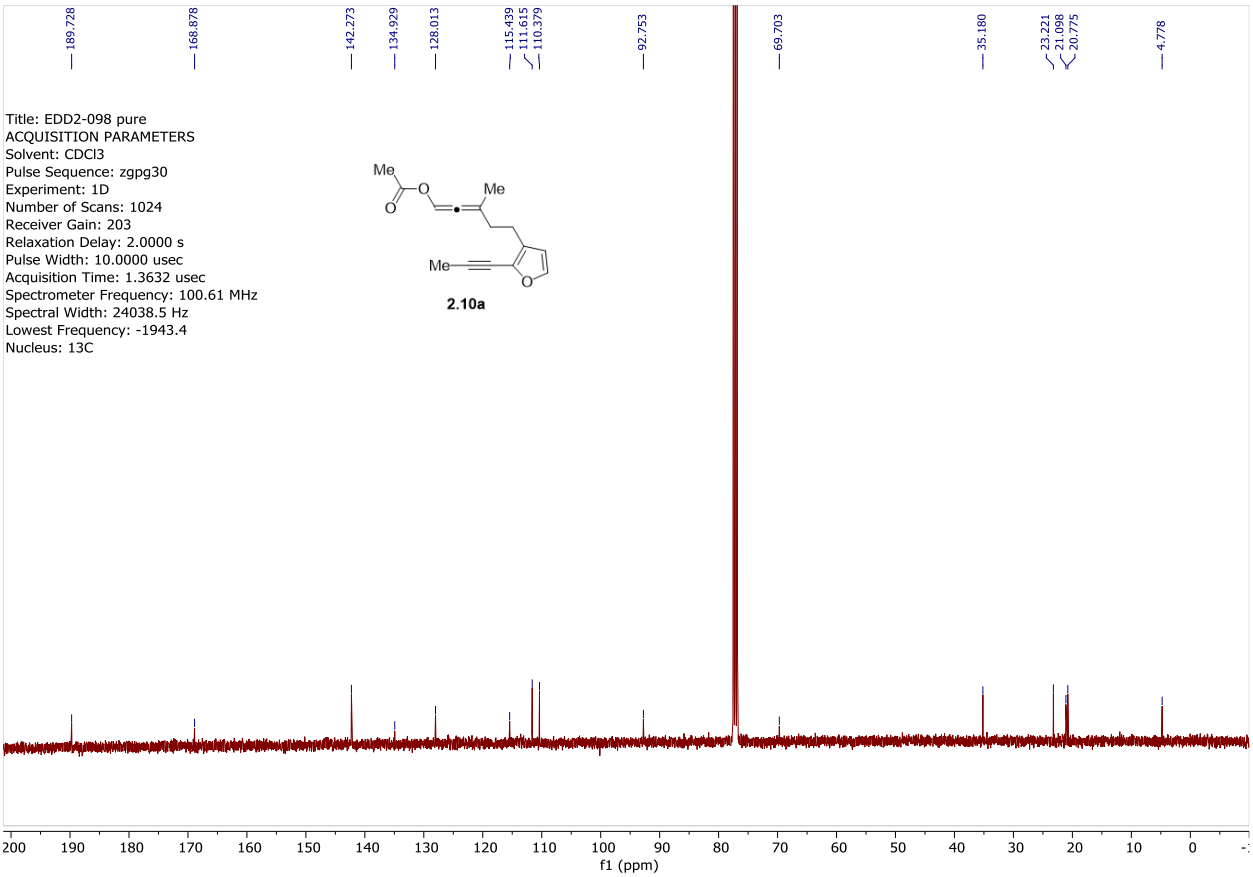
189.728
168.878
142.273
134.929
128.013
115.439
111.615
110.379
92.753
69.703
35.180
23.221
21.098
20.775
4.778
Title: EDD2-098 pure
ACQUISITION PARAMETERS
Solvent: CDCl3
Pulse Sequence: zgpg30
Experiment: 1D
Number of Scans: 1024
Receiver Gain: 203
Relaxation Delay: 2.0000 s
Pulse Width: 10.0000 usec
Acquisition Time: 1.3632 usec
Spectrometer Frequency: 100.61 MHz
Spectral Width: 24038.5 Hz
Lowest Frequency: -1943.4
Nucleus: 13C
Me
O
O
Me
Me
O
2.10a
200
190
180
170
160
150
140
130
120
110
100
90
80
70
60
50
40
30
20
10
0
f1 (ppm)

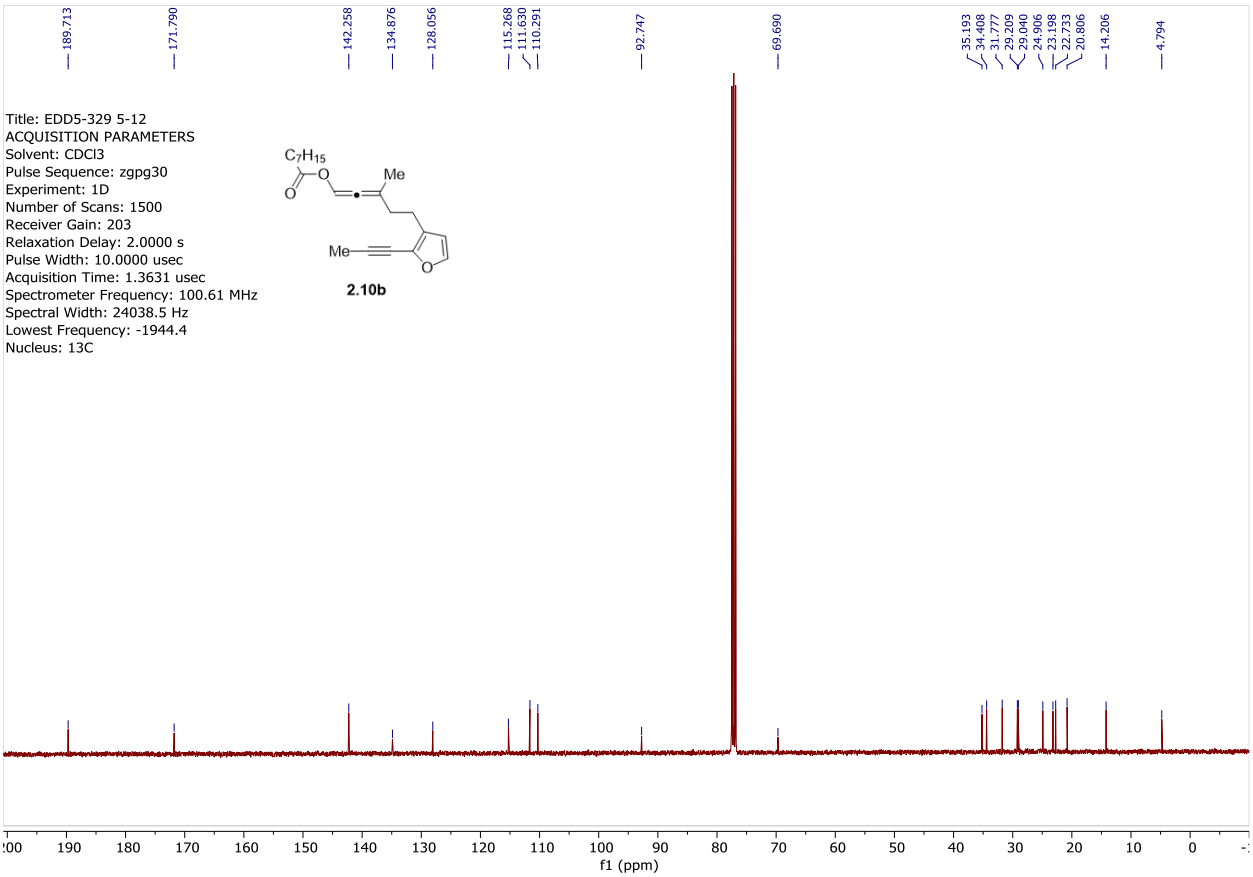
189.713
171.790
142.258
134.876
128.056
115.268
111.630
110.291
92.747
69.690
35.193
34.408
31.777
29.209
29.040
24.906
23.198
22.733
20.806
14.206
4.794
Title: EDD5-329 5-12
ACQUISITION PARAMETERS
Solvent: CDCl3
Pulse Sequence: zgpg30
Experiment: 1D
Number of Scans: 1500
Receiver Gain: 203
Relaxation Delay: 2.0000 s
Pulse Width: 10.0000 usec
Acquisition Time: 1.3631 usec
Spectrometer Frequency: 100.61 MHz
Spectral Width: 24038.5 Hz
Lowest Frequency: -1944.4
Nucleus: 13C
C7H15
O
O
Me
Me
O
2.10b
190
180
170
160
150
140
130
120
110
100
90
80
70
60
50
40
30
20
10
0
f1 (ppm)

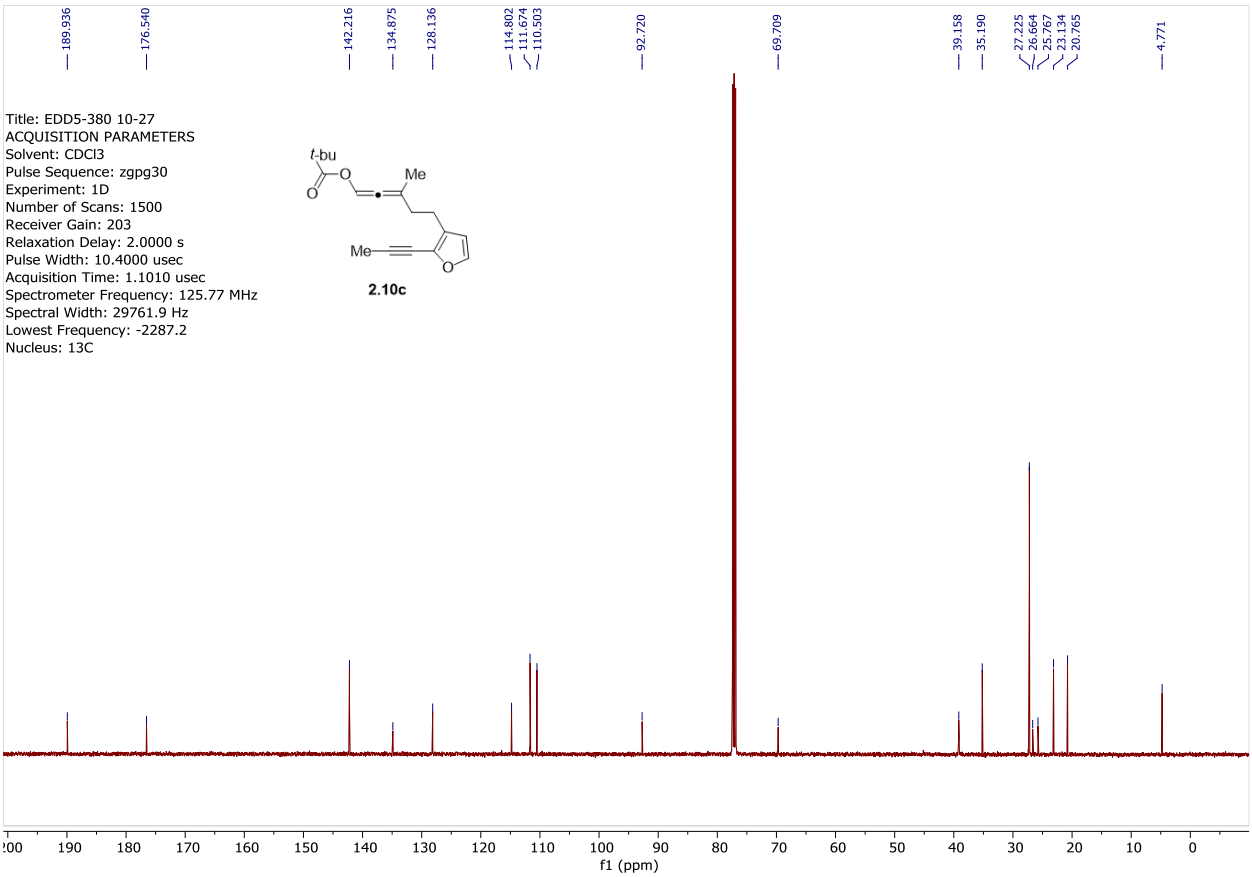
189.936
176.540
142.216
134.875
128.136
114.802
111.674
110.503
92.720
69.709
39.158
35.190
27.225
26.664
25.767
23.134
20.765
4.771
Title: EDD5-380 10-27
ACQUISITION PARAMETERS
Solvent: CDCl3
Pulse Sequence: zgpg30
Experiment: 1D
Number of Scans: 1500
Receiver Gain: 203
Relaxation Delay: 2.0000 s
Pulse Width: 10.4000 usec
Acquisition Time: 1.1010 usec
Spectrometer Frequency: 125.77 MHz
Spectral Width: 29761.9 Hz
Lowest Frequency: -2287.2
Nucleus: 13C
t-bu
O
O
Me
Me
O
2.10c
200
190
180
170
160
150
140
130
120
110
100
90
80
70
60
50
40
30
20
10
0
f1 (ppm)

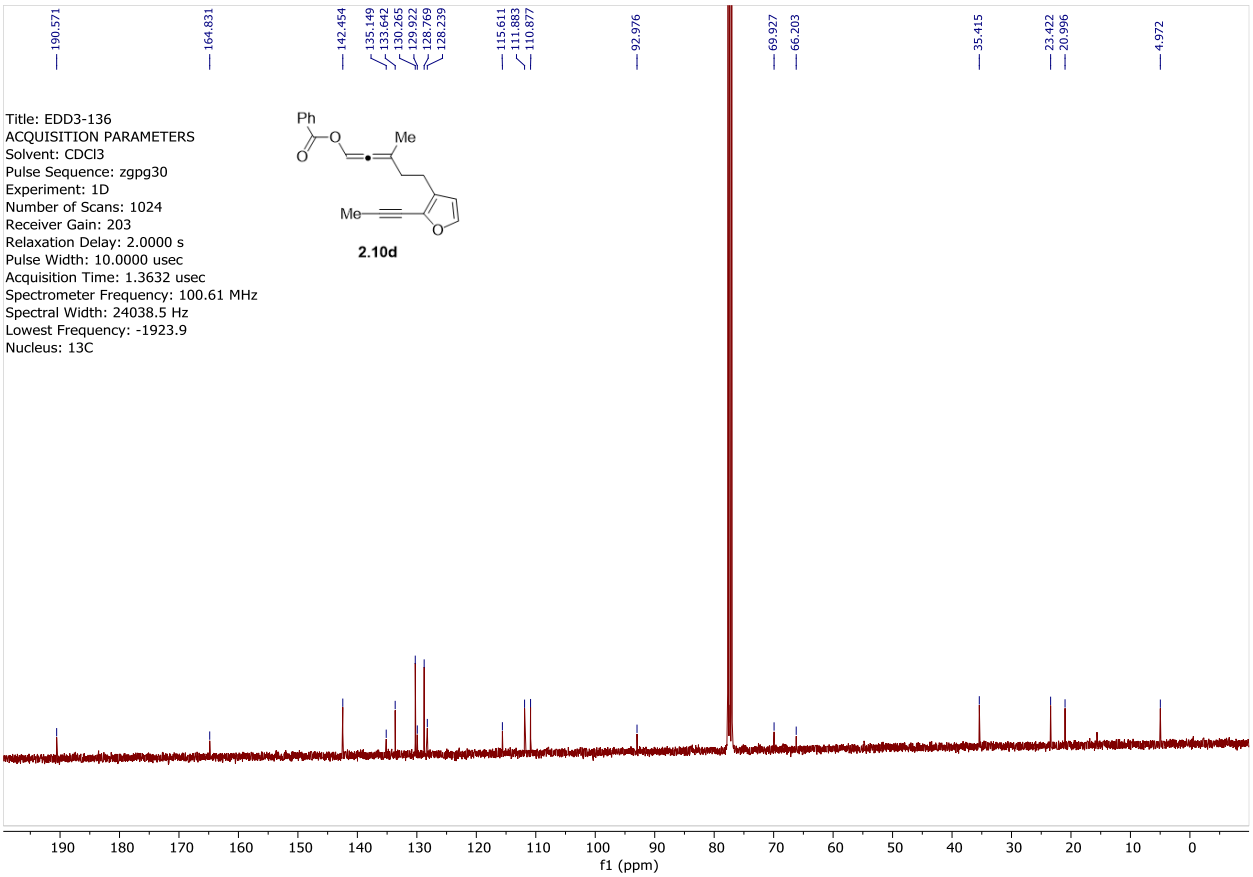
190.571
164.831
142.454
135.149
133.642
130.265
129.922
128.769
128.239
115.611
111.883
110.877
92.976
69.927
66.203
35.415
23.422
20.996
4.972
Title: EDD3-136
ACQUISITION PARAMETERS
Solvent: CDCl3
Pulse Sequence: zgpg30
Experiment: 1D
Number of Scans: 1024
Receiver Gain: 203
Relaxation Delay: 2.0000 s
Pulse Width: 10.0000 usec
Acquisition Time: 1.3632 usec
Spectrometer Frequency: 100.61 MHz
Spectral Width: 24038.5 Hz
Lowest Frequency: -1923.9
Nucleus: 13C
Ph
O
O
Me
Me
O
2.10d
190
180
170
160
150
140
130
120
110
100
90
80
70
60
50
40
30
20
10
0
f1 (ppm)

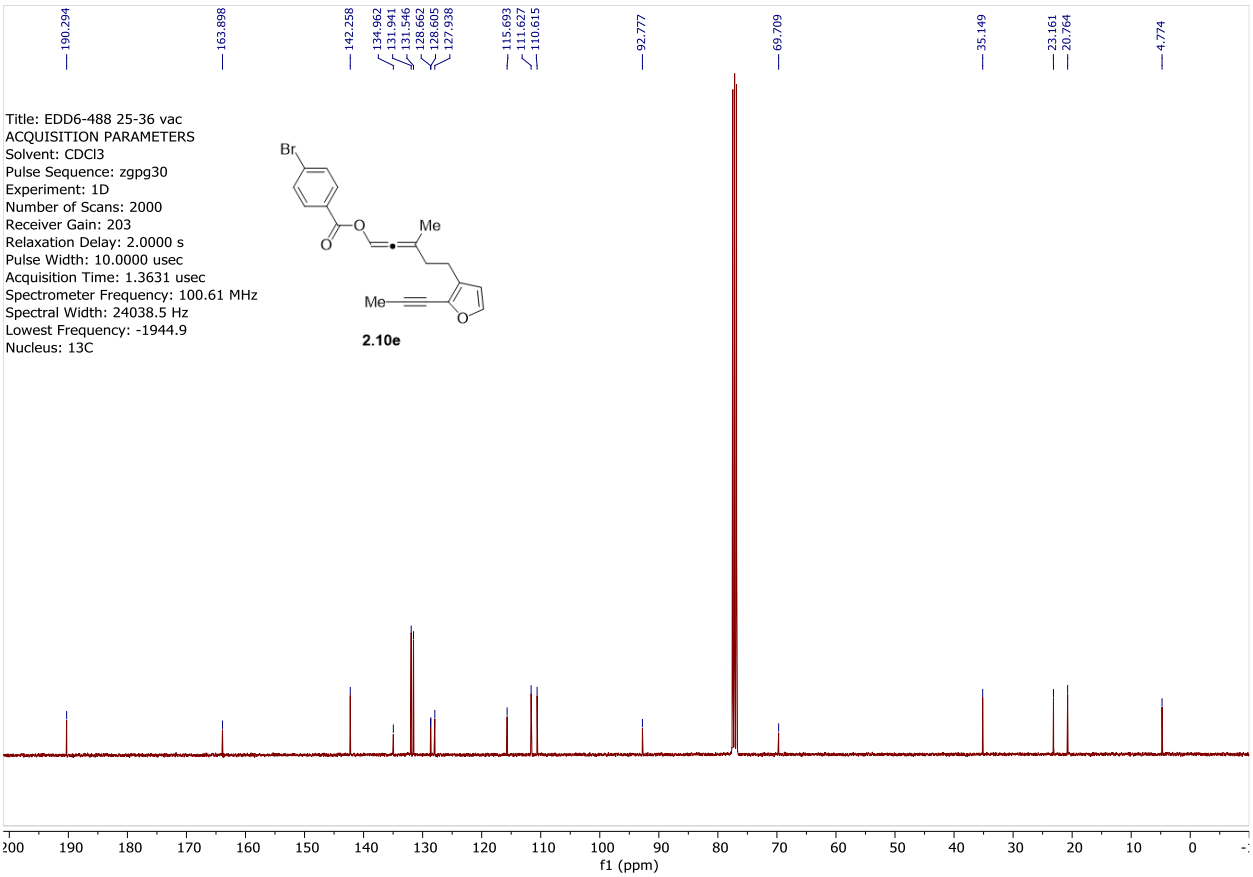
190.294
163.898
142.258
134.962
131.941
131.546
128.662
128.605
127.938
115.693
111.627
110.615
92.777
69.709
35.149
23.161
20.764
4.774
Title: EDD6-488 25-36 vac
ACQUISITION PARAMETERS
Solvent: CDCl3
Pulse Sequence: zgpg30
Experiment: 1D
Number of Scans: 2000
Receiver Gain: 203
Relaxation Delay: 2.0000 s
Pulse Width: 10.0000 usec
Acquisition Time: 1.3631 usec
Spectrometer Frequency: 100.61 MHz
Spectral Width: 24038.5 Hz
Lowest Frequency: -1944.9
Nucleus: 13C
Br
O
O
Me
Me
O
2.10e
200
190
180
170
160
150
140
130
120
110
100
90
80
70
60
50
40
30
20
10
0
f1 (ppm)

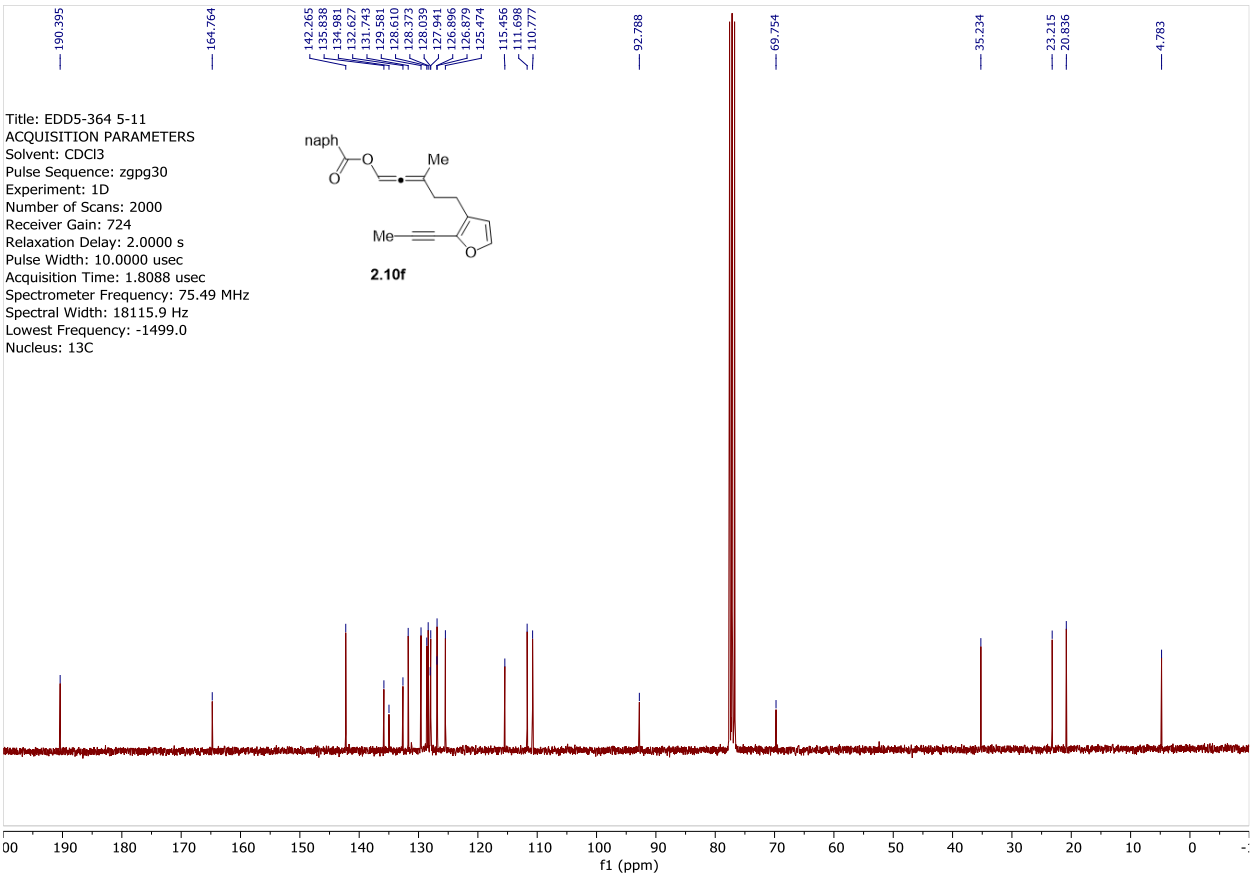
190.395
164.764
142.265
135.838
134.981
132.627
131.743
129.581
128.610
128.373
128.039
127.941
126.896
126.879
125.474
115.456
111.698
110.777
92.788
69.754
35.234
23.215
20.836
4.783
Title: EDD5-364 5-11
ACQUISITION PARAMETERS
Solvent: CDCl3
Pulse Sequence: zgpg30
Experiment: 1D
Number of Scans: 2000
Receiver Gain: 724
Relaxation Delay: 2.0000 s
Pulse Width: 10.0000 usec
Acquisition Time: 1.8088 usec
Spectrometer Frequency: 75.49 MHz
Spectral Width: 18115.9 Hz
Lowest Frequency: -1499.0
Nucleus: 13C
naph
O
O
Me
Me
O
2.10f
f1 (ppm)

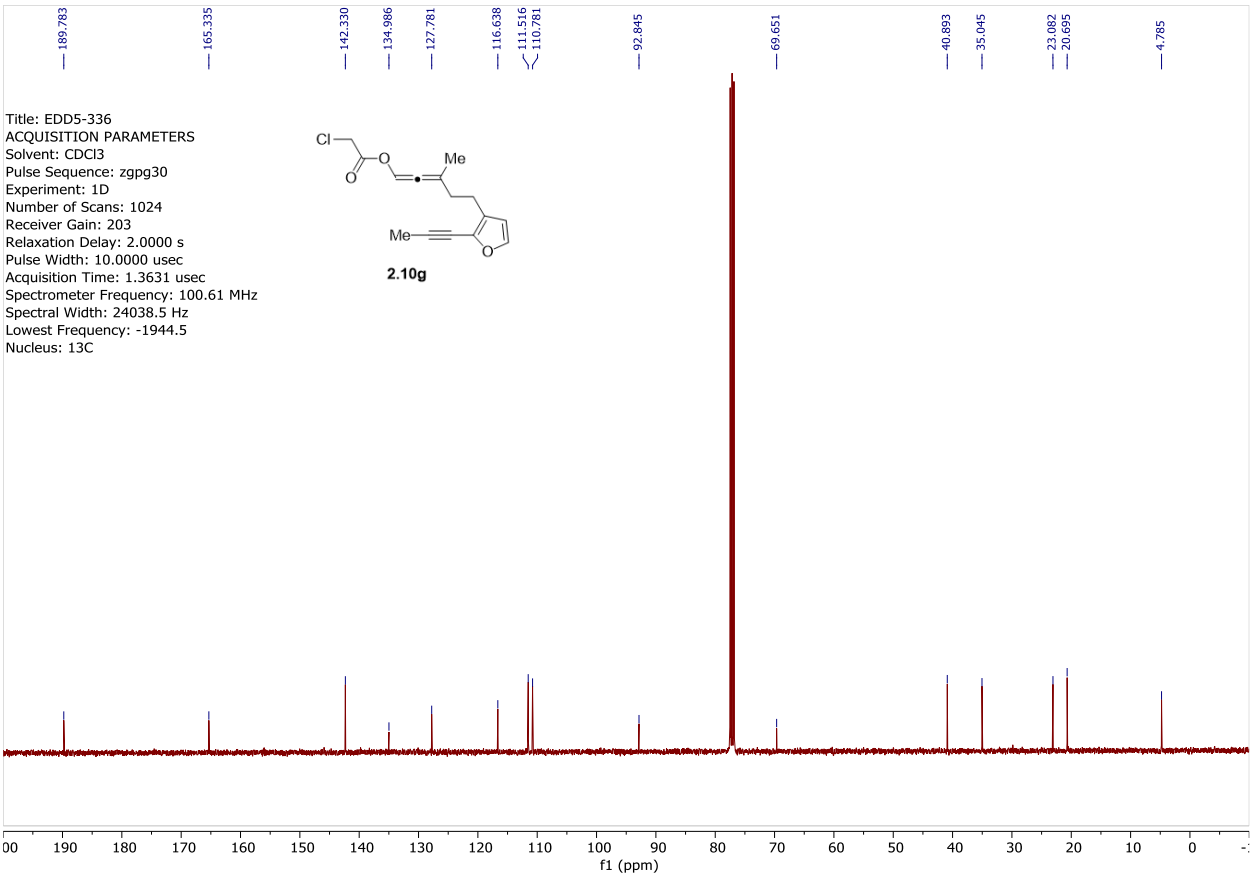
189.783
165.335
142.330
134.986
127.781
116.638
111.516
110.781
92.845
69.651
40.893
35.045
23.082
20.695
4.785
Title: EDD5-336
ACQUISITION PARAMETERS
Solvent: CDCl3
Pulse Sequence: zgpg30
Experiment: 1D
Number of Scans: 1024
Receiver Gain: 203
Relaxation Delay: 2.0000 s
Pulse Width: 10.0000 usec
Acquisition Time: 1.3631 usec
Spectrometer Frequency: 100.61 MHz
Spectral Width: 24038.5 Hz
Lowest Frequency: -1944.5
Nucleus: 13C
Cl
O
O
Me
Me
O
2.10g
f1 (ppm)

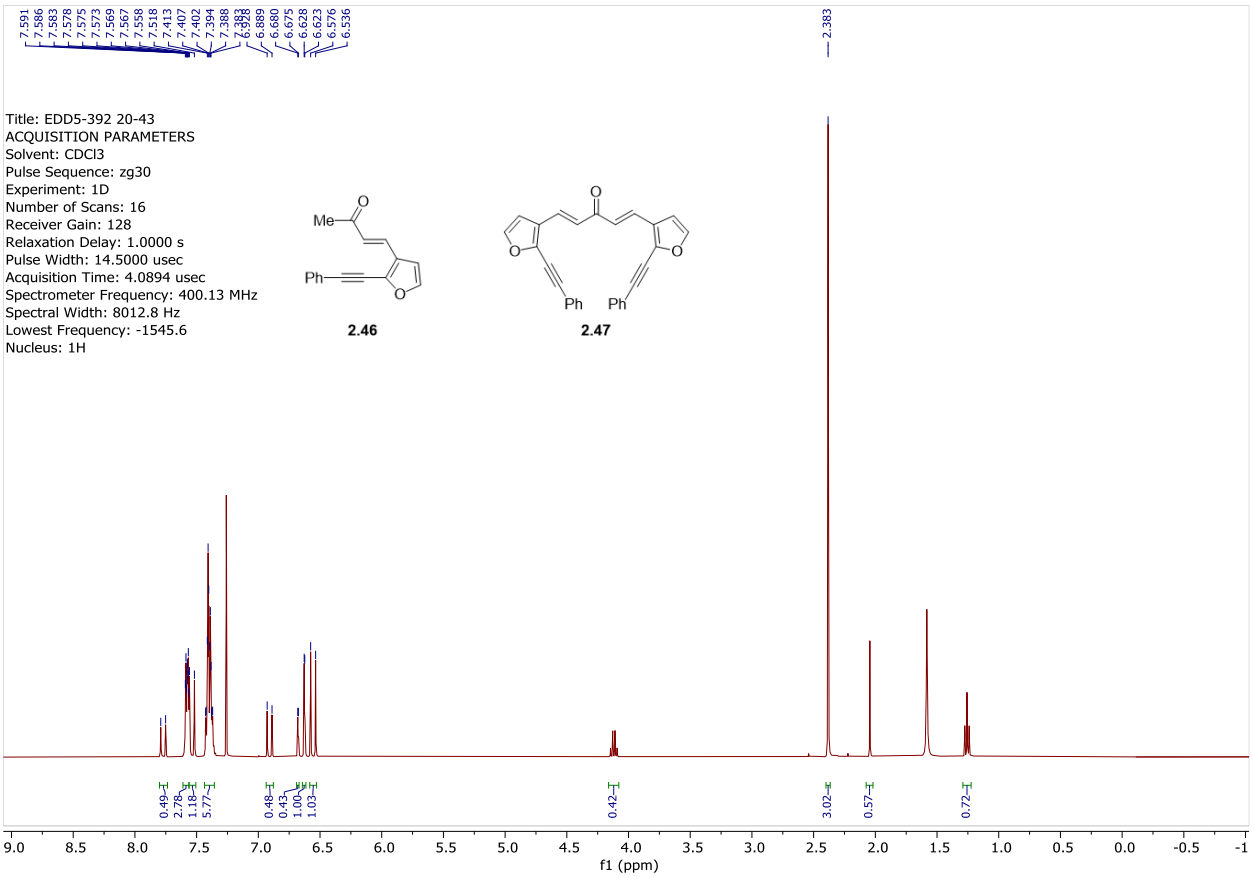
7.591
7.586
7.583
7.578
7.575
7.573
7.569
7.567
7.558
7.518
7.413
7.407
7.402
7.394
7.388
6.889
6.680
6.675
6.628
6.623
6.576
6.536
2.383
Title: EDD5-392 20-43
ACQUISITION PARAMETERS
Solvent: CDCl3
Pulse Sequence: zg30
Experiment: 1D
Number of Scans: 16
Receiver Gain: 128
Relaxation Delay: 1.0000 s
Pulse Width: 14.5000 usec
Acquisition Time: 4.0894 usec
Spectrometer Frequency: 400.13 MHz
Spectral Width: 8012.8 Hz
Lowest Frequency: -1545.6
Nucleus: 1H
Me
O
Ph
O
2.46
O
O
O
Ph
Ph
2.47
0.49
2.78
1.18
5.77
0.48
0.43
1.00
1.03
0.42
3.02
0.57
0.72
9.0
8.5
8.0
7.5
7.0
6.5
6.0
5.5
5.0
4.5
4.0
3.5
3.0
2.5
2.0
1.5
1.0
0.5
0.0
-0.5
-1
f1 (ppm)

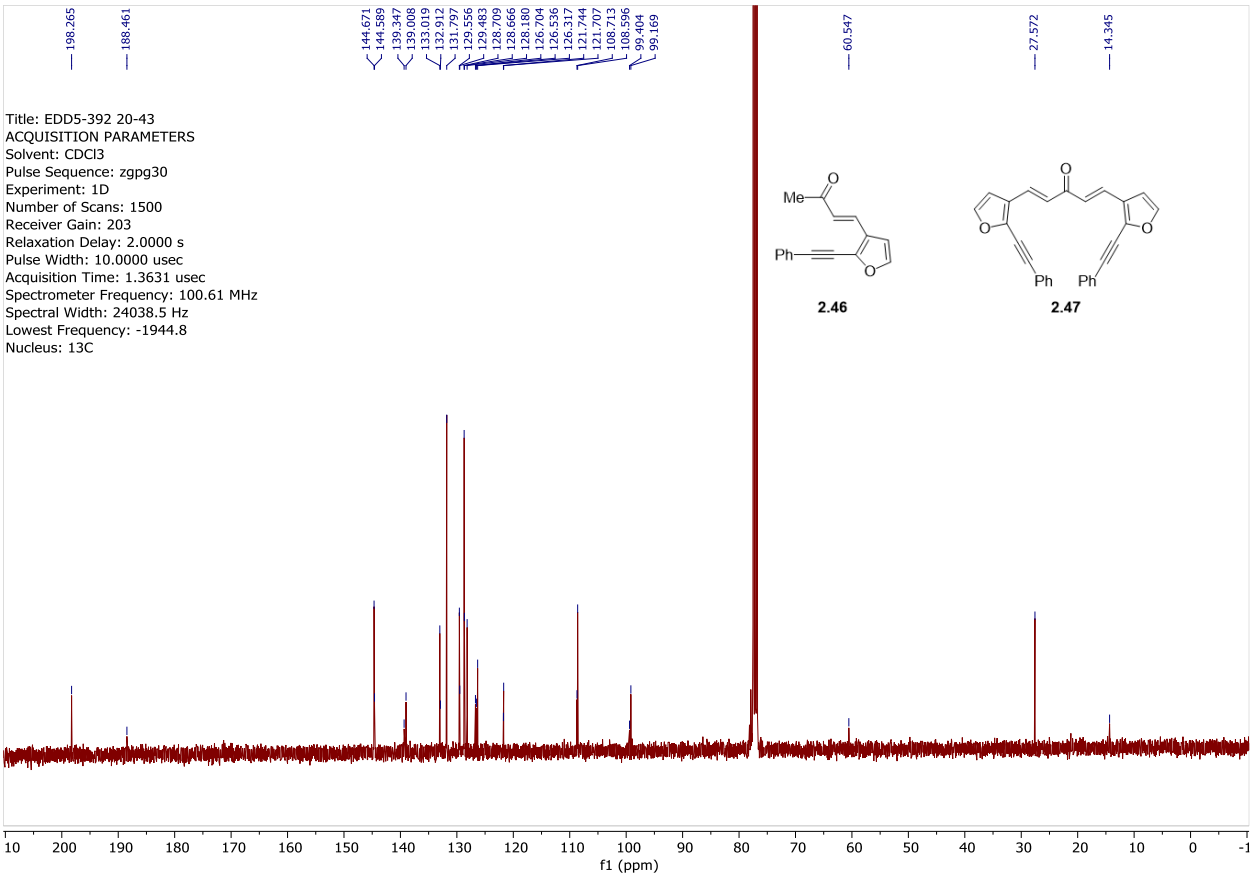
198.265
188.461
144.671
144.589
139.347
139.008
133.019
132.912
131.797
129.556
129.483
128.709
128.666
128.180
126.704
126.536
126.317
121.744
121.707
108.713
108.596
99.404
99.169
60.547
27.572
14.345
Title: EDD5-392 20-43
ACQUISITION PARAMETERS
Solvent: CDCl3
Pulse Sequence: zgpg30
Experiment: 1D
Number of Scans: 1500
Receiver Gain: 203
Relaxation Delay: 2.0000 s
Pulse Width: 10.0000 usec
Acquisition Time: 1.3631 usec
Spectrometer Frequency: 100.61 MHz
Spectral Width: 24038.5 Hz
Lowest Frequency: -1944.8
Nucleus: 13C
Me
O
Ph
O
2.46
O
O
O
Ph
Ph
2.47
10 200 190 180 170 160 150 140 130 120 110 100 90 80 70 60 50 40 30 20 10 0 -1
f1 (ppm)

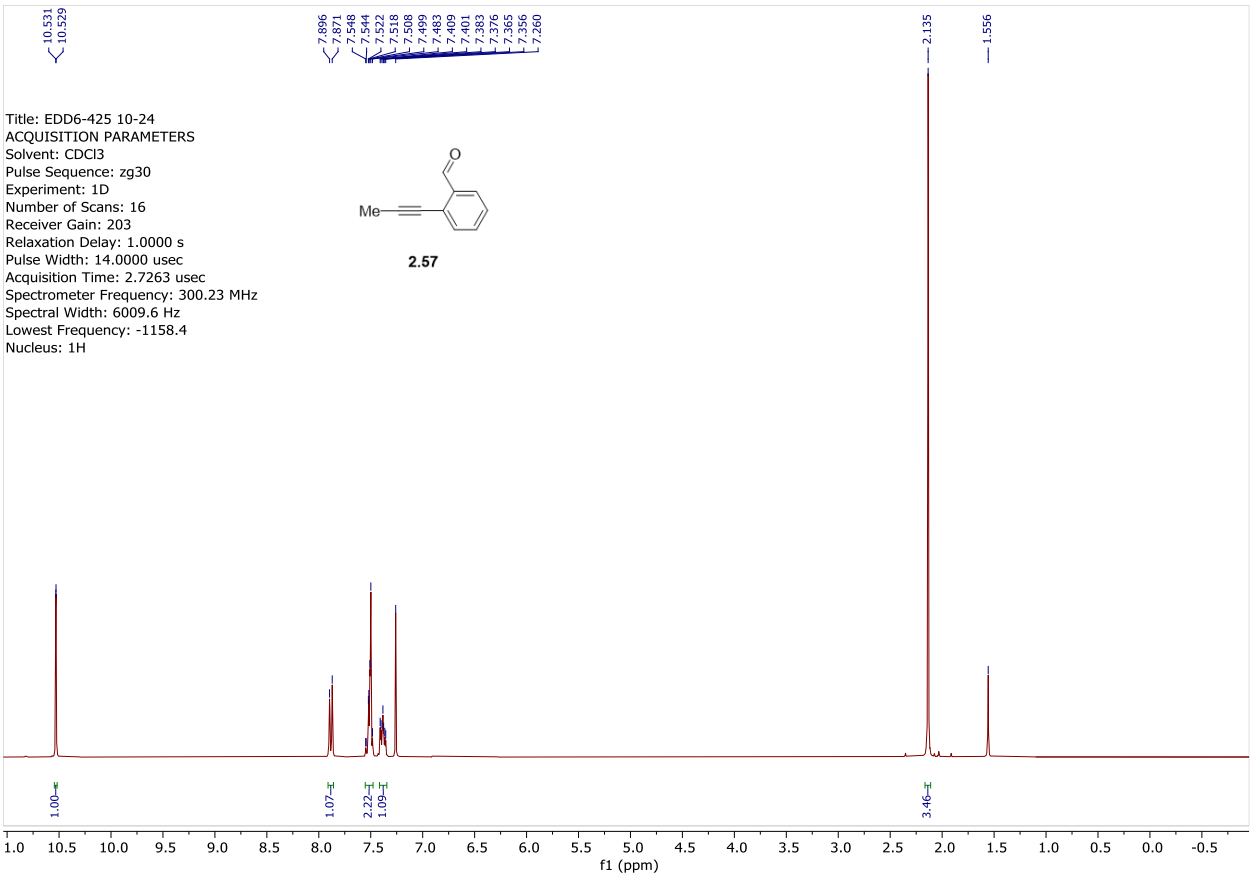
10.531
10.529
7.896
7.871
7.548
7.544
7.522
7.518
7.508
7.499
7.483
7.409
7.401
7.383
7.376
7.365
7.356
7.260
2.135
1.556
Title: EDD6-425 10-24
ACQUISITION PARAMETERS
Solvent: CDCl3
Pulse Sequence: zg30
Experiment: 1D
Number of Scans: 16
Receiver Gain: 203
Relaxation Delay: 1.0000 s
Pulse Width: 14.0000 usec
Acquisition Time: 2.7263 usec
Spectrometer Frequency: 300.23 MHz
Spectral Width: 6009.6 Hz
Lowest Frequency: -1158.4
Nucleus: 1H
O
Me
2.57
1.00
1.07
2.22
1.09
3.46
f1 (ppm)

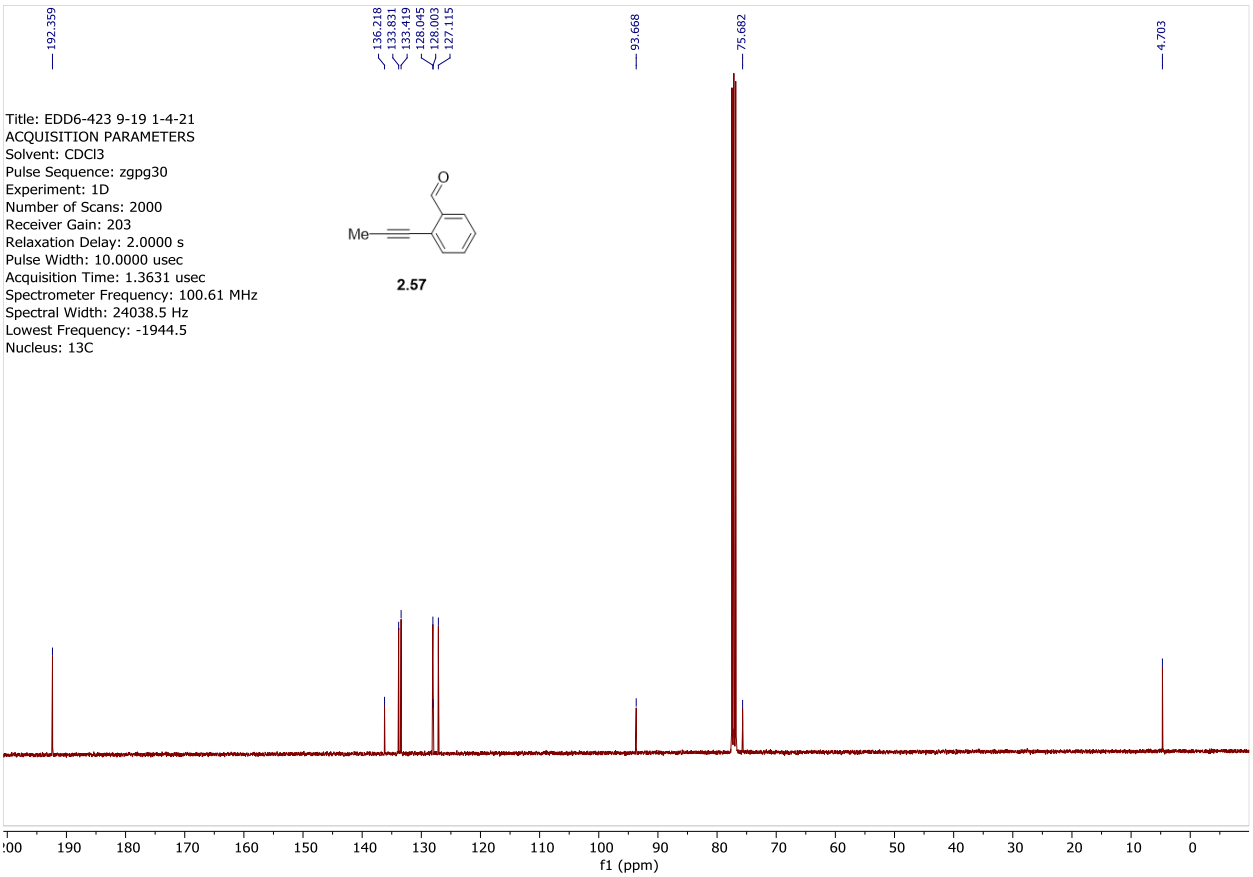
192.359
136.218
133.831
133.419
128.045
128.003
127.115
93.668
75.682
4.703
Title: EDD6-423 9-19 1-4-21
ACQUISITION PARAMETERS
Solvent: CDCl3
Pulse Sequence: zgpg30
Experiment: 1D
Number of Scans: 2000
Receiver Gain: 203
Relaxation Delay: 2.0000 s
Pulse Width: 10.0000 usec
Acquisition Time: 1.3631 usec
Spectrometer Frequency: 100.61 MHz
Spectral Width: 24038.5 Hz
Lowest Frequency: -1944.5
Nucleus: 13C
O
Me
2.57
190
180
170
160
150
140
130
120
110
100
90
80
70
60
50
40
30
20
10
0
f1 (ppm)

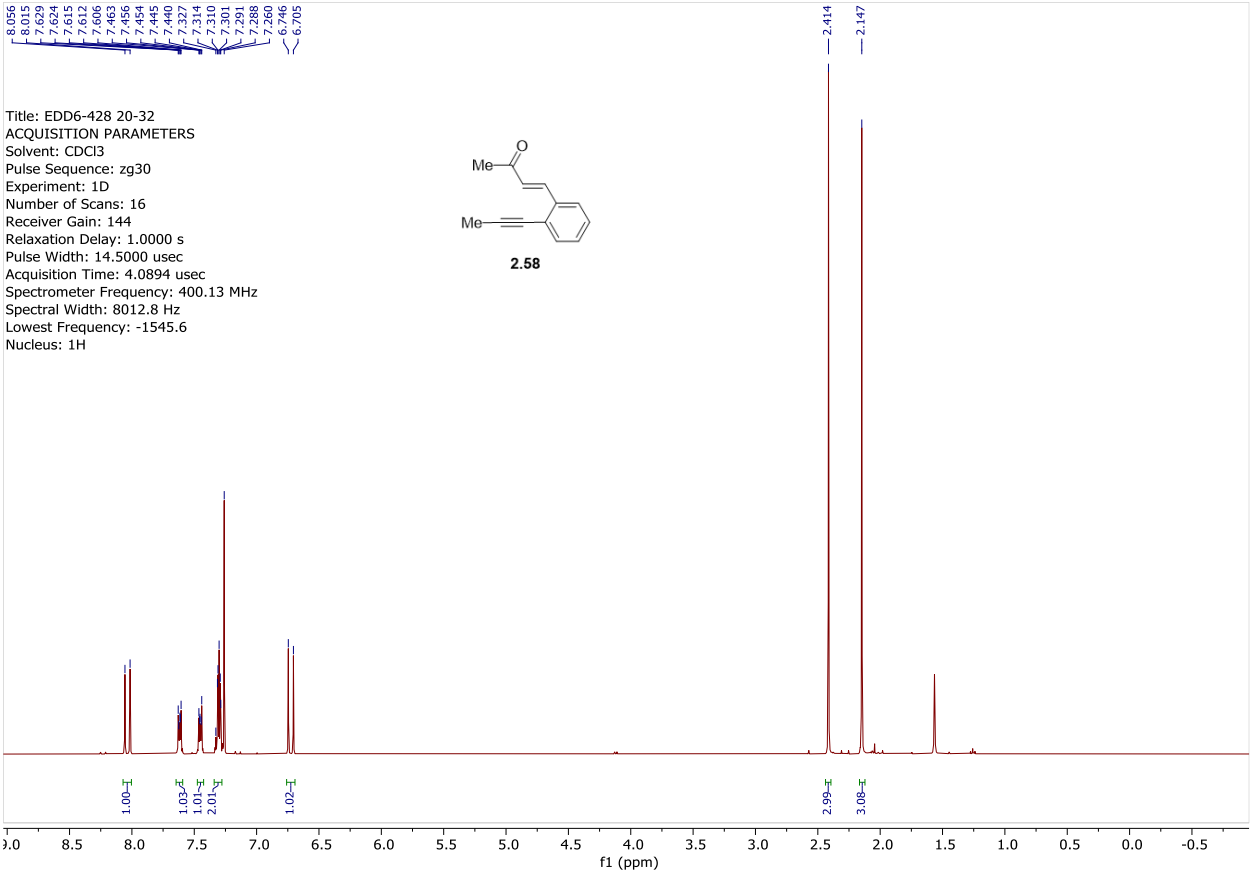
8.056
8.015
7.629
7.624
7.615
7.612
7.606
7.463
7.456
7.454
7.445
7.440
7.327
7.314
7.310
7.301
7.291
7.288
7.260
6.746
6.705
2.414
2.147
Title: EDD6-428 20-32
ACQUISITION PARAMETERS
Solvent: CDCl3
Pulse Sequence: zg30
Experiment: 1D
Number of Scans: 16
Receiver Gain: 144
Relaxation Delay: 1.0000 s
Pulse Width: 14.5000 usec
Acquisition Time: 4.0894 usec
Spectrometer Frequency: 400.13 MHz
Spectral Width: 8012.8 Hz
Lowest Frequency: -1545.6
Nucleus: 1H
Me
O
Me
2.58
1.00
1.03
1.01
2.01
1.02
2.99
3.08
f1 (ppm)

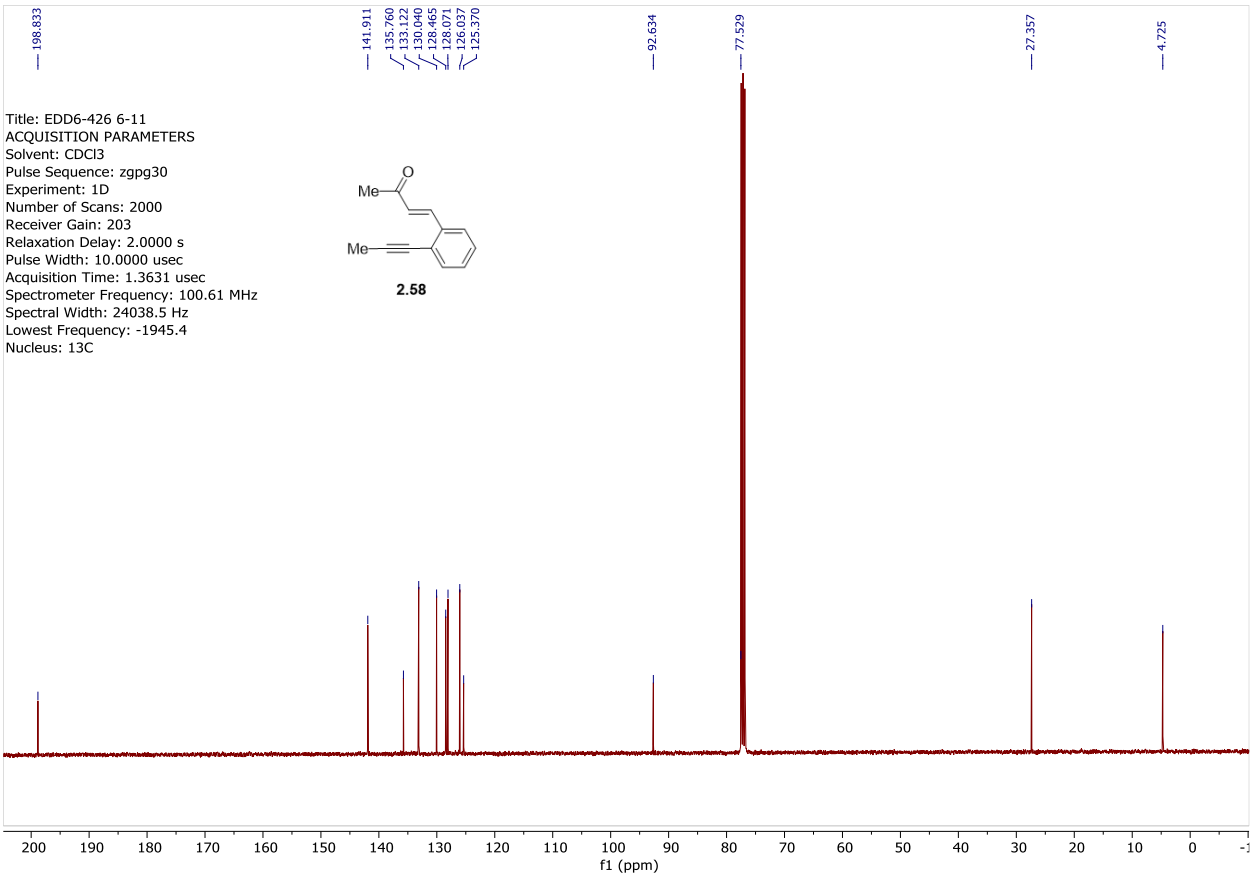
198.833
141.911
135.760
133.122
130.040
128.465
128.071
126.037
125.370
92.634
77.529
27.357
4.725
Title: EDD6-426 6-11
ACQUISITION PARAMETERS
Solvent: CDCl3
Pulse Sequence: zgpg30
Experiment: 1D
Number of Scans: 2000
Receiver Gain: 203
Relaxation Delay: 2.0000 s
Pulse Width: 10.0000 usec
Acquisition Time: 1.3631 usec
Spectrometer Frequency: 100.61 MHz
Spectral Width: 24038.5 Hz
Lowest Frequency: -1945.4
Nucleus: 13C
Me
O
Me
2.58
200 190 180 170 160 150 140 130 120 110 100 90 80 70 60 50 40 30 20 10 0
f1 (ppm)

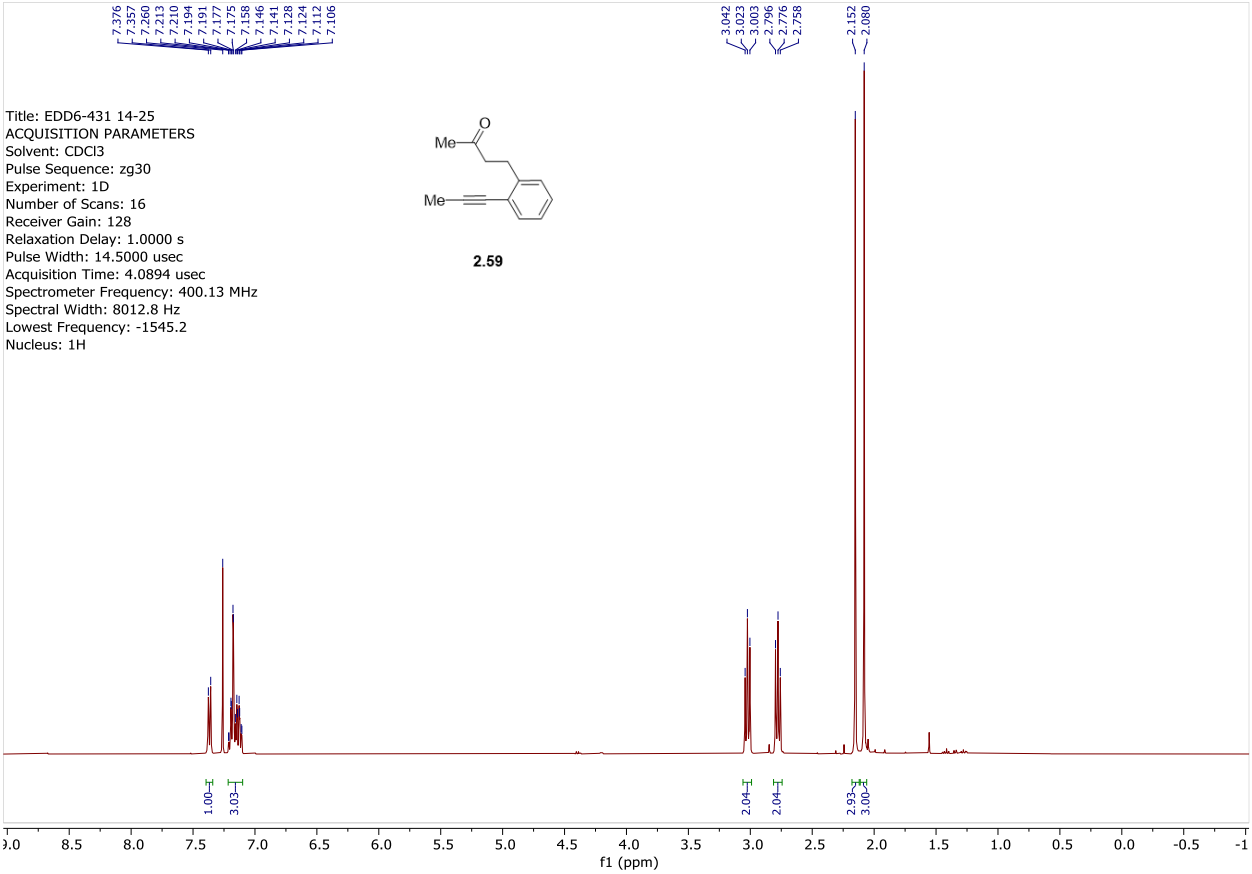
7.376
7.357
7.260
7.213
7.210
7.194
7.191
7.177
7.175
7.158
7.146
7.141
7.128
7.124
7.112
7.106
3.042
3.023
3.003
2.796
2.776
2.758
2.152
2.080
Title: EDD6-431 14-25
ACQUISITION PARAMETERS
Solvent: CDCl3
Pulse Sequence: zg30
Experiment: 1D
Number of Scans: 16
Receiver Gain: 128
Relaxation Delay: 1.0000 s
Pulse Width: 14.5000 usec
Acquisition Time: 4.0894 usec
Spectrometer Frequency: 400.13 MHz
Spectral Width: 8012.8 Hz
Lowest Frequency: -1545.2
Nucleus: 1H
Me
O
Me
2.59
1.00
3.03
2.04
2.04
2.93
3.00
f1 (ppm)

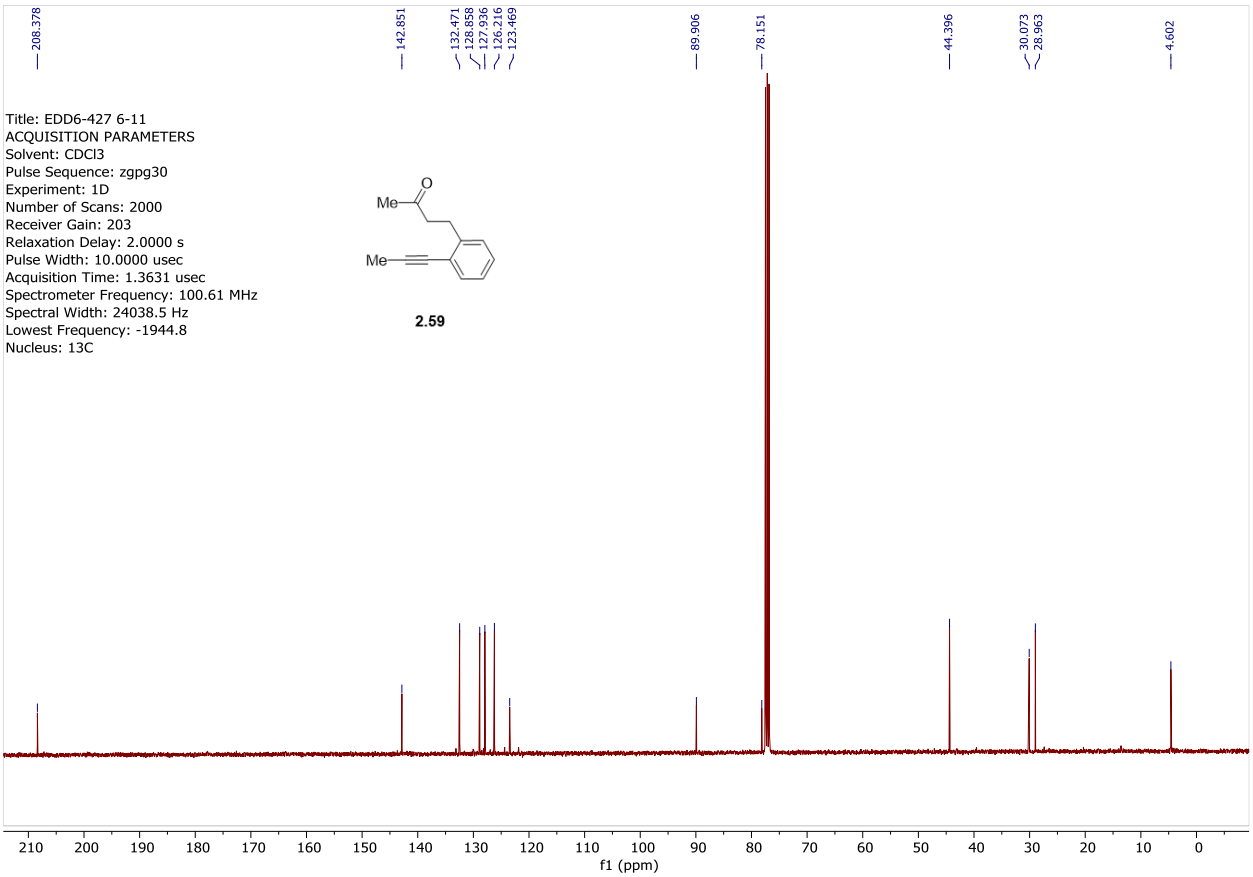
208.378
142.851
132.471
128.858
127.936
126.216
123.469
89.906
78.151
44.396
30.073
28.963
4.602
Title: EDD6-427 6-11
ACQUISITION PARAMETERS
Solvent: CDCl3
Pulse Sequence: zgpg30
Experiment: 1D
Number of Scans: 2000
Receiver Gain: 203
Relaxation Delay: 2.0000 s
Pulse Width: 10.0000 usec
Acquisition Time: 1.3631 usec
Spectrometer Frequency: 100.61 MHz
Spectral Width: 24038.5 Hz
Lowest Frequency: -1944.8
Nucleus: 13C
Me
O
Me
2.59
210 200 190 180 170 160 150 140 130 120 110 100 90 80 70 60 50 40 30 20 10 0
f1 (ppm)

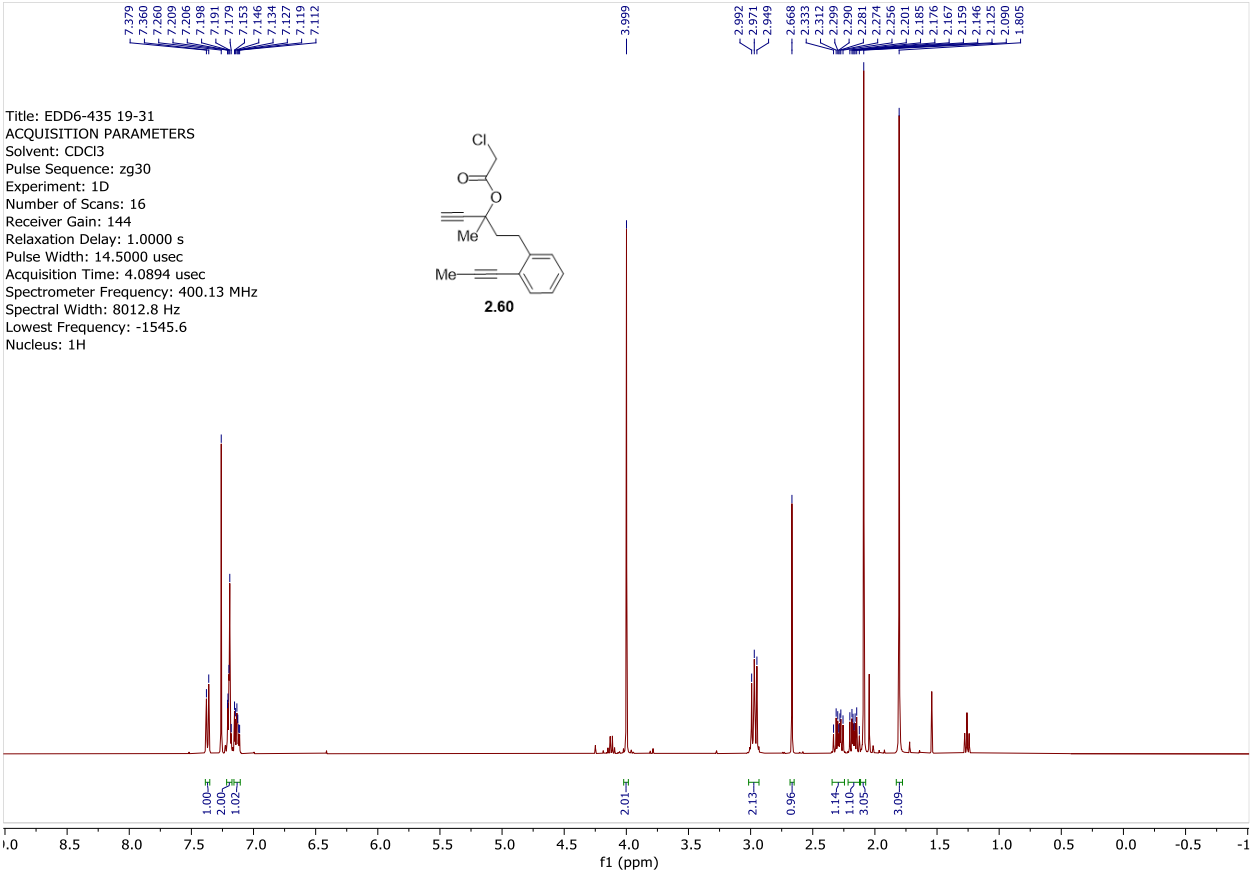
Title: EDD6-435 19-31
ACQUISITION PARAMETERS
Solvent: CDCl3
Pulse Sequence: zg30
Experiment: 1D
Number of Scans: 16
Receiver Gain: 144
Relaxation Delay: 1.0000 s
Pulse Width: 14.5000 usec
Acquisition Time: 4.0894 usec
Spectrometer Frequency: 400.13 MHz
Spectral Width: 8012.8 Hz
Lowest Frequency: -1545.6
Nucleus: 1H
Cl
O
O
Me
Me
2.60
f1 (ppm)

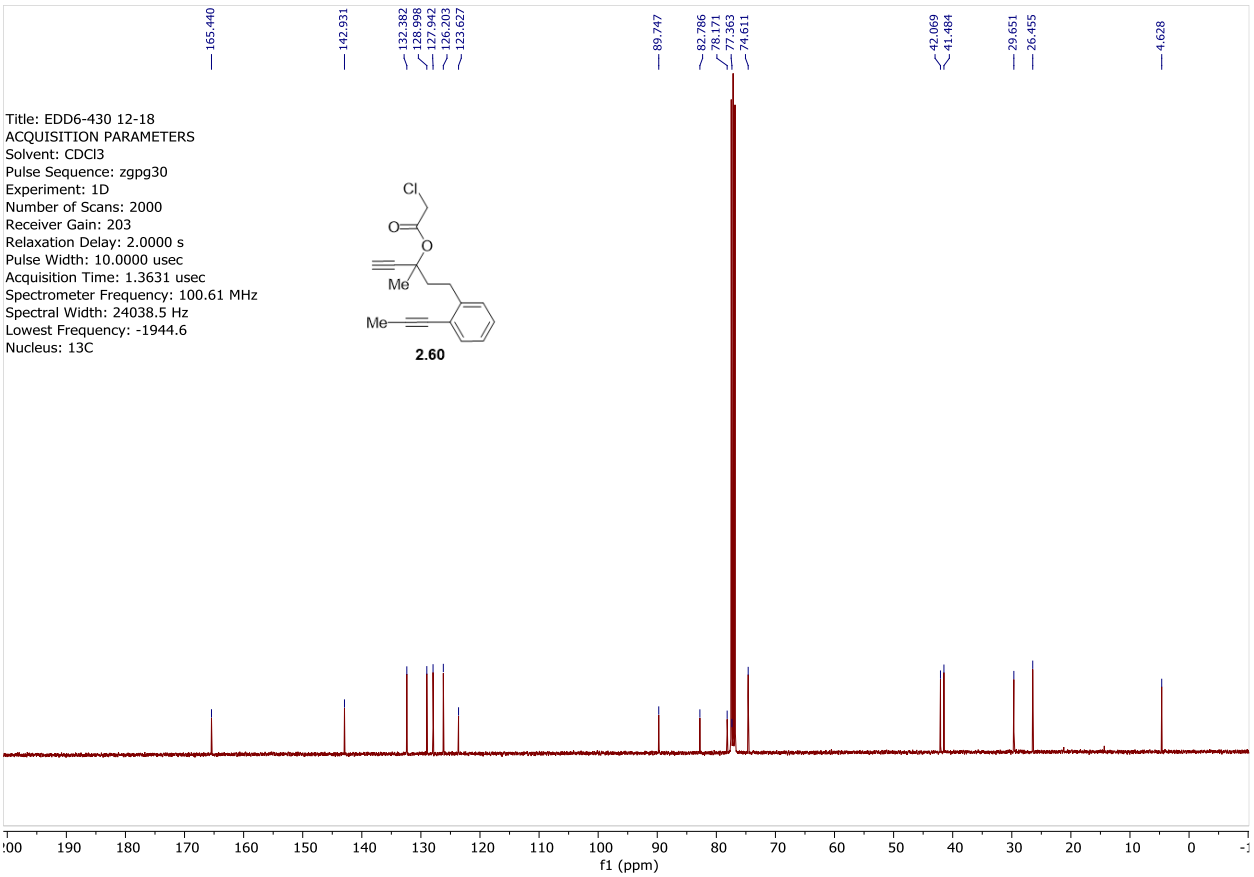
165.440
142.931
132.382
128.998
127.942
126.203
123.627
89.747
82.786
78.171
77.363
74.611
42.069
41.484
29.651
26.455
4.628
Title: EDD6-430 12-18
ACQUISITION PARAMETERS
Solvent: CDCl3
Pulse Sequence: zgpg30
Experiment: 1D
Number of Scans: 2000
Receiver Gain: 203
Relaxation Delay: 2.0000 s
Pulse Width: 10.0000 usec
Acquisition Time: 1.3631 usec
Spectrometer Frequency: 100.61 MHz
Spectral Width: 24038.5 Hz
Lowest Frequency: -1944.6
Nucleus: 13C
Cl
O
O
Me
Me
2.60
190
180
170
160
150
140
130
120
110
100
90
80
70
60
50
40
30
20
10
0
f1 (ppm)

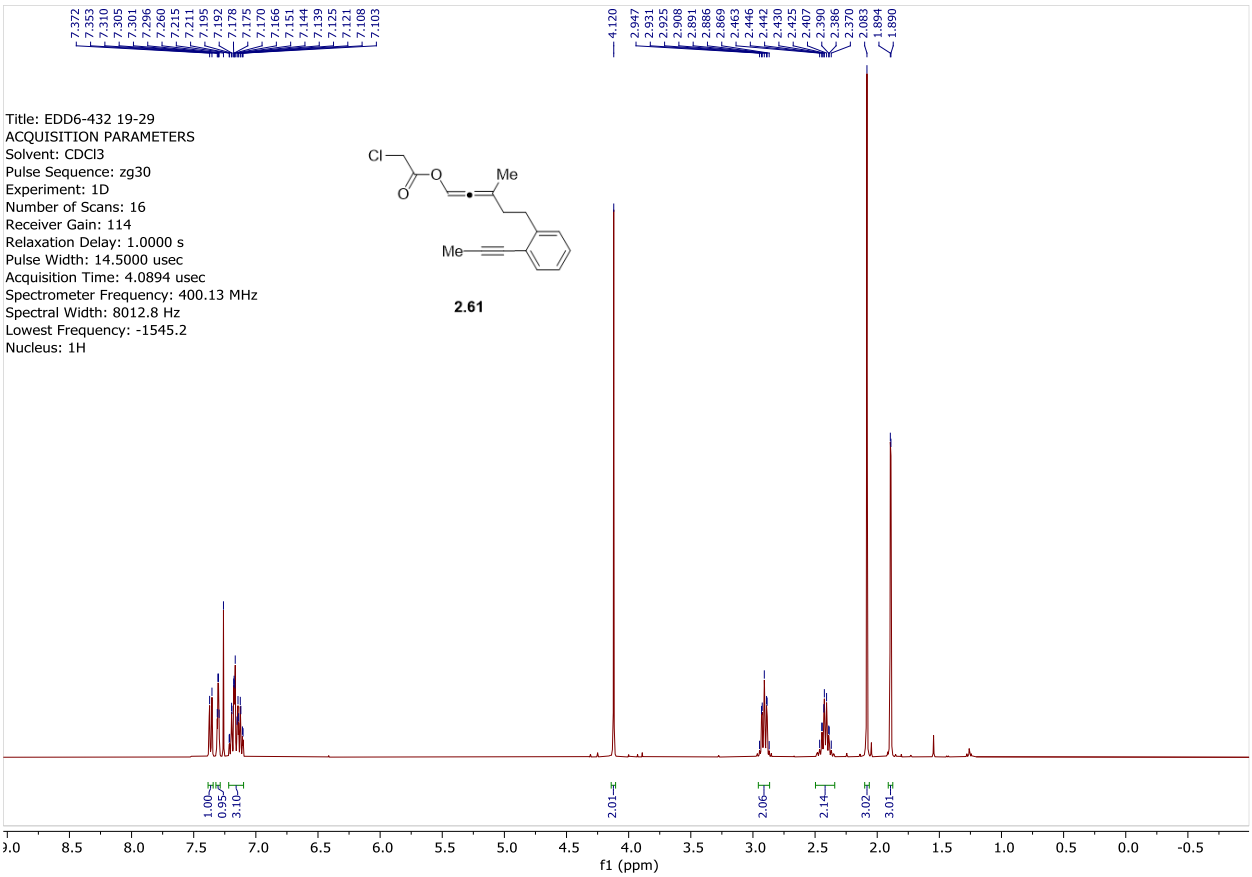
Title: EDD6-432 19-29
ACQUISITION PARAMETERS
Solvent: CDCl3
Pulse Sequence: zg30
Experiment: 1D
Number of Scans: 16
Receiver Gain: 114
Relaxation Delay: 1.0000 s
Pulse Width: 14.5000 usec
Acquisition Time: 4.0894 usec
Spectrometer Frequency: 400.13 MHz
Spectral Width: 8012.8 Hz
Lowest Frequency: -1545.2
Nucleus: 1H
Cl
O
O
Me
Me
2.61
f1 (ppm)

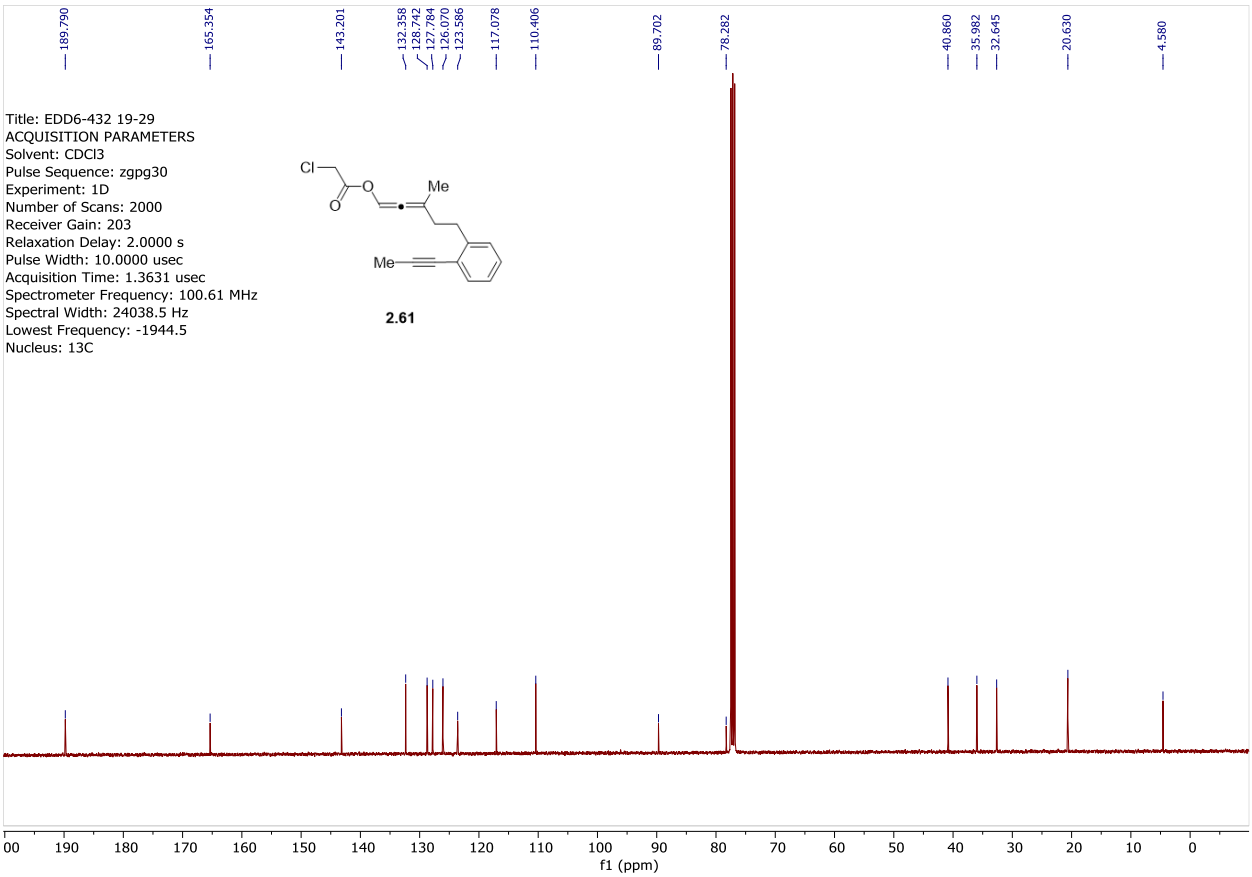
189.790
165.354
143.201
132.358
128.742
127.784
126.070
123.586
117.078
110.406
89.702
78.282
40.860
35.982
32.645
20.630
4.580
Title: EDD6-432 19-29
ACQUISITION PARAMETERS
Solvent: CDCl3
Pulse Sequence: zgpg30
Experiment: 1D
Number of Scans: 2000
Receiver Gain: 203
Relaxation Delay: 2.0000 s
Pulse Width: 10.0000 usec
Acquisition Time: 1.3631 usec
Spectrometer Frequency: 100.61 MHz
Spectral Width: 24038.5 Hz
Lowest Frequency: -1944.5
Nucleus: 13C
Cl
O
O
Me
Me
2.61
00 190 180 170 160 150 140 130 120 110 100 90 80 70 60 50 40 30 20 10 0
f1 (ppm)

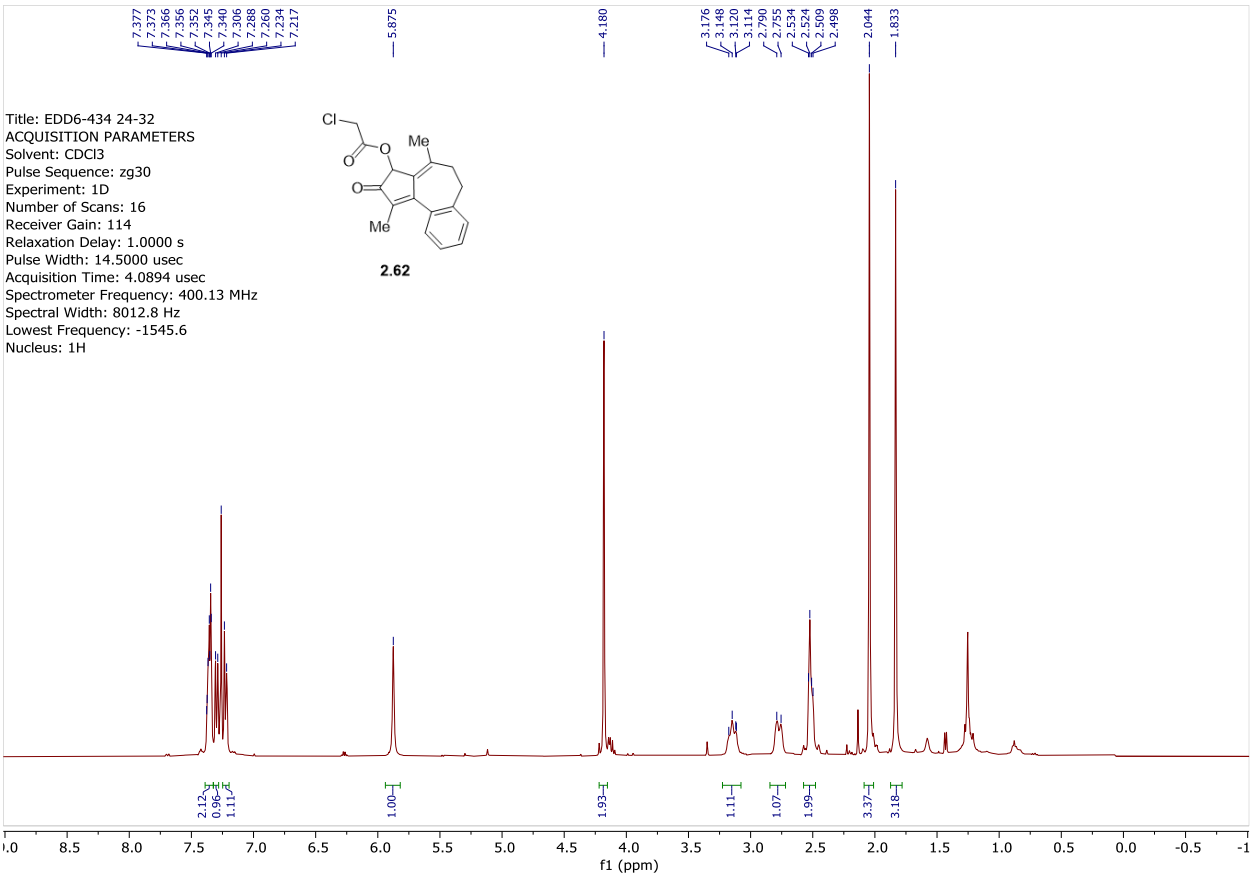
7.377
7.373
7.366
7.356
7.352
7.345
7.340
7.306
7.288
7.260
7.234
7.217
5.875
4.180
3.176
3.148
3.120
3.114
2.790
2.755
2.534
2.524
2.509
2.498
2.044
1.833
Title: EDD6-434 24-32
ACQUISITION PARAMETERS
Solvent: CDCl3
Pulse Sequence: zg30
Experiment: 1D
Number of Scans: 16
Receiver Gain: 114
Relaxation Delay: 1.0000 s
Pulse Width: 14.5000 usec
Acquisition Time: 4.0894 usec
Spectrometer Frequency: 400.13 MHz
Spectral Width: 8012.8 Hz
Lowest Frequency: -1545.6
Nucleus: 1H
Cl
O
O
Me
O
Me
2.62
2.12
0.96
1.11
1.00
1.93
1.11
1.07
1.99
3.37
3.18
8.5
8.0
7.5
7.0
6.5
6.0
5.5
5.0
4.5
4.0
3.5
3.0
2.5
2.0
1.5
1.0
0.5
0.0
-0.5
f1 (ppm)

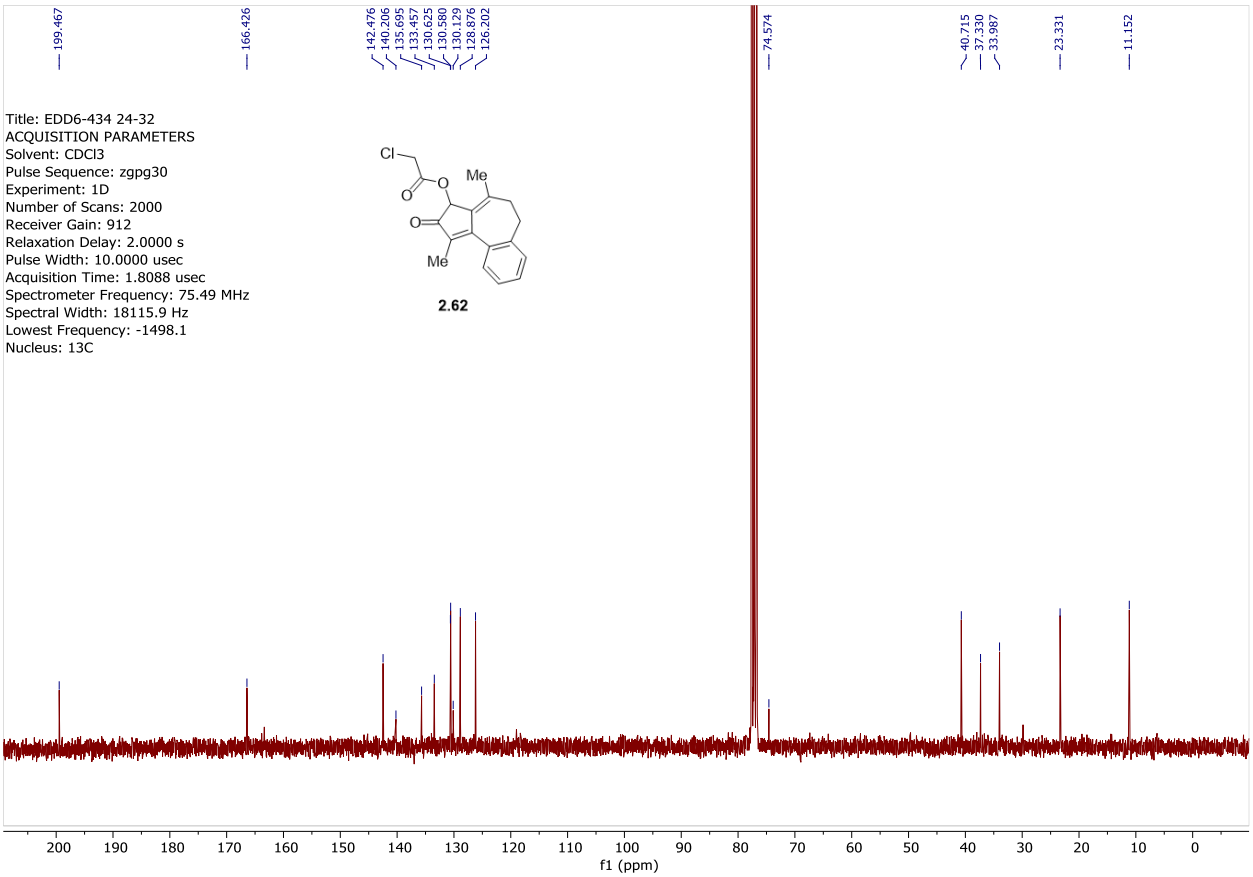
199.467
166.426
142.476
140.206
135.695
133.457
130.625
130.580
130.129
128.876
126.202
74.574
40.715
37.330
33.987
23.331
11.152
Title: EDD6-434 24-32
ACQUISITION PARAMETERS
Solvent: CDCl3
Pulse Sequence: zgpg30
Experiment: 1D
Number of Scans: 2000
Receiver Gain: 912
Relaxation Delay: 2.0000 s
Pulse Width: 10.0000 usec
Acquisition Time: 1.8088 usec
Spectrometer Frequency: 75.49 MHz
Spectral Width: 18115.9 Hz
Lowest Frequency: -1498.1
Nucleus: 13C
Cl
O
O
Me
O
Me
2.62
200 190 180 170 160 150 140 130 120 110 100 90 80 70 60 50 40 30 20 10 0
f1 (ppm)

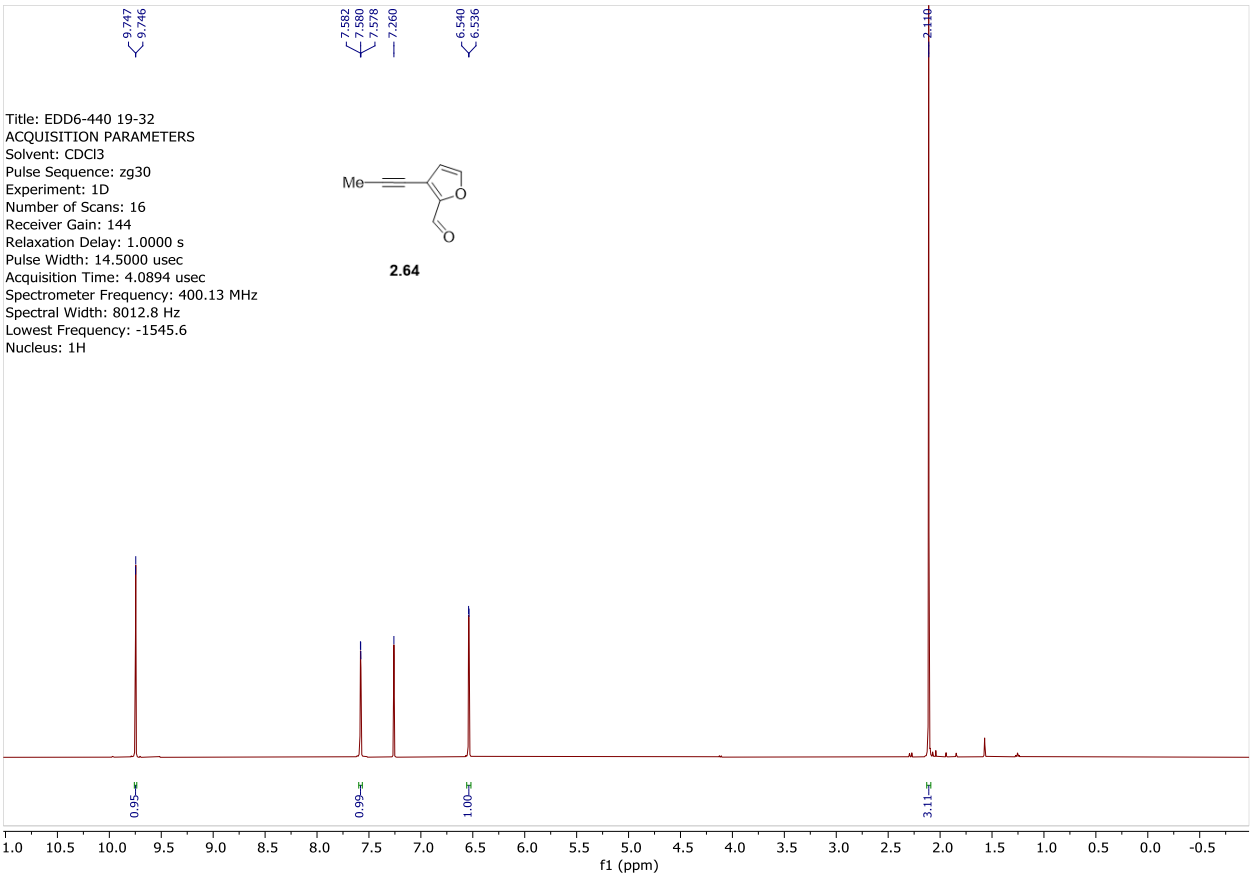
9.747
9.746
7.582
7.580
7.578
7.260
6.540
6.536
2.110
Title: EDD6-440 19-32
ACQUISITION PARAMETERS
Solvent: CDCl3
Pulse Sequence: zg30
Experiment: 1D
Number of Scans: 16
Receiver Gain: 144
Relaxation Delay: 1.0000 s
Pulse Width: 14.5000 usec
Acquisition Time: 4.0894 usec
Spectrometer Frequency: 400.13 MHz
Spectral Width: 8012.8 Hz
Lowest Frequency: -1545.6
Nucleus: 1H
Me
O
O
2.64
0.95
0.99
1.00
3.11
1.0 10.5 10.0 9.5 9.0 8.5 8.0 7.5 7.0 6.5 6.0 5.5 5.0 4.5 4.0 3.5 3.0 2.5 2.0 1.5 1.0 0.5 0.0 -0.5
f1 (ppm)

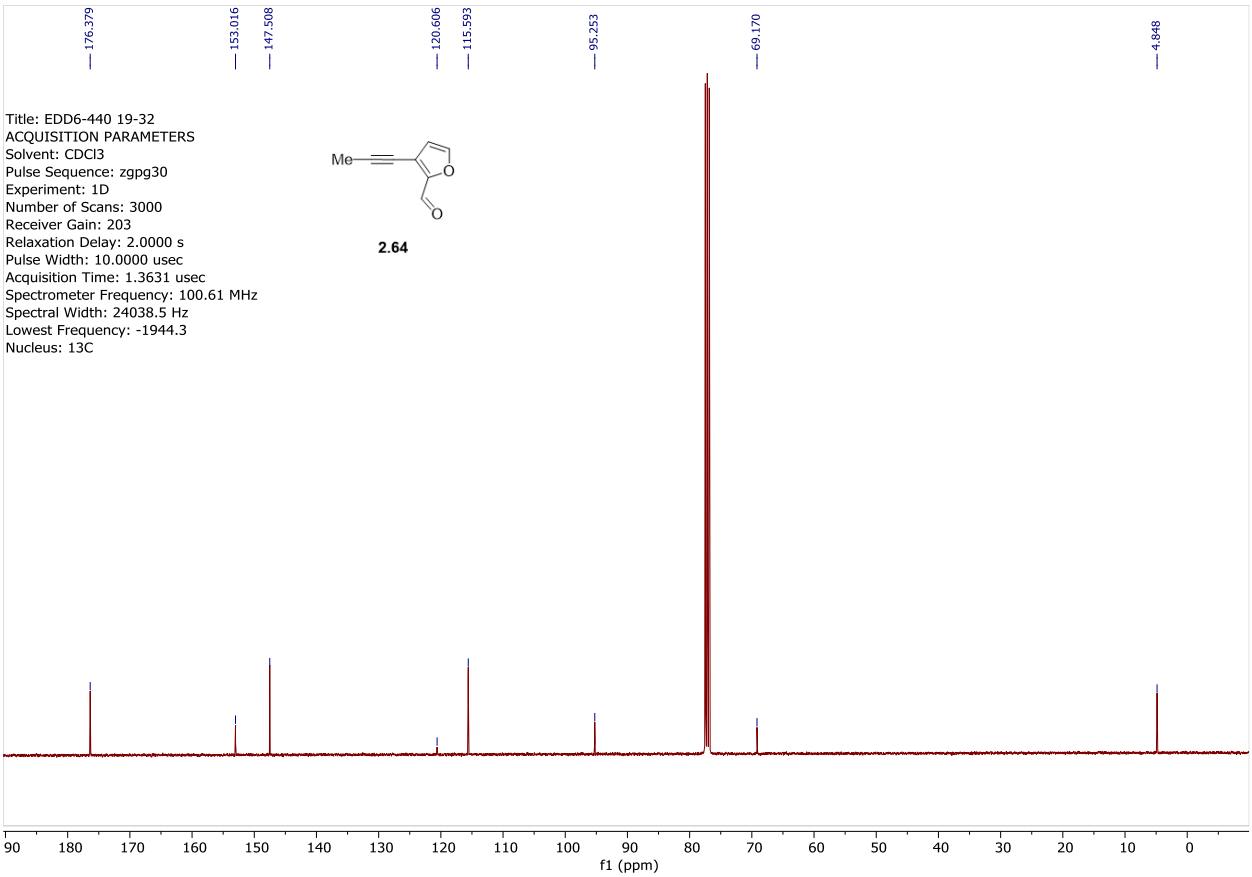
176.379
153.016
147.508
120.606
115.593
95.253
69.170
4.848
Title: EDD6-440 19-32
ACQUISITION PARAMETERS
Solvent: CDCl3
Pulse Sequence: zgpg30
Experiment: 1D
Number of Scans: 3000
Receiver Gain: 203
Relaxation Delay: 2.0000 s
Pulse Width: 10.0000 usec
Acquisition Time: 1.3631 usec
Spectrometer Frequency: 100.61 MHz
Spectral Width: 24038.5 Hz
Lowest Frequency: -1944.3
Nucleus: 13C
Me
O
O
2.64
90 180 170 160 150 140 130 120 110 100 90 80 70 60 50 40 30 20 10 0
f1 (ppm)

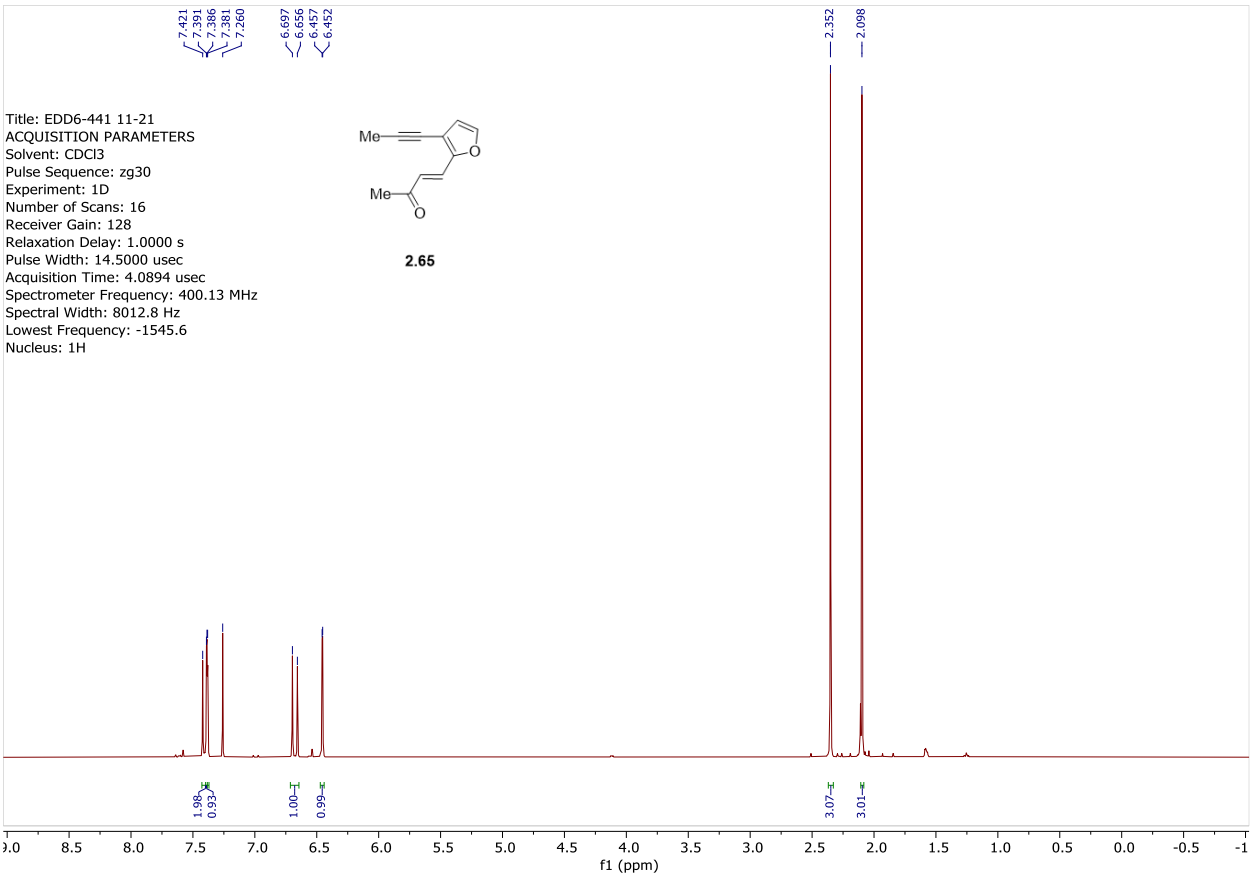
7.421
7.391
7.386
7.381
7.260
6.697
6.656
6.457
6.452
2.352
2.098
Title: EDD6-441 11-21
ACQUISITION PARAMETERS
Solvent: CDCl3
Pulse Sequence: zg30
Experiment: 1D
Number of Scans: 16
Receiver Gain: 128
Relaxation Delay: 1.0000 s
Pulse Width: 14.5000 usec
Acquisition Time: 4.0894 usec
Spectrometer Frequency: 400.13 MHz
Spectral Width: 8012.8 Hz
Lowest Frequency: -1545.6
Nucleus: 1H
Me
O
Me
O
2.65
1.98
0.93
1.00
0.99
3.07
3.01
f1 (ppm)

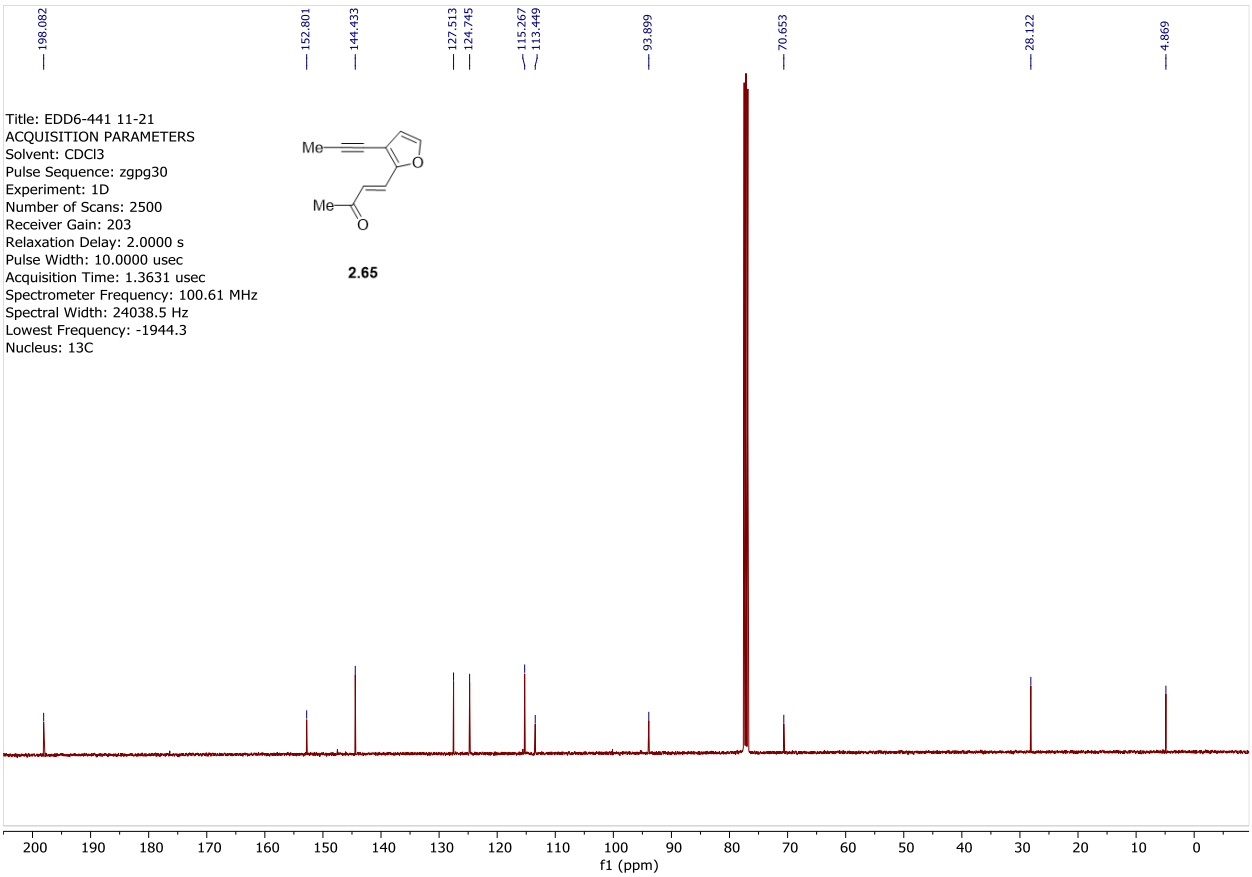
198.082
152.801
144.433
127.513
124.745
115.267
113.449
93.899
70.653
28.122
4.869
Title: EDD6-441 11-21
ACQUISITION PARAMETERS
Solvent: CDCl3
Pulse Sequence: zgpg30
Experiment: 1D
Number of Scans: 2500
Receiver Gain: 203
Relaxation Delay: 2.0000 s
Pulse Width: 10.0000 usec
Acquisition Time: 1.3631 usec
Spectrometer Frequency: 100.61 MHz
Spectral Width: 24038.5 Hz
Lowest Frequency: -1944.3
Nucleus: 13C
Me
O
Me
O
2.65
200 190 180 170 160 150 140 130 120 110 100 90 80 70 60 50 40 30 20 10 0
f1 (ppm)

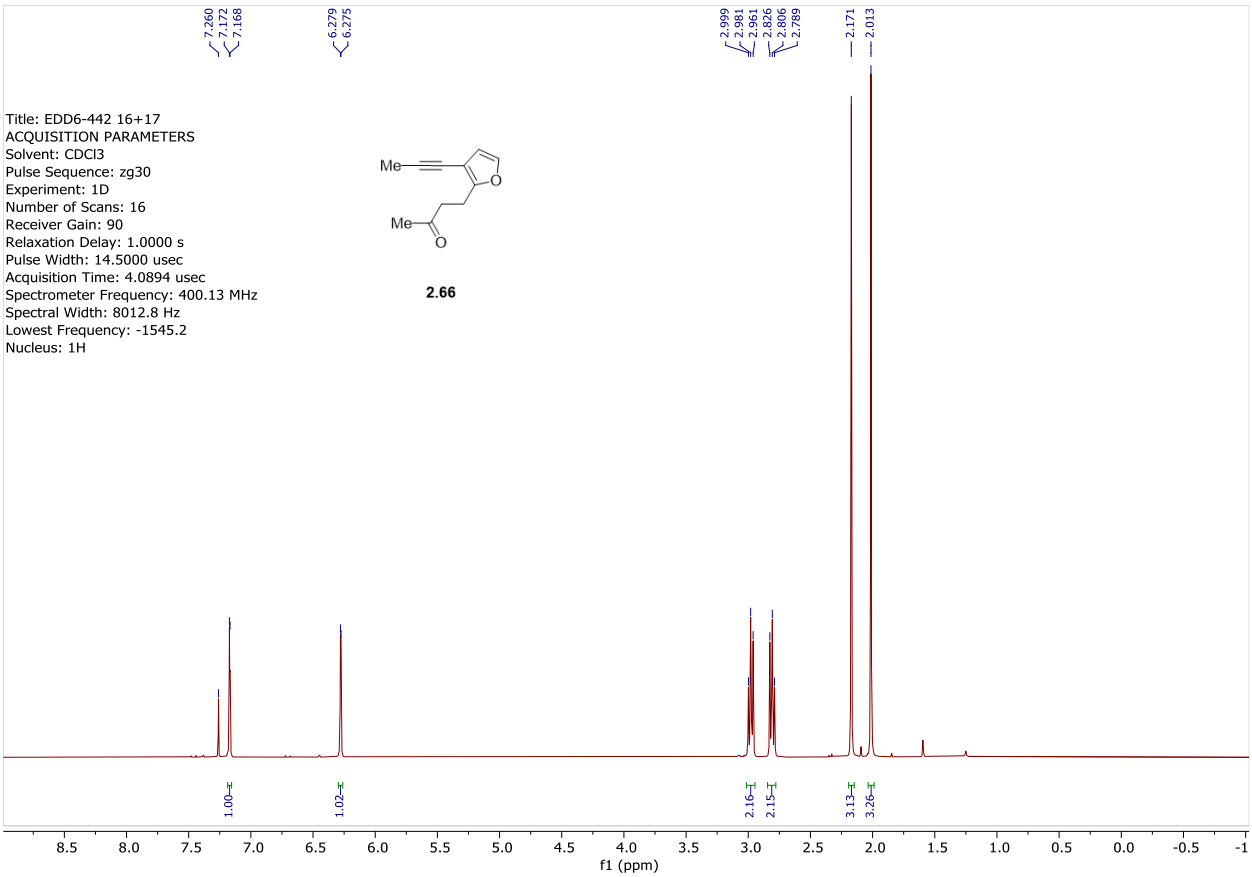
7.260
7.172
7.168
6.279
6.275
2.999
2.981
2.961
2.826
2.806
2.789
2.171
2.013
Title: EDD6-442 16+17
ACQUISITION PARAMETERS
Solvent: CDCl3
Pulse Sequence: zg30
Experiment: 1D
Number of Scans: 16
Receiver Gain: 90
Relaxation Delay: 1.0000 s
Pulse Width: 14.5000 usec
Acquisition Time: 4.0894 usec
Spectrometer Frequency: 400.13 MHz
Spectral Width: 8012.8 Hz
Lowest Frequency: -1545.2
Nucleus: 1H
Me
O
Me
O
2.66
1.00
1.02
2.16
2.15
3.13
3.26
8.5
8.0
7.5
7.0
6.5
6.0
5.5
5.0
4.5
4.0
3.5
3.0
2.5
2.0
1.5
1.0
0.5
0.0
-0.5
-1
f1 (ppm)

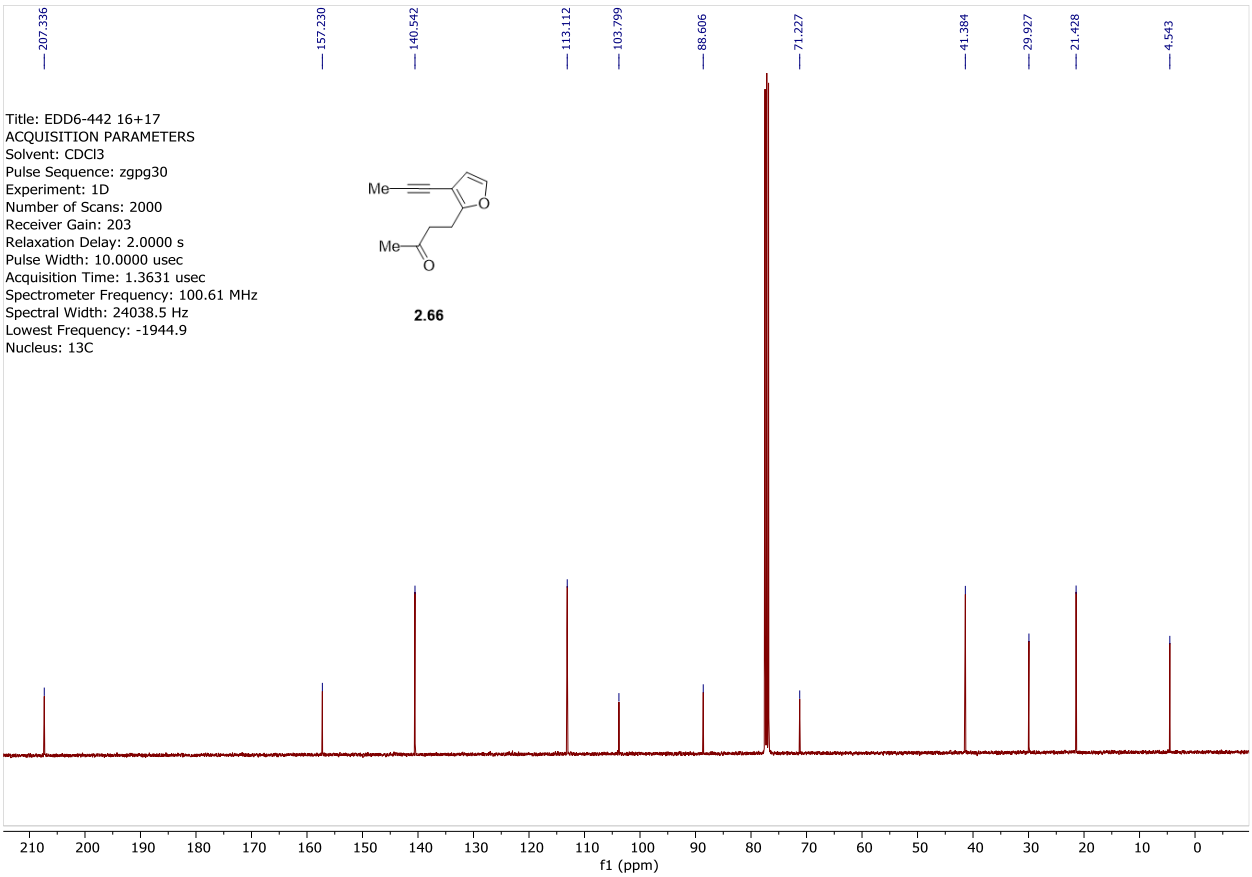
207.336
157.230
140.542
113.112
103.799
88.606
71.227
41.384
29.927
21.428
4.543
Title: EDD6-442 16+17
ACQUISITION PARAMETERS
Solvent: CDCl3
Pulse Sequence: zgpg30
Experiment: 1D
Number of Scans: 2000
Receiver Gain: 203
Relaxation Delay: 2.0000 s
Pulse Width: 10.0000 usec
Acquisition Time: 1.3631 usec
Spectrometer Frequency: 100.61 MHz
Spectral Width: 24038.5 Hz
Lowest Frequency: -1944.9
Nucleus: 13C
Me
O
Me
O
2.66
210 200 190 180 170 160 150 140 130 120 110 100 90 80 70 60 50 40 30 20 10 0
f1 (ppm)

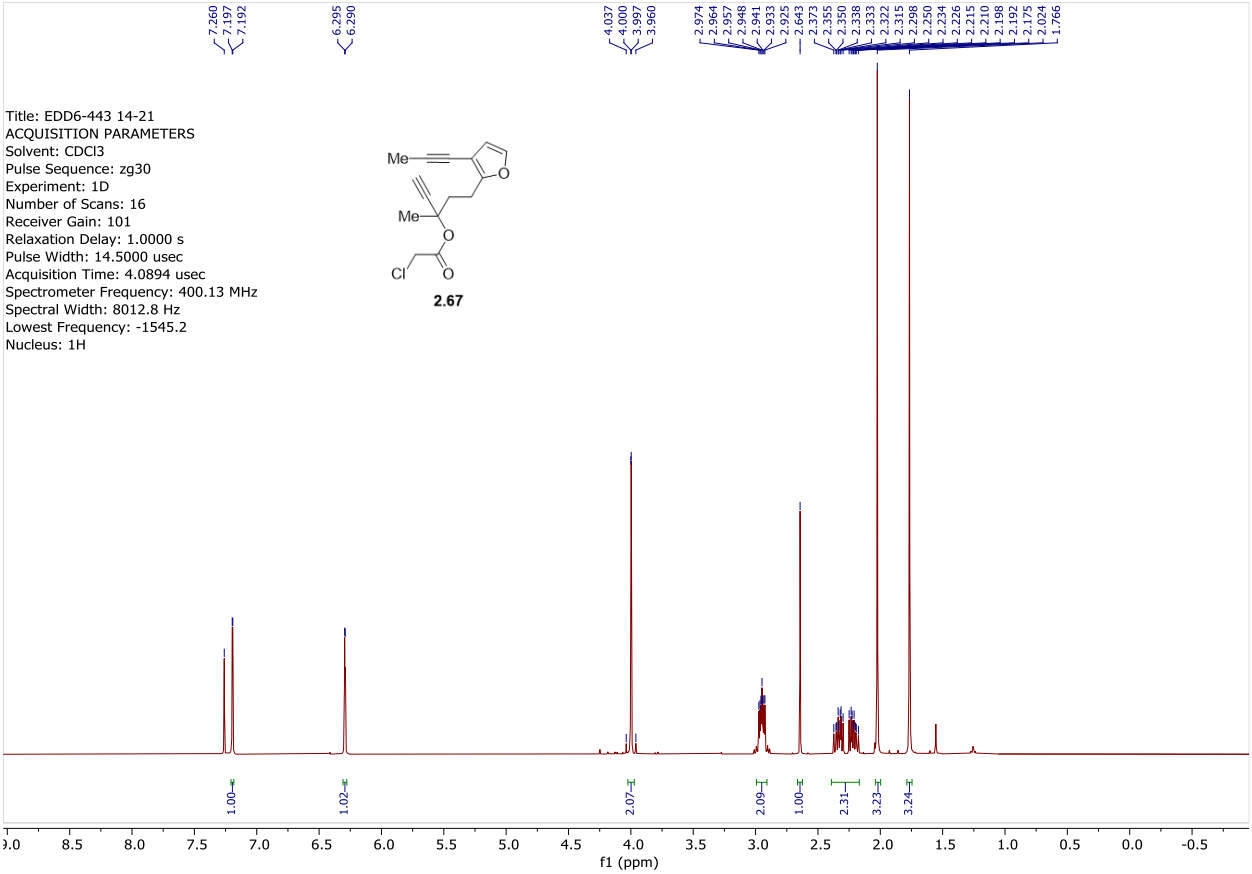
Title: EDD6-443 14-21
ACQUISITION PARAMETERS
Solvent: CDCl3
Pulse Sequence: zg30
Experiment: 1D
Number of Scans: 16
Receiver Gain: 101
Relaxation Delay: 1.0000 s
Pulse Width: 14.5000 usec
Acquisition Time: 4.0894 usec
Spectrometer Frequency: 400.13 MHz
Spectral Width: 8012.8 Hz
Lowest Frequency: -1545.2
Nucleus: 1H
Me
Me
O
Cl
O
O
2.67
7.260
7.197
7.192
6.295
6.290
4.037
4.000
3.997
3.960
2.974
2.964
2.957
2.948
2.941
2.933
2.925
2.643
2.373
2.355
2.350
2.338
2.333
2.322
2.315
2.298
2.250
2.234
2.226
2.215
2.210
2.198
2.192
2.175
2.024
1.766
1.00
1.02
2.07
2.09
1.00
2.31
3.23
3.24
f1 (ppm)

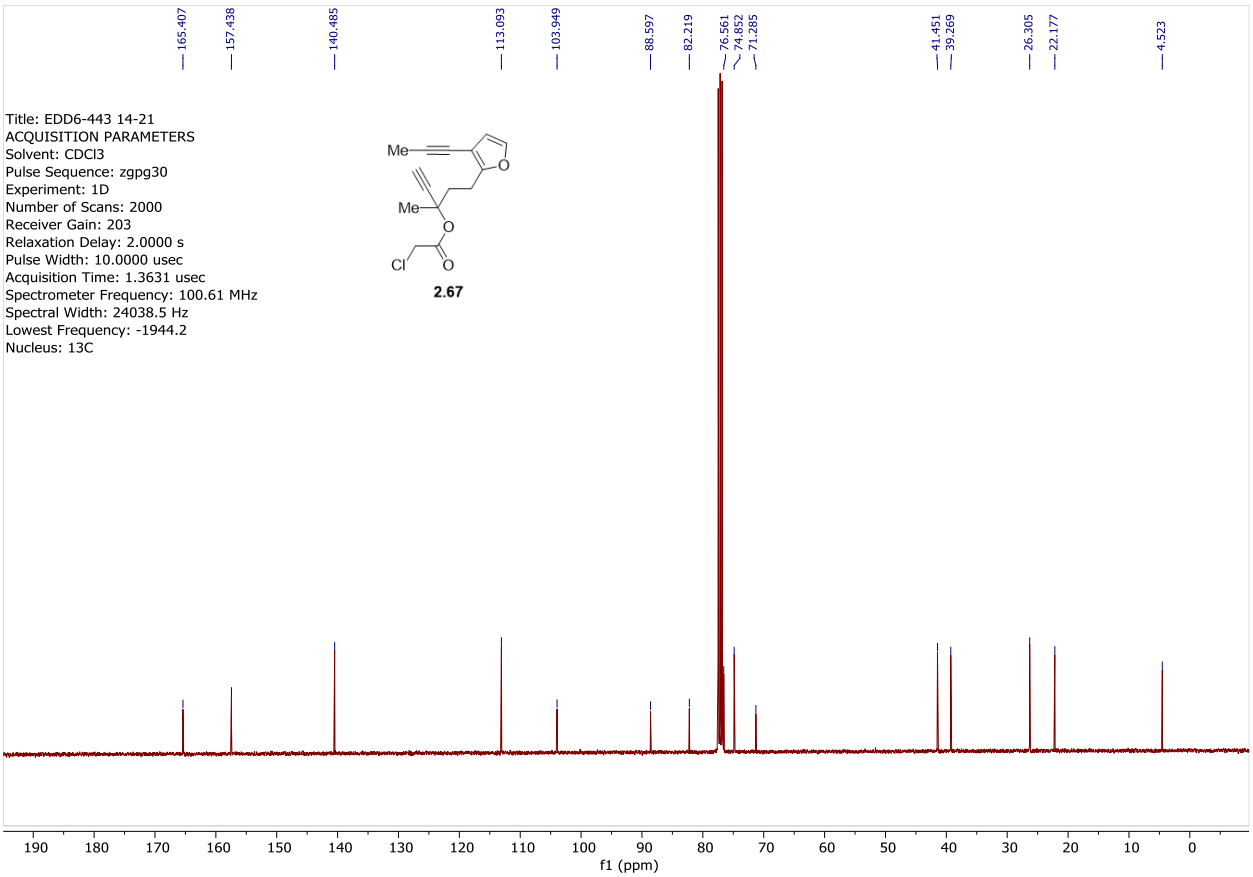
165.407
157.438
140.485
113.093
103.949
88.597
82.219
76.561
74.852
71.285
41.451
39.269
26.305
22.177
4.523
Title: EDD6-443 14-21
ACQUISITION PARAMETERS
Solvent: CDCl3
Pulse Sequence: zgpg30
Experiment: 1D
Number of Scans: 2000
Receiver Gain: 203
Relaxation Delay: 2.0000 s
Pulse Width: 10.0000 usec
Acquisition Time: 1.3631 usec
Spectrometer Frequency: 100.61 MHz
Spectral Width: 24038.5 Hz
Lowest Frequency: -1944.2
Nucleus: 13C
Me
O
Me
O
Cl
O
2.67
190
180
170
160
150
140
130
120
110
100
90
80
70
60
50
40
30
20
10
0
f1 (ppm)

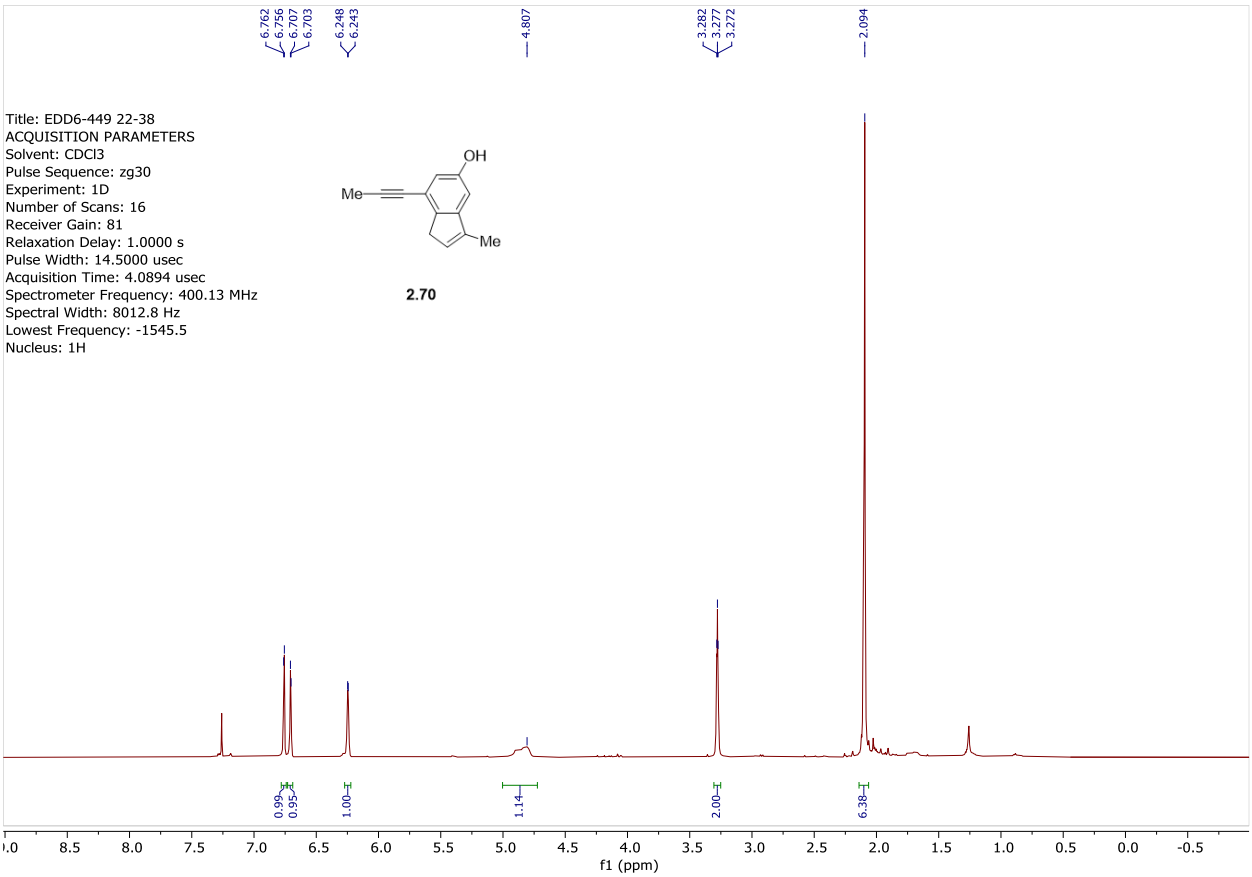
6.762
6.756
6.707
6.703
6.248
6.243
4.807
3.282
3.277
3.272
2.094
Title: EDD6-449 22-38
ACQUISITION PARAMETERS
Solvent: CDCl3
Pulse Sequence: zg30
Experiment: 1D
Number of Scans: 16
Receiver Gain: 81
Relaxation Delay: 1.0000 s
Pulse Width: 14.5000 usec
Acquisition Time: 4.0894 usec
Spectrometer Frequency: 400.13 MHz
Spectral Width: 8012.8 Hz
Lowest Frequency: -1545.5
Nucleus: 1H
OH
Me
Me
2.70
0.99
0.95
1.00
1.14
2.00
6.38
f1 (ppm)

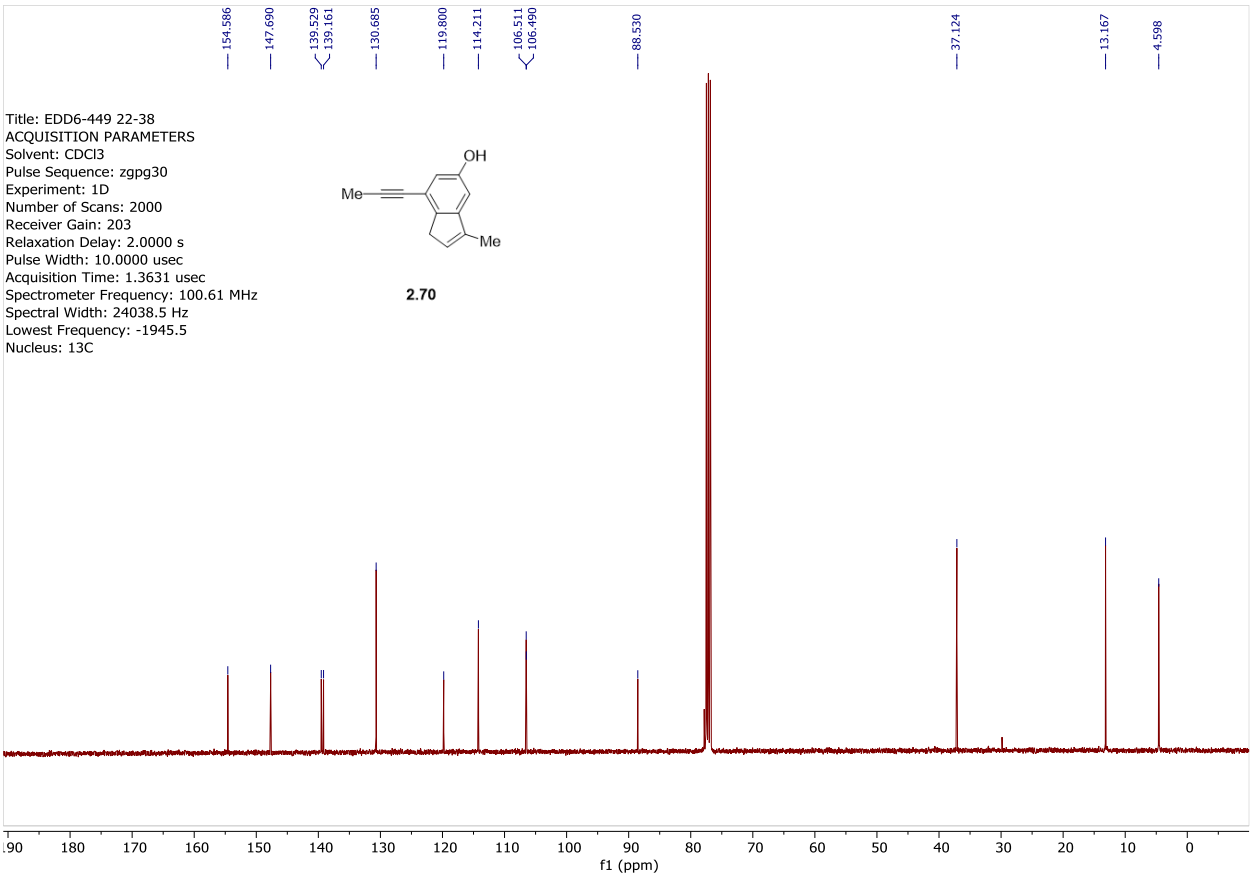
154.586
147.690
139.529
139.161
130.685
119.800
114.211
106.511
106.490
88.530
37.124
13.167
4.598
Title: EDD6-449 22-38
ACQUISITION PARAMETERS
Solvent: CDCl3
Pulse Sequence: zgpg30
Experiment: 1D
Number of Scans: 2000
Receiver Gain: 203
Relaxation Delay: 2.0000 s
Pulse Width: 10.0000 usec
Acquisition Time: 1.3631 usec
Spectrometer Frequency: 100.61 MHz
Spectral Width: 24038.5 Hz
Lowest Frequency: -1945.5
Nucleus: 13C
OH
Me
Me
2.70
f1 (ppm)

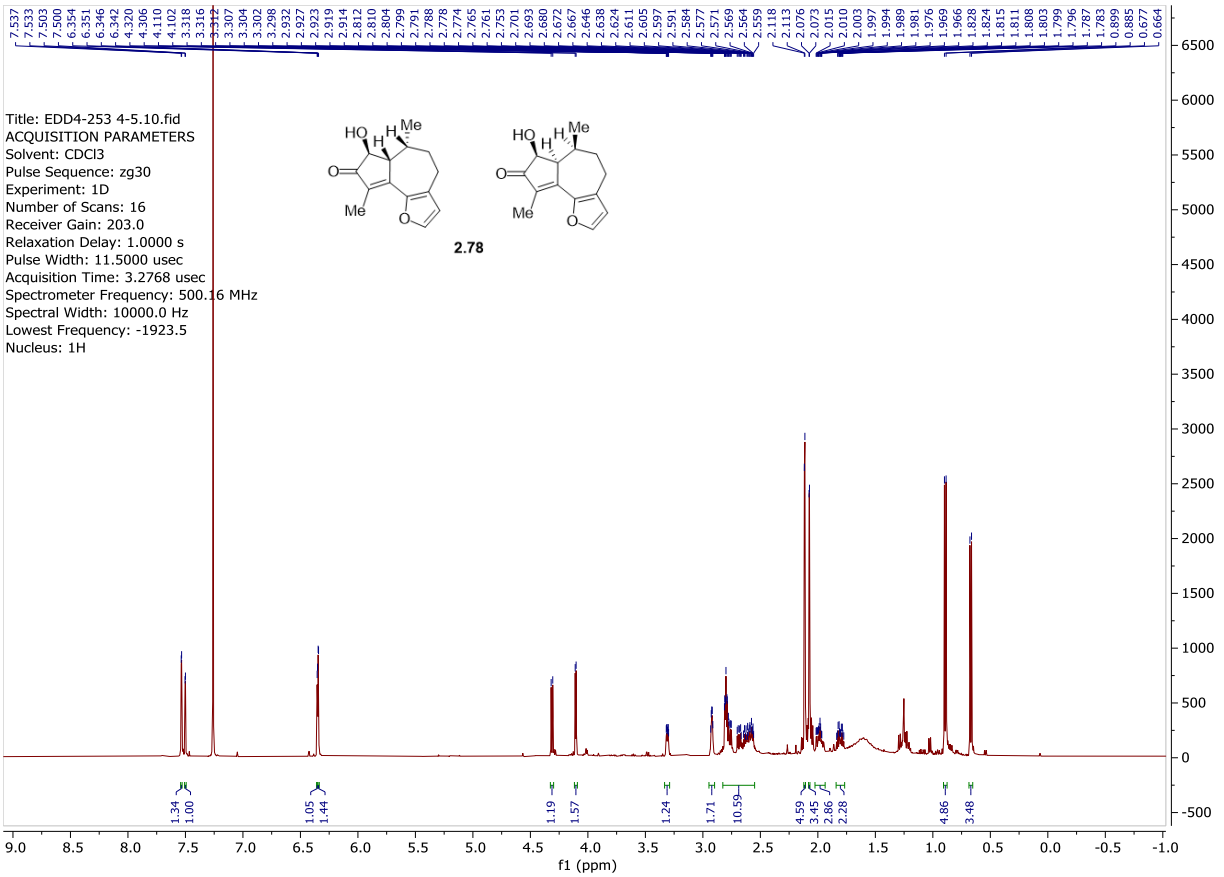
Title: EDD4-253 4-5.10.fid
ACQUISITION PARAMETERS
Solvent: CDCl3
Pulse Sequence: zg30
Experiment: 1D
Number of Scans: 16
Receiver Gain: 203.0
Relaxation Delay: 1.0000 s
Pulse Width: 11.5000 usec
Acquisition Time: 3.2768 usec
Spectrometer Frequency: 500.16 MHz
Spectral Width: 10000.0 Hz
Lowest Frequency: -1923.5
Nucleus: 1H
HO
H
Me
O
Me
2.78
f1 (ppm)

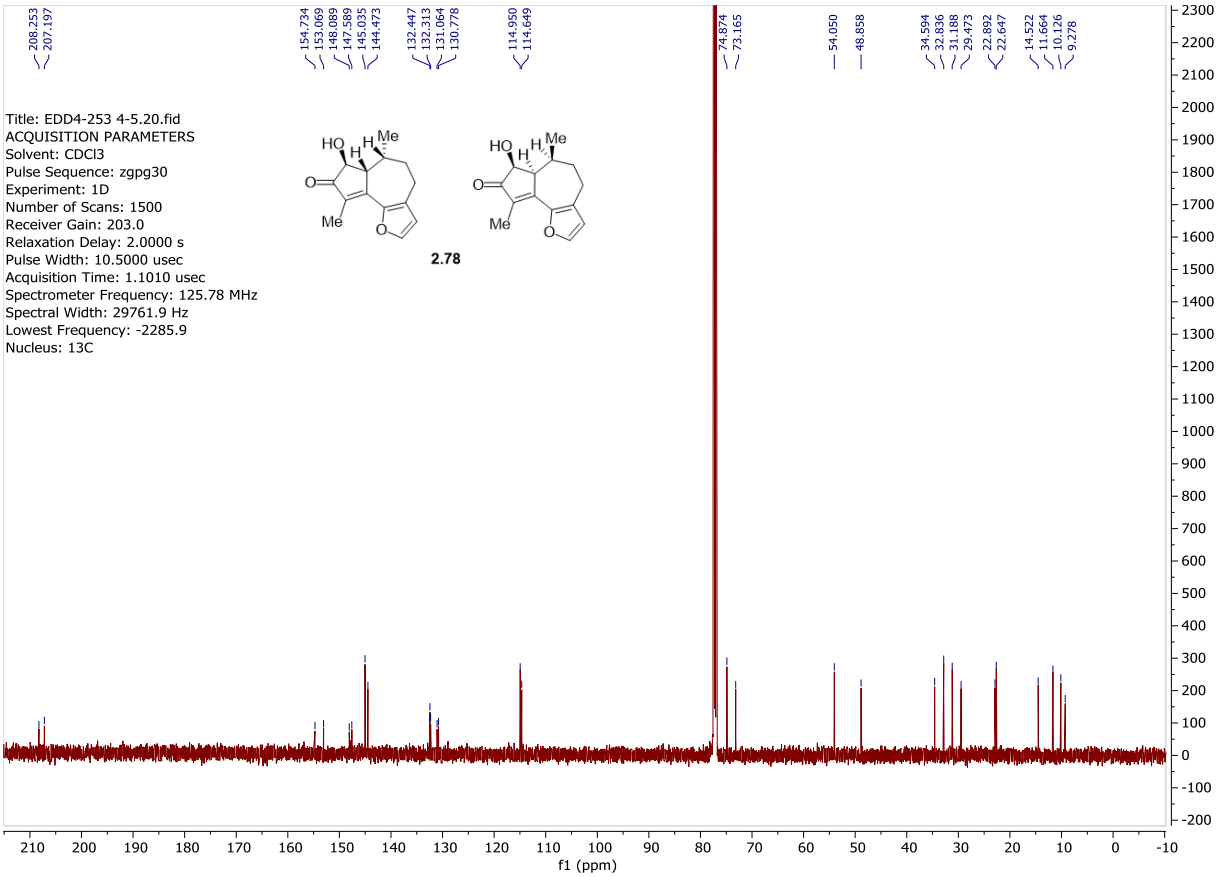
208.253
207.197
154.734
153.069
148.089
147.589
145.035
144.473
132.447
132.313
131.064
130.778
114.950
114.649
74.874
73.165
54.050
48.858
34.594
32.836
31.188
29.473
22.892
22.647
14.522
11.664
10.126
9.278
Title: EDD4-253 4-5.20.fid
ACQUISITION PARAMETERS
Solvent: CDCl3
Pulse Sequence: zgpg30
Experiment: 1D
Number of Scans: 1500
Receiver Gain: 203.0
Relaxation Delay: 2.0000 s
Pulse Width: 10.5000 usec
Acquisition Time: 1.1010 usec
Spectrometer Frequency: 125.78 MHz
Spectral Width: 29761.9 Hz
Lowest Frequency: -2285.9
Nucleus: 13C
HO
H
H
Me
O
Me
O
2.78
f1 (ppm)

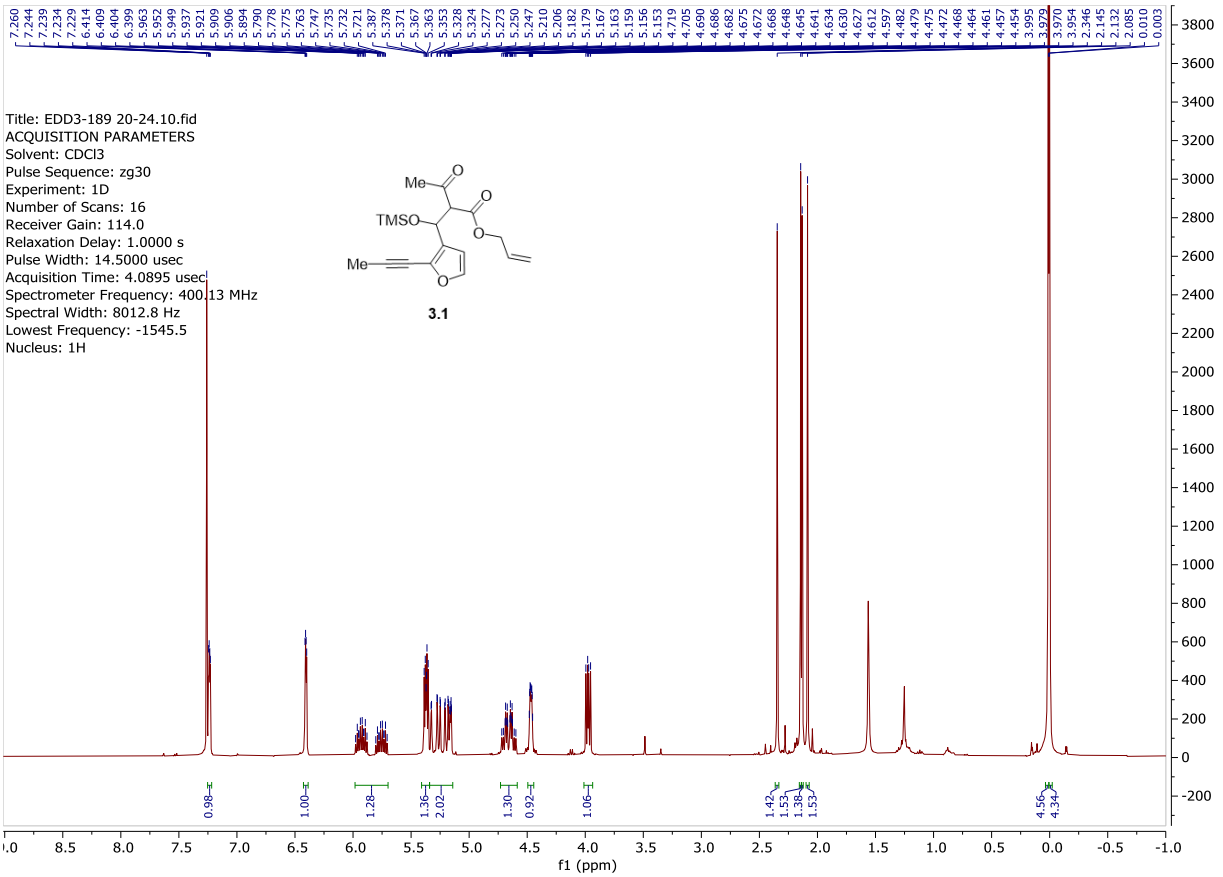
Title: EDD3-189 20-24.10.fid
ACQUISITION PARAMETERS
Solvent: CDCl3
Pulse Sequence: zg30
Experiment: 1D
Number of Scans: 16
Receiver Gain: 114.0
Relaxation Delay: 1.0000 s
Pulse Width: 14.5000 usec
Acquisition Time: 4.0895 usec
Spectrometer Frequency: 400.13 MHz
Spectral Width: 8012.8 Hz
Lowest Frequency: -1545.5
Nucleus: 1H
Me
O
TMSO
O
O
Me
O
3.1
f1 (ppm)

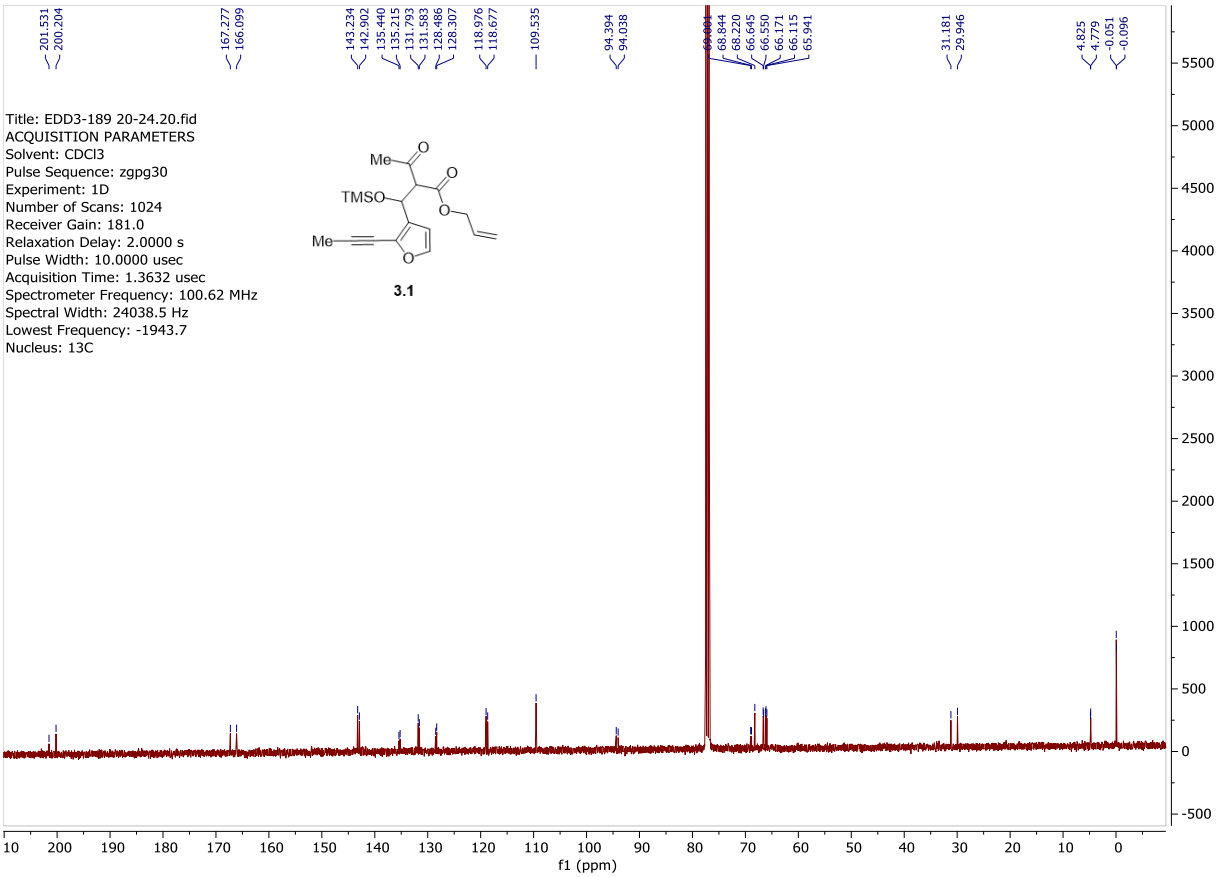
201.531
200.204
167.277
166.099
143.234
142.902
135.440
135.215
131.793
131.583
128.486
128.307
118.976
118.677
109.535
94.394
94.038
68.844
68.220
66.645
66.550
66.171
66.115
65.941
31.181
29.946
4.825
4.779
-0.051
-0.096
Title: EDD3-189 20-24.20.fid
ACQUISITION PARAMETERS
Solvent: CDCl3
Pulse Sequence: zgpg30
Experiment: 1D
Number of Scans: 1024
Receiver Gain: 181.0
Relaxation Delay: 2.0000 s
Pulse Width: 10.0000 usec
Acquisition Time: 1.3632 usec
Spectrometer Frequency: 100.62 MHz
Spectral Width: 24038.5 Hz
Lowest Frequency: -1943.7
Nucleus: 13C
Me
O
O
TMSO
O
Me
O
3.1
5500
5000
4500
4000
3500
3000
2500
2000
1500
1000
500
0
-500
10
200
190
180
170
160
150
140
130
120
110
100
90
80
70
60
50
40
30
20
10
0
f1 (ppm)

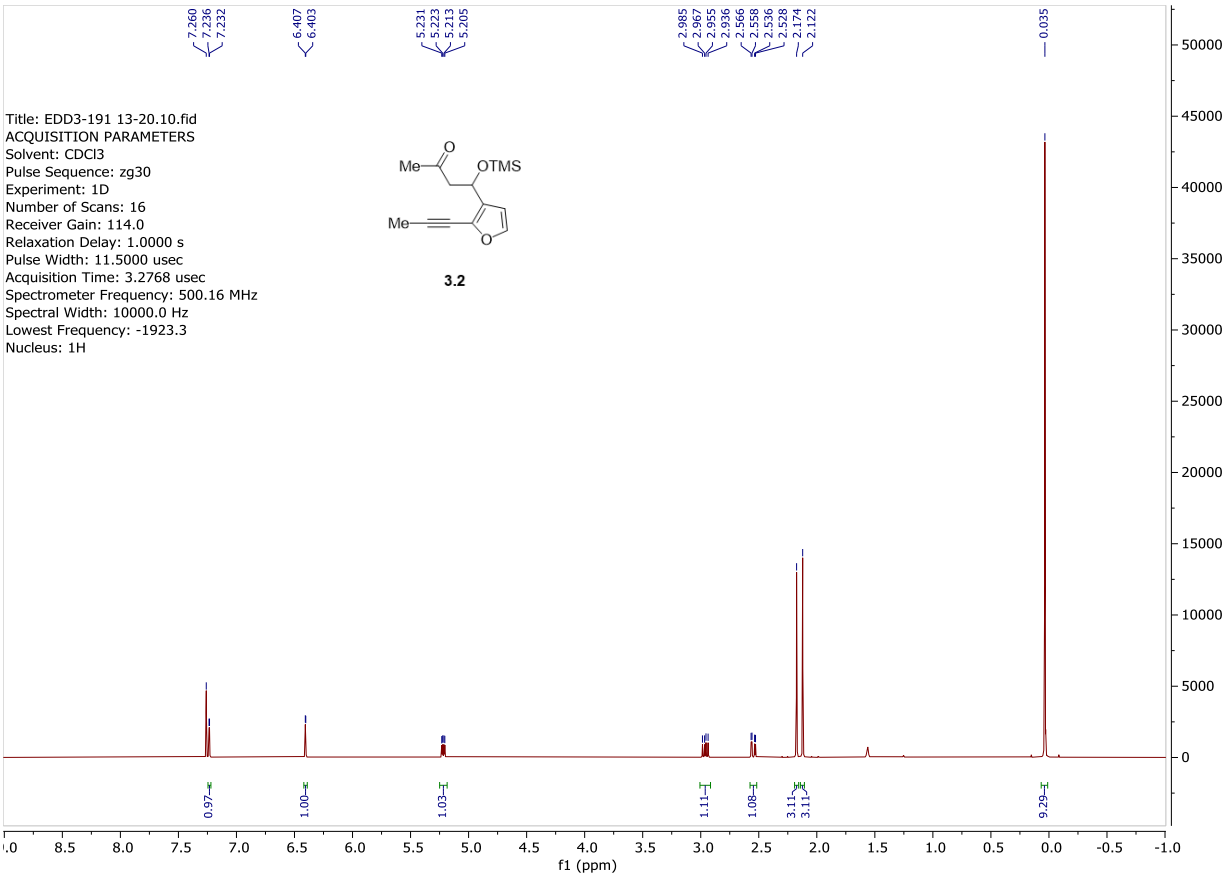
7.260
7.236
7.232
6.407
6.403
5.231
5.223
5.213
5.205
2.985
2.967
2.955
2.936
2.566
2.558
2.536
2.528
2.174
2.122
0.035
Title: EDD3-191 13-20.10.fid
ACQUISITION PARAMETERS
Solvent: CDCl3
Pulse Sequence: zg30
Experiment: 1D
Number of Scans: 16
Receiver Gain: 114.0
Relaxation Delay: 1.0000 s
Pulse Width: 11.5000 usec
Acquisition Time: 3.2768 usec
Spectrometer Frequency: 500.16 MHz
Spectral Width: 10000.0 Hz
Lowest Frequency: -1923.3
Nucleus: 1H
Me
O
OTMS
Me
O
3.2
0.97
1.00
1.03
1.11
1.08
3.11
3.11
9.29
50000
45000
40000
35000
30000
25000
20000
15000
10000
5000
0
8.5
8.0
7.5
7.0
6.5
6.0
5.5
5.0
4.5
4.0
3.5
3.0
2.5
2.0
1.5
1.0
0.5
0.0
-0.5
-1.0
f1 (ppm)

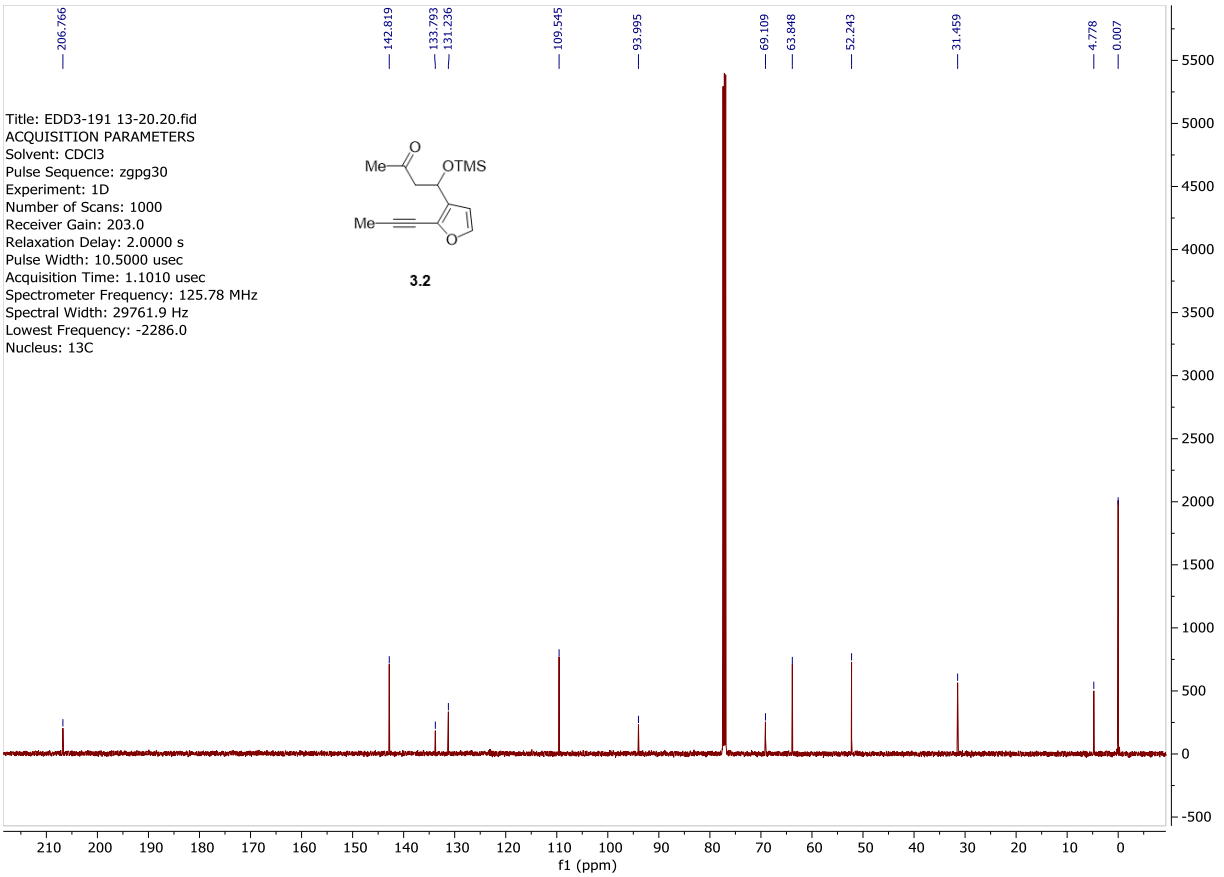
206.766
142.819
133.793
131.236
109.545
93.995
69.109
63.848
52.243
31.459
4.778
0.007
Title: EDD3-191 13-20.20.fid
ACQUISITION PARAMETERS
Solvent: CDCl3
Pulse Sequence: zgpg30
Experiment: 1D
Number of Scans: 1000
Receiver Gain: 203.0
Relaxation Delay: 2.0000 s
Pulse Width: 10.5000 usec
Acquisition Time: 1.1010 usec
Spectrometer Frequency: 125.78 MHz
Spectral Width: 29761.9 Hz
Lowest Frequency: -2286.0
Nucleus: 13C
Me
O
OTMS
Me
O
3.2
f1 (ppm)

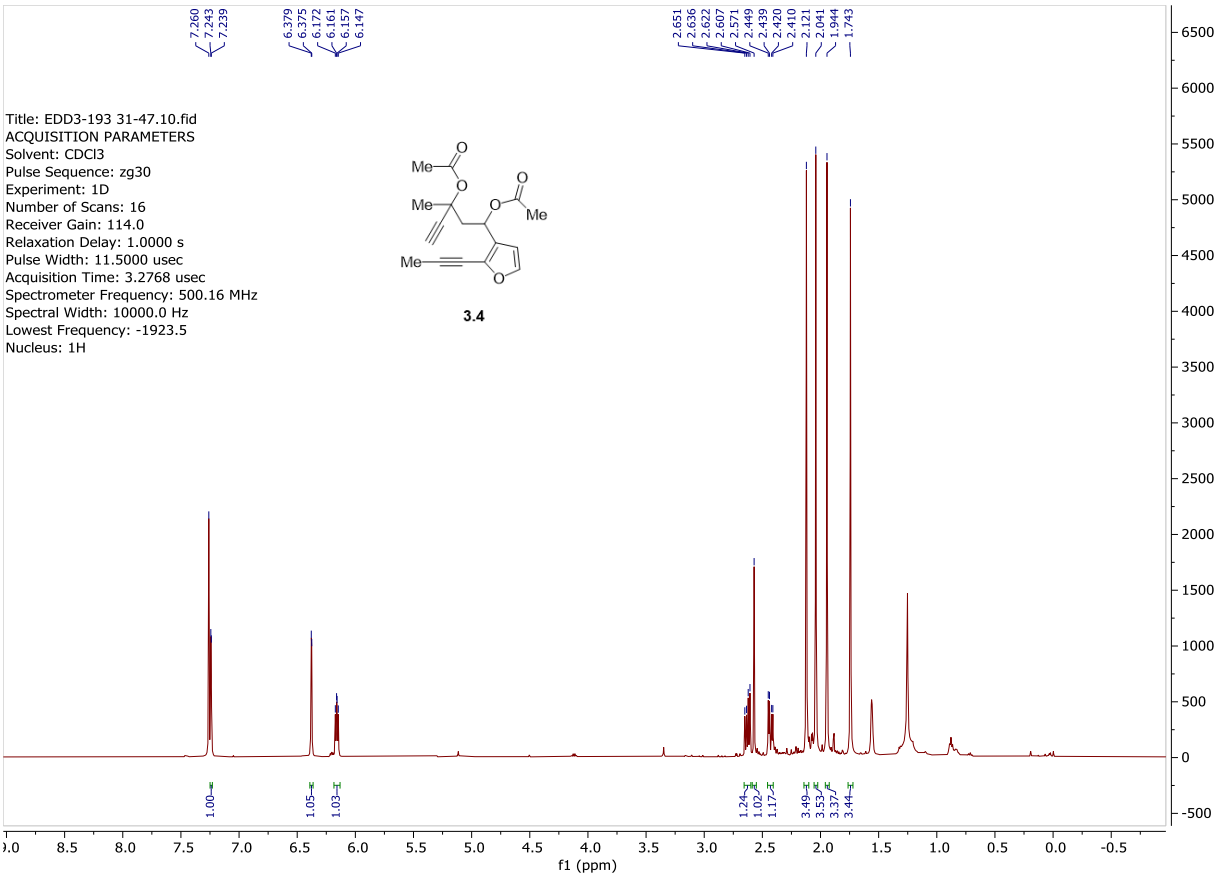
7.260
7.243
7.239
6.379
6.375
6.172
6.161
6.157
6.147
2.651
2.636
2.622
2.607
2.571
2.449
2.439
2.420
2.410
2.121
2.041
1.944
1.743
Title: EDD3-193 31-47.10.fid
ACQUISITION PARAMETERS
Solvent: CDCl3
Pulse Sequence: zg30
Experiment: 1D
Number of Scans: 16
Receiver Gain: 114.0
Relaxation Delay: 1.0000 s
Pulse Width: 11.5000 usec
Acquisition Time: 3.2768 usec
Spectrometer Frequency: 500.16 MHz
Spectral Width: 10000.0 Hz
Lowest Frequency: -1923.5
Nucleus: 1H
Me
O
Me
O
O
Me
Me
O
3.4
1.00
1.05
1.03
1.24
1.02
1.17
3.49
3.53
3.37
3.44
f1 (ppm)

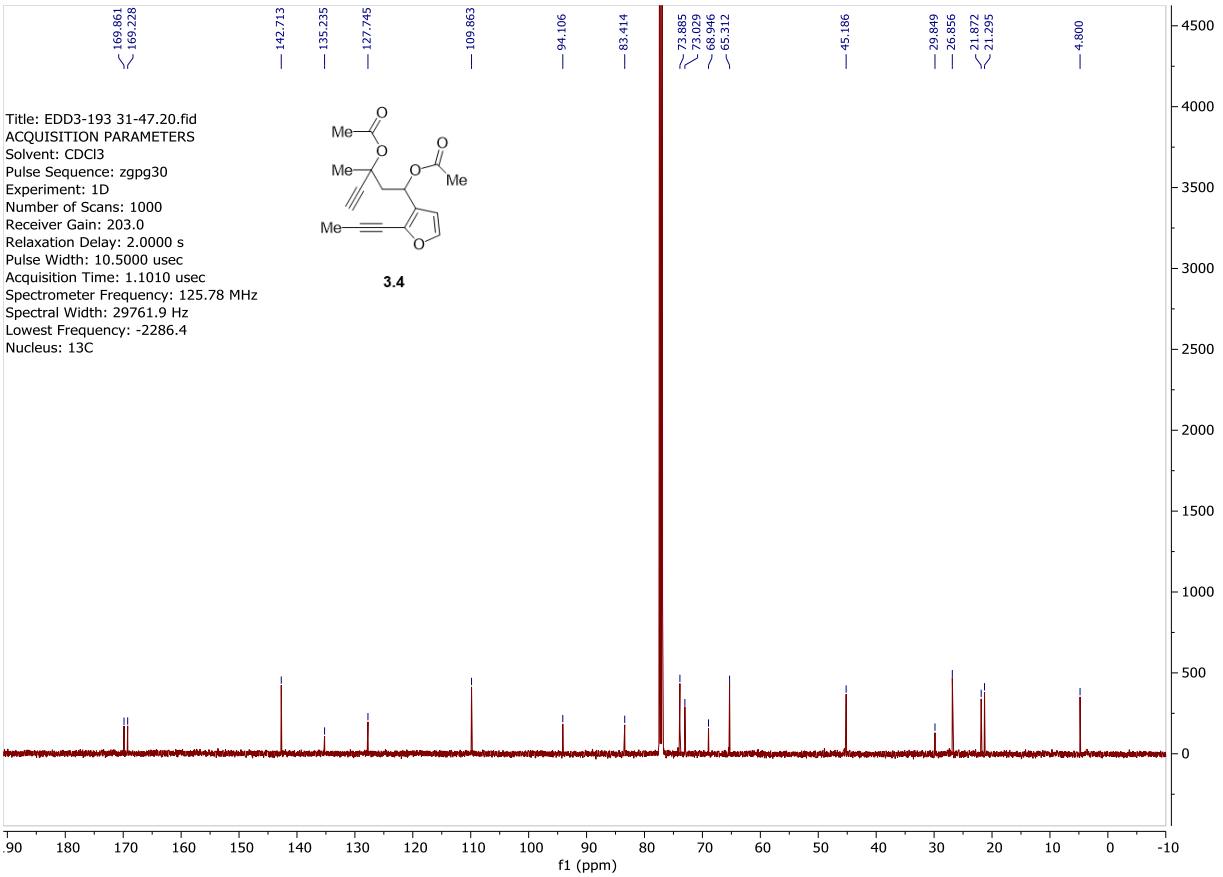
169.861
169.228
142.713
135.235
127.745
109.863
94.106
83.414
73.885
73.029
68.946
65.312
45.186
29.849
26.856
21.872
21.295
4.800
Title: EDD3-193 31-47.20.fid
ACQUISITION PARAMETERS
Solvent: CDCl3
Pulse Sequence: zgpg30
Experiment: 1D
Number of Scans: 1000
Receiver Gain: 203.0
Relaxation Delay: 2.0000 s
Pulse Width: 10.5000 usec
Acquisition Time: 1.1010 usec
Spectrometer Frequency: 125.78 MHz
Spectral Width: 29761.9 Hz
Lowest Frequency: -2286.4
Nucleus: 13C
Me
O
Me
O
O
Me
Me
O
3.4
4500
4000
3500
3000
2500
2000
1500
1000
500
0
f1 (ppm)

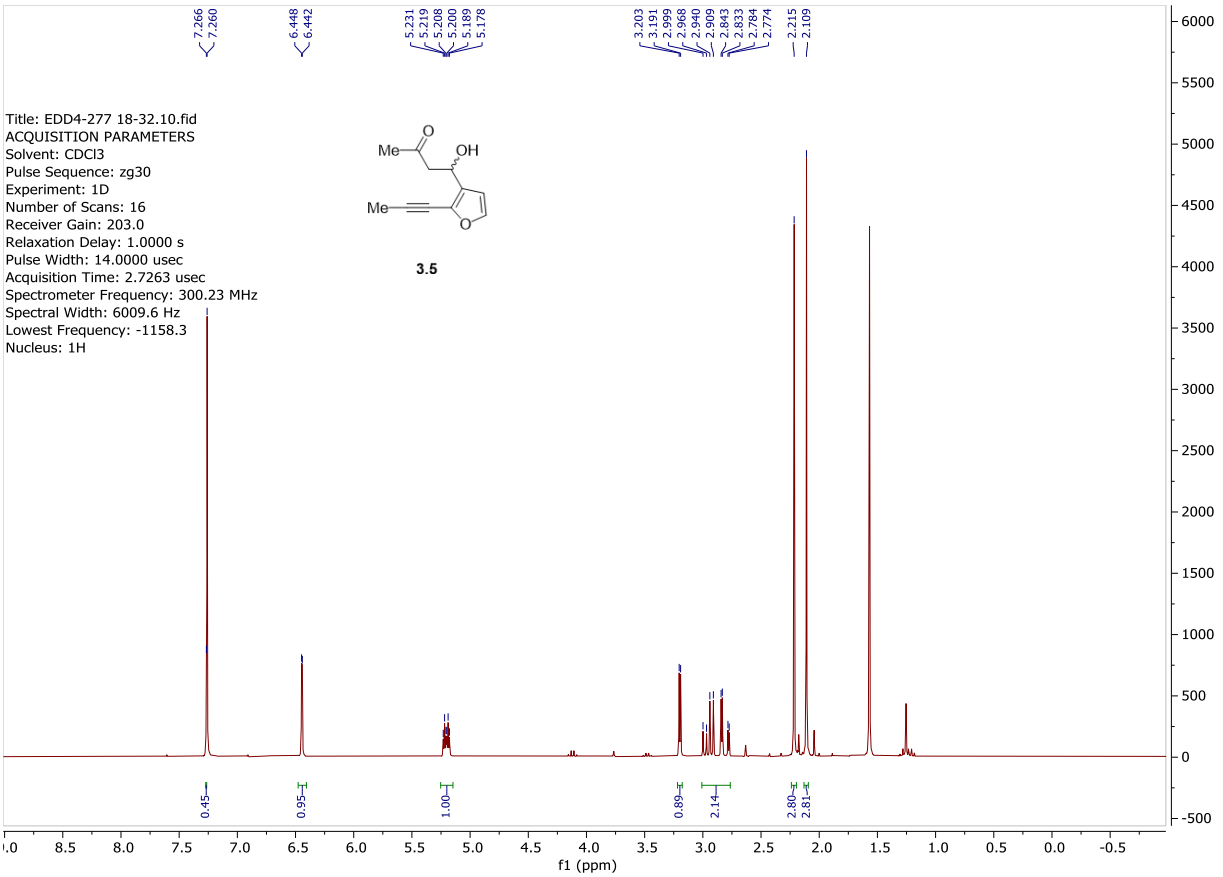
Title: EDD4-277 18-32.10.fid
ACQUISITION PARAMETERS
Solvent: CDCl3
Pulse Sequence: zg30
Experiment: 1D
Number of Scans: 16
Receiver Gain: 203.0
Relaxation Delay: 1.0000 s
Pulse Width: 14.0000 usec
Acquisition Time: 2.7263 usec
Spectrometer Frequency: 300.23 MHz
Spectral Width: 6009.6 Hz
Lowest Frequency: -1158.3
Nucleus: 1H
Me
O
OH
Me
O
3.5
7.266
7.260
6.448
6.442
5.231
5.219
5.208
5.200
5.189
5.178
3.203
3.191
2.999
2.968
2.940
2.909
2.843
2.833
2.784
2.774
2.215
2.109
0.45
0.95
1.00
0.89
2.14
2.80
2.81
f1 (ppm)

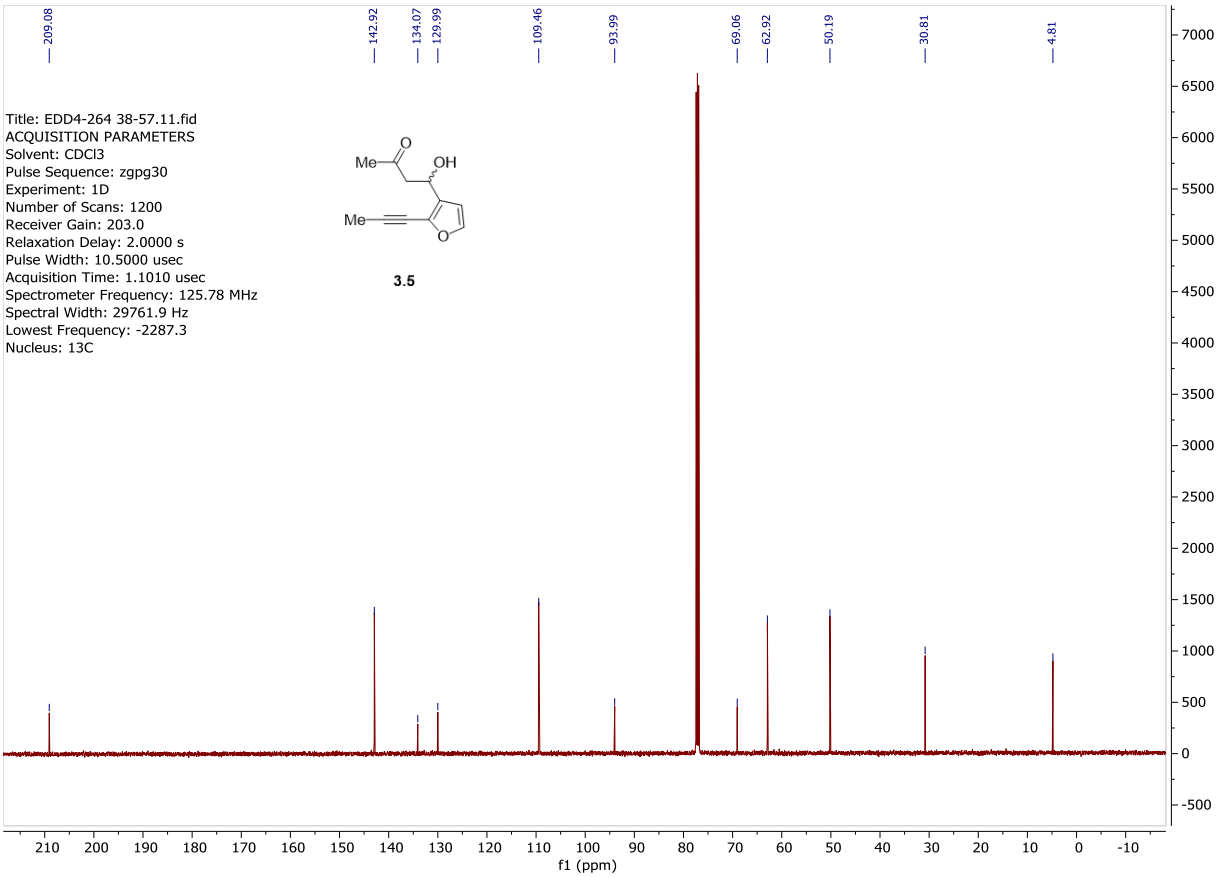
209.08
142.92
134.07
129.99
109.46
93.99
69.06
62.92
50.19
30.81
4.81
Title: EDD4-264 38-57.11.fid
ACQUISITION PARAMETERS
Solvent: CDCl3
Pulse Sequence: zgpg30
Experiment: 1D
Number of Scans: 1200
Receiver Gain: 203.0
Relaxation Delay: 2.0000 s
Pulse Width: 10.5000 usec
Acquisition Time: 1.1010 usec
Spectrometer Frequency: 125.78 MHz
Spectral Width: 29761.9 Hz
Lowest Frequency: -2287.3
Nucleus: 13C
Me
O
OH
Me
O
3.5
f1 (ppm)

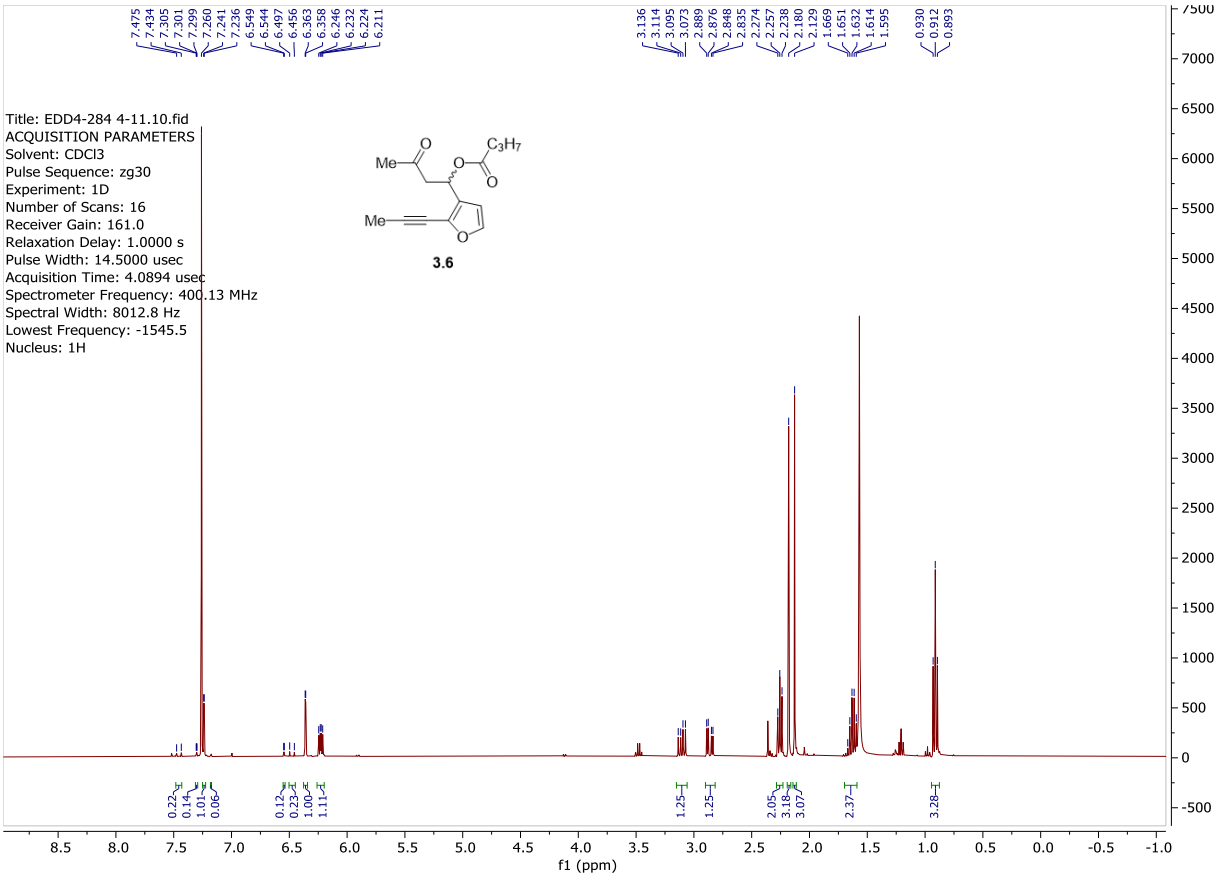
Title: EDD4-284 4-11.10.fid
ACQUISITION PARAMETERS
Solvent: CDCl3
Pulse Sequence: zg30
Experiment: 1D
Number of Scans: 16
Receiver Gain: 161.0
Relaxation Delay: 1.0000 s
Pulse Width: 14.5000 usec
Acquisition Time: 4.0894 usec
Spectrometer Frequency: 400.13 MHz
Spectral Width: 8012.8 Hz
Lowest Frequency: -1545.5
Nucleus: 1H
Me
O
O
C3H7
O
Me
O
3.6
f1 (ppm)

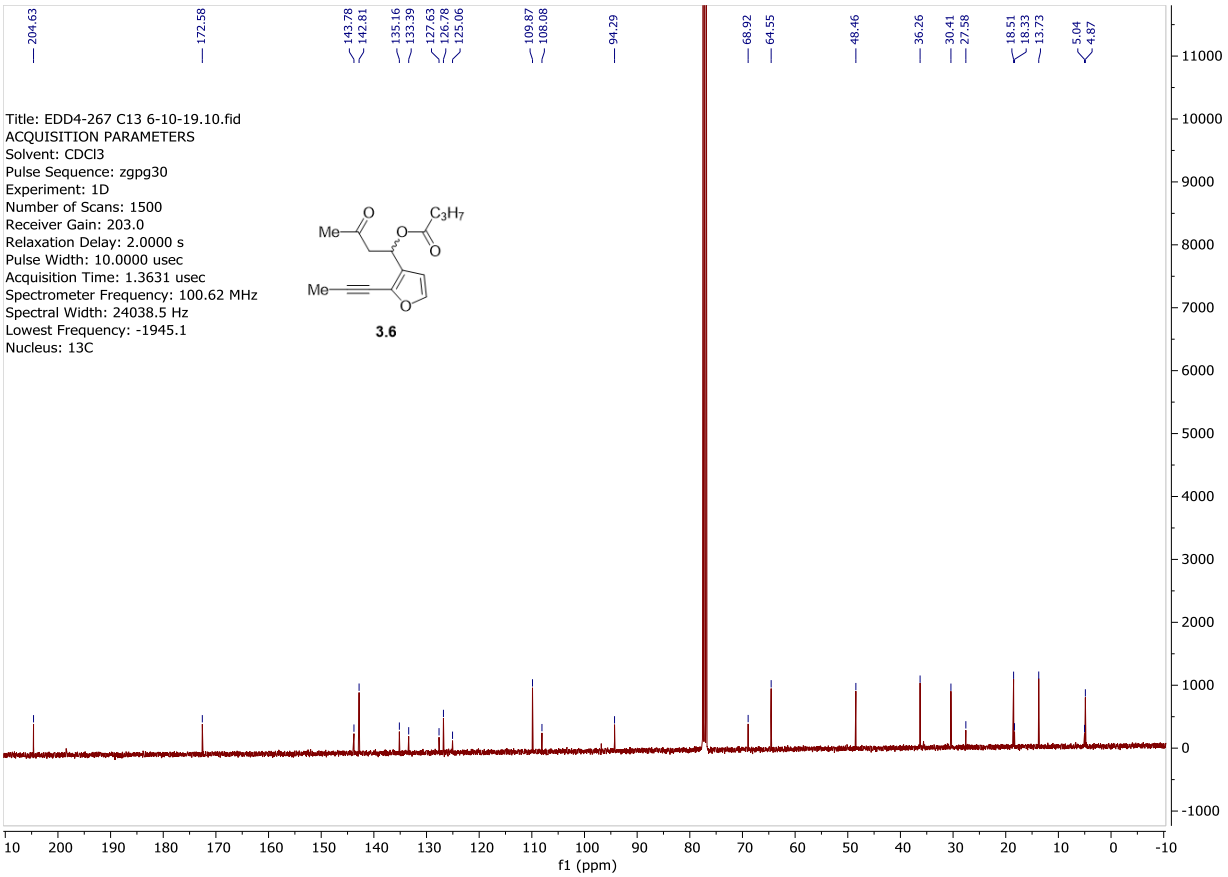
204.63
172.58
143.78
142.81
135.16
133.39
127.63
126.78
125.06
109.87
108.08
94.29
68.92
64.55
48.46
36.26
30.41
27.58
18.51
18.33
13.73
5.04
4.87
Title: EDD4-267 C13 6-10-19.10.fid
ACQUISITION PARAMETERS
Solvent: CDCl3
Pulse Sequence: zgpg30
Experiment: 1D
Number of Scans: 1500
Receiver Gain: 203.0
Relaxation Delay: 2.0000 s
Pulse Width: 10.0000 usec
Acquisition Time: 1.3631 usec
Spectrometer Frequency: 100.62 MHz
Spectral Width: 24038.5 Hz
Lowest Frequency: -1945.1
Nucleus: 13C
Me
O
O
C3H7
O
Me
O
3.6
11000
10000
9000
8000
7000
6000
5000
4000
3000
2000
1000
0
-1000
10
200
190
180
170
160
150
140
130
120
110
100
90
80
70
60
50
40
30
20
10
0
-10
f1 (ppm)

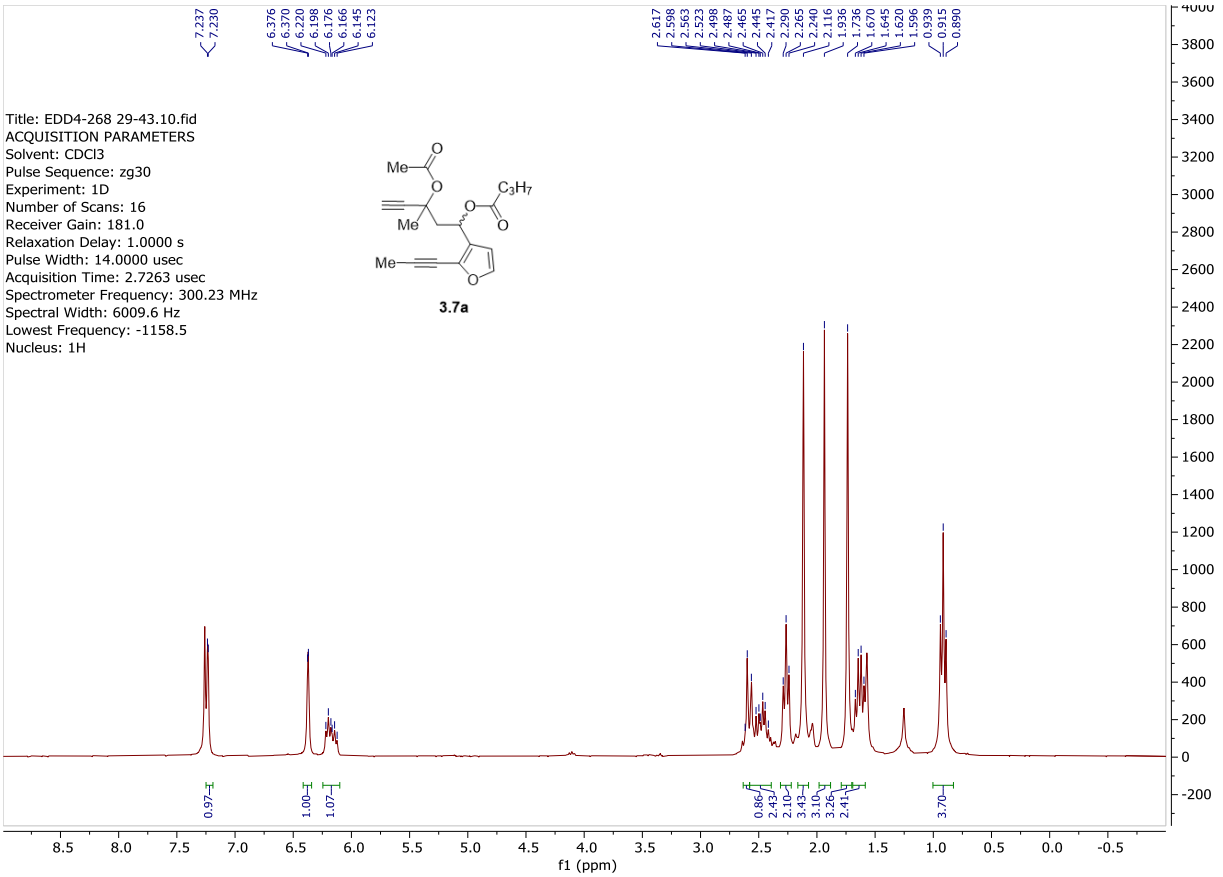
Title: EDD4-268 29-43.10.fid
ACQUISITION PARAMETERS
Solvent: CDCl3
Pulse Sequence: zg30
Experiment: 1D
Number of Scans: 16
Receiver Gain: 181.0
Relaxation Delay: 1.0000 s
Pulse Width: 14.0000 usec
Acquisition Time: 2.7263 usec
Spectrometer Frequency: 300.23 MHz
Spectral Width: 6009.6 Hz
Lowest Frequency: -1158.5
Nucleus: 1H
3.7a
f1 (ppm)

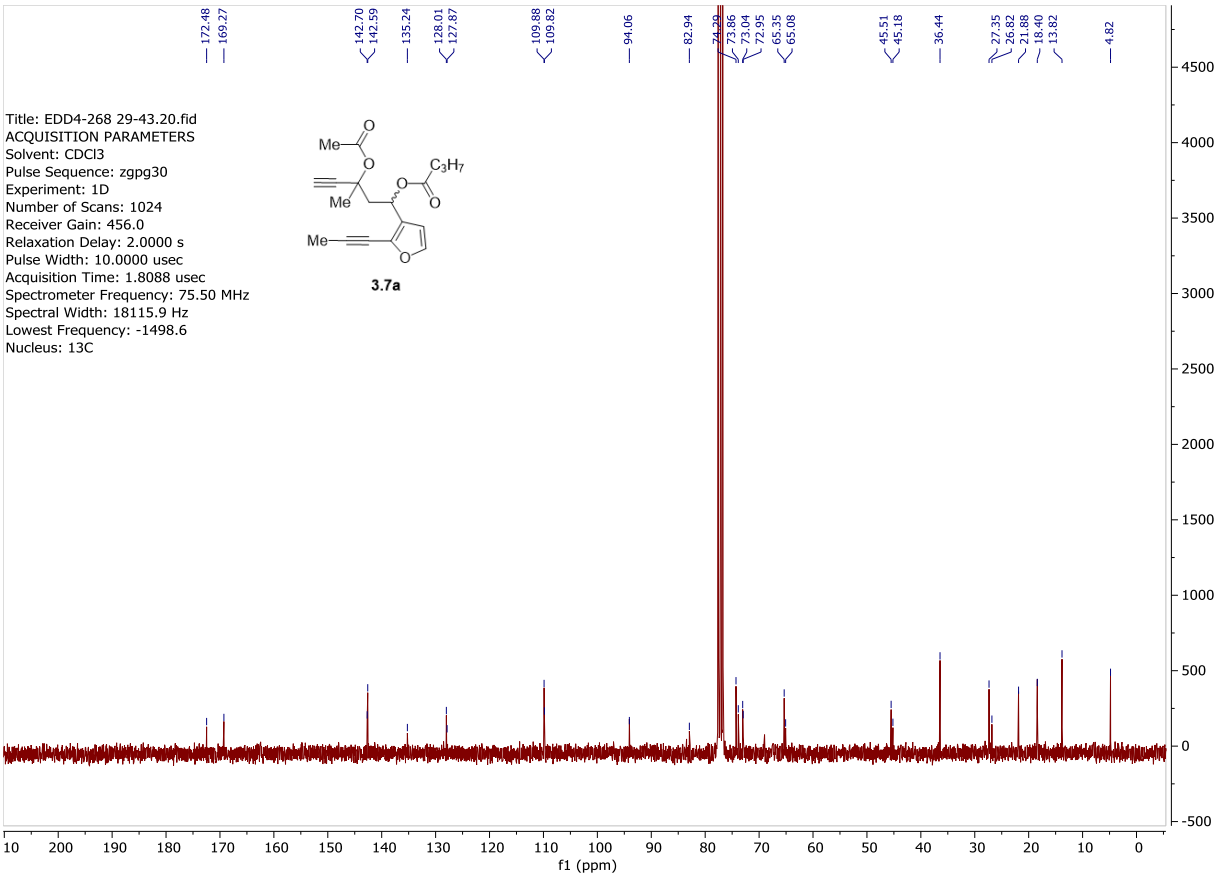
172.48
169.27
142.70
142.59
135.24
128.01
127.87
109.88
109.82
94.06
82.94
74.39
73.86
73.04
72.95
65.35
65.08
45.51
45.18
36.44
27.35
26.82
21.88
18.40
13.82
4.82
Title: EDD4-268 29-43.20.fid
ACQUISITION PARAMETERS
Solvent: CDCl3
Pulse Sequence: zgpg30
Experiment: 1D
Number of Scans: 1024
Receiver Gain: 456.0
Relaxation Delay: 2.0000 s
Pulse Width: 10.0000 usec
Acquisition Time: 1.8088 usec
Spectrometer Frequency: 75.50 MHz
Spectral Width: 18115.9 Hz
Lowest Frequency: -1498.6
Nucleus: 13C
Me
O
O
C3H7
Me
O
O
Me
O
3.7a
4500
4000
3500
3000
2500
2000
1500
1000
500
0
-500
10
200
190
180
170
160
150
140
130
120
110
100
90
80
70
60
50
40
30
20
10
0
f1 (ppm)

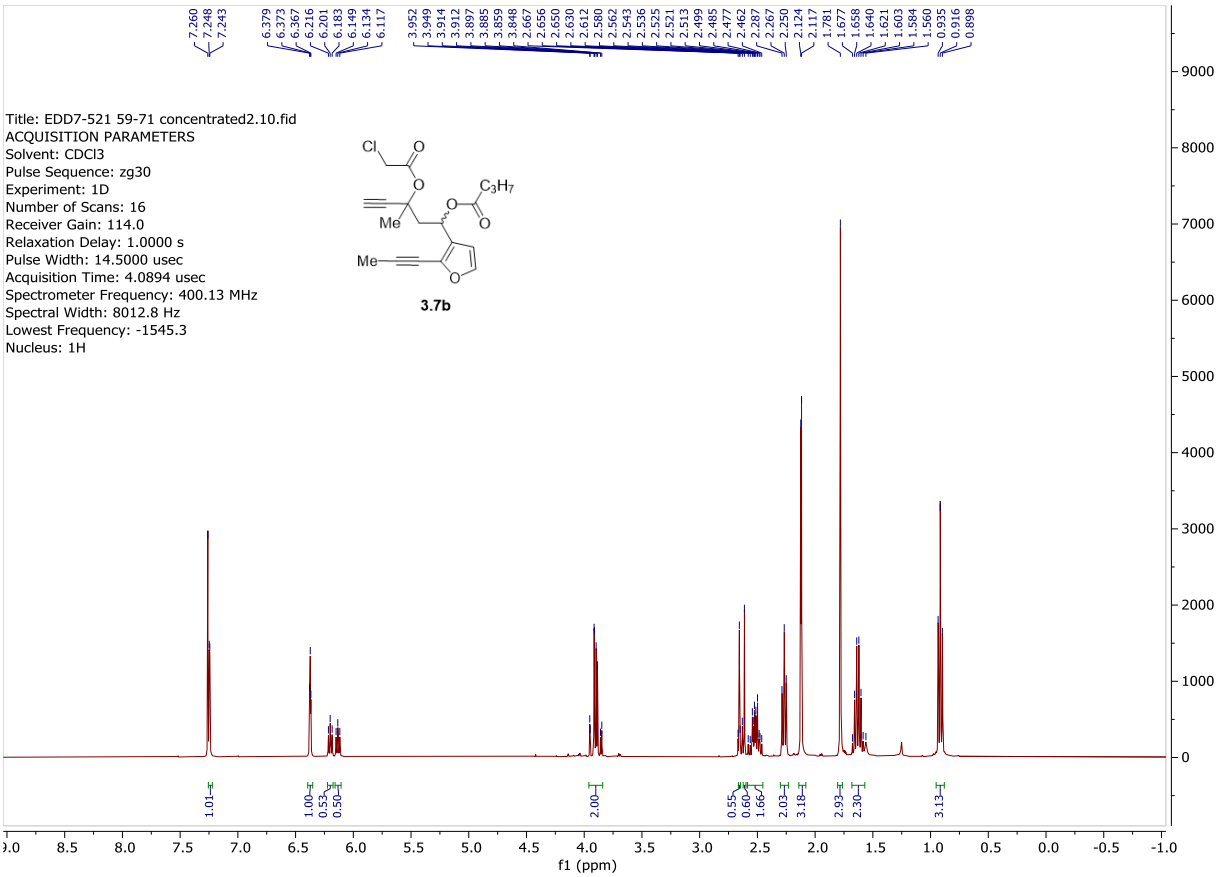
Title: EDD7-521 59-71 concentrated2.10.fid
ACQUISITION PARAMETERS
Solvent: CDCl3
Pulse Sequence: zg30
Experiment: 1D
Number of Scans: 16
Receiver Gain: 114.0
Relaxation Delay: 1.0000 s
Pulse Width: 14.5000 usec
Acquisition Time: 4.0894 usec
Spectrometer Frequency: 400.13 MHz
Spectral Width: 8012.8 Hz
Lowest Frequency: -1545.3
Nucleus: 1H
3.7b
f1 (ppm)

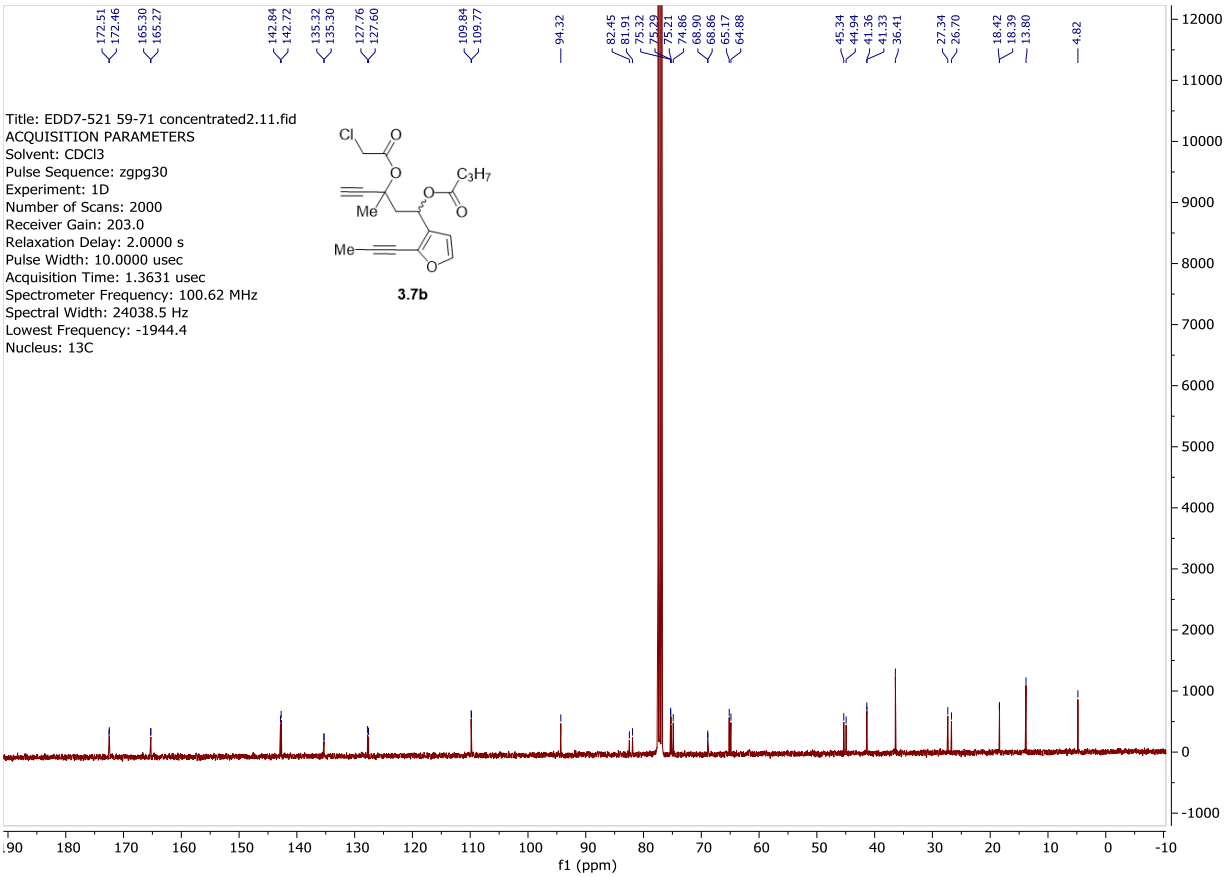
172.51
172.46
165.30
165.27
142.84
142.72
135.32
135.30
127.76
127.60
109.84
109.77
94.32
82.45
81.91
75.32
75.29
75.21
74.86
68.90
68.86
65.17
64.88
45.34
44.94
41.36
41.33
36.41
27.34
26.70
18.42
18.39
13.80
4.82
Title: EDD7-521 59-71 concentrated2.11.fid
ACQUISITION PARAMETERS
Solvent: CDCl3
Pulse Sequence: zgpg30
Experiment: 1D
Number of Scans: 2000
Receiver Gain: 203.0
Relaxation Delay: 2.0000 s
Pulse Width: 10.0000 usec
Acquisition Time: 1.3631 usec
Spectrometer Frequency: 100.62 MHz
Spectral Width: 24038.5 Hz
Lowest Frequency: -1944.4
Nucleus: 13C
Cl
O
O
C3H7
O
O
Me
Me
O
3.7b
12000
11000
10000
9000
8000
7000
6000
5000
4000
3000
2000
1000
0
-1000
190
180
170
160
150
140
130
120
110
100
90
80
70
60
50
40
30
20
10
0
-10
f1 (ppm)

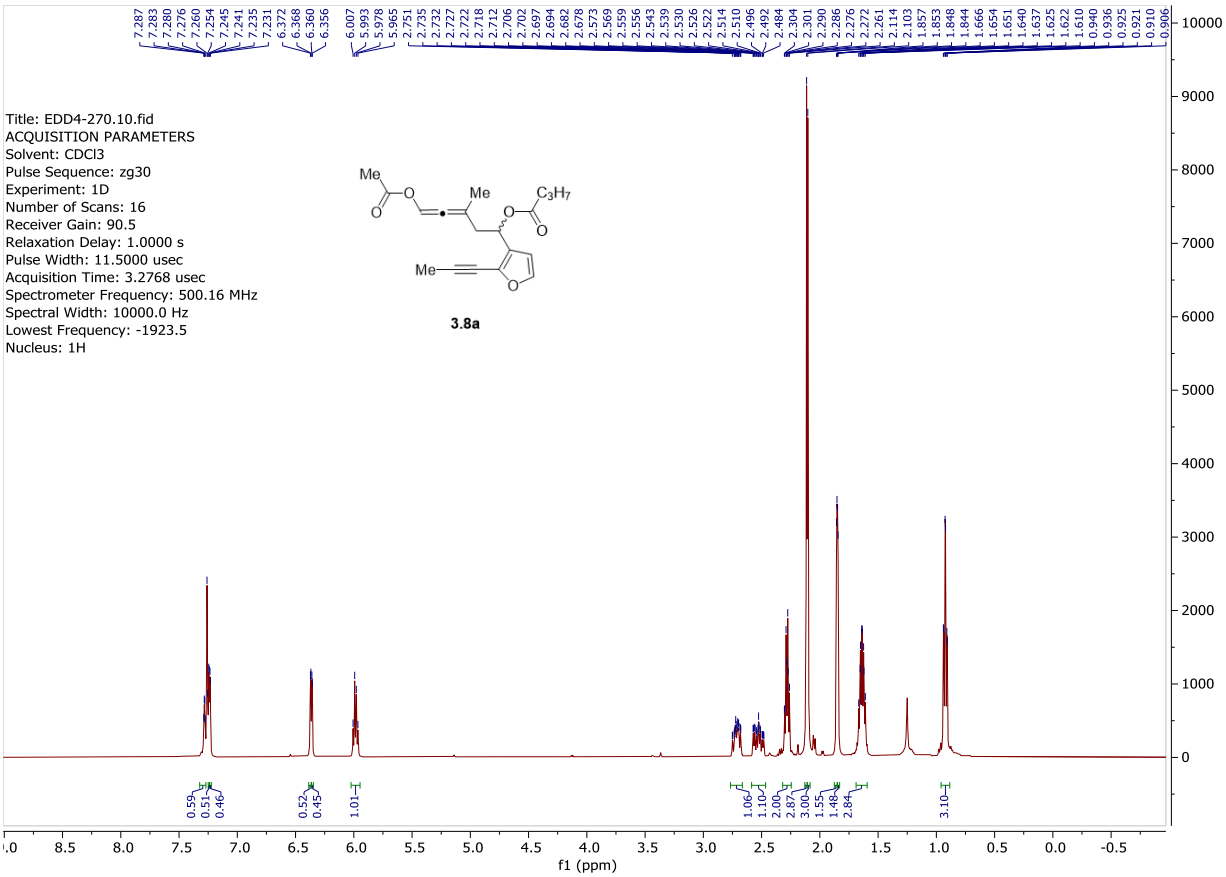
Title: EDD4-270.10.fid
ACQUISITION PARAMETERS
Solvent: CDCl3
Pulse Sequence: zg30
Experiment: 1D
Number of Scans: 16
Receiver Gain: 90.5
Relaxation Delay: 1.0000 s
Pulse Width: 11.5000 usec
Acquisition Time: 3.2768 usec
Spectrometer Frequency: 500.16 MHz
Spectral Width: 10000.0 Hz
Lowest Frequency: -1923.5
Nucleus: 1H
3.8a
f1 (ppm)

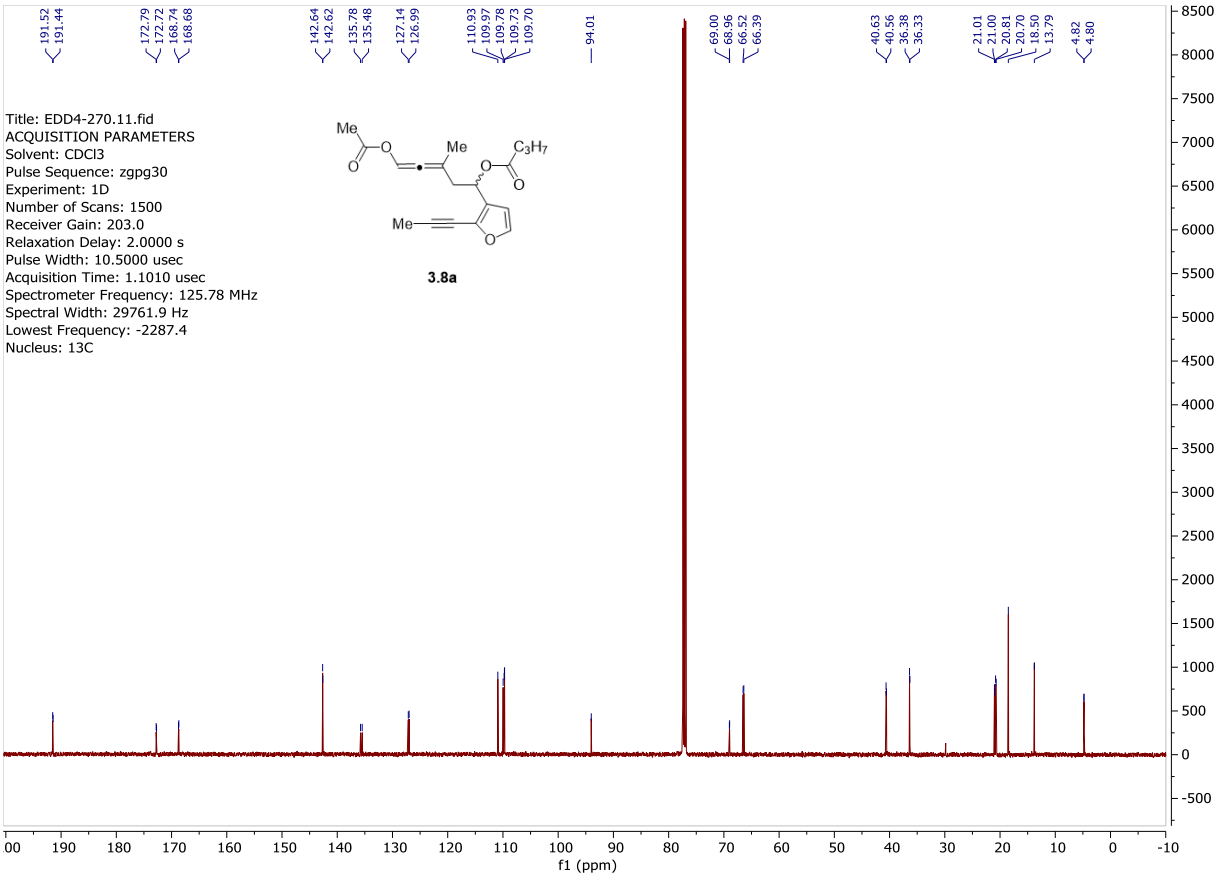
191.52
191.44
172.79
172.72
168.74
168.68
142.64
142.62
135.78
135.48
127.14
126.99
110.93
109.97
109.78
109.73
109.70
94.01
69.00
68.96
66.52
66.39
40.63
40.56
36.38
36.33
21.01
21.00
20.81
20.70
18.50
13.79
4.82
4.80
Title: EDD4-270.11.fid
ACQUISITION PARAMETERS
Solvent: CDCl3
Pulse Sequence: zgpg30
Experiment: 1D
Number of Scans: 1500
Receiver Gain: 203.0
Relaxation Delay: 2.0000 s
Pulse Width: 10.5000 usec
Acquisition Time: 1.1010 usec
Spectrometer Frequency: 125.78 MHz
Spectral Width: 29761.9 Hz
Lowest Frequency: -2287.4
Nucleus: 13C
Me
O
O
Me
O
C3H7
O
Me
O
3.8a
f1 (ppm)

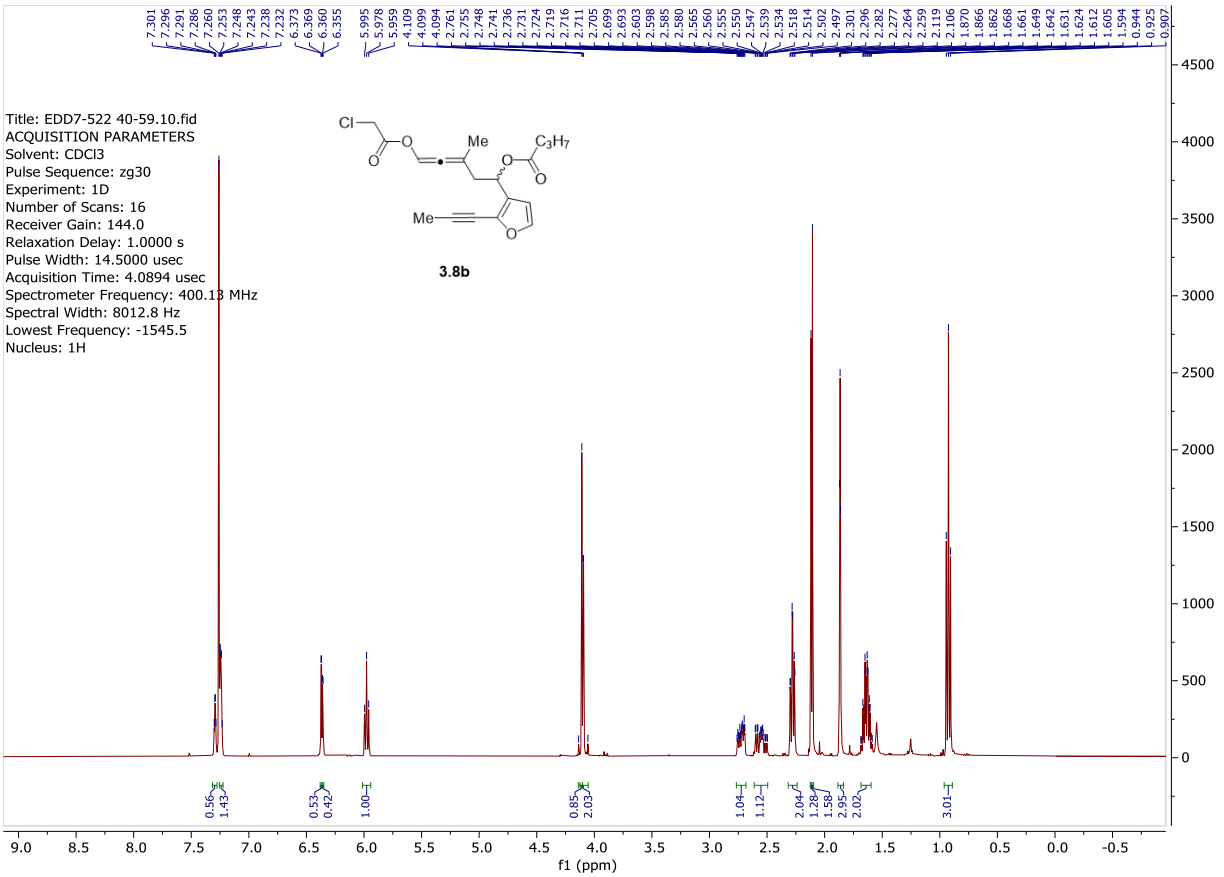
Title: EDD7-522 40-59.10.fid
ACQUISITION PARAMETERS
Solvent: CDCl3
Pulse Sequence: zg30
Experiment: 1D
Number of Scans: 16
Receiver Gain: 144.0
Relaxation Delay: 1.0000 s
Pulse Width: 14.5000 usec
Acquisition Time: 4.0894 usec
Spectrometer Frequency: 400.13 MHz
Spectral Width: 8012.8 Hz
Lowest Frequency: -1545.5
Nucleus: 1H
3.8b
f1 (ppm)

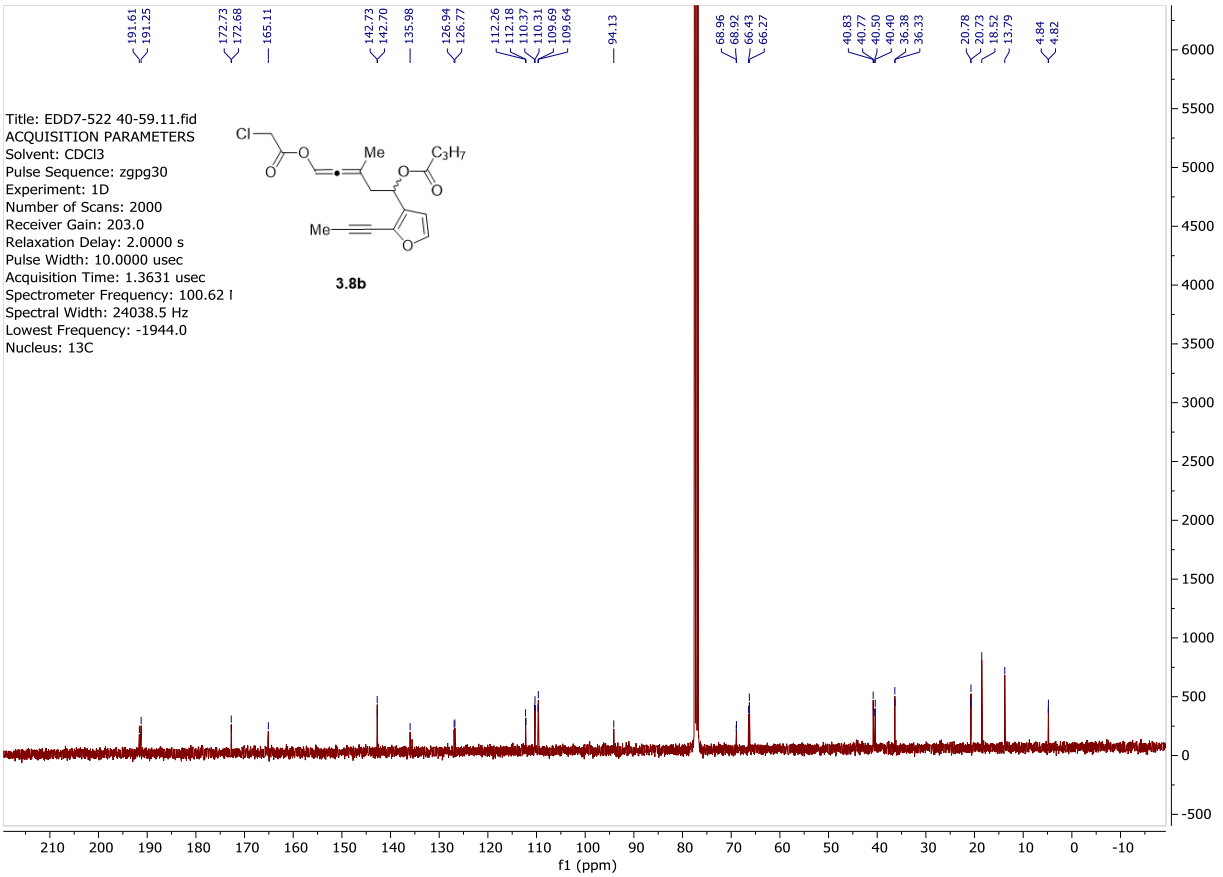
191.61
191.25
172.73
172.68
165.11
142.73
142.70
135.98
126.94
126.77
112.26
112.18
110.37
110.31
109.69
109.64
94.13
68.96
68.92
66.43
66.27
40.83
40.77
40.50
40.40
36.38
36.33
20.78
20.73
18.52
13.79
4.84
4.82
Title: EDD7-522 40-59.11.fid
ACQUISITION PARAMETERS
Solvent: CDCl3
Pulse Sequence: zgpg30
Experiment: 1D
Number of Scans: 2000
Receiver Gain: 203.0
Relaxation Delay: 2.0000 s
Pulse Width: 10.0000 usec
Acquisition Time: 1.3631 usec
Spectrometer Frequency: 100.62 I
Spectral Width: 24038.5 Hz
Lowest Frequency: -1944.0
Nucleus: 13C
Cl
O
O
Me
O
C3H7
O
Me
O
3.8b
6000
5500
5000
4500
4000
3500
3000
2500
2000
1500
1000
500
0
-500
210
200
190
180
170
160
150
140
130
120
110
100
90
80
70
60
50
40
30
20
10
0
-10
f1 (ppm)

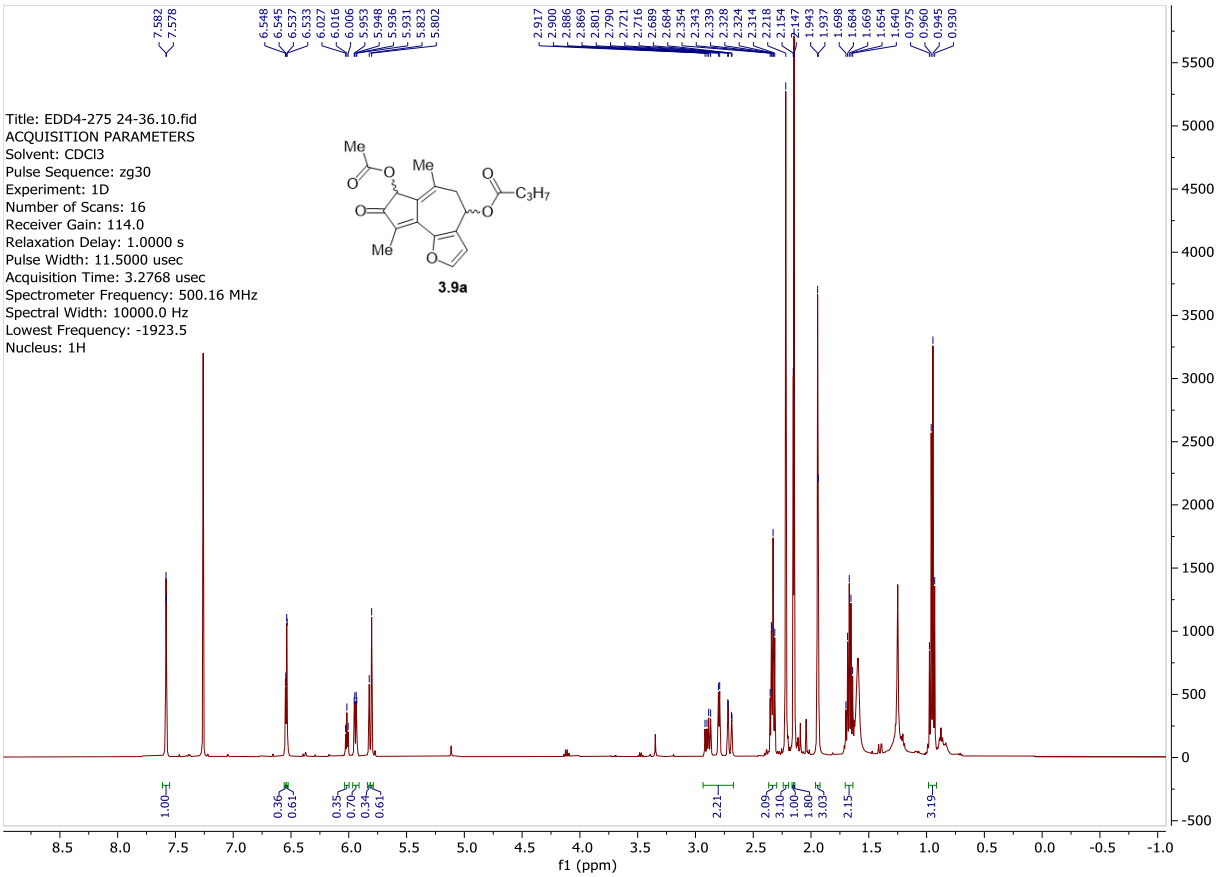
Title: EDD4-275 24-36.10.fid
ACQUISITION PARAMETERS
Solvent: CDCl3
Pulse Sequence: zg30
Experiment: 1D
Number of Scans: 16
Receiver Gain: 114.0
Relaxation Delay: 1.0000 s
Pulse Width: 11.5000 usec
Acquisition Time: 3.2768 usec
Spectrometer Frequency: 500.16 MHz
Spectral Width: 10000.0 Hz
Lowest Frequency: -1923.5
Nucleus: 1H
3.9a
f1 (ppm)

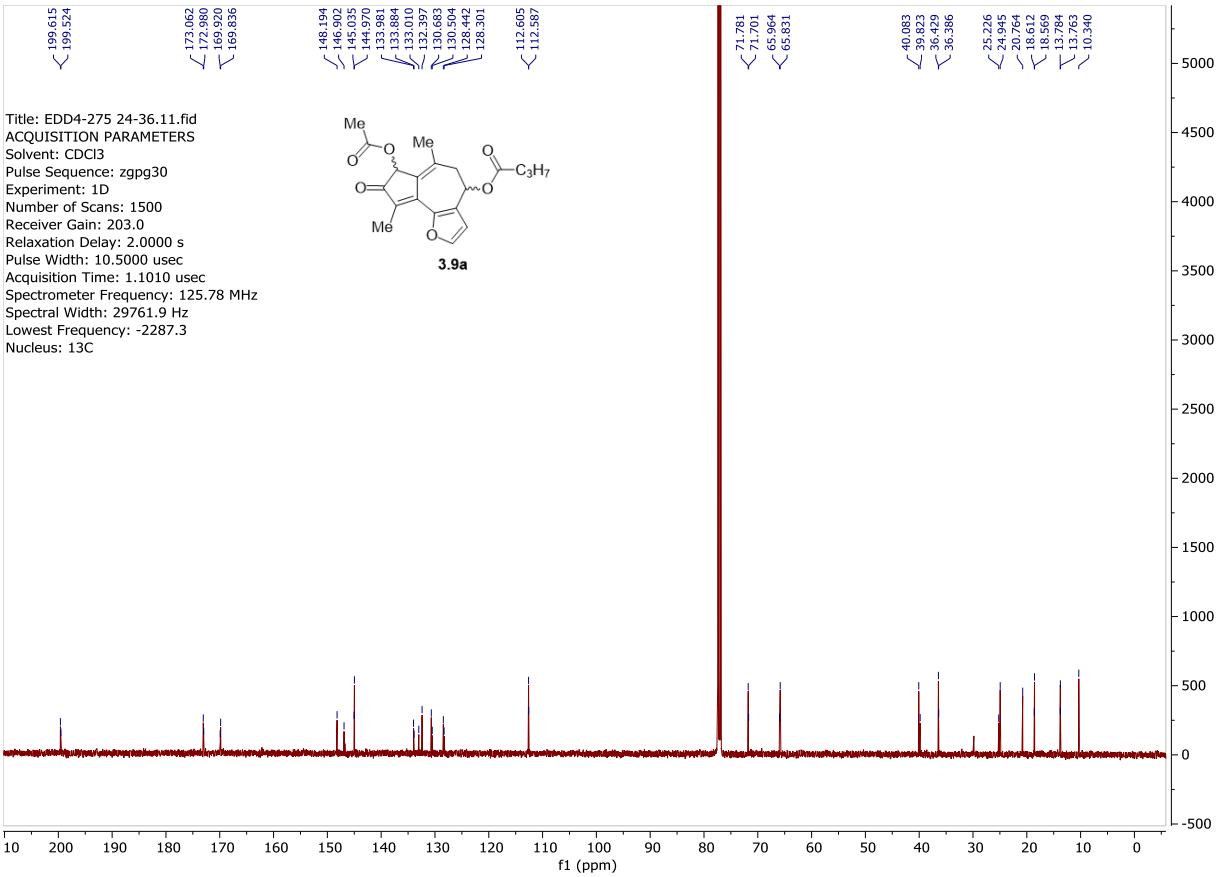
199.615
199.524
173.062
172.980
169.920
169.836
148.194
146.902
145.035
144.970
133.981
133.884
133.010
132.397
130.683
130.504
128.442
128.301
112.605
112.587
71.781
71.701
65.964
65.831
40.083
39.823
36.429
36.386
25.226
24.945
20.764
18.612
18.569
13.784
13.763
10.340
Title: EDD4-275 24-36.11.fid
ACQUISITION PARAMETERS
Solvent: CDCl3
Pulse Sequence: zgpg30
Experiment: 1D
Number of Scans: 1500
Receiver Gain: 203.0
Relaxation Delay: 2.0000 s
Pulse Width: 10.5000 usec
Acquisition Time: 1.1010 usec
Spectrometer Frequency: 125.78 MHz
Spectral Width: 29761.9 Hz
Lowest Frequency: -2287.3
Nucleus: 13C
Me
O
O
Me
O
O
C3H7
Me
O
3.9a
5000
4500
4000
3500
3000
2500
2000
1500
1000
500
0
-500
10
200
190
180
170
160
150
140
130
120
110
100
90
80
70
60
50
40
30
20
10
0
f1 (ppm)

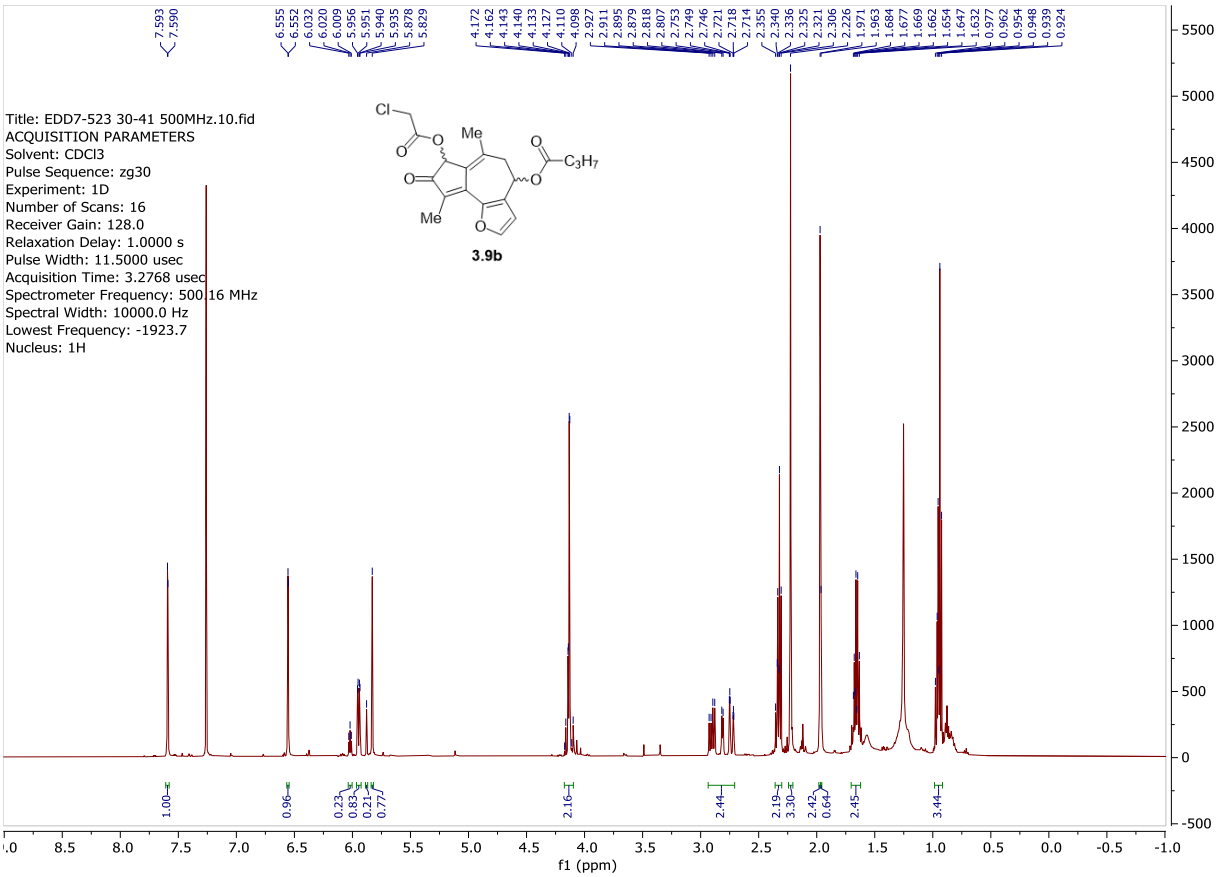
Title: EDD7-523 30-41 500MHz.10.fid
ACQUISITION PARAMETERS
Solvent: CDCl3
Pulse Sequence: zg30
Experiment: 1D
Number of Scans: 16
Receiver Gain: 128.0
Relaxation Delay: 1.0000 s
Pulse Width: 11.5000 usec
Acquisition Time: 3.2768 usec
Spectrometer Frequency: 500.16 MHz
Spectral Width: 10000.0 Hz
Lowest Frequency: -1923.7
Nucleus: 1H
3.9b
f1 (ppm)

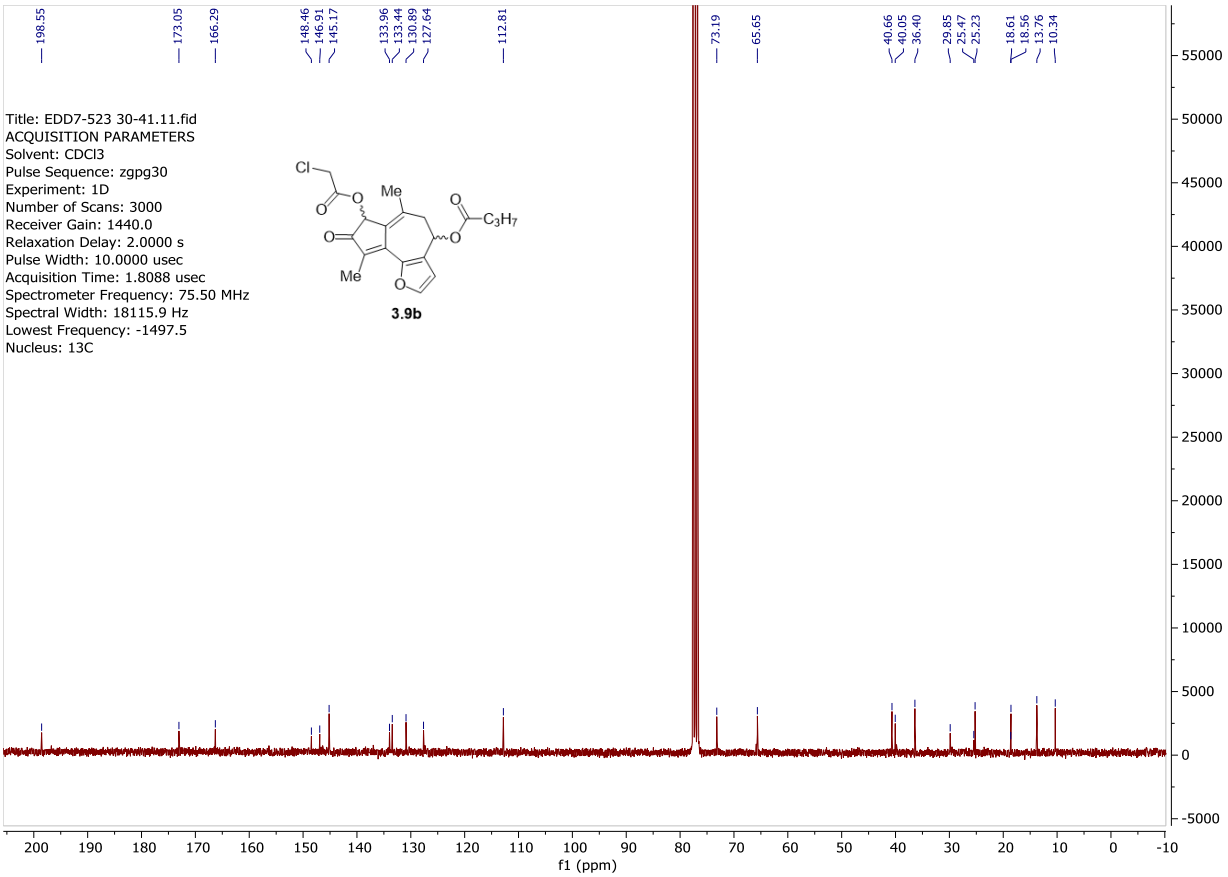
198.55
173.05
166.29
148.46
146.91
145.17
133.96
133.44
130.89
127.64
112.81
73.19
65.65
40.66
40.05
36.40
29.85
25.47
25.23
18.61
18.56
13.76
10.34
Title: EDD7-523 30-41.11.fid
ACQUISITION PARAMETERS
Solvent: CDCl3
Pulse Sequence: zgpg30
Experiment: 1D
Number of Scans: 3000
Receiver Gain: 1440.0
Relaxation Delay: 2.0000 s
Pulse Width: 10.0000 usec
Acquisition Time: 1.8088 usec
Spectrometer Frequency: 75.50 MHz
Spectral Width: 18115.9 Hz
Lowest Frequency: -1497.5
Nucleus: 13C
Cl
O
O
Me
O
C3H7
O
O
Me
O
3.9b
55000
50000
45000
40000
35000
30000
25000
20000
15000
10000
5000
0
-5000
200
190
180
170
160
150
140
130
120
110
100
90
80
70
60
50
40
30
20
10
0
-10
f1 (ppm)

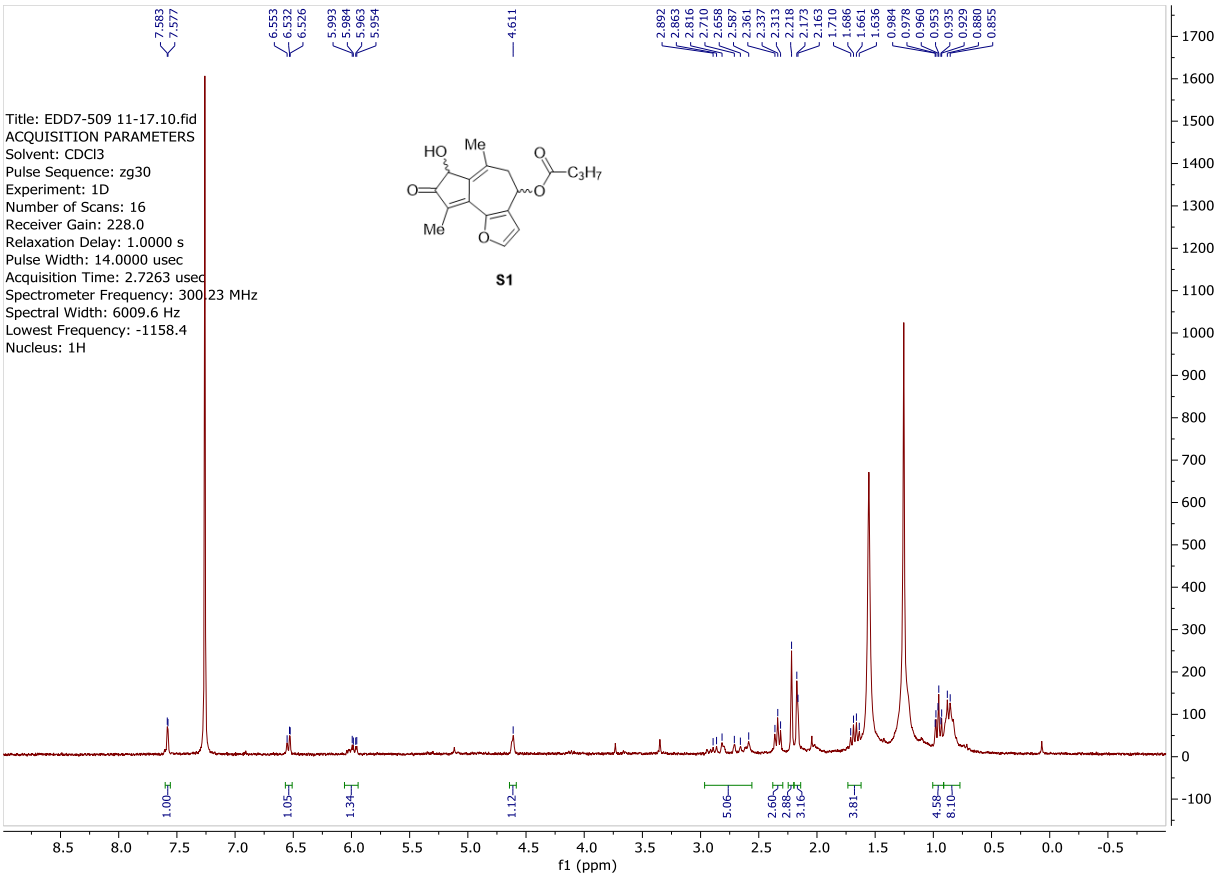
Title: EDD7-509 11-17.10.fid
ACQUISITION PARAMETERS
Solvent: CDCl3
Pulse Sequence: zg30
Experiment: 1D
Number of Scans: 16
Receiver Gain: 228.0
Relaxation Delay: 1.0000 s
Pulse Width: 14.0000 usec
Acquisition Time: 2.7263 usec
Spectrometer Frequency: 300.23 MHz
Spectral Width: 6009.6 Hz
Lowest Frequency: -1158.4
Nucleus: 1H
S1
f1 (ppm)

Bibliography

1. Christensen, S. B.; Norup, E., Absolute Configurations of the Histamine Liberating Sesquiterpene Lactones Thapsigargin and Trilobolide. *Tetrahedron Letters* **1985,** *26* (1), 107-110.

2. Thastrup, O.; Cullen, P. J.; Drøbak, B. K.; Hanley, M. R.; Dawson, A. P., Thapsigargin, a Tumor Promoter, Discharges Intracellular Ca2+ Stores by Specific Inhibition of the Endoplasmic Reticulum Ca2(+)-ATPase. *Proceedings of the National Academy of Sciences* **1990,** *87* (7), 2466.

3. Sagara, Y.; Inesi, G., Inhibition of the Sarcoplasmic Reticulum Ca2+ Transport ATPase by Thapsigargin at Subnanomolar Concentrations. *Journal of Biological Chemistry* **1991,** *266* (21), 13503-13506.

4. Chemaly, E. R.; Troncone, L.; Lebeche, D., SERCA Control of Cell Death and Survival. *Cell Calcium* **2018,** *69*, 46-61.

5. Doan, N. T. Q.; Paulsen, E. S.; Sehgal, P.; Møller, J. V.; Nissen, P.; Denmeade, S. R.; Isaacs, J. T.; Dionne, C. A.; Christensen, S. B., Targeting Thapsigargin Towards Tumors. *Steroids* **2015,** *97*, 2-7.

6. Christensen, S. B.; Simonsen, H. T.; Engedal, N.; Nissen, P.; Møller, J. V.; Denmeade, S. R.; Isaacs, J. T., From Plant to Patient: Thapsigargin, a Tool for Understanding Natural Product Chemistry, Total Syntheses, Biosynthesis, Taxonomy, ATPases, Cell Death, and Drug Development. In *Progress in the Chemistry of Organic Natural Products 115*, Kinghorn, A. D.; Falk, H.; Gibbons, S.; Asakawa, Y.; Liu, J.-K.; Dirsch, V. M., Eds. Springer International Publishing: Cham, 2021; pp 59-114.

7. Nhu Thi Quynh, D.; Soren Brogger, C., Thapsigargin, Origin, Chemistry, Structure-Activity Relationships and Prodrug Development. *Current Pharmaceutical Design* **2015,** *21* (38), 5501-5517.

8. Chang, S. S.; Reuter, V. E.; Heston, W. D. W.; Bander, N. H.; Grauer, L. S.; Gaudin, P. B., Five Different Anti-Prostate-specific Membrane Antigen (PSMA) Antibodies Confirm PSMA Expression in Tumor-associated Neovasculature1. *Cancer Research* **1999,** *59* (13), 3192-3198.

9. Mahalingam, D.; Wilding, G.; Denmeade, S.; Sarantopoulas, J.; Cosgrove, D.; Cetnar, J.; Azad, N.; Bruce, J.; Kurman, M.; Allgood, V. E.; Carducci, M., Mipsagargin, a Novel Thapsigargin-Based PSMA-Activated Prodrug: Results of a First-in-Man Phase I Clinical Trial in Patients with Refractory, Advanced or Metastatic Solid Tumours. *British Journal of Cancer* **2016,** *114* (9), 986-994.

10. Mahalingam, D.; Peguero, J.; Cen, P.; Arora, P. S.; Sarantopoulos, J.; Rowe, J.; Allgood, V.; Tubb, B.; Campos, L., A Phase II, Multicenter, Single-Arm Study of Mipsagargin (G-202) as

a Second-Line Therapy Following Sorafenib for Adult Patients with Progressive Advanced Hepatocellular Carcinoma. *Cancers* **2019,** *11* (6).

11. Piccioni, D.; Juarez, T.; Brown, B.; Rose, L.; Allgood, V.; Kesari, S., ATCT-18Phase II Study of Mipsagargin (G-202), a PSMA-Activated Prodrug Targeting the Tumor Endothelium, in Adult Patients with Recurrent or Progressive Glioblastoma. *Neuro-Oncology* **2015,** *17* (suppl_5), v5-v5.

12. Roti, G.; Qi, J.; Kitara, S.; Sanchez-Martin, M.; Saur Conway, A.; Varca, A. C.; Su, A.; Wu, L.; Kung, A. L.; Ferrando, A. A.; Bradner, J. E.; Stegmaier, K., Leukemia-Specific Delivery of Mutant NOTCH1 Targeted Therapy. *The Journal of Experimental Medicine* **2018,** *215* (1), 197.

13. Brøgger Christensen, S.; Andersen, A.; Kromann, H.; Treiman, M.; Tombal, B.; Denmeade, S.; Isaacs, J. T., Thapsigargin Analogues for Targeting Programmed Death of Androgen-Independent Prostate Cancer Cells. *Bioorganic & Medicinal Chemistry* **1999,** *7* (7), 1273-1280.

14. Skytte, D. M.; Møller, J. V.; Liu, H.; Nielsen, H. Ø.; Svenningsen, L. E.; Jensen, C. M.; Olsen, C. E.; Christensen, S. B., Elucidation of the Topography of the Thapsigargin Binding Site in the Sarco-Endoplasmic Calcium ATPase. *Bioorganic & Medicinal Chemistry* **2010,** *18* (15), 5634-5646.

15. Akinboye, E. S.; Rogers, O. C.; Isaacs, J. T., 2-Fluoro-5-maleimidobenzoic Acid-Linked Albumin Drug (MAD) Delivery for Selective Systemic Targeting of Metastatic Prostate Cancer. *The Prostate* **2018,** *78* (9), 655-663.

16. Ishikawa, T.; Mizuta, S.; Kaneko, O.; Yahata, K., Fragment Molecular Orbital Study of the Interaction between Sarco/Endoplasmic Reticulum Ca2+-ATPase and its Inhibitor Thapsigargin toward Anti-Malarial Development. *The Journal of Physical Chemistry B* **2018,** *122* (33), 7970-7977.

17. Wei, Y.; Meng, M.; Tian, Z.; Xie, F.; Yin, Q.; Dai, C.; Wang, J.; Zhang, Q.; Liu, Y.; Liu, C.; Yan, F.; Jiang, F.; Guo, X., Pharmacological Preconditioning with the Cellular Stress Inducer Thapsigargin Protects Against Experimental Sepsis. *Pharmacological Research* **2019,** *141*, 114-122.

18. Bravo-Santano, N.; Capilla-Lasheras, P.; Mateos, L. M.; Calle, Y.; Behrends, V.; Letek, M., Identification of Novel Targets for Host-Directed Therapeutics Against Intracellular Staphylococcus aureus. *Scientific Reports* **2019,** *9* (1), 15435.

19. Goulding, L. V.; Yang, J.; Jiang, Z.; Zhang, H.; Lea, D.; Emes, R. D.; Dottorini, T.; Pu, J.; Liu, J.; Chang, K.-C., Thapsigargin at Non-Cytotoxic Levels Induces a Potent Host Antiviral Response that Blocks Influenza A Virus Replication. *Viruses* **2020,** *12* (10).

20. Al-Beltagi, S.; Preda, C. A.; Goulding, L. V.; James, J.; Pu, J.; Skinner, P.; Jiang, Z.; Wang, B. L.; Yang, J.; Banyard, A. C.; Mellits, K. H.; Gershkovich, P.; Hayes, C. J.; Nguyen-Van-Tam, J.; Brown, I. H.; Liu, J.; Chang, K.-C., Thapsigargin Is a Broad-Spectrum Inhibitor of Major Human Respiratory Viruses: Coronavirus, Respiratory Syncytial Virus and Influenza A Virus. *Viruses* **2021,** *13* (2).

21. Shaban, M. S.; Müller, C.; Mayr-Buro, C.; Weiser, H.; Meier-Soelch, J.; Albert, B. V.; Weber, A.; Linne, U.; Hain, T.; Babayev, I.; Karl, N.; Hofmann, N.; Becker, S.; Herold, S.; Schmitz, M. L.; Ziebuhr, J.; Kracht, M., Multi-Level Inhibition of Coronavirus Replication by Chemical ER Stress. *Nature Communications* **2021,** *12* (1), 5536.

22. Al-Beltagi, S.; Goulding, L. V.; Chang, D. K. E.; Mellits, K. H.; Hayes, C. J.; Gershkovich, P.; Coleman, C. M.; Chang, K.-C., Emergent SARS-CoV-2 Variants: Comparative Replication Dynamics and High Sensitivity to Thapsigargin. *Virulence* **2021,** *12* (1), 2946-2956.

23. Kumar, N.; Khandelwal, N.; Kumar, R.; Chander, Y.; Rawat, K. D.; Chaubey, K. K.; Sharma, S.; Singh, S. V.; Riyesh, T.; Tripathi, B. N.; Barua, S., Inhibitor of Sarco/Endoplasmic Reticulum Calcium-ATPase Impairs Multiple Steps of Paramyxovirus Replication. *Frontiers in Microbiology* **2019,** *10*.

24. Shaban, M. S.; Mayr-Buro, C.; Meier-Soelch, J.; Albert, B. V.; Schmitz, M. L.; Ziebuhr, J.; Kracht, M., Thapsigargin: Key to New Host-Directed Coronavirus Antivirals? *Trends in Pharmacological Sciences* **2022**.

25. Mohamed Ibrahim, A. M.; Martinez-Swatson, K. A.; Benkaci-Ali, F.; Cozzi, F.; Zoulikha, F.; Simonsen, H. T., Effects of Gamma Irradiation and Comparison of Different Extraction Methods on Sesquiterpene Lactone Yields from the Medicinal Plant Thapsia garganica L. (Apiaceae). *Journal of Applied Research on Medicinal and Aromatic Plants* **2018,** *8*, 26-32.

26. Moujir, L.; Callies, O.; Sousa, P. M. C.; Sharopov, F.; Seca, A. M. L., Applications of Sesquiterpene Lactones: A Review of Some Potential Success Cases. *Applied Sciences* **2020,** *10* (9).

27. Andersen, B. T.; López, Q. C.; Manczak, T.; Martinez, K.; Simonsen, T. H., Thapsigargin—From Thapsia L. to Mipsagargin. *Molecules* **2015,** *20* (4).

28. Ball, M.; Andrews, S. P.; Wierschem, F.; Cleator, E.; Smith, M. D.; Ley, S. V., Total Synthesis of Thapsigargin, a Potent SERCA Pump Inhibitor. *Organic Letters* **2007,** *9* (4), 663-666.

29. Ley, S. V.; Antonello, A.; Balskus, E. P.; Booth, D. T.; Christensen, S. B.; Cleator, E.; Gold, H.; Högenauer, K.; Hünger, U.; Myers, R. M.; Oliver, S. F.; Simic, O.; Smith, M. D.; Søhoel, H.; Woolford, A. J. A., Synthesis of the Thapsigargins. *Proceedings of the National Academy of Sciences of the United States of America* **2004,** *101* (33), 12073.

30. Andrews, S. P.; Ball, M.; Wierschem, F.; Cleator, E.; Oliver, S.; Högenauer, K.; Simic, O.; Antonello, A.; Hünger, U.; Smith, M. D.; Ley, S. V., Total Synthesis of Five Thapsigargins: Guaianolide Natural Products Exhibiting Sub-Nanomolar SERCA Inhibition. *Chemistry – A European Journal* **2007,** *13* (20), 5688-5712.

31. Chu, H.; Smith, J. M.; Felding, J.; Baran, P. S., Scalable Synthesis of (−)-Thapsigargin. *ACS Central Science* **2017,** *3* (1), 47-51.

32. Chen, D.; Evans, P. A., A Concise, Efficient and Scalable Total Synthesis of Thapsigargin and Nortrilobolide from (R)-(−)-Carvone. *Journal of the American Chemical Society* **2017,** *139* (17), 6046-6049.

33. Jouanneau, M.; Bonepally, K. R.; Jeuken, A.; Tap, A.; Guillot, R.; Ardisson, J.; Férézou, J.-P.; Prunet, J., Diastereoselective Synthesis of an Advanced Intermediate of Thapsigargin and Other 6,12-Guaianolides Using a RCEYM Strategy. *Organic Letters* **2018,** *20* (8), 2176-2180.

34. Sanogo, Y.; Othman, R. B.; Dhambri, S.; Selkti, M.; Jeuken, A.; Prunet, J.; Férézou, J.-P.; Ardisson, J.; Lannou, M.-I.; Sorin, G., Ti(II) and Rh(I) Complexes as Reagents toward a Thapsigargin Core. *The Journal of Organic Chemistry* **2019,** *84* (9), 5821-5830.

35. Tap, A.; Jouanneau, M.; Galvani, G.; Sorin, G.; Lannou, M.-I.; Férézou, J.-P.; Ardisson, J., Asymmetric Synthesis of a Highly Functionalized Enantioenriched System Close to Thapsigargin Framework. *Organic & Biomolecular Chemistry* **2012,** *10* (40), 8140-8146.

36. Tap, A.; Lecourt, C.; Dhambri, S.; Arnould, M.; Galvani, G.; Nguyen Van Buu, O.; Jouanneau, M.; Férézou, J.-P.; Ardisson, J.; Lannou, M.-I.; Sorin, G., Alkoxyallene-ynes: Selective Preparation of Bicyclo[5.3.0] Ring Systems Including a δ-Alkoxy Cyclopentadienone. *Chemistry – A European Journal* **2016,** *22* (14), 4938-4944.

37. Manzano, F. L.; Guerra, F. M.; Moreno-Dorado, F. J.; Jorge, Z. D.; Massanet, G. M., Toward the Synthesis of Thapsigargin: Enantioselective Synthesis of 7,11-Dihydroxyguaianolides. *Organic Letters* **2006,** *8* (13), 2879-2882.

38. Marín-Barrios, R.; García-Cabeza, A. L.; Moreno-Dorado, F. J.; Guerra, F. M.; Massanet, G. M., Acyloxylation of Cyclic Enones: Synthesis of Densely Oxygenated Guaianolides. *The Journal of Organic Chemistry* **2014,** *79* (14), 6501-6509.

39. Grillet, F.; Huang, C.; Brummond, K. M., An Allenic Pauson–Khand Approach to 6,12-Guaianolides. *Organic Letters* **2011,** *13* (23), 6304-6307.

40. Crestey, F.; Toma, M.; Christensen, S. B., Concise Synthesis of Thapsigargin from Nortrilobolide. *Tetrahedron Letters* **2015,** *56* (43), 5896-5898.

41. Zimmermann, T.; Drašar, P.; Rimpelová, S.; Christensen, S. B.; Khripach, V. A.; Jurášek, M., Large Scale Conversion of Trilobolide into the Payload of Mipsagargin: 8-O-(12-Aminododecanoyl)-8-O-Debutanoylthapsigargin. *Biomolecules* **2020,** *10* (12).

42. Chu, H.; Dünstl, G.; Felding, J.; Baran, P. S., Divergent Synthesis of Thapsigargin Analogs. *Bioorganic & Medicinal Chemistry Letters* **2018,** *28* (16), 2705-2707.

43. Andrews, S. P.; Tait, M. M.; Ball, M.; Ley, S. V., Design and Total Synthesis of Unnatural Analogues of the Sub-Nanomolar SERCA inhibitor thapsigargin. *Organic & Biomolecular Chemistry* **2007,** *5* (9), 1427-1436.

44. Jaskulska, A.; Janecka, A. E.; Gach-Janczak, K., Thapsigargin—From Traditional Medicine to Anticancer Drug. *International Journal of Molecular Sciences* **2021,** *22* (1).

45. Abbasov, M. E.; Alvariño, R.; Chaheine, C. M.; Alonso, E.; Sánchez, J. A.; Conner, M. L.; Alfonso, A.; Jaspars, M.; Botana, L. M.; Romo, D., Simplified Immunosuppressive and Neuroprotective Agents Based on Gracilin A. *Nature Chemistry* **2019,** *11* (4), 342-350.

46. Tao, Y.; Reisenauer, K. N.; Masi, M.; Evidente, A.; Taube, J. H.; Romo, D., Pharmacophore-Directed Retrosynthesis Applied to Ophiobolin A: Simplified Bicyclic Derivatives Displaying Anticancer Activity. *Organic Letters* **2020,** *22* (21), 8307-8312.

47. Truax, N. J.; Ayinde, S.; Van, K.; Liu, J. O.; Romo, D., Pharmacophore-Directed Retrosynthesis Applied to Rameswaralide: Synthesis and Bioactivity of Sinularia Natural Product Tricyclic Cores. *Organic Letters* **2019,** *21* (18), 7394-7399.

48. Truax, N. J.; Romo, D., Bridging the Gap Between Natural Product Synthesis and Drug Discovery. *Natural Product Reports* **2020,** *37* (11), 1436-1453.

49. Khand, I. U.; Knox, G. R.; Pauson, P. L.; Watts, W. E., Organocobalt Complexes. Part I. Arene Complexes Derived from Dodecacarbonyltetracobalt. *Journal of the Chemical Society, Perkin Transactions 1* **1973,** (0), 975-977.

50. Brummond, K. M.; Kent, J. L., Recent Advances in the Pauson–Khand Reaction and Related [2+2+1] Cycloadditions. *Tetrahedron* **2000,** *56* (21), 3263-3283.

51. Ma, K.; Martin, B. S.; Yin, X.; Dai, M., Natural Product Syntheses via Carbonylative Cyclizations. *Natural Product Reports* **2019,** *36* (1), 174-219.

52. Narasaka, K.; Shibata, T., Conversion of 1-(ω-Alkynyl)-1,2-propadienyl Sulfides to Bicyclic Dienones by the Use of Iron Carbonyl Complex. *Chemistry Letters* **1994,** *23* (2), 315-318.

53. Kent, J. L.; Wan, H.; Brummond, K. M., A New Allenic Pauson-Khand Cycloaddition for the Preparation of α-Methylene Cyclopentenones. *Tetrahedron Letters* **1995,** *36* (14), 2407-2410.

54. Williams, D. R.; Shah, A. A.; Mazumder, S.; Baik, M.-H., Studies of Iron-Mediated Pauson–Khand Reactions of 1,1-Disubstituted-Allenylsilanes: Mechanistic Implications for a Reactive Three-Membered Iron Metallacycle. *Chemical Science* **2013,** *4* (1), 238-247.

55. González-Gómez, Á.; Añorbe, L.; Poblador, A.; Domínguez, G.; Pérez-Castells, J., Intermolecular and Intramolecular Pauson–Khand Reactions of Functionalized Allenes. *European Journal of Organic Chemistry* **2008,** *2008* (8), 1370-1377.

56. Antras, F.; Laurent, S.; Ahmar, M.; Chermette, H.; Cazes, B., Pauson–Khand Reaction of Allenic Hydrocarbons: Synthesis of 4-Alkylidenecyclopentenones. *European Journal of Organic Chemistry* **2010,** *2010* (17), 3312-3336.

57. Brummond, K. M.; Chen, H.; Fisher, K. D.; Kerekes, A. D.; Rickards, B.; Sill, P. C.; Geib, S. J., An Allenic Pauson−Khand-Type Reaction: A Reversal in π-Bond Selectivity and the Formation of Seven-Membered Rings. *Organic Letters* **2002,** *4* (11), 1931-1934.

58. Kobayashi, T.; Koga, Y.; Narasaka, K., The rhodium-catalyzed Pauson–Khand reaction. *Journal of Organometallic Chemistry* **2001,** *624* (1), 73-87.

59. Mukai, C.; Nomura, I.; Yamanishi, K.; Hanaoka, M., Rh(I)-Catalyzed Intramolecular Allenic Pauson−Khand Reaction: Construction of a Bicyclo[5.3.0]dec-1,7-dien-9-one Skeleton. *Organic Letters* **2002,** *4* (10), 1755-1758.

60. Shibata, T.; Koga, Y.; Narasaka, K., Intra- and Intermolecular Allene–Alkyne Coupling Reactions by the Use of Fe(CO)4(NMe3). *Bulletin of the Chemical Society of Japan* **1995,** *68* (3), 911-919.

61. Aumann, R.; Weidenhaupt, H.-J., Organische Synthesen mit übergangsmetallkomplexen, 19 ß-Methylencyclopentenone durch templatgesteuerte [2 + 2 + 1]-Cycloaddition von Alkinen an Allene und Kohlenmonoxid mit Eisencarbonyl. *Chemische Berichte* **1987,** *120* (1), 23-27.

62. Brummond, K. M.; Chen, D.; Davis, M. M., A General Synthetic Route to Differentially Functionalized Angularly and Linearly Fused [6−7−5] Ring Systems: A Rh(I)-Catalyzed Cyclocarbonylation Reaction. *The Journal of Organic Chemistry* **2008,** *73* (13), 5064-5068.

63. Brummond, K. M.; Davis, M. M.; Huang, C., Rh(I)-Catalyzed Cyclocarbonylation of Allenol Esters To Prepare Acetoxy 4-Alkylidenecyclopent-3-en-2-ones. *The Journal of Organic Chemistry* **2009,** *74* (21), 8314-8320.

64. Inagaki, F.; Kawamura, T.; Mukai, C., Rh(I)-Catalyzed Pauson–Khand Reaction of 1-Phenylsulfonyl-1,2-octadien-7-yne Derivatives. *Tetrahedron* **2007,** *63* (24), 5154-5160.

65. Bayden, A. S.; Brummond, K. M.; Jordan, K. D., Computational Insight Concerning Catalytic Decision Points of the Transition Metal Catalyzed [2 + 2 + 1] Cyclocarbonylation Reaction of Allenes. *Organometallics* **2006,** *25* (22), 5204-5206.

66. Shibata, T.; Kadowaki, S.; Hirase, M.; Takagi, K., Iridium Complex-Catalyzed Pauson-Khand-Type Reaction of Allenynes. *Synlett* **2003,** *2003* (04), 0573-0575.

67. Hicks, F. A.; Kablaoui, N. M.; Buchwald, S. L., Titanocene-Catalyzed Cyclocarbonylation of Enynes to Cyclopentenones. *Journal of the American Chemical Society* **1996,** *118* (39), 9450-9451.

68. Brummond, K. M.; Wan, H.; Kent, J. L., An Intramolecular Allenic [2 + 2 + 1] Cycloaddition. *The Journal of Organic Chemistry* **1998,** *63* (19), 6535-6545.

69. Han, Y.; Zhao, Y.; Ma, S., Rhodium-Catalyzed Pauson–Khand-Type Cyclization of 1,5-Allene-Alkynes: A Chirality Transfer Strategy for Optically Active Bicyclic Ketones. *Chemistry – A European Journal* **2019,** *25* (40), 9529-9533.

70. Grillet, F.; Brummond, K. M., Enantioselective Synthesis of 5,7-Bicyclic Ring Systems from Axially Chiral Allenes Using a Rh(I)-Catalyzed Cyclocarbonylation Reaction. *The Journal of Organic Chemistry* **2013,** *78* (8), 3737-3754.

71. Defieber, C.; Ariger, M. A.; Moriel, P.; Carreira, E. M., Iridium-Catalyzed Synthesis of Primary Allylic Amines from Allylic Alcohols: Sulfamic Acid as Ammonia Equivalent. *Angewandte Chemie International Edition* **2007,** *46* (17), 3139-3143.

72. Rössler, S. L.; Petrone, D. A.; Carreira, E. M., Iridium-Catalyzed Asymmetric Synthesis of Functionally Rich Molecules Enabled by (Phosphoramidite,Olefin) Ligands. *Accounts of Chemical Research* **2019,** *52* (9), 2657-2672.

73. Burrows, L. C.; Jesikiewicz, L. T.; Lu, G.; Geib, S. J.; Liu, P.; Brummond, K. M., Computationally Guided Catalyst Design in the Type I Dynamic Kinetic Asymmetric Pauson–Khand Reaction of Allenyl Acetates. *Journal of the American Chemical Society* **2017,** *139* (42), 15022-15032.

74. Bhat, V.; Welin, E. R.; Guo, X.; Stoltz, B. M., Advances in Stereoconvergent Catalysis from 2005 to 2015: Transition-Metal-Mediated Stereoablative Reactions, Dynamic Kinetic Resolutions, and Dynamic Kinetic Asymmetric Transformations. *Chemical Reviews* **2017,** *117* (5), 4528-4561.

75. Wang, Y.-M.; Kuzniewski, C. N.; Rauniyar, V.; Hoong, C.; Toste, F. D., Chiral (Acyclic Diaminocarbene)Gold(I)-Catalyzed Dynamic Kinetic Asymmetric Transformation of Propargyl Esters. *Journal of the American Chemical Society* **2011,** *133* (33), 12972-12975.

76. Trost, B. M.; Fandrick, D. R.; Dinh, D. C., Dynamic Kinetic Asymmetric Allylic Alkylations of Allenes. *Journal of the American Chemical Society* **2005,** *127* (41), 14186-14187.

77. Tran, D. N.; Cramer, N., Rhodium-Catalyzed Dynamic Kinetic Asymmetric Transformations of Racemic Allenes by the [3+2] Annulation of Aryl Ketimines. *Angewandte Chemie International Edition* **2013,** *52* (40), 10630-10634.

78. Ogasawara, M.; Nagano, T.; Hayashi, T., A New Route to Methyl (R,E)-(−)-Tetradeca-2,4,5-trienoate (Pheromone of Acanthoscelides obtectus) Utilizing a Palladium-Catalyzed Asymmetric Allene Formation Reaction. *The Journal of Organic Chemistry* **2005,** *70* (14), 5764-5767.

79. Deihl, E. D.; Jesikiewicz, L. T.; Newman, L. J.; Liu, P.; Brummond, K. M., Rh(I)-Catalyzed Allenic Pauson–Khand Reaction to Access the Thapsigargin Core: Influence of Furan and Allenyl Chloroacetate Groups on Enantioselectivity. *Organic Letters* **2022,** *24* (4), 995-999.

80. Mace, L. H.; Shanmugham, M. S.; White, J. D.; Drew, M. G. B., A New Route to Furanoeremophilane Sesquiterpenoids. Synthesis of Senecio Metabolites (±)-6-Hydroxyeuryopsin, (±)-1,10-Epoxy-6-hydroxyeuryopsin, (±)-Toluccanolide A and (±)-Toluccanolide C. *Organic & Biomolecular Chemistry* **2006,** *4* (6), 1020-1031.

81. Chen, K.; Richter, J. M.; Baran, P. S., 1,3-Diol Synthesis via Controlled, Radical-Mediated C−H Functionalization. *Journal of the American Chemical Society* **2008,** *130* (23), 7247-7249.

82. Chen, K.; Baran, P. S., Total synthesis of eudesmane terpenes by site-selective C–H oxidations. *Nature* **2009,** *459*, 824.

83. Crabtree, R., Iridium Compounds in Catalysis. *Accounts of Chemical Research* **1979,** *12* (9), 331-337.

84. Gill, G. S.; Grobelny, D. W.; Chaplin, J. H.; Flynn, B. L., An Efficient Synthesis and Substitution of 3-Aroyl-2-bromobenzo[b]furans. *The Journal of Organic Chemistry* **2008,** *73* (3), 1131-1134.

85. Flynn, B. L.; Gill, G. S.; Grobelny, D. W.; Chaplin, J. H.; Paul, D.; Leske, A. F.; Lavranos, T. C.; Chalmers, D. K.; Charman, S. A.; Kostewicz, E.; Shackleford, D. M.; Morizzi, J.; Hamel, E.; Jung, M. K.; Kremmidiotis, G., Discovery of 7-Hydroxy-6-methoxy-2-methyl-3-(3,4,5-trimethoxybenzoyl)benzo[b]furan (BNC105), a Tubulin Polymerization Inhibitor with Potent Antiproliferative and Tumor Vascular Disrupting Properties. *Journal of Medicinal Chemistry* **2011,** *54* (17), 6014-6027.

86. List, B.; Lerner, R. A.; Barbas, C. F., Proline-Catalyzed Direct Asymmetric Aldol Reactions. *Journal of the American Chemical Society* **2000,** *122* (10), 2395-2396.

87. Mukherjee, S.; Yang, J. W.; Hoffmann, S.; List, B., Asymmetric Enamine Catalysis. *Chemical Reviews* **2007,** *107* (12), 5471-5569.

88. Bures, E. J.; Keay, B. A., The 1,4 O→C Silyl Migrations of Various 3-[(Trialkylsilyl)oxymethyl]-furans and -thiophenes. *Tetrahedron Letters* **1987,** *28* (48), 5965-5968.

89. Bures, E. J.; Keay, B. A., The Regiospecific Formation and Reactions of 4-Lithio-2-(t-butyldimethylsilyl)- 3-(hydroxymethyl)furan: An Approach to 3,4-Disubstituted Furans. *Tetrahedron Letters* **1988,** *29* (11), 1247-1250.

90. Hao, H.-D.; Trauner, D., Furans as Versatile Synthons: Total Syntheses of Caribenol A and Caribenol B. *Journal of the American Chemical Society* **2017,** *139* (11), 4117-4122.

91. Mukai, C.; Hirose, T.; Teramoto, S.; Kitagaki, S., Rh(I)-Catalyzed Allenic Pauson–Khand Reaction: First Construction of the Bicyclo[6.3.0]undecadienone Ring System. *Tetrahedron* **2005,** *61* (46), 10983-10994.

92. Lv, C.; Tu, Q.; Gong, J.; Hao, X.; Yang, Z., Asymmetric Total Synthesis of (−)-Perforanoid A. *Tetrahedron* **2017,** *73* (26), 3612-3621.

93. Peterson, L. A., Reactive Metabolites in the Biotransformation of Molecules Containing a Furan Ring. *Chemical Research in Toxicology* **2013,** *26* (1), 6-25.

94. Kelly, A. R.; Kerrigan, M. H.; Walsh, P. J., Addition/Oxidative Rearrangement of 3-Furfurals and 3-Furyl Imines: New Approaches to Substituted Furans and Pyrroles. *Journal of the American Chemical Society* **2008,** *130* (12), 4097-4104.

95. Paquette, L. A.; Efremov, I., Teubrevin G and Teubrevin H: The First Total Syntheses of Rearranged neo-Clerodanes Including Solutions to the Problems of Chirality Merger and Furan Ring Assembly. *Journal of the American Chemical Society* **2001,** *123* (19), 4492-4501.

96. Pearson, D. E.; Cowan, D.; Beckler, J. D., A Study of the Entrainment Method for Making Grignard Reagents. *The Journal of Organic Chemistry* **1959,** *24* (4), 504-509.

97. Gregg, B. T.; Golden, K. C.; Quinn, J. F.; Wang, H.-J.; Zhang, W.; Wang, R.; Wekesa, F.; Tymoshenko, D. O., Rapid, One-Pot Synthesis of α,α-Disubstituted Primary Amines by the Addition of Grignard Reagents to Nitriles Under Microwave Heating Conditions. *Tetrahedron Letters* **2009,** *50* (27), 3978-3981.

98. Weiberth, F. J.; Hall, S. S., Copper(I)-Activated Addition of Grignard Reagents to Nitriles. Synthesis of Ketimines, Ketones, and Amines. *The Journal of Organic Chemistry* **1987,** *52* (17), 3901-3904.

99. Padwa, A.; Akiba, M.; Chou, C. S.; Cohen, L., Photochemistry of Cyclopropene Derivatives. Synthesis and Photorearrangement of a 3-Acyl-Substituted Cyclopropene. *The Journal of Organic Chemistry* **1982,** *47* (2), 183-191.

100. Hauser, C. R.; Humphlett, W. J., The Influence of Structure on the Reactions of Grignard Reagents with Nitriles Having α-Hydrogen. *The Journal of Organic Chemistry* **1950,** *15* (2), 359-366.

101. Sumrell, G., Investigation of the Reaction of Organolithium Reagents with Nitriles Having α-Hydrogen. *The Journal of Organic Chemistry* **1954,** *19* (5), 817-819.

102. Grissom, J. W.; Klingberg, D.; Meyenburg, S.; Stallman, B. L., Enediyne- and Tributyltin Hydride-Mediated Aryl Radical Additions onto Various Radical Acceptors. *The Journal of Organic Chemistry* **1994,** *59* (25), 7876-7888.

103. Cheng, S.-W.; Chiou, D.-Y.; Lai, Y.-Y.; Yu, R.-H.; Lee, C.-H.; Cheng, Y.-J., Synthesis and Molecular Properties of Four Isomeric Dialkylated Angular-Shaped Naphthodithiophenes. *Organic Letters* **2013,** *15* (20), 5338-5341.

104. Wang, K. K.; Zhang, Q.; Liao, J., Synthesis of 5-Methylene-1,3-cyclohexadienes (o-Isotoluenes) via Electrocyclization of (4Z)-1,2,4,6-Heptatetraenes. *Tetrahedron Letters* **1996,** *37* (24), 4087-4090.

105. Kuzmin, A. V.; Popik, V. V., Dual Reactivity of a Photochemically-Generated Cyclic Enyne–Allene. *Chemical Communications* **2009,** (38), 5707-5709.

106. Mironov, M. E.; Bagryanskaya, I. Y.; Shults, E. E., Synthesis of 3-Trimethylsiloxy-1-(furan-3-yl)butadiene and its Reactions with Dienophiles. *Chemistry of Heterocyclic Compounds* **2016,** *52* (6), 364-373.

107. Nakamura, K.; Fujii, M.; Ohno, A.; Oka, S., NAD(P)+-NAD(P)H model. 52. Reduction of Olefins by Hantzsch Ester on Silica Gel. *Tetrahedron Letters* **1984,** *25* (36), 3983-3986.

108. Fujii, M.; Aida, T.; Yoshihara, M.; Ohno, A., NAD(P)+–NAD(P)H Models. 71. A Convenient Route to the Synthesis of Juvabione. *Bulletin of the Chemical Society of Japan* **1990,** *63* (4), 1255-1257.

109. Che, J.; Lam, Y., Rapid and Regioselective Hydrogenation of α,β-Unsaturated Ketones and Alkylidene Malonic Diesters Using Hantzsch Ester Catalyzed by Titanium Tetrachloride. *Synlett* **2010,** *2010* (16), 2415-2420.

110. Reese, C. B.; Stewart, J. C. M.; van Boom, J. H.; de Leeuw, H. P. M.; Nagel, J.; de Rooy, J. F. M., The Synthesis of Oligoribonucleotides. Part XI. Preparation of Ribonucleoside 2′-Acetal 3′-esters by Selective Deacylation. *Journal of the Chemical Society, Perkin Transactions 1* **1975,** (10), 934-942.

111. Kajiro, H.; Mitamura, S.; Mori, A.; Hiyama, T., Scandium Trifluoromethanesulfonate-Catalyzed Cleavage of Esters Bearing a Coordinative Group at a Vicinal Position. *Bulletin of the Chemical Society of Japan* **1999,** *72* (7), 1553-1560.

112. Cikotiene, I.; Buksnaitiene, R.; Sazinas, R., Rapid Access to Benzo-Annelated Heterocycles, Naphthalenes, and Polysubstituted Benzenes through a Novel Benzannulation Reaction. *Tetrahedron* **2011,** *67* (4), 706-717.

113. Lipshutz, B. H., Five-Membered Heteroaromatic Rings as Intermediates in Organic Synthesis. *Chemical Reviews* **1986,** *86* (5), 795-819.

114. Oliver Kappe, C.; Shaun Murphree, S.; Padwa, A., Synthetic Applications of Furan Diels-Alder Chemistry. *Tetrahedron* **1997,** *53* (42), 14179-14233.

115. Vivek Kumar, S.; Yen, A.; Lautens, M.; Guiry, P. J., Catalytic Asymmetric Transformations of Oxa- and Azabicyclic Alkenes. *Chemical Society Reviews* **2021,** *50* (5), 3013-3093.

116. Zhao, J.; Hughes, C. O.; Toste, F. D., Synthesis of Aromatic Ketones by a Transition Metal-Catalyzed Tandem Sequence. *Journal of the American Chemical Society* **2006,** *128* (23), 7436-7437.

117. Cariou, K.; Mainetti, E.; Fensterbank, L.; Malacria, M., Tandem PtCl2 Catalyzed–Thermal [3,3] Rearrangements of Enyne Acetates. *Tetrahedron* **2004,** *60* (43), 9745-9755.

118. Zhang, L., Tandem Au-Catalyzed 3,3-Rearrangement−[2 + 2] Cycloadditions of Propargylic Esters: Expeditious Access to Highly Functionalized 2,3-Indoline-Fused Cyclobutanes. *Journal of the American Chemical Society* **2005,** *127* (48), 16804-16805.

119. Hoveyda, A. H.; Evans, D. A.; Fu, G. C., Substrate-Directable Chemical Reactions. *Chemical Reviews* **1993,** *93* (4), 1307-1370.

120. Brown, J. M., Directed Homogeneous Hydrogenation [New Synthetic Methods (65)]. *Angewandte Chemie International Edition in English* **1987,** *26* (3), 190-203.

121. Takagi, M.; Yamamoto, K., Carbamate-Directed Stereoselective Hydrogenation and Kinetic Resolution of N-Protected α-(α-Aminoalkyl)acrylates. *Tetrahedron* **1991,** *47* (42), 8869-8882.

122. Trost, B. M.; Rudd, M. T., Ruthenium-Catalyzed Alkyne−Propargyl Alcohol Addition. An Asymmetric Total Synthesis of (+)-α-Kainic Acid. *Organic Letters* **2003,** *5* (9), 1467-1470.

123. Hirose, T.; Miyakoshi, N.; Mukai, C., Total Synthesis of (+)-Achalensolide Based on the Rh(I)-Catalyzed Allenic Pauson−Khand-Type Reaction. *The Journal of Organic Chemistry* **2008,** *73* (3), 1061-1066.

124. Thompson, H. W., Stereochemical Control of Reductions. Directive Effect of Carbomethoxy vs. Hydroxymethyl Groups in Catalytic Hydrogenation. *The Journal of Organic Chemistry* **1971,** *36* (18), 2577-2581.

125. Thompson, H. W.; Wong, J. K., Stereochemical Control of Reductions. 8. Exploration of the Inner Limits of the Haptophilic Effect with 2-Exo-Substituted 7-Methylenenorbornanes. *The Journal of Organic Chemistry* **1985,** *50* (22), 4270-4276.

126. Metz, P.; Bertels, S.; Froehlich, R., An Enantioselective Approach to 3.Alpha.-hydroxy-15-rippertene. Construction of the Tetracyclic Ring System. *Journal of the American Chemical Society* **1993,** *115* (26), 12595-12596.

127. Hans Reich's Collection. NMR Spectroscopy. https://organicchemistrydata.org/hansreich/resources/nmr/?index=nmr_index%2F1H_coupling (accessed May, 17, 2022).

128. Christensen, S. B.; Andersen, A.; Poulsen, J.-C. J.; Treiman, M., Derivatives of Thapsigargin as Probes of its Binding Site on Endoplasmic Reticulum Ca2+ ATPase: Stereoselectivity and Important Functional Groups. *FEBS Letters* **1993,** *335* (3), 345-348.

129. More, V.; Di Mola, A.; Croce, G.; Tedesco, C.; Petronzi, C.; Peduto, A.; De Caprariis, P.; Filosa, R.; Massa, A., Multi-Component, Regio-Selective aldol Addition of β-Ketoesters to Aldehydes: Scope and Applications. *Organic & Biomolecular Chemistry* **2011,** *9* (24), 8483-8488.

130. Hori, M.; Sakakura, A.; Ishihara, K., Enantioselective 1,3-Dipolar Cycloaddition of Azomethine Imines with Propioloylpyrazoles Induced by Chiral π–Cation Catalysts. *Journal of the American Chemical Society* **2014,** *136* (38), 13198-13201.

131. Lingham, A. R.; Hügel, H. M.; Rook, T. J., Studies Towards the Synthesis of Salvinorin A. *Australian Journal of Chemistry* **2006,** *59* (5), 340-348.

132. Trost, B. M.; Brindle, C. S., The Direct Catalytic Asymmetric Aldol Reaction. *Chemical Society Reviews* **2010,** *39* (5), 1600-1632.

133. McCreary, M. D.; Lewis, D. W.; Wernick, D. L.; Whitesides, G. M., Determination of Enantiomeric Purity using Chiral Lanthanide Shift Reagents. *Journal of the American Chemical Society* **1974,** *96* (4), 1038-1054.